Apoptoseresistenz und Vermeidung von anti-Tumor-Immunität – zwei verwandte (?) Überlebensstrategien maligner Gliomzellen

Resistance to apoptosis and escape from host immune surveillance - two related (?) survival mechanisms of malignant glioma cells

DISSERTATION

der Fakultät für Chemie und Pharmazie
der Eberhard-Karls-Universität Tübingen

zur Erlangung des Grades eines Doktors
der Naturwissenschaften

2004

vorgelegt von

Jörg Hinrich Wischhusen

Tag der mündlichen Prüfung: 14. Oktober 2004

Dekan: Professor Dr. S. Laufer

1. Berichterstatter: Professor Dr. Michael Weller

2. Berichterstatter: Professor Dr. Hans-Georg Rammensee

3. Berichterstatter: Professor Dr. Peter H. Krammer

There are two rules for a good scientific presentation:

1.) Never tell everything you know...

Accordingly, the projects summarized in this thesis sought to explore and possibly overcome human glioma cells´ resistance to apoptosis as well as their escape from host immune surveillance. Work from other areas to which I also contributed has been omitted (see attached reference list).

Proprietary Declaration

The work presented here has been performed under the guidance of Prof. Dr. Michael Weller from January 2000 until May 2004 in the Department of Neurology at the University of Tübingen Medical School. I hereby declare that this PhD thesis is the product of my own work and has been written autonomously. Wherever further resources have been used, this has been indicated. In all sections that contain work from my colleagues, I have specified the extent of my contribution. Parts of this work have already been published and are referenced accordingly, others have been submitted for publication.

Table of Contents

List of Abbreviations

Ad-dE1	adenovirus delta exon 1 (control virus)
Ad-eGFP	adenovirus encoding enhanced green fluorescent protein
Ad-MICA	adenovirus encoding MHC class I chain-related protein A
ALLN	N-acetyl-Leu-Leu-Nle-CHO
ANCOVA	analysis of covariance
AnxV	annexinV
Apaf-1	apoptotic protease activating factor 1
APC	antigen presenting cell
ASPP	apoptosis-stimulating protein for p53
ATA	aurintricarboxylic acid
BAK	BCL2-antagonist/killer2
BAX	BCL2-associated X protein
BCL-2	B-cell lymphoma/leukemia-2
BCL-XL	B cell lymphoma mutant, extra long
BH3	Bcl homology 3
BHK	baby hamster kidney
BID	BH3-interacting domain death agonist
BSA	bovine serum albumin
CA-074ME	L-3-trans-(prolylcarbamoyl)oxirane-2-carbonyl)-L-isoleucyl-L-proline methyl ester
caspase	cysteine aspartyl protease
CCR7	chemokine (CC motif) receptor 7
CD	cluster of differentiation
CD40L	CD40 ligand
CD95L	CD95 ligand
cDNA	complementary DNA
CHX	cycloheximide
CMV	cytomegalovirus
CSF	cerebrospinal fluid
CTL	cytotoxic T lymphocytes
CTLA-4	common T lymphocyte antigen 4
CTS-1	chimeric tumour suppressor 1

DAB	diaminobenzidine
DAPI	4,6-diamidino-2-phenylindole
DC	dendritic cell(s)
DCFH-DA	2´,7´-dichlorodihydrofluorescein diacetate
DEVD-amc	Asp-Glu-Val-Asp-7-amino-4-methylcoumarin
DEX	DC-derived exosomes
DISC	death-inducing signalling complex
DMEM	Dulbecco´s Modified Eagle´s Medium
DMSO	dimethylsulfoxide
DNA	deoxyribonucleic acid
DR4/5	death receptor 4/5
DTAF	di-chlorotriazinyl-fluoresceine
E:T ratio	effector target ratio
EBV	Epstein-Barr virus
EC_{50}	50% effective concentration, i.e. the concentration at which the half-maximal effect is achieved
ECL	enhanced chemiluminescence
EDTA	ethylene diamine tetraacetic acid
eGFP	enhanced green fluorescent protein
EGFR	epidermal growth factor receptor
ELISA	enzyme-linked immunosorbent assay
EMSA	electrophoretic mobility shift assay
ER	endoplasmatic reticulum
Fab	antigen-binding fragment
FADD	Fas-associated protein with death domain
FasL	Fas ligand
FCS	foetal calf serum
FITC	fluorescein isothiocyanate
FLICE	FADD-like interleukin-1 -converting enzyme
FLIP	FLICE inhibitory protein
GM-CSF	granulocyte macrophage colony stimulating factor
HCMV	human cytomegalovirus
HHV	human herpes virus
HLA	human leukocyte antigen

HRP	horseradish peroxidase
hsp70	heat shock protein 70
IAP	inhibitor of apoptosis
iASPP	inhibitory member of the ASPP family
IFN-γ	interferon-γ
Ig	immunoglobulin
IL	interleukin
KIR	killing inhibitory receptor
LAK	lymphokine-activated killer
LDH	lactate dehydrogenase
mAb	monoclonal antibody
Mdm2	mouse double minute 2
Melan-A	melanocyte differentiation antigen (MART-1)
MEM	modified Eagle´s medium
MG-132	carbobenzoxy-L-leucyl-L-leucyl-leucinaldehyde
MHC class I	major histocompatibility complex class I
MICA/B	MHC class I chain-related proteins A and B
MLR	mixed lymphocyte reaction
MMP	matrix metalloproteinase
mt	mutant
NAC	N-acetylcysteine
NIH	National Institute of Health (USA)
NK	natural killer
NKG2D	natural killer group 2D
NKG2DL	NKG2D ligand
oPA	o-phenanthroline
p53-luc	p53-inducible luciferase reporter gene
PAMP	pathogen-associated molecular patterns
PARC	p53-associated, parkin-like cytoplasmic protein
PARP	poly (ADP-ribose) polymerase
PBL	peripheral blood lymphocytes
PBMC	peripheral blood mononuclear cells
PBN	N-t-butyl-α-phenylnitrone
PBS	phosphate-buffered saline

pCMV-RL	plasmid encoding renilla reniformis luciferase under the CMV promoter
PCR	polymerase chain reaction
PE	phycoerithrin
PHA	phytohemagglutinin
PI	propidium iodide
PMA	phorbol 12-myristate 13-acetate
PRIMA-1	p53 reactivation and induction of massive apoptosis
PRR	pattern recognition receptors
p-Smad	phosphorylated Smad
pSUPER	plasmid for suppression of endogenous RNA
PTEN	phosphatase and tensin homolog deleted on chromosome ten
PUMA	p53-upregulated modulator of apoptosis
RAG	recombinase activating gene
RNA	ribonucleic acid
RNAi	RNA interference
RPMI	Roswell Park Memorial Institute
RT-PCR	reverse transcription polymerase chain reaction
SBE	Smad binding element
sCD27	soluble CD27
SDS- PAGE	sodium dodecylsulfate polyacrylamide gel electrophoresis
SEM	standard error of the mean
SEREX	serological analysis of tumour antigens by recombinant cDNA expression cloning
SFI	specific fluorescence index
shRNA	short hairpin RNA
siRNA	short interfering RNA
sMICA	soluble MICA
SN	supernatant
SSCP	single strand conformational polymorphism
TAP	transporter associated with antigen processing
tBID	truncated BID
TBS	Tris-buffered saline
TCR	T cell receptor
TEX	tumour cell-derived exosomes

TGF-ß	transforming growth factor-β
TGF-βRI	TGF-β receptor I
TLR	toll-like receptor
TMB	tetramethylbenzidine
TNF	tumour necrosis factor
TNFR	TNF receptor
TRAF	TNF receptor-associated factor
TRAIL	TNF-related apoptosis-inducing ligand
TRAIL-R	TRAIL receptor
TRAMP	tyrosine rich acidic matrix protein
TREC	T cell receptor excision circles
ULBP	UL-16-binding proteins
WHO	world health organisation
wt	wild-type
XIAP	X-linked inhibitor of apoptosis
zFA-fmk	N-tert-butoxy-carbonyl-Phe-Ala-fluoromethylketone
zVAD-fmk	N-tert-butoxy-carbonyl-Val-Ala-DL-Asp-fluoromethylketone
ΔNp63/73	delta N p63/73 (N-terminally deleted p63/p73)

Introductory Remark

In order to give this PhD thesis more structured contours, I decided to split it into various chapters by projects, each consisting of an introduction, a material and methods section, the results paragraph and a discussion. All references as well as a summary are provided at the end. The introductory paragraphs on apoptosis and on tumour immunology are intended to provide the background for the understanding of the work that follows. This format should enable readers who are interested in a specific part of the work outlined here to find all relevant information within a concise standard format. All sections represent the state-of-the-art when the respective project was prepared for publication and have been supplemented with the most relevant recent findings.

I. Introduction

Glioma biology and therapy

Prognosis and current treatment

Glioblastoma is a primary brain tumour of unknown origin carrying an extremely poor prognosis. The pathological diagnosis is based on nuclear atypia, mitoses, microvascular proliferation and necrosis observed in the most malignant region of the tumour (1). In order of increasing anaplasia, the WHO distinguishes (2) pilocytic astrocytoma (grade I), diffuse astrocytoma (grade II), anaplastic astrocytoma (grade III), and eventually glioblastoma (grade IV), the most common subtype in adults, which is among the most lethal of all cancers. Traditionally, cancer is resected and treated with radiotherapy and cytotoxic agents supposed to have a greater effect on proliferating cancer cells than on non-cancerous cells. For some types of cancer, this approach has translated into increased survival. However, despite advanced neurosurgery, optimized radiation therapy regimens and a wide variety of cytotoxic chemotherapies (3), the median survival of glioblastoma patients is approximately one year from the time of diagnosis—the same as it was 10 years ago (1, 4-6).

Glioblastomas are characterized by localized, non-metastatic growth. Inside the brain, however, glioma cells tend to migrate and diffusely infiltrate irreplaceable neuronal tissue. Surgical approaches are limited by the delicacy of intervening in the human brain: Even if the bulk of the tumour mass can be surgically removed, the surrounding tissue which is likely to be invaded by glioma cells must be spared. Thus resection does not prevent recurrence and has little impact on the life-span of glioma patients. The more optimistic estimates suggest that neurosurgery can prolong a patient's life by two to three months and there is little hope that this clinical outcome will be greatly improved (7).

The most effective current treatment modality is radiotherapy (8): median survival after resection is increased from 4 months without irradiation to 10 months. Since glioma cell lines do not undergo apoptosis upon treatment with γ-irradiation up to 8 Gy, the sensitivity of the endothelial cells of the tumour vasculature may be the major determinant of tumour responses (9). Therefore, the effect of radiotherapy may at least partially be mediated by an anti-angiogenic mechanism involving endothelial cell apoptosis. Traditional chemotherapy aims at inducing apoptosis selectively in cancer cells. Delivery of anti-cancer drugs into the brain does not present a major problem since the blood-brain barrier is largely destroyed in the

areas of glioblastoma growth. However, the efficiency of chemotherapeutics is limited because of the intrinsic apoptosis resistance observed in glioma cells. Thus chemotherapy helps to increase the rate of survivors at 18 months from less than 5% to 15-20%, but the majority of patients seems to draw very little benefit from this treatment (10, 11). This still leaves us with the need for an effective therapy that directly targets the glioma cells. Thus, new approaches for the treatment of glioma are badly needed.

Perspectives

The design of novel anti-tumour therapeutics should be guided by our substantially improved understanding of cancer biology that has become possible through major advances in molecular biology, cellular biology and genomics (12, 13). The hallmark of primary glioblastoma is amplification of the oncogenic epidermal growth factor receptor (EGFR) (14). Constitutive signalling through EGFR enhances survival of glioma cells *in vivo*. Another common event in malignant gliomas that contributes to resistance to apoptosis is loss of the tumour suppressor phosphatase and tensin homolog deleted on chromosome ten (PTEN) (15, 16). Mutational inactivation of the tumour suppressor protein p53 is found in >50% of all human cancers and in 65% of secondary gliomas (15, 17). These alterations are thought to be critical for tumour growth and survival and may paradoxically represent the tumour's "Achilles heel": while promoting malignant behaviour, they also provide molecularly defined targets for new therapeutic approaches. Approaches aiming at the inhibition of the oncogenic EGFR (18) are already undergoing clinical trials for a variety of cancers, strategies for the rescue of mutant p53 function (19, 20) have successfully been tested in murine tumour models. These approaches can build upon substantial advances in the understanding of apoptosis, a biological principle that is thought to physiologically protect multicellular organisms against the occurrence of cancer.

Apoptosis:

Physiological significance

The term “apoptosis” is of Greek origin and describes the defoliation of a tree in autumn or the falling of petals from a flower. In 1972, Kerr, Wyllie and Currie introduced this term to describe a cellular suicide program morphologically defined by nuclear condensation and fragmentation, membrane blebbing and the formation of apoptotic bodies (21). Apoptotic cell death allows for the elimination of large numbers of cells no longer needed without inflammation of the surrounding tissue. All of these features distinguish apoptosis from necrosis which is commonly induced by external trauma in its broadest sense (mechanical trauma, heat, bacterial inflammation, and others) and affects continuous tissues rather than single cells within tissues. The cellular suicide program called apoptosis is an essential part of life for any multicellular organism and is largely conserved from worms to mammals (22, 23). In humans, optimum body maintenance requires about 10 billion of our cells to die on a normal day just to balance the new cells arising through mitosis. This process has to be tightly regulated (24) since too little or too much cell death may lead to developmental defects, neurodegeneration, autoimmune diseases or cancer.

During development apoptosis helps to sculpture the body, shape the organs, and carve out fingers and toes (25). It is only by apoptotic elimination of the cells in between that the fingers can separate (26). The nervous system arises through overproduction of cells followed by the death of those that fail to establish functional synaptic connections (27). However, once a functional nervous system has been established, apoptotic deletion of neuronal cell types must be kept to a minimum. Pathological apoptosis in the adult brain may play a role in neurodegenerative diseases such as Alzheimer’s, Parkinson’s, Huntington’s disease or amyotrophic lateral sclerosis (28).

In the immune system that must cope, on the one hand, with a broad variety of antigens and, on the other hand, with the danger of autoimmunity, more cells than finally needed are produced, followed by apoptotic elimination of autoreactive and dysfunctional T cells (29). Another distinctive feature in the immune system is its homeostatic control: after a clonal expansion phase, the number of antigen-reactive lymphocytes must be titrated back until the pool of lymphoid cells reaches the baseline level again (30). This is achieved by balanced fine-tuning between growth/expansion and death by apoptosis. Thus it is not surprising that too little or too much apoptosis results in immunodeficiency or autoimmunity.

In dividing cells, apoptosis is a common response to DNA injury. Accumulation of genetic alterations and subsequent malignant transformation can only occur when a cell fails to initiate apoptosis upon DNA damage. This implies that a defective apoptotic pathway is a prerequisite for tumour development – and the alterations responsible for this defect will also reduce sensitivity towards treatment with apoptosis-inducing anticancer agents (31). Therefore understanding apoptosis is often considered a key to understand the genesis of tumours and to devise innovative strategies for their treatment.

Mechanisms (I): the intrinsic pathway

Apoptosis can be initiated via two different pathways, the so-called intrinsic and the extrinsic (death receptor) pathway. The intrinsic pathway is activated by signals from within the cell such as genotoxic stress leading to DNA damage or nutrient deprivation (32, 33). Upstream sensors, including p53 and pro-apoptotic "BH3-only" proteins of the BCL-2 family (Bad, Bim, Noxa, and Puma, among others) (34-37), respond to select death signals and subsequently trigger the activation of the multidomain death effectors BAX and BAK (38, 39). Activation of BAX and BAK can be prevented through sequestration of translocated BH-3 only molecules by antiapoptotic BCL-2 or BCL-X_L (40). In most cell types, BAX and BAK constitute an essential gateway to the intrinsic death pathway operating at the level of both mitochondria and endoplasmic reticulum Ca^{2+} dynamics (41). Activated homo-oligomerized BAX or BAK result in the permeabilization of the mitochondrial outer membrane and the release of proteins including cytochrome c (42). Released cytochrome c binds to monomers of Apaf-1 in the cytosol, inducing a conformational change that enables stable association with (deoxy)adenosine triphosphate. Apaf-1 monomers then assemble into the heptameric apoptosome, a caspase-activating scaffold which in turn binds to procaspase-9. Once procaspase-9 has been recruited to the apoptosome, it acquires catalytic competency, is proteolytically cleaved, and activates in turn the downstream effectors caspase-3, -6, and -7. These cysteine aspartyl proteases are the central executioners of most apoptotic processes (43). They are synthesized as inactive pro-enzymes and become activated upon proteolytical cleavage by upstream caspases. This cascade of mutual caspase activation culminates in apoptotic cell death.

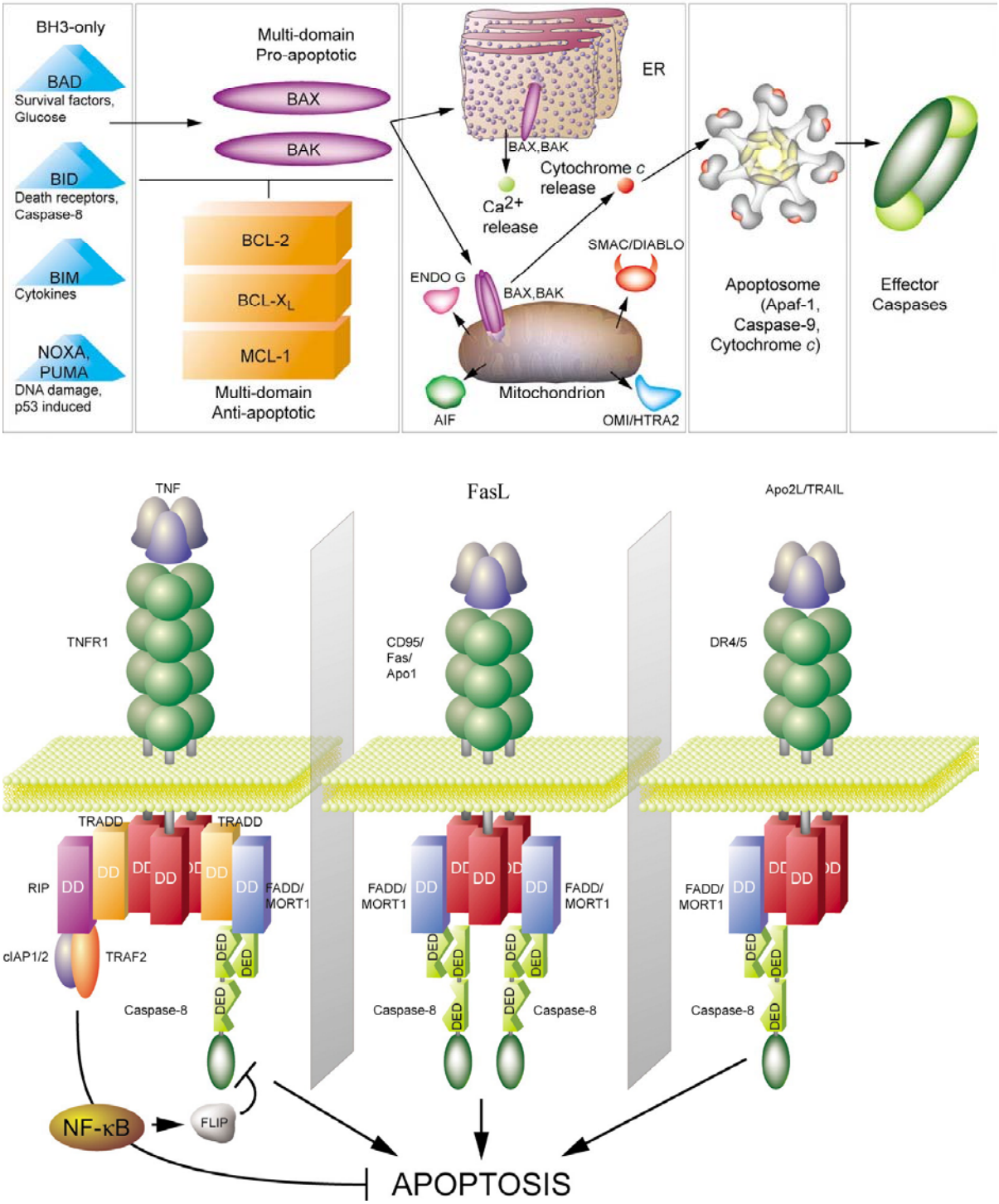

Fig. 1.1: The intrinsic (upper panel) and the extrinsic/death receptor (lower panel) pathway for apoptosis. Figures are modified from (24), Danial and Korsmeyer, 2004. See text for details.

In many experimental paradigms, apoptotic cell death can be prevented by pharmacological inhibition of caspases by suicide substrates such as zVAD-fmk. Inhibition of caspase–9, -3 and –7 by elevated expression of XIAP (X-linked inhibitor of apoptosis) (44) contributes to the apoptosis resistance of many cancer cell lines (including glioma cells). However, it would be dangerous for an organism to depend on a single protease family for the clearance of unwanted and potentially harmful cells. Consequently, other proteases, including granzymes, lysosomal cathepsins, matrix metalloproteinases, and proteasomal proteases have also been implicated in apoptotic cell death. While these mechanisms are not fully consistent with classical apoptosis, they contribute to an active process that depends on signalling events in the dying cell and is thus distinct from necrosis. Often, this caspase-independent cell death also shows some characteristics of apoptosis.

Mechanisms (II): the extrinsic pathway

The detection of endogenous death ligands mediating the death of distinct target cell populations via activation of specific death receptors at the cell surface has led to the concept of what is now commonly called the extrinsic apoptotic pathway. The most important death ligands are tumour necrosis factor alpha (TNF-α) (45), CD95 ligand (CD95L), also known as Fas ligand or Apo-1 ligand (46), and Apo-2 ligand/TNF-related apoptosis-inducing ligand (Apo2L/TRAIL) (47). The receptors for these death ligands belong to the superfamily of TNF receptors (TNFR) (48). These membrane-bound receptors can be divided into two main subgroups on the basis of the cytoplasmic region of the receptor: the death receptor subfamily of TNFR contains a cytoplasmic death domain whereas the other subfamily does not. The death domain is crucial for the signalling of apoptotic cell death. It mediates the homotypic interaction of the death receptor with an adaptor protein containing both a death and a death effector domain. The members of this subfamily are TNF-R1, Fas/CD95, DR-3/Apo-3/TRAMP, TRAIL-R1/DR4, TRAIL-R2/DR5/Killer and DR6. The TNFR family members TNFR2, CD27, CD30 and CD40 do not contain a death domain and need to recruit adaptor proteins such as SIVA-1 (49) in order to transduce apoptotic signals. However, in most cases these receptors transmit survival rather than death signals. Further, there are decoy receptors for TRAIL (TRAIL-R3, TRAIL-R4, osteoprotegerin) (50) and CD95/FasL (DcR3) (51, 52) that seem to have, if any, antiapoptotic properties. The differential distribution of agonistic and decoy receptors in normal tissue and in tumour cells may underlie the selective activity of Apo2L/TRAIL against tumour cells. Activation of death receptors requires engagement by trimeric ligand, leading to the formation of multimeric protein complexes. The CD95/Fas-associated DISC (death-inducing signalling complex) (53) consists of the death receptor

Fas/CD95 itself, its adaptor protein FADD (Fas-associating protein with death domain) and procaspase 8. Instead of procaspase 8, its anti-apoptotic homologue c-FLIP (54, 55) may be incorporated into the complex where it prevents activation of the caspase cascade. However, if procaspase-8 assembles in the DISC to a high local concentration, this will lead to autoproteolytic cleavage and release of active caspase 8 into the cytosol. In SKW6.4 cells (56, 57), where the Fas/CD95 pathway for apoptosis was discovered, caspase 8 may directly activate the downstream effector caspase 3 by proteolytic cleavage (see lower panel, Figure 1.1). In most other cell types (including glioma cell lines), the DISC is formed quite poorly and only a small amount of active caspase 8 is produced. This small amount of activated caspase 8 may, however, initiate a cascade leading to the release of cytochrome *c* from the mitochondrial intermembrane space, the assembly of the apoptosome, the activation of caspase 9 and the subsequent activation of caspases 3, 6 and 7. The molecular mechanisms underlying the amplification of the initial pro-apoptotic signal have not yet been fully resolved. In HeLa, Jurkat or MCF7 cells, caspase 8-mediated cleavage of the BH3 domain containing Bcl-2 family member BID (58, 59) may induce the proapoptotic functions of the mitochondria by causing aggregation of Bax or Bak (60), whereas similar experiments in glioma cells failed to reveal a critical role for tBID (61). Nevertheless, these experiments confirmed the requirement for mitochondrial amplification of the receptor-mediated pro-apoptotic signal since overexpression of the antiapoptotic members of the Bcl-2 family was found to protect glioma cells against CD95L or Apo-2L/TRAIL-induced apoptosis (61, 62). Consequently, the intrinsic and the extrinsic apoptotic pathway converge at the mitochondria, which appear to be the central integrators of pro- and anti-apoptotic signalling.

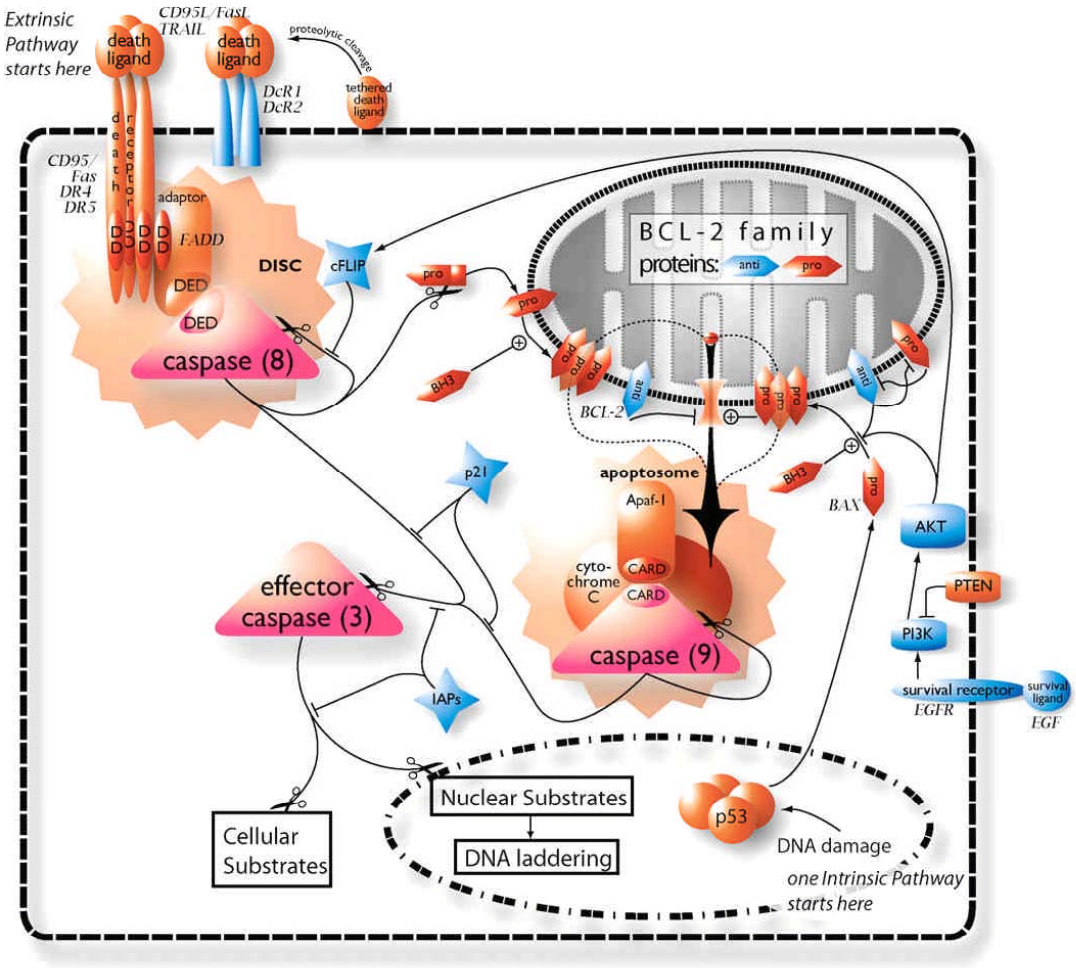

Fig. 1.2. A schematic representation of the apoptotic pathways in glioma cells, showing the convergence of the intrinsic and the extrinsic apoptotic pathway at the level of effector caspases and the mitochondrion. In the extrinsic pathway the engagement of death receptors by death ligand results in the formation of the death-inducing signaling complex (DISC) together with adaptor molecules, leading to the proteolytic activation of regulatory caspases, typically caspase 8, and thereby caspases 3 and 7. In one instance of the intrinsic pathway, DNA damage, expression of multi-domain pro-apoptotic members of the bcl-2 family, for example BAX or BAK, or other unknown events causes mitochondrial pore formation and the release of cytochrome c. This in turn allows the formation of the apoptosome together with APAF-1 and the activation of a regulatory caspase, usually caspase 9, and thereby caspases 3 and 7. In addition survival signals emanating from survival ligands and receptors can inhibit the pro-apoptotic members of the bcl-2 family, or caspases via caspase inhibitors such as IAP or XIAP. Under conditions, where caspase activation is blocked (or triggered inefficiently), Ca^{2+} mobilization or cytochrome C release may also result in caspase-independent cell death. Cross talk between the pathways is indicated by the proteolytic activation of a pro-apoptotic member of the bcl-2 family by caspase 8 (modified from (431), Bögler and Weller, 2002).

Apoptosis in cancer therapy

Selective induction of apoptosis in cancer cells is a key concept for the therapy of malignant gliomas (62, 63). Current therapeutic strategies, including radiotherapy and chemotherapy, do probably not induce a substantial degree of apoptosis in human malignant gliomas, since current glioma treatments, if successful at all, seem to stop growth rather than actually kill (as judged from the failure to induce a regression of the tumour size). This is likely to be due to an overexpression of antiapoptotic (BCL-2, BCL-X_L, XIAP) relative to proapoptotic (BAX, BAD, BAK) regulators of apoptosis (64, 65). However, death receptors of the tumour necrosis factor (TNF)-receptor family are (over)expressed on tumour cells (66) and therefore represent potential therapeutic targets. Sensitization of glioma cells to TRAIL/Apo-2L-induced apoptosis can be achieved *in vitro* and *in vivo* by antagonizing BCL-2 and BCL-X_L using Smac peptides (67). Given the increased selectivity achieved through combined treatment with an appropriate sensitizer and an apoptotic stimulus (that may be regionally delivered), therapeutic regimens inducing a substantial degree of apoptosis in glioma cells without detectable toxicity to normal brain tissue may become possible in the future.

The ultimate goal of an anti-glioma therapy based on the selective induction of apoptosis in tumour cells would, of course, be the complete eradication of the tumour. Further, it has been shown that apoptotic tumour cells can be taken up by antigen-presenting cells and induce a potent anti-tumour immune response *in vivo* (68-71). Therefore, successful induction of apoptosis in a reasonably large proportion of glioma cells might trigger a subsequent immunological response, leading to a more favourable clinical outcome than would be expected based on the efficiency of the pro-apoptotic strategy alone.

Tumour immunology and immunotherapy:

The concept of immune surveillance – a historical overview

Tumour immunotherapy was initiated in 1893 when William Coley used extracts of pyogenic bacteria to cause sporadic anti-tumour responses (72). The concept that the immune system can recognize and eliminate developing tumours in the absence of external therapeutic intervention has first been proposed in 1909 by Paul Ehrlich (73). In 1959, Lewis Thomas described homograft rejection as a primary defence against neoplasia (74). The term "tumour immune surveillance" was coined by Frank Macfarlane Burnet in 1967 (75-77). Clinically, a highly elevated incidence of virally induced malignancies such as HHV-8 (human herpes virus type 8)-dependent Kaposi's sarcoma and EBV (Epstein-Barr-virus)-associated primary cerebral lymphoma has been documented in immunodeficient or immunosuppressed individuals. However, the hypothesis of immune surveillance against non-viral cancers was challenged in 1974 when nude mice, lacking T cells, did not show a higher incidence of cancer than syngeneic immunocompetent mice (78, 79). These experiments were considered to be so convincing that it led most researchers to give up the cancer immunosurveillance hypothesis. What was not recognized at that time is that nude mice are an imperfect model for immunodeficiency: They possess a fully functional innate and a residual adaptive immune system. Improved models of immunodeficiency have now led to a renaissance of the concept of immunosurveillance. Compared to their wild-type counterparts, IFN-$\gamma^{-/-}$ C57BL/6 mice show an increased incidence of disseminated lymphomas, and IFN-$\gamma^{-/-}$ BALB/c mice display an increased incidence of spontaneous lung adenocarcinomas (80). Mice lacking perforin ($pfp^{-/-}$) are more susceptible to chemically induced and spontaneous tumour formation than the respective control mice (81). Finally, the existence of a lymphocyte-dependent cancer immunosurveillance process has been demonstrated in experiments employing gene-targeted mice that lack the recombinase activating gene (RAG)-2 (82). These mice cannot rearrange lymphocyte antigen receptors and thus lack T, B, and NKT cells (83). Since RAG-2 expression is limited to cells of the immune system, the knockout of RAG has no direct effects on nonlymphoid cells undergoing transformation. Thus RAG-2$^{-/-}$ mice provide a suitable system for studying the effects of host immunodeficiency on tumour development. Within 2 years, all of 26 RAG-2$^{-/-}$ mice succumbed to spontaneous epithelial tumours whereas only 5 of 20 wild-type control mice developed (predominantly benign) spontaneous neoplasias. Based on these observations, the concept of immunological anti-tumour surveillance has now been widely accepted.

Basic functions of the immune system

In order to understand how the immune system can protect an organism against cancer, it is necessary to understand the basic principles of immunological recognition of cellular targets. The principal function of the immune system is to protect the organism against the attack of foreign pathogenic organisms, such as parasites, fungi, bacteria and viruses. An efficient destruction of pathogens is essential for survival in any non-sterile environment while harmless environmental influences (such as pollen) should not induce an immune reaction. Tolerance towards the components of the own body is crucial for the prevention of autoimmunity while reactivity against aberrant cells is required for tumour immunosurveillance. Thus the immune system has to discriminate between "self", "altered self" (84) and "non-self" – and, in the case of "non-self", to decide whether it is necessary to launch an attack against the detected antigen.

These complex requirements can only be met by a well-organized ensemble of cells with different specificities. All cells of the immune system derive from the pluripotent haematopoietic stem cells in the bone marrow. In newborns, only the innate immune system is fully evolved whereas the adaptive immune system arises through constant learning from environmental influences.

Innate immunity

The innate immune system consists of anatomical barriers such as skin and mucosae, of soluble factors including lysozyme, interferons and complement and of cellular components, namely granulocytes, macrophages, monocytes, mast cells, natural killer (NK) and γ:δ T cells. These components of the innate immune system can destroy invading pathogens without deliberate immunization or activation. Innate immune cells recognize *pathogen-associated molecular patterns* (PAMPs), i.e. structural motifs that are conserved on pathogenic microorganisms and absent from eukaryotic cells via *pattern recognition receptors* (PRR). Endocytic pattern-recognition receptors (mannose or scavenger receptors) are found on the surface of phagocytes like macrophages or neutrophilic granulocytes. Their activation promotes the engulfment and destruction of microorganisms (85). Signalling PRR include CD14 and the group of *toll-like receptors* (TLR). Importantly, expression of TLR is not restricted to innate immune cells (86).

NK cells (87) are cytotoxic effectors (88) of innate immunity that can lyse tumour cells or virus-infected cells without prior activation (89). However, they also respond to stimuli from antigen-presenting cells sensing pathogens or cellular stress signals (90). NK cells preferentially attack targets lacking the "self" recognition signal provided by expression of the major histocompatibility complex (MHC) class I antigen found on the surface of most nucleated cells (91). Further, they transmit danger signals (92) by the release of inflammatory cytokines, triggering a subsequent, antigen-specific adaptive immune response.

Recent studies have shown that the innate arm of the human immune system may also participate in cancer immunosurveillance. Discrimination between tumour cells and normal cells can be achieved through "induced self-recognition": The activation state of NK cells is regulated by the equilibrium between the input received from stimulatory (NKp, NKG2D) and inhibitory (NKG2A, KIR) NK cell receptors (93). Cellular stress like viral infection or malignant transformation induces MHC class I chain-related proteins A and B (MICA/B) and UL-16 binding proteins (ULBP1-4), all of which are absent from normal somatic cells. Some expression is found on intestinal epithelia, most likely due to the continuous presence of symbiotic bacteria on these tissues. Activation of the NKG2D receptor by these ligands (94, 95) may overcome the inhibitory effect of "self recognition". Activated NK cells would then induce apoptosis in the recognized target cell by releasing cytotoxic granules containing perforin and granzyme B and by upregulating death ligands (88, 96, 97). This NK cell

response may therefore clear malignant cells before they can form a tumour (98). Further, IFN-γ and other inflammatory cytokines are released by activated NK cells. Innate immunity thus provides a strong activation stimulus for the adaptive immune system while specific T cells can build up in the lymph nodes.

Adaptive immunity (I): Lymphocytes

The main features of the adaptive immune system are specificity, diversity, long-term memory and the ability to distinguish between self, altered self and non-self. These attributes are guaranteed by subsets of professional antigen presenting cells (APC) and lymphocytes. In birds, B lymphocytes mature in the *bursa fabriciis*, in humans, they originate (like all other lymphocytes) from lymphoid progenitors in the bone marrow. B cells are responsible for antibody production and thus for humoral immunity. The cellular effectors of the adaptive immune system are T cells.

Antigen recognition by T cells

T cells recognize fragments from proteins degraded in the cytosol or nucleus or generated in the endocytic pathway when these peptides are presented on MHC (major histocompatibility complex) molecules. MHC class I enables the immune system to spot hidden pathogens. Once the proteasome has cleaved proteins into peptide fragments, these are translocated into the lumen of the endoplasmatic reticulum by a specific transporter associated with antigen processing (TAP).

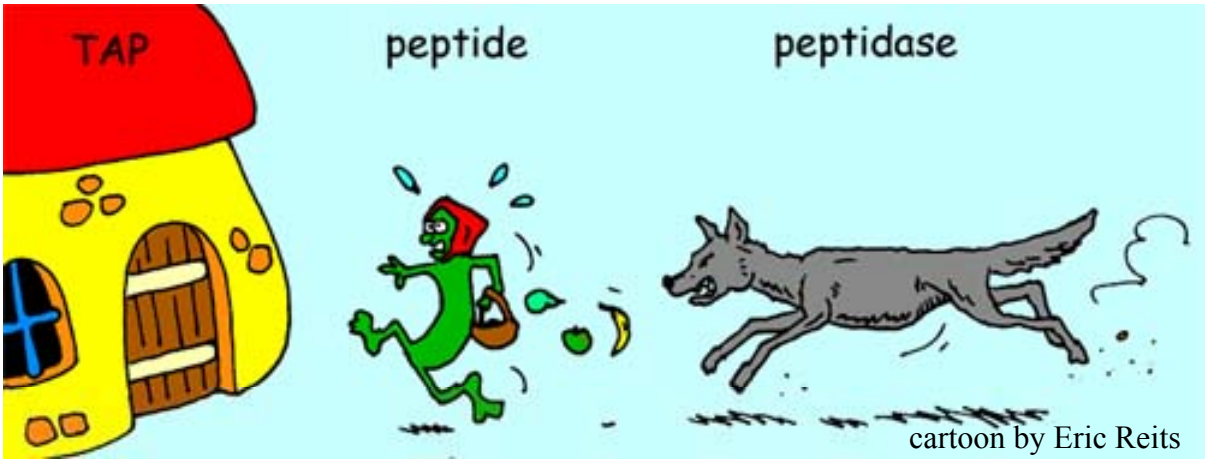

Fig. 1.3: The generation of antigenic peptides for MHC class I. (With kind permission from Eric Reits)

In the endoplasmatic reticulum, peptide binding to the MHC class I complex occurs. This MHC class I complex consists of an α or heavy chain encoded in the MHC and a smaller, non-covalently associated chain, β_2-microglobulin, which is not encoded in the MHC. Upon loading with peptide, the MHC class I complex is transported to the plasma membrane where the antigenic peptide is presented to $CD8^+$ T cells (CTL).

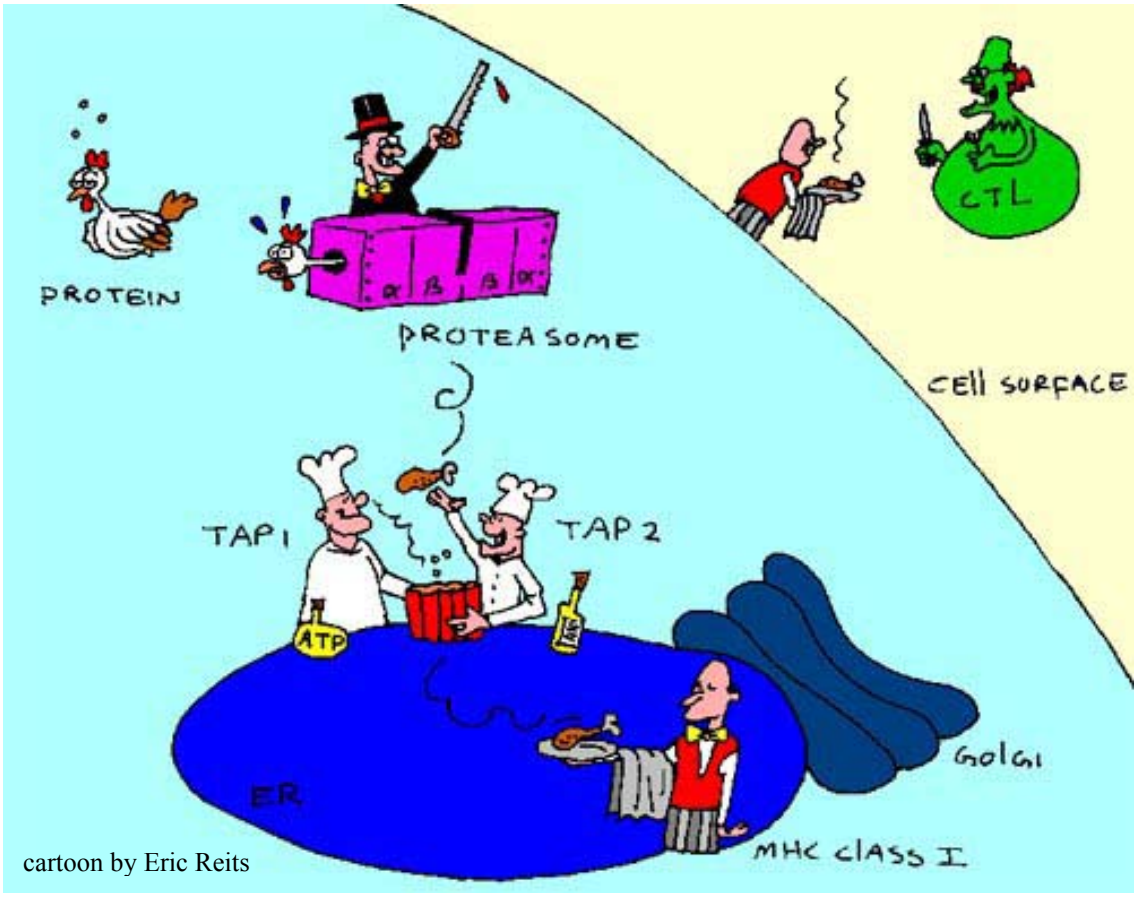

Fig. 1.4: MHC class I loading with antigen. (With kind permission from Eric Reits)

$CD4^+$ T "helper" cells recognize antigens presented on MHC class II. MHC class II epitopes are generated by cathepsin-dependent cleavage of antigens taken up in the endocytotic pathway. Peptide-loading of MHC class II molecules is supported by the chaperone HLA-DM. HLA-DO can interact with HLA-DM and restrict peptide loading of HLA-class II molecules to late endocytic structures (99).

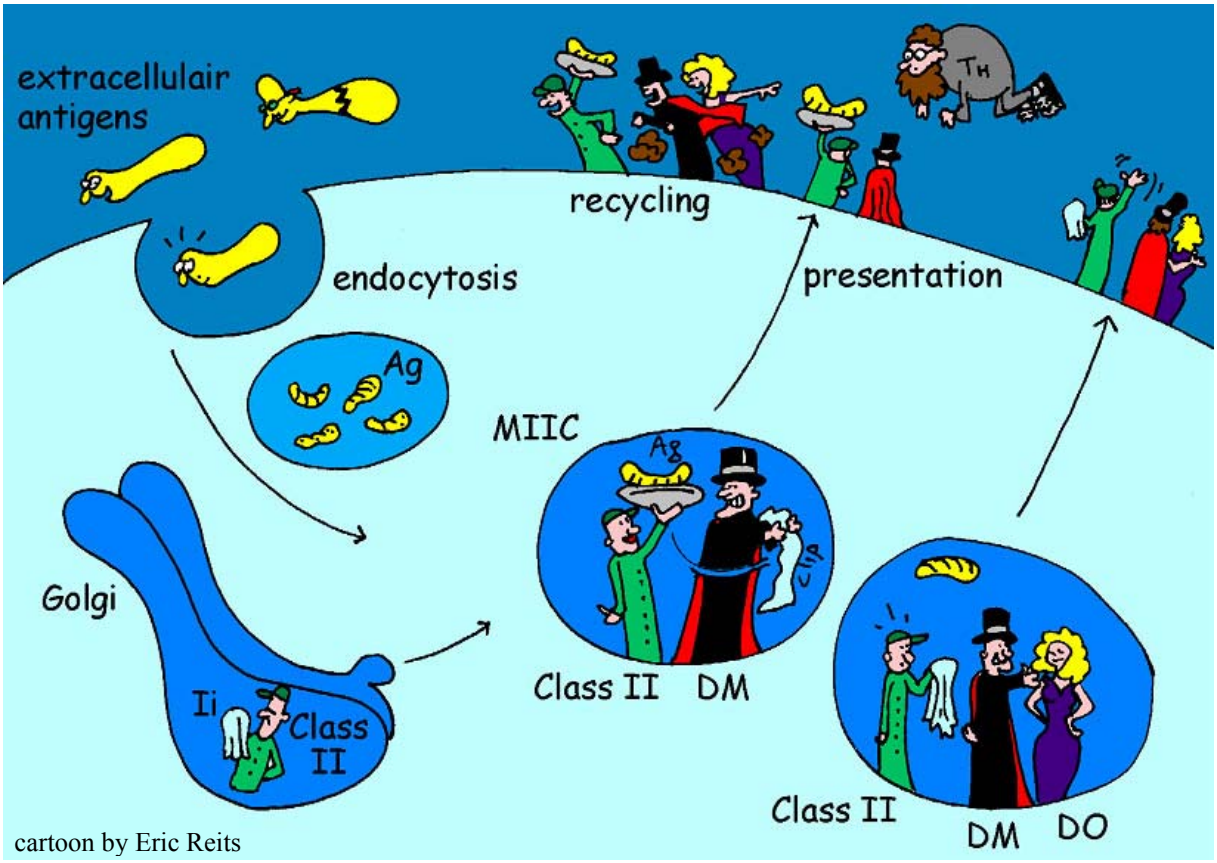

Fig. 1.5. MHC class II loading (with kind permission from Eric Reits).

T cell development

During their development, T cells have to pass through the thymus where a diverse and polymorphic T cell repertoire is generated by random recombination of discrete T cell receptor gene segments. Recombinatorial diversity would allow for a calculated 10^{16} different T cell receptor specificities, even though there are only up to 10^{12} T cells in the human body. This repertoire is then shaped by intrathymic selection for two criteria: Dysfunctional T cells that fail to express a T cell receptor that recognizes self-MHC are deleted during positive selection (100). Cells that react with self-antigens presented in the thymic medulla are eliminated during negative selection (101). The former requirement guarantees that T cells recognize presented peptides only in the context of self-MHC, named "self restriction" (102).

The second selection step secures that autoreactive T cells, i.e. T cells specific for "self"-peptides presented on "self"-MHC, are eliminated, leading to self-tolerance. During this thymic selection process, 96-98% of all T cell precursors are deleted through apoptosis. The selected T cell repertoire still comprises an estimated $2.5x10^7$ T cell clones with different specificities (103). Thus, the naïve T cell repertoire is shaped to show a rather high diversity - at the expense of a limited number of copies of each clone in the body. This highly diverse pool of cells expressing the αβ T cell receptor can be divided in two major subsets defined by expression of the respective co-receptor: $CD8^+$ T cells or cytotoxic T lymphocytes (CTL) can secrete cytotoxic granules and upregulate death ligands when they "see" their cognate peptide (8-10 amino acids) presented in the context of MHC class I (104-106). $CD4^+$ T cells recognize their antigen (15-20 amino acid epitopes) through presentation on MHC class II (107). The cytotoxic potential of $CD4^+$ T cells is restricted to the expression of death ligands (CD95/FasL, Apo2L/TRAIL). The main function of $CD4^+$ "helper" T cells is to secrete cytokines (chemical messengers) that activate and regulate B cells, CTL and APC.

Adaptive immunity (II): antigen-presenting cells

"Nature's best antigen-presenting cells" are the so-called dendritic cells (DC) (108, 109). The two major subsets of DC are myeloid-derived DC (110, 111) and plasmacytoid DC (112). However, it is not yet clear whether they fulfil different functions. Immature DC (and macrophages) can take up antigen via pinocytosis and, more importantly, via receptor-mediated endocytosis of apoptotic and necrotic cellular material. This has been explained by expression of CD36, $\alpha_v\beta_3$- and $\alpha_v\beta_5$-integrins on immature, but not on mature dendritic cells (113). CD36 is a receptor for phosphatidylserine that is normally restricted to the inner leaflet of the cell membrane, but becomes exposed on the outside during apoptosis and late necrosis. In the presence of danger signals (92, 114), DC then maturate. Danger signals can be stimulatory cytokines like TNF-α, TNF-related cellular (or soluble) ligands like CD40L, but also microbial products recognized by TLR that are abundantly expressed on DC (115, 116). Mature DC upregulate their antigen processing machinery (the so-called immunoproteasome) to generate and present antigenic peptides derived from the engulfed material. Interestingly, certain components of the immunoproteasome assemble in an IFN-γ-dependent manner. Thus, the quality and quantity of antigenic peptides generated from a certain target antigen is likely to change in the course of an ongoing immune reaction (117). Presentation of antigens by professional APC has, at least, two distinct advantages. While virtually all somatic cells except testis and some transformed cells express MHC class I and can therefore present

peptide epitopes to CTL, MHC class II is mainly expressed on APC. Therefore the helper T cells required to orchestrate the adaptive immune response are only insufficiently activated by presentation of pathogenic material on non-professional APC. Further, activated DC provide co-stimulation to T cells, mainly via expression of B7.1 (CD80) and B7.2 (CD86) (118).

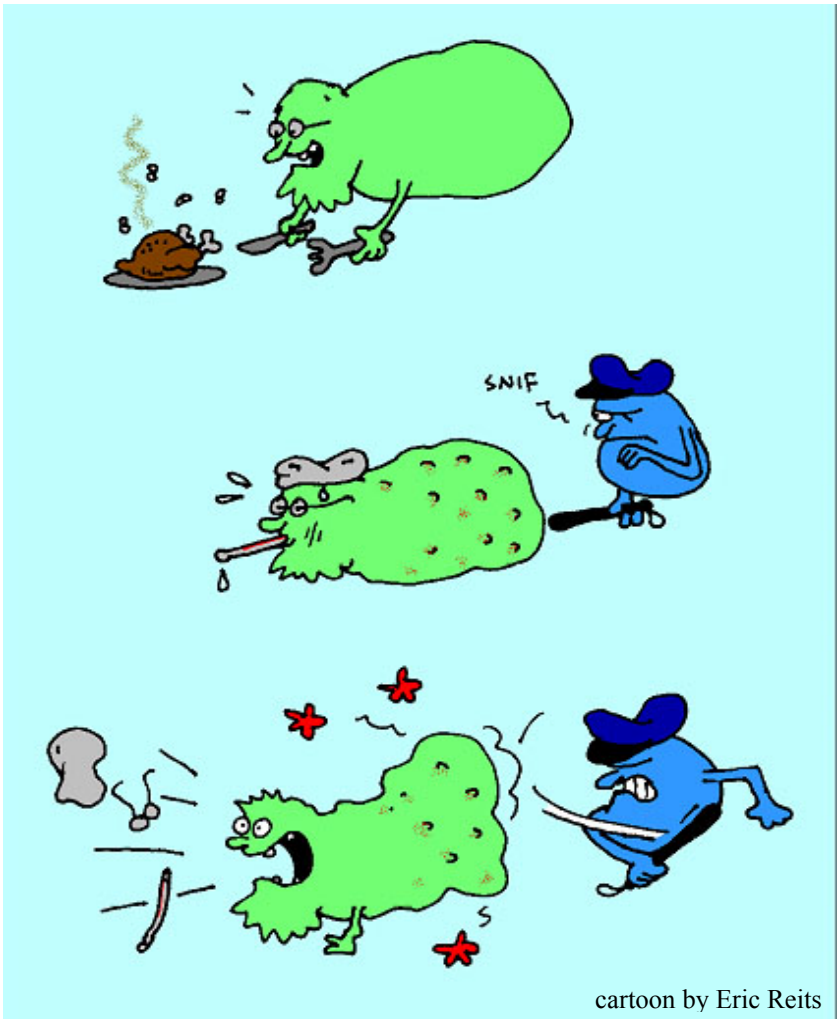

Fig. 1.6. The importance of co-stimulation for T cell activation .

Presentation of antigen on MHC (signal I) in the absence of co-stimulation (signal II) or in the presence of negative co-stimulation (via signals to CTL-A4 or PD-1) (119) renders the T cell bearing the cognate receptor inactive (anergic) (120) and therefore promotes tolerance. On the other hand, T cells sensing their cognate peptide in the presence of appropriate co-stimulation will become fully activated, start to proliferate and attack cells that express the cognate antigen. Once the respective target cells have been eliminated, the majority of the clonally expanded T cells is deleted through apoptosis (30). However, a pool of “memory T cells” is retained that may confer protection against tumour recurrence.

Tumour cell recognition by the adaptive immune system

In order to understand the basis for the recognition of cancer cells by the components of the adaptive immune system it has to be envisaged that cancer is a genetic disease. Cancer cells are "altered self" by virtue of aberrant gene expression. The genetic alterations occurring during tumorigenesis lead to expression of proteins that are not found in normal cells, or not expressed at high levels in normal cells, or only expressed in normal cells at certain stages of development. While overexpression of self may not necessarily be immunogeneic, *de novo* induced tumour-associated antigens (121) should be recognized by the immune system as altered self.

Despite strong evidence supporting the existence of a functional cancer immunosurveillance process (122, 123), immunocompetent individuals still develop cancer. This may be due to cancer cells simply overgrowing the response – or to the outgrowth of tumours that interfere with the cascade from tumour cell recognition to tumour cell elimination. Immunotherapy now aims at overcoming this inhibition (124). In order to devise a rationally designed immunotherapy, the possible shortcomings of the spontaneous anti-tumour response have to be analysed.

Evidently, the concept of anti-cancer immunotherapy requires the respective tumour to be immunogenic. Consequently, identification of tumour antigens that might enable T cell recognition of transformed cells is of major interest. Serological analysis of tumour antigens by recombinant cDNA expression cloning (SEREX) (125) relies on antibody responses in cancer patients and cancer-free individuals. One major shortcoming of SEREX is that responses against post-translationally modified proteins cannot be detected since the method screens for serum reactivity against a bacterially expressed cancer cell cDNA library. Expressing the tumour cell cDNA library in yeast rather than in bacteria may overcome this limitation. A further problem is posed by the assumption that antigens which induce a B cell and $CD4^+$ T cell-dependent antibody response may also be suitable targets for CTL activation. While this seems to be true in some cases, the number of tumour antigens defined by SEREX screening currently greatly exceeds the number of tumour-specific CTL epitopes known.

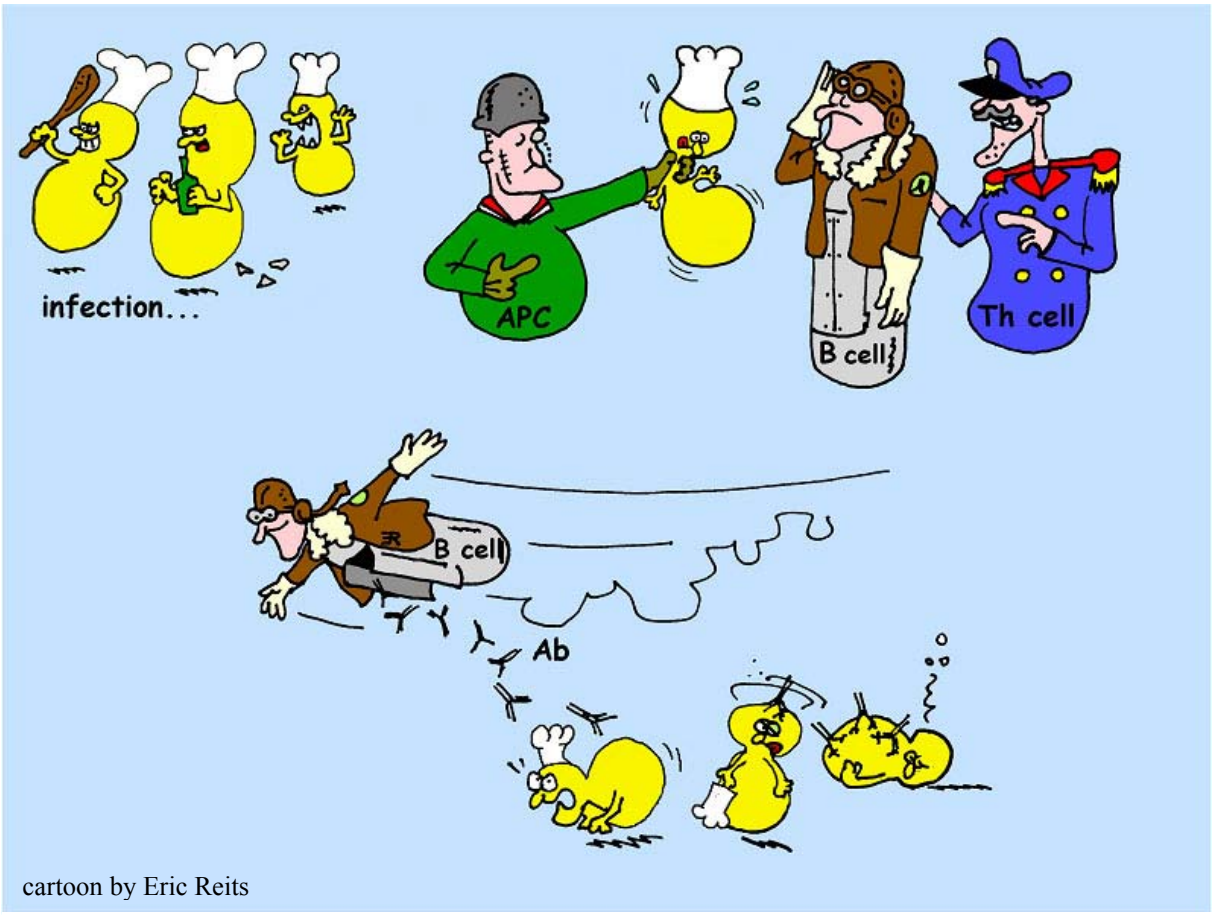

Fig. 1.7. Induction of B cell responses by APC and $CD4^+$ T cells (with kind permission from Eric Reits).

An approach aiming at the direct identification of immunogenic CTL epitopes on tumour cells is being pursued in Tübingen (126): Protein and mRNA from tumour and surrounding tissue are extracted in parallel and MHC complexes from tumour and normal tissue are eluted to determine tumour-specific peptides. Then the immunogenicity of these peptides is determined using autologous PBMC. Further, a gene chip array screens for tumour-specific antigen expression. The results of this array are then correlated with the antigenic peptides found in the respective tumour - and with the individual HLA isotype of the patient. Since each HLA molecule owns its own peptide specificity, the target epitopes that are presented (and recognized) do not only depend on the expression of the respective tumour antigen, but also on the HLA context in which they are presented. Eventually this approach may enable the prediction of an individually-customized selection of antigenic peptides for each tumour patient according to the results of a gene chip array and his or her HLA isotypes.

Immunogenic tumour antigens have now been identified for most human tumour types, including glioma (127). Of the greatest interest are those tumour-associated antigens that are not found in adult normal tissues. Typically these are differentiation antigens (e.g., melanocyte differentiation antigen, Melan-A/MART-1, tyrosinase, gp-100), expressed

exclusively in germ cells in the testis and therefore named “cancer testis” or “cancer germline antigens” (128). However, since germ cells do not express MHC molecules, immunological presentation of these antigens is strictly confined to tumour cells. Further, mutational antigens (e.g., abnormal forms of p53) may be highly tumour-specific. Also overexpressed/amplified antigens (e.g., HER-2/neu, telomerase) and viral antigens (e.g., Epstein Barr virus and human papilloma virus) may be good targets for an anti-tumour immune response, especially when they are both immunogenic and responsible for the malignant phenotype – otherwise the genomic instability of tumour cells (129) may lead to antigen loss, giving rise to new tumour cell variants displaying increased resistance to immune attack. Thus the selection of a good target antigen, or, much better, simultaneous targeting of different tumour antigens, is critical for immunotherapy.

Cancer immunotherapy: current strategies

The problem of defining an optimal antigen is circumvented by approaches that attempt to stimulate anti-tumour immunity in general and do not target specific antigens. This may be achieved by the administration of cytokines (130). Clinical trials have shown some tumour regressions in response to IL-2, GM-CSF, IL-15 and IL-18. However, while cytokines may well be used as adjuvants in combination with other treatments, on their own they only have a modest therapeutic effect.

An innate immune response can be elicited by administration of autologous, irradiated tumour cells that have been engineered to overexpress stimulatory NK cell ligands. These “therapeutic tumour cells” are thought to be lysed by NK cells. Further, this vaccine stimulates NK cells to produce IFN-γ, thus setting up an inflammatory cascade. As a result of these processes, a source of tumour antigens from apoptotic tumour cells becomes available and the adaptive immune system is recruited into the process. For gliomas, this approach has been successfully employed in a mouse model (131). Basically any process that causes limited destruction of tumour material which can then be taken up and transported into the lymph nodes by DC could provide such a trigger to the adaptive immune system. Thus, spontaneous or therapeutically induced apoptosis of tumour cells in conjunction with inflammatory cytokines might also assist in the initiation of an anti-tumour immune response.

However, while most tumours display antigens that could - upon appropriate presentation by DC - initiate an anti-tumour T cell response, antigen presentation is compromised in tumour

patients. Treatment of DC with tumour cell supernatant leads to a decreased expression of the components of the antigen-processing machinery and inhibits maturation and expression of costimulatory molecules. T cells “seeing” their cognate antigen on such immature DC become anergic. Still, infiltration of tumour with DC can be predictive for long-term survival (132), providing a good rationale for a DC-based cancer immunotherapy. Further, a clinical trial using DC with mRNA encoding a tumour antigen (in this case, prostate specific antigen) yielded some clinical responses (133).

Considering the importance of DC maturation states, *ex vivo* antigen loading with apoptotic tumour cells or tumour cell mRNA, followed by cytokine-induced maturation and subsequent adoptive transfer has been chosen for most clinical trials (134-136). However, in the *in vivo* situation, external loading may not be necessary, since a wide variety of antigens is constantly taken up by immature DC. When maturation and activation of immature DC is induced *in vivo* (e.g. by injection of suitable adjuvants), these matured DC migrate towards the lymph nodes where the naturally ingested antigens are presented to T cells. Upon antigen encounter on mature DC, these T cells expand, downregulate their homing receptors CD62L and CCR7 and locate to the tumour. This may have happened in those cancer patients that were treated with bacterial extracts by William Coley in 1893 (72). A molecularly more defined approach is the administration of unmethylated cytidine-phosphate-guanosine dinucleotides in specific sequence contexts. These CpG-oligodeoxynucleotides (CpG-ODN) mimic the immunostimulatory characteristic of bacterial cDNA and provide a strong maturation stimulus for TLR9 (137, 138). While CpG-ODN on their own (139) or as adjuvants (140) can elicit potent anti-tumour responses in mice, they have strong side-effects (141). A safer alternative may be the use of stabilized single-stranded RNA molecules that activate TLR7 (142, 143).

A DC-related approach is based on the use of DC-derived exosomes (DEX) (144). These are small vesicles (60-80 nm) containing MHC class I, MHC class II, hsc73, hsp54 and CD86, among others. DEX can be obtained from leukapheresis and loaded with antigens indirectly via DC or directly with peptides. They can stimulate T cell responses when co-stimulation is provided by some other means. A clinical phase I trial has shown that DEX can be obtained from cancer patients, are generally well tolerated and elicit NK cell-dependent anti-tumour responses. DEX-induced, specific CTL can be found, but show poor killing capacity.

Tumour cell derived exosomes (TEX) exist *in* vivo, too (145). TEX content differs from whole cell protein content in that it is enriched in MHC class I and contain neither MHC class II nor heat shock proteins. Ascites-derived TEX elicit an immune response in otherwise poorly immunogenic mouse models. Also peptide-hsp70-gp96 complexes may be eluted from tumours. Administration of autologous, tumour-derived peptide-heat shock protein complexes (Oncophage) appears to be a safe, but laborious method that induced anti-tumour $CD8^+$ T cell responses in about 50% of the treated patients (146). A major advantage is the large peptide repertoire contained in these complexes as well as in TEX.

Vaccination strategies using distinct antigenic peptides are also being employed. Since natural antigenic peptides are suboptimal immunogens, most studies use adjuvants or modified peptides to enhance the vaccination effect. Further, simultaneous targeting of several antigens could reduce the danger of immune escape by antigen loss (147). Long peptides that require processing by professional APC may have more favourable pharmacokinetics since they cannot be loaded on MHC molecules on non-professional antigen-presenting cells where they would be presented in the absence of co-stimulation and could induce tolerance. Finally, peptides encompassing both MHC class I and MHC class II epitopes have turned out to be most effective in a mouse model, supporting a role for $CD4^+$ helper T cells as well as for CTL (148).

Irrespective of the stimulus provided, any successful immunotherapy must induce a sufficient number of fully activated tumour-specific CTL that go into the tumour. Therefore a monitoring of T cell responses in cancer patients should include the therapeutically induced expansion of antigen-reactive T cells as well as their functional characteristics and localisation. The relative frequency of tumour-specific T cells induced upon vaccination can be analysed by tetramer staining for antigen reactivity (detection limit 1: 5000). In order to distinguish between clonal expansion and high thymic output, the proliferative history of T cells can further be traced by T cell receptor excision circles (TREC) (149) and telomere lengths (150). Functional criteria for tumour-specific CTL are IFN-γ production and lytic activity in response to challenge with antigenic peptide or syngeneic tumour cells.

Cancer immunotherapy: clinical responses

Cancer immunotherapy has already shown that it can be clinically effective, even though this is rather the exception than the rule. This may partly be due to immunotherapy being largely restricted to late-stage cancer patients that have already gone through several (unsuccessful) conventional therapies. Throughout most clinical trials, however, tumour regression is observed in a small but significant proportion of patients that respond to vaccination with selective expansion of antigen-specific CTL whereas regression hardly occurs in the absence of T cell expansion. Surprisingly, data from melanoma patients vaccinated with MAGE3.A1 peptide together with different adjuvants suggest that clinical efficacy does not critically depend on the immunogenicity of the vaccine. Neither does the rate of expansion of peptide-specific CTL clones correlate with clinical outcome. Low-frequency CTL may be sufficient to induce a relevant response. Instead, tumour regression was found to be associated with the presence of a broad repertoire of CTL that did not necessarily recognize the initial vaccine, but displayed lytic activity against autologous tumour cells. Frequency calculations suggested that these T cell clones had been activated *in vivo* after the vaccination (151). Apparently a successful vaccination can induce one or more tumour-specific T cell clones that may destroy some tumour tissue which can then be taken up by professional APCs, most likely by DC. If these can present the ingested antigens appropriately, they will induce responses from new precursors. This is called “epitope spreading” and appears to be crucial for the clinical outcome. However, antigen spreading seems to occur in only ~ 20% of cancer patients. Intriguingly, the clinical efficacy through all immunotherapeutical trials is rather constantly ~ 20% (personal communication from Pierre Coulie, Brussels), suggesting that 80% of non-responders have their immune-response compromised by tumour-derived immunosuppressive factors.

Tolerization of T cells against tumour cells has been observed in melanoma patients that were vaccinated with MART-1 specific peptides (152). Antigen-driven expansion of MART-1-reactive T cells was found in tumour-infiltrated lymph nodes of all responders (T cell frequency: 1,4 ± 3 %). However, these $CD8^+$ T cells contained hardly any perforin or granzyme B and showed no detectable IFN-γ release upon challenge with an antigenic peptide, while responding normally to PMA/ionomycin. Since MART-1-reactive T cells from the peripheral blood of these patients were fully functional, tolerization must have occurred in the metastatic lymph nodes. *In vitro* stimulation with IL-2 could re-functionalize these cells. Other studies also described massive lymphocyte apoptosis in the tumour microenvironment.

While TREC numbers indicated increased T cell proliferation rates, apoptosis (as assessed by AnnnexinV-staining) was dominant, leading to lymphopenia, a symptom that is frequently observed in tumour patients. In particular, 97% of MART1-reactive $CD8^+$ T cells were apoptotic.

Cancer immunoediting and immune escape

These strong immunosuppressive properties of tumour cells have led to the concept of "cancer immunoediting" (153, 154). Tumours are shaped by a constant interaction with the host's immune system. During tumorigenesis the majority of transformed cells may be eliminated by the immune system. However, new variants carrying different mutations are likely to arise. A continuous Darwinian selection process will eventually lead to a population of tumour cell clones with reduced immunogenicity that have a better chance of survival in an immunocompetent host. Finally, genetic and epigenetic alterations will have produced tumour cells that are resistant to immune detection and/or elimination, allowing the tumours to expand and become clinically detectable. Accordingly, tumorigenicity dominates immunogenicity in any clinically manifest tumour. Stimulating the immune system or relieving tumour-dependent immunosuppression may both tilt that balance towards improved tumour cell recognition and elimination.

Glioma-dependent immunosuppression

Glioblastoma is paradigmatic for tumour-induced immunosuppression. Further, glioblastomas grow in the "immune-privileged" context of the brain (155). This "immune privilege" has formerly been explained by the blood-brain barrier that excludes naïve T cells from the brain. However, T cells with an activated phenotype may well enter the inflamed brain (156, 157) where they, surprisingly, secrete neurotrophic factors (158, 159). Since the blood-brain barrier is largely destroyed at least within the bulk tumour mass in glioma patients, it does not preclude anti-tumour immune reactions. The infiltration of malignant gliomas by lymphocytes and macrophages confirms a potential for lymphocyte homing and presentation of processed tumour antigens (155). However, the exact mechanisms for intracerebral antigen presentation remain to be clarified. It is thought to be mediated mainly by microglia, astrocytes, endothelial cells and capillary pericytes and thus substantially different from antigen presentation in the periphery (160). Further, there is no anatomically defined drainage from the brain to the lymph nodes which may explain difficulties in amplifying an initial immune response. Instead, the role of lymphatic drainage may be subserved by the movement of

cerebrospinal and brain fluid (transporting a bulk of potentially antigenic material) to cervical lymph nodes (161-163). Further factors contributing to the immune privilege are a high local concentration of immunosuppressive mediators such as neurotransmitters, neurotrophins and TGF-β (164), the expression of CD95/FasL and Apo2L/TRAIL on residential brain cells that may induce immune cell apoptosis (165) and tolerogenic DC in the brain (166).

The importance of these immunologically unfavourable surroundings is stressed by the fact that gliomas do not metastasize outside the brain. This suggests that outside of their immune-privileged compartment, the immunogenicity of glioma cells can dominate their tumorigenicity. Nevertheless, it has now become clear that antigens in the brain, including those expressed by cerebral malignancies, can induce immune responses *in vivo* (167, 168). Accordingly, glioma infiltration by tumour-reactive T cells has been described (169). Still, the intracerebral tumour-host immune response is in favour of the tumour and immune responses are severely compromised in glioma patients (155). Tumour infiltrating (and peripheral) lymphocytes show high rates of apoptosis. Glioma-infiltrating T cells show delayed hypersensitivity responses, depressed mitogen responsiveness and impaired T cell cytotoxicity. Further, activatory T and NK cell receptors become downregulated even in the peripheral blood of glioma patients (unpublished observation, see section 8). Lymphocytes from healthy donors are similarly compromised in the presence of glioma cells or supernatant, proving that glioma cells exert acute immunosuppression (and that the tumour did not arise opportunistically as a result of impaired immune function). Antigen presentation is also inhibited by glioma cells: glioma cell supernatant strongly inhibits the maturation of dendritic cells (unpublished observation). Further, microglial cells, that might serve as APC in the brain, seem to support rather than suppress glioma growth (170), indicating that they may be functionally controlled by the tumour.

Relieving glioma-induced immunosuppression could tilt the balance of tumour-host immune interactions in favour of the host, especially when a good source of antigen (a defined vaccine or appropriately presented apoptotic tumour cell material) was provided. Therefore a combined approach that induces apoptosis in glioma cells and ameliorates glioma-dependent immunosuppression at the same time might enable a therapeutic T cell response. Tumour-reactive T cells are highly specific, display potent cytotoxicity against their targets (while sparing the surrounding tissue), generate long-term immunological memory and would therefore be eminently suitable for eliminating dispersed glioma cells in the brain.

Experimental overview

Induction of glioma cell death by rescue of mutant p53 using the experimental drug CP-31398

The first parts of the results section of this PhD thesis describe novel strategies for the selective induction of cell death in glioma cells. In this context, the effects of the experimental p53 rescue drug CP-31398 (19) on malignant glioma cells were investigated. Mutational inactivation of the tumour suppressor protein p53 is the most frequent molecular alteration in all human cancers (>50%). Sequencing confirmed that this "guardian of the genome" (171) is mutated in 8/12 human glioma cell lines. Functional p53 senses genotoxic stress that may lead to DNA damage. Through activation of various p53 response genes, including p21 and bax, damaged cells are arrested in G0/1 or G2/M phase. In case of an irreparable cellular damage, p53 initiates apoptosis by transcription-dependent and transcription-independent mechanisms (39, 172-174). Approaches aiming at pharmacological reactivation of mutant p53 should therefore specifically inhibit the growth and survival of cancer cells bearing mutant p53 (175). As will be outlined in **chapter 2**, treatment of malignant glioma cell lines with the experimental p53-rescue drug CP-31398 (19) resulted in the induction of p53-dependent target genes and in caspase-independent cell death displaying some features of apoptosis. However, cell lines harbouring wild-type p53 and $p53^{-/-}$ cell lines were also affected by this reagent, showing that the specificity of the experimental drug needs to be greatly improved. The present work also sought to characterize the undesirable effects of CP-31398. A better understanding of the p53-independent effects of this lead substance may guide the development of compounds hitting solely at p53 – or at p53 and its homologues p63 and p73 (176). In fact, some effects that have been attributed to p53 may rather be mediated by p63 or p73 – and they may be repressed by the presence of an excess of mutant p53. This would explain the surprising induction of p53-like reporter gene activity in a p53 mutant cell line following siRNA-mediated knock-down of mutant p53 (177, 178). Based on this observation, the specificity of a commonly used reporter gene for p53 was investigated **(chapter 3)**. It turned out that p63 or p73 may be even stronger activators of p53-dependent consensus sequences than p53 itself. These data therefore show that much of the literature on p53 may represent an oversimplified picture and should be treated with caution. Still, the quantification of a net effect derived from p53, p63 and p73 may provide a perfectly sensible physiological parameter.

Activating the extrinsic apoptotic pathway via CD40

An alternative to the selective activation of the intrinsic apoptotic pathway would be the selective induction of apoptosis in cancer cells by triggering the extrinsic or death receptor pathway. However, the massive hepatotoxicity of CD95/FasL (179) and the uncertain activity of clinically applicable Apo2L/TRAIL preparations (180) have so far prevented the translation of this approach into the clinic. Strategies to overcome these obstacles involve the regional delivery of Apo2L/TRAIL (181) and the directed killing of target cells via bispecific antibodies (182). Another, presumably safe option might be the triggering of CD40. While CD40 transduces survival signals in somatic cells, induction of apoptosis has been reported exclusively in transformed cell lines (183). Based on this rationale, expression and function of CD40 in malignant glioma cells were investigated **(chapter 4)**.

A further advantage of CD40L as a cancer therapeutic is that it may not only induce apoptosis in tumour cells. CD40L can also promote the priming of a potent antitumour immune response in the presence of apoptotic tumour cells (148, 184). Since glioma-derived inhibitory signals dominate tumour-host interactions in patients, the generation of apoptotic tumour cell material alone will probably be insufficient to trigger a productive anti-tumour immune response. It may further be necessary to provide additional immune stimulation and to overcome glioma-dependent immunosuppression. While a modest enhancement of anti-lymphoma immune responses by CD40L has already been shown in a clinical trial (185), the potential targets for relieving glioma-dependent immunosuppression are less well defined.

Glioma-induced T cell apoptosis via CD70/CD27 as a mechanism for immune escape

In this context, **chapter 5** of the present work describes a novel mechanism by which glioma cells may compromise anti-tumour immunosurveillance. The TNF family member CD70/CD27L (186) had previously thought to be expressed exclusively on activated B and T cells where it provides co-stimulatory signals to T cells and a strong activatory signal to NK cells. However, aberrant expression of CD70 on glioma cells can induce apoptosis of immune effector cells via its receptor CD27 that is constitutively expressed on T cells. Such a dichotomy is characteristic for members of the TNF family: TNF-α can activate NF-κB which then transmits survival signals and protects cells from apoptosis. However, if NF-κB signalling is inhibited, TNF-α becomes a strong pro-apoptotic stimulus (187). Also CD95/FasL can act both as a growth factor (188) and as a death signal (63) in tumour cells. CD40L (CD154) can induce apoptosis exclusively in cancer cells (183) and, apparently,

CD70/CD27L only leads to the apoptotic elimination of non-transformed immune cells when it is expressed in the context of further immune-regulatory molecules expressed by malignant cells. This shows that the physiological outcome of TNF receptor signalling is fine-tuned by further input from related or interfering pathways.

Glioma-dependent immunosuppression through expression of the non-classical MHC class I molecule HLA-G

Some important determinants of the immunosuppressive milieu induced by glioma cells have been defined during the past few years´ research. It has become evident that tumour cells rely on more than one mechanism for securing their escape from the host's immunosurveillance. An interesting candidate molecule that may provide an alternative strategy for the immune escape of malignant is the non-classical MHC class I molecule HLA-G (189). Membrane-bound and soluble HLA-G are physiologically important for mediating foetal semi-allograft tolerance in the placenta. In the pathological condition of a tumour, they are also thought to promote immune tolerance, thus preventing an effective anti-tumour immune response (190). This and the following is work from joint projects with my colleagues where I contributed to both the intellectual framework and its experimental execution. The extent of my contribution is explained in the respective chapter **(chapter 6)**.

Transforming growth factor (TGF)-β as a principal target for the immunotherapy of malignant gliomas

The strongest mediator of glioma-induced immunosuppression is TGF-β. TGF-β_2 was named "glioblastoma-derived immunosuppressive factor" when it was discovered by Adriano Fontana in 1987 (191, 192). TGF-β is the cytokine with the strongest known immunosuppressive activity. While the direct effects of TGF-β on immune effector cells are well-documented (193) and have been further characterized in our group using the novel receptor kinase inhibitor SD-208 **(chapter 7)**, its modulatory influence on other immunological pathways (explicitly, on the regulation of the expression of NKG2D and its ligands) is only now being recognized **(chapter 8)** (194). An intriguing aspect of these novel findings is that anti-TGF-β strategies do not only improve the compromised immune responses in the presence of glioma cells, but have also strong effects on growth, migration and invasion of glioma cells. Antagonizing TGF-β by RNA interference (177, 178) also results in a massive upregulation of activatory NK and costimulatory T cell ligands on the surface of glioma cells, adding a further rationale to the concept of an anti-TGF-β glioma

therapy. By targeting TGF-β the relief of glioma-induced immunosuppression could be combined with the active induction of NK and T cell responses against cancer cells. Given the current lack of well-defined CTL epitopes for a peptide vaccination against glioma cells, this strategy may represent the most promising option for an immunotherapy of human glioblastoma.

II. CP-31398, a novel p53-stabilizing agent, induces p53-dependent and p53-independent glioma cell death

A related manuscript has been published in Oncogene. 2003 Nov 13;22(51):8233-45.

Sequencing of p53 for this project (Table 2.1) was performed by Dr. Hiroko Ohgaki and Mrs. Marie-Anne Camus (International Agency for Research on Cancer, F-69372 Lyon Cedex 08, France). Thanks also go to Dr. Farzan Rastinejad (Cancer Drug Discovery Group, Pfizer Global Research and Development, Eastern Point Road, Groton, CT 06340) who discovered CP-31398. He did not only supply CP-31398, but also gave helpful advice during many stages of this project.

Introduction

Mutational inactivation of p53 is one of the most common genetic alterations in human cancers. The p53 gene encodes a 53 kD transcription factor which appears to require the integrity of at least three functional domains to exert its full transcriptional activity: the aminoterminal transcription activation domain, the central DNA binding domain and the carboxyterminal tetramerization/regulatory domain. The vast majority of mutations in the p53 gene in human cancers (>95%) affect the DNA binding domain (195). Whether functions other than transcriptional regulation are exerted by the wild-type p53 protein under physiological conditions has long remained controversial. Recent findings indicate that p53 can induce apoptosis in the absence of transcription, but still dependent on the functional integrity of the DNA binding domain (172, 173).

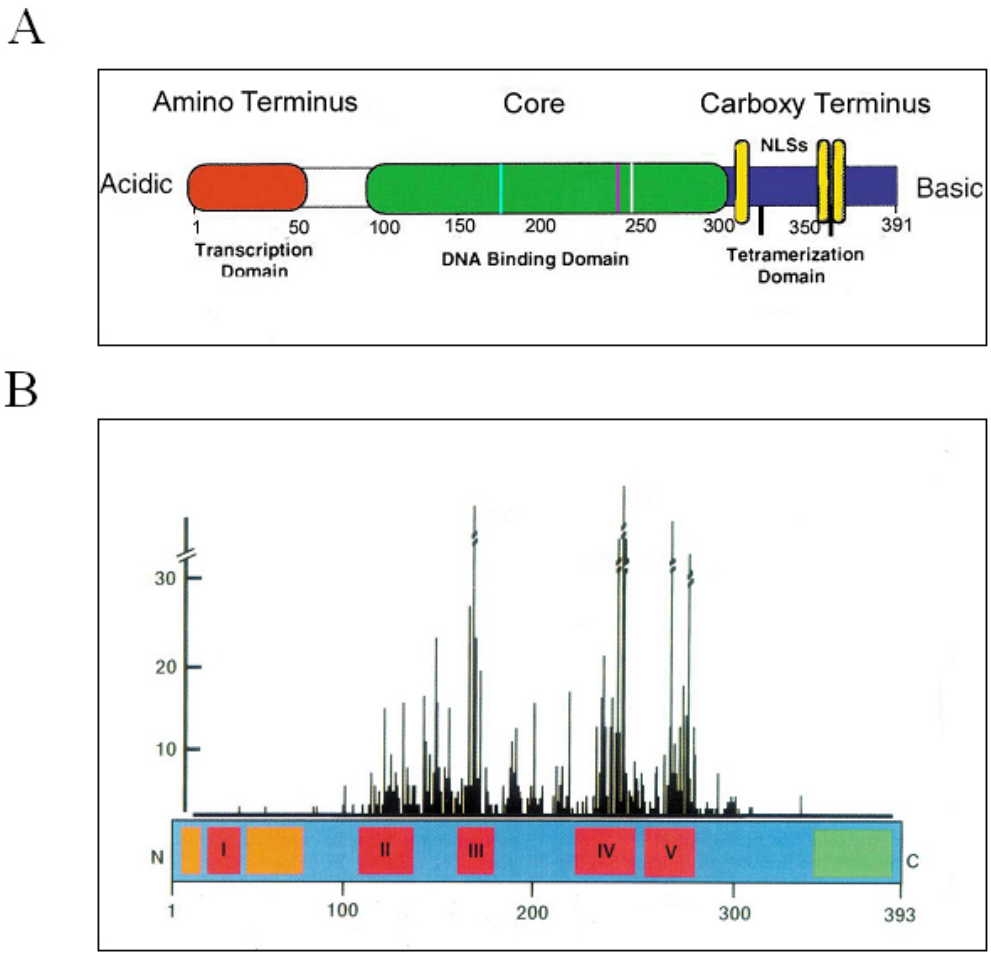

Fig. 2.1: **p53 – domains and mutational frequency.** A. Schematic representation of the different domains of p53. B. The relative positional frequencies of p53 mutations found in cancer cell lines. (Diagrams modified from Cho et al., 1994)

The DNA binding domain of p53 is conformationally labile and is further destabilized in the majority of cancer-derived mutant p53 proteins. A novel type of anticancer agents which promote the proper folding of mutant p53 protein has recently been described (19). It is assumed that these agents act in a chaperone-like manner on newly synthesized p53 to promote and maintain a correctly folded conformation. The effects of one such compound, the styrylquinazoline CP-31398, were studied here in a panel of human malignant glioma cell lines with various genetic alterations of the p53 genes (Table 1).

Table 2.1. **Human malignant glioma cell lines: genetic p53 status, p53 reporter activity and sensitivity to CP-31398.**

Cell line	Genetic p53 status[1]	p53 reporter activity [%] (196)	CP-31398 sensitivity (EC_{50}, 24 h) [μM]	CP-31398 sensitivity (EC_{50}, 4 h pulse) [μM]
LN-18	238 Cys→Ser	1 (n.s.)[2]	12.6 ± 2.1	21.8 ± 3.5
U138MG	273 Arg→His heterozygous	9	19.2 ± 2.6	37.5 ± 3.8
U87MG	wild-type	36	11.2 ± 1.4	32.0 ± 2.1
LN-428	173 Val→Met 282 Arg→Trp	0	17.9 ± 2.3	26.3 ± 2.6
D247MG	wild-type	77	12.6 ± 2.0	34.2 ± 3.1
T98G	237 Met→Ile	0	10.1 ± 1.9	22.8 ± 2.5
LN-319	175 Arg→His	1 (n.s.)	26 ± 3.4	34.7± 1.8
LN-229	wild-type	100	14.1 ± 2.2	38.2 ± 4.2
A172	wild-type	25	22.2 ± 2.6	35.1 ± 1.8
U251MG	273 Arg→His homozygous	0	16.8 ± 2.5	29.4 ± 3.3
U373MG	273 Arg→His homozygous	0	12.8 ± 1.7	31.6 ± 3.5
LN-308	deletion	0	36 ± 4.2	> 120

[1]see Methods; data correspond in essence to (17) and (15); however, LN-229 cells used here are homozygous wild-type (not heterozygous mutant) and U138MG cells used here are heterozygous with a mutation not previously described. [2]n.s., not significant

Materials and Methods

Materials and cell lines. CP-31398-01 (Lot #035035-106-02), prepared as described (19), was dissolved directly in medium. zVAD-fmk, obtained from Bachem (Heidelberg, Germany), was dissolved in dimethylsulfoxide (DMSO). AnxV-FITC was obtained from Pharmingen (Heidelberg, Germany), Fluo-3AM from Biorad (Munich, Germany). CHX, PI, ATA, PBN, 2′,7′-dichlorodihydrofluorescein diacetate (DCFH-DA) and all other reagents, unless indicated otherwise, were purchased from Sigma (St. Louis, MO). zFA-fmk was from ESP (Livermore, CA), ALLN from Calbiochem (San Diego, CA), CA-074ME from Peptide Institute Inc. (Osaka, Japan). The human malignant glioma cell lines, kindly provided by Dr. N. de Tribolet (Lausanne, Switzerland), have been characterized (15, 197). Unlike LN-229 cells grown in other laboratories, the LN-229 cell line used for this study still harbours wild-type p53 (see Table 2.1). The cells were cultured in Dulbecco`s modified Eagle medium (DMEM) containing 10% foetal calf serum, 2 mM glutamine and penicillin (100 IU/ml)/streptomycin (100 µg/ml). Viable cell counts were obtained by crystal violet staining. For the determination of EC_{50} values, the drug effects were monitored in serial dilutions (1:2) over a broad range of concentrations. Rat primary cerebellar granule neurons were prepared as described previously (198).

p53 sequencing. Prescreening for mutations by polymerase chain reaction (PCR) and single strand conformational polymorphism (SSCP) analysis was carried out on exons 5-8 of the p53 gene (14). Samples showing mobility shifts on SSCP were further analyzed by direct DNA sequencing. After PCR amplification with the same set of primers as used for SSCP, the PCR products were sequenced on a Genetic Analyzer (ABI PRISM^{TM} 310, Perkin-Elmer Biosystems, Shelton, CT) using an ABI PRISM BigDye Terminator Cycle Sequencing Ready Reaction Kit. Primers for DNA sequencing were as follows: 5′-TCT GTC TCC TTC CTC TTC CTA C-3′ (sense) and 5′-AAC CAG CCC TGT CGT CTC TCC A-3′ (antisense) for exon 5; 5′-ACA GGG CTG GTT GCC CAG GGT-3′ (sense) and 5′-AGT TGC AAA CCA GAC CTC-3′ (antisense) for exon 6; 5′-TGC CAC AGG TCT CCC CAA GG-3′ (sense) and 5′-GGG TCA GAG GCA AGC AGA GG-3′ (antisense) for exon 7; 5′-TCC TTA CTG CCT CTT GCT TC-3′ (sense) and 5′-TCT CCT CCA CCG CTT CTT GT-3′ (antisense) for exon 8.

p53 silencing. The p53 specific oligonucleotide sequences GATCCCC**GACTCCAG TGGTAATCTAC**ttcaagaga**GTAGATTACCACTGGAGTC**TTTTTGGAAA and TCGATTTCCAAAAA**GACTCCAGTGGTAATCTAC**tctcttgaa**GTAGATTACCAC TGGAGTC**GGG were obtained from Metabion (Munich, Germany) and cloned into Bgl II and Sal I-sites of the pSUPER vector (177), generously provided by Dr. Reuven Agami (Amsterdam, NL). The p53-specific parts of the sequence are depicted in bold letters and underlined. The resulting pSUPERp53 plasmid was stably cotransfected (10:1) with a pBABEpuro (199) plasmid and puromycin-resistant bulk transfectants were generated. Control transfectants were generated by co-transfecting pSUPER together with pBABEpuro**.**

p53 and NF-κB *reporter assay.* The cells were transfected with the PathDetect® p53 and NF-κB cis-reporter gene plasmids (#219092 and #219077, Stratagene) using FuGene (Roche, Mannheim, Germany) (196). The p53-responsive enhancer is $(TGCCTGGACTTGCCTGG)_{15}$, the NF-κB–responsive element is $(TGGGGACTTTC CGC)_5$. Cotransfection with pFC-p53 which encodes human wild-type p53 was used as a positive control. The p53 null cell line, LN-308, was included as a negative control in all experiments. At 24 h after transfection, CP-31398 was added to some samples. Another 6 h later, the cells were washed and lysed using Reporter Lysis Buffer (Promega, Madison, WI). Following one freeze-thaw cycle, the lysates were transferred to a LumiNuncTM plate (Nunc, Roskilde, Denmark), Luciferase assay substrate (100 µl, Promega) was added automatically, and the luminescence was measured in a LumimatPlus (EG&G Berthold, Pforzheim, Germany). The background was subtracted from all values.

Immunoblot analysis. The general procedure has been described (200). The cells were untreated or treated with CP-31398 as indicated and lysed. Soluble protein levels were analysed by immunoblot using 20 µg of protein per lane separated on 10-12% acrylamide gels (Biorad, Munich, Germany). After transfer to a nitrocellulose membrane, the blots were pretreated for 2 h with phosphate buffered saline (PBS) containing 5% skim milk and 0.05% Tween 20 and then incubated overnight at 4°C with the following antibodies: murine anti-human p53 monoclonal antibody Bp53-12 (2 µg/ml), murine anti-mammalian p53 monoclonal antibody Pab240 (for the detection of

murine p53^{V135A}) (2 µg/ml), rabbit anti-human p21 polyclonal antibody C-19 (2 µg/ml), rabbit anti-mammalian Bax polyclonal antibody N-20 (1 µg/ml), goat anti-mammalian β-actin polyclonal antibody I-19 (1 µg/ml), mouse anti-mammalian Mdm2 monoclonal antibody SMP14 (1 µg/ml), mouse anti-human Bcl-2 antibody 100 (2 µg/ml), rabbit anti-human bak polyclonal antibody G-23 (0.5 µg/ml), rabbit anti-mammalian caspase 8 polyclonal antibody p20 (0.5 µg/ml) (all from Santa Cruz, Santa Cruz, CA), mouse anti-mammalian Bcl-x_L monoclonal antibody 2H12 (2 µg/ml) (Pharmingen, Heidelberg, Germany), and mouse anti-human caspase 3 C31720 (1 µg/ml) (Transduction Laboratories, Lexington, KY). Mouse anti-human caspase 7 (clone 7-1-10) and caspase 9 (clone 2-22) antibodies were generous gifts of Y. Lazebnik (Cold Spring Harbor, NY). Visualization of protein bands was accomplished using horseradish peroxidase (HRP)-coupled IgG secondary antibody (Sigma) and enhanced chemiluminescence (ECL) (Amersham, Braunschweig, Germany). Quantification was performed by multiplying the respective signal area with its mean intensity using Corel Photo-Paint 11 software (Corel Corporation, Ottawa, CA).

Northern blot analysis. Denatured total RNA (10 µg) was loaded on a 1% agarose gel containing 6.7% formaldehyde. The RNA was separated at 100 V, transferred to a Hybond N+ membrane (Amersham, Freiburg, Germany) using capillary blotting and cross-linked in a UV stratalinker 1800 (Stratagene, La Jolla, CA) at 1200 J. Methylene blue staining was performed as a loading control. The membrane was preincubated for 2 h in Church buffer at 65°C. The probes were constructed by isolating the respective cDNA sequences from expression plasmids. A cDNA encoding PUMA was generously provided by Dr. B. Vogelstein (Baltimore, MD), the NOXA cDNA was a generous gift of Dr. E. Oda (Tokyo, Japan). The respective full-length cDNAs were purified by gel extraction (Qiagen, Hilden, Germany) and labeled using 5 µl (~1.6 Mbq) dCTP and the Rediprime II random labelling system (Amersham). Filters were hybridized overnight at 65°C in a hybridization oven with a rotisserie device using Church-buffer. Binding of radioactive probes was visualized using a PhosphoImager (FujiBasReader 1500, Fuji, Kangawa, Japan) and quantified using TINA software (Fuji). Loading was controlled by assessing ß-actin mRNA expression.

Flow cytometry. For cell cycle analysis, the glioma cells were treated with CP-31398 as indicated, harvested, fixed and permeabilized overnight in ice-cold 70% ethanol

(Merck, Darmstadt, Germany). The cells were washed twice with PBS. RNA was digested with RNase A (Gibco Life Technologies, Paisley, GB). The DNA was stained with PI (50 µg/ml). Fluorescence was recorded on channel Fl-2A in a FACScalibur (Becton Dickinson, Heidelberg, Germany). Instrument settings were adjusted to move the G1 peak to 200 relative fluorescence units. Cells to the left of this peak appear to have a DNA content below 2n, indicative of cell death. Aggregated cells were detected in channel Fl-2W and gated out. 10,000 events per condition were recorded. Evidence for apoptosis was also obtained by AnxV-FITC staining which measures the exposure of phophatidylserine on the cell membrane. The cells were collected, washed with PBS and resuspended in a buffer containing 10 mM HEPES/NaOH, pH 7.4, 140 mM NaCl and 2.5 mM $CaCl_2$. AnxV-FITC (1:100) and PI (50 µg/ml) were added.

Free radical formation. The cells (2 x 10^5/well) were seeded in 6 well plates, adhered overnight and treated with CP-31398 or ethacrinic acid as a positive control. A solution of DCFH-DA in DMSO (stock: 2 mM) was added to a final concentration of 5 µM. After 15 min the cells were washed with ice-cold PBS, trypsinized and washed again with cold medium. The fluorescence originating from intracellular DCF (the oxidation product of DCFH-DA) was measured in channel Fl-1H in a Becton Dickinson FACScalibur. Dead cells were excluded by simultaneous staining with PI (50 µg/ml).

Cell-free peroxide assay. CP-31398 was co-incubated in serum-free medium with serum, Fe^{2+} or PBN. Cell culture supernatant containing CP-31398 was also examined. The samples (20 µl) were collected at various times and ongoing reactions were stopped by addition of 180 µl 25 mM H_2SO_4. After a total incubation period of 30 min 200 µl reaction mixture containing 0.5 mM $(NH_4)_2Fe(SO_4)_2$, 200 µM xylenol orange and 200 µM sorbitol in 25 mM H_2SO_4 were added to each well of the microtiter plate. The absorption at 540 nm was determined using a microtiter plate reader (Titertek Multiscan MCC, Flow Laboratories/ICN, Eschwege, Germany) 45 min later and compared with the absorbance read at standard concentrations of the peroxides (201, 202).

Calcium assay. Fluo-3AM was reconstituted in DMSO and a 1:500 dilution was prepared in serum-free medium. Treated cells were washed and loaded with Fluo-3 AM for 30 min while still adherent. After further washing the cells were detached,

resuspended in PBS and analysed by flow cytometry. The signal from Fluo-3 bound to Ca^{2+} was detected in channel Fl-1H. Dead cells were gated out by PI (double) staining.

DEVD-cleaving caspase activity. The cells (0.5×10^4) were seeded in 96 well plates, treated as indicated, lysed in 25 mM TrisHCl, pH 8.0, 60 mM NaCl, 2.5 mM EDTA, 0.25% Nonidet-P40 for 10 min, and DEVD-amc was added at 12.5 μM. Caspase activity was assessed by fluorescence using a Millipore fluorimeter at 360 nm excitation and 480 nm emission wave lengths.

Statistical analysis. Data are representative of experiments performed three times with similar results. Viability studies were performed using triplicate wells. Significance was assessed by t-test ($p<0.05$) or covariance analysis (ANCOVA).

Results

CP-31398 is cytotoxic to human malignant glioma cell lines

Light microscopic monitoring revealed that CP-31398-treated cells from all glioma cell lines rounded up and detached from the tissue culture plates. Trypan blue staining confirmed that the detached cells were dead. Cell death rather than inhibition of proliferation became also apparent on flow cytometry which showed accumulation of cell remnants in the sub-G0/1 peak (Fig. 2.2A). There was a dramatic loss of cells in the G2/M phase, suggesting that death occurred out of S-phase. However, synchronisation of LN-229 cells in S-phase by aphidicolin did not affect cell death induced by CP-31398 (data not shown). Representative concentration response curves for LN-18, U87MG, LN-229 and LN-308 cells are shown in Fig. 2.2B.

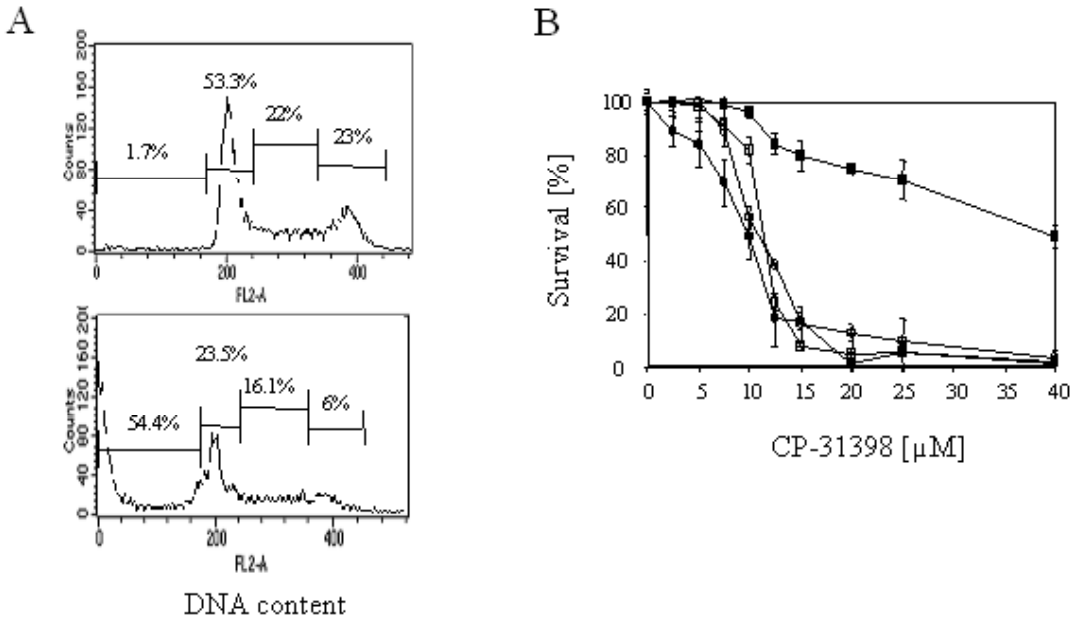

Fig. 2.2. **CP-31398 is cytotoxic to human glioma cell lines.** A. LN-18 cells were untreated (top) or treated with CP-31398 (9 µM) for 24 h (bottom) and studied by flow cytometry. B. The glioma cells (LN-18, filled circles; U87MG; open circles, dashed lines; LN-229, open squares, dashed lines; LN-308, filled squares) were treated with CP-31398 for 24 h. Survival was assessed by crystal violet staining. All crystal violet data are expressed as mean percentages of survival and standard error of the mean (SEM, n=3).

Next, the mode of cell death induced by CP-31398 was explored. p53 is supposed to induce apoptosis rather than necrosis, but cell death induced by a synthetic super-p53, CTS-1, was caspase-independent in glioma cells (203). Flow cytometry for annexinV-FITC/propidium iodide (AnxV-FITC/PI) labelling revealed the exposure of phosphatidylserine on the cell membrane preceding the loss of membrane integrity detected by PI uptake (Fig. 2.3). Early apoptotic cells are AnxV-FITC-positive, but PI-negative, and therefore move to the lower right quadrant.

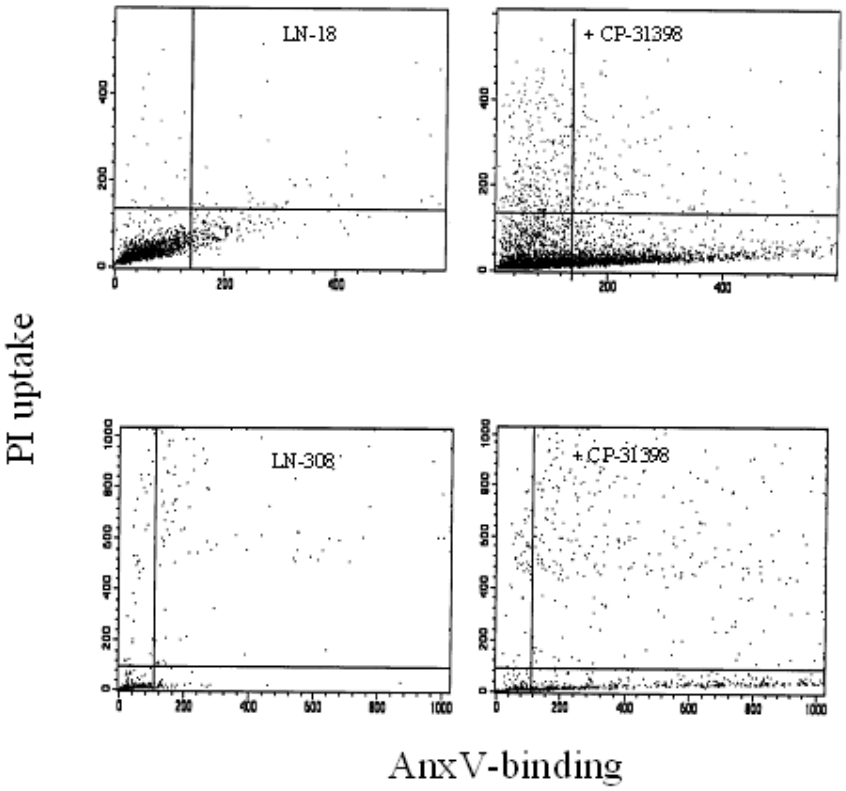

Fig. 2.3. **CP-31398-induced cell death has features of apoptosis.** LN-18 or LN-308 cells were left untreated (left) or treated for 16 h with CP-31398 (12 μM) (right) and analysed for AnxV-FITC binding and PI uptake by flow cytometry. Similar results were obtained for U87MG and T98G cells (data not shown).

In contrast, almost no cells are PI-positive, but AnxV-negative (left upper quadrant). Asp-Glu-Val-Asp-7-amino-4-methylcoumarin (DEVD-amc) cleavage assays showed that even high concentrations of CP-31398 did not significantly increase caspase activity from baseline, as assessed in LN-18, T98G, LN-229 and LN-308 cells at 6 or 18 h. In contrast, CD95 ligand (CD95L), as a positive control (204), induced prominent DEVD-amc cleavage in these cells (Fig. 2.4A). Accordingly, CD95L induced massive processing of caspases 3, 7, 8 and 9, whereas no effects of CP-31398 on caspase 8 and 9 levels were observed in any cell line. In LN-18 and U87MG cells, a slight decrease in the levels of pro-caspase 3 was observed when the cells were treated with 36 μM of CP-31398 for 16 h, and these conditions also induced cleavage of caspase 7 (Fig. 2.4B). However, the concentrations required for caspase cleavage were far above the EC_{50} values for these cell lines (Table 2.1). Further, the time-point of caspase activation seemed to lie behind the point of commitment for cell death, suggesting that caspase activation is not essential for CP-31398-induced cell death. Accordingly, N-tert-butoxy-carbonyl-Val-Ala-DL-Asp-fluoromethylketone (zVAD-fmk), a broad spectrum caspase inhibitor previously shown to inhibit CD95L- and drug-induced apoptosis in glioma cells (204), did not significantly modulate CP-31398 cytotoxicity in LN-18, LN-229, T98G, U87MG, U251MG, U373MG or LN-308 cells at concentrations up to 100 μM (Fig. 2.4C, data not shown). The viral preferential caspase 1 and 8 inhibitor, crm-A, which abrogates CD95-mediated apoptosis, had no effect on CP-31398 cytotoxicity either (data not shown). Neither had inhibition of calpains by N-tert-butoxy-carbonyl-Phe-Ala-fluoromethylketone (zFA-fmk), N-acetyl-Leu-Leu-Nle-CHO (ALLN) or L-3-trans-(prolylcarbamoyl)oxirane-2-carbonyl)-L-isoleucyl-L-proline methyl ester (CA-074Me). Although no evidence was obtained for a role of caspases in CP-31398-induced cell death, cytochrome c was released in LN-18, U87MG and T98G cells, but not in LN-308 cells, in response to CP-31398 (Fig. 2.4D, data not shown). It was also asked whether the ectopic expression of a bcl-x_L transgene inhibited CP-31398-induced cell death. While T98G and LN-229 cells transfected with a bcl-x_L transgene acquired resistance to CD95L-mediated apoptosis (61) (data not shown), Bcl-x_L did not inhibit CP-31398 cytotoxicity (Fig. 2.4E). Immunoblot accordingly showed that cytochrome c release induced by CP-31398 was insensitive to Bcl-x_L whereas cytochrome c release induced by CD95L was blocked (data not shown).

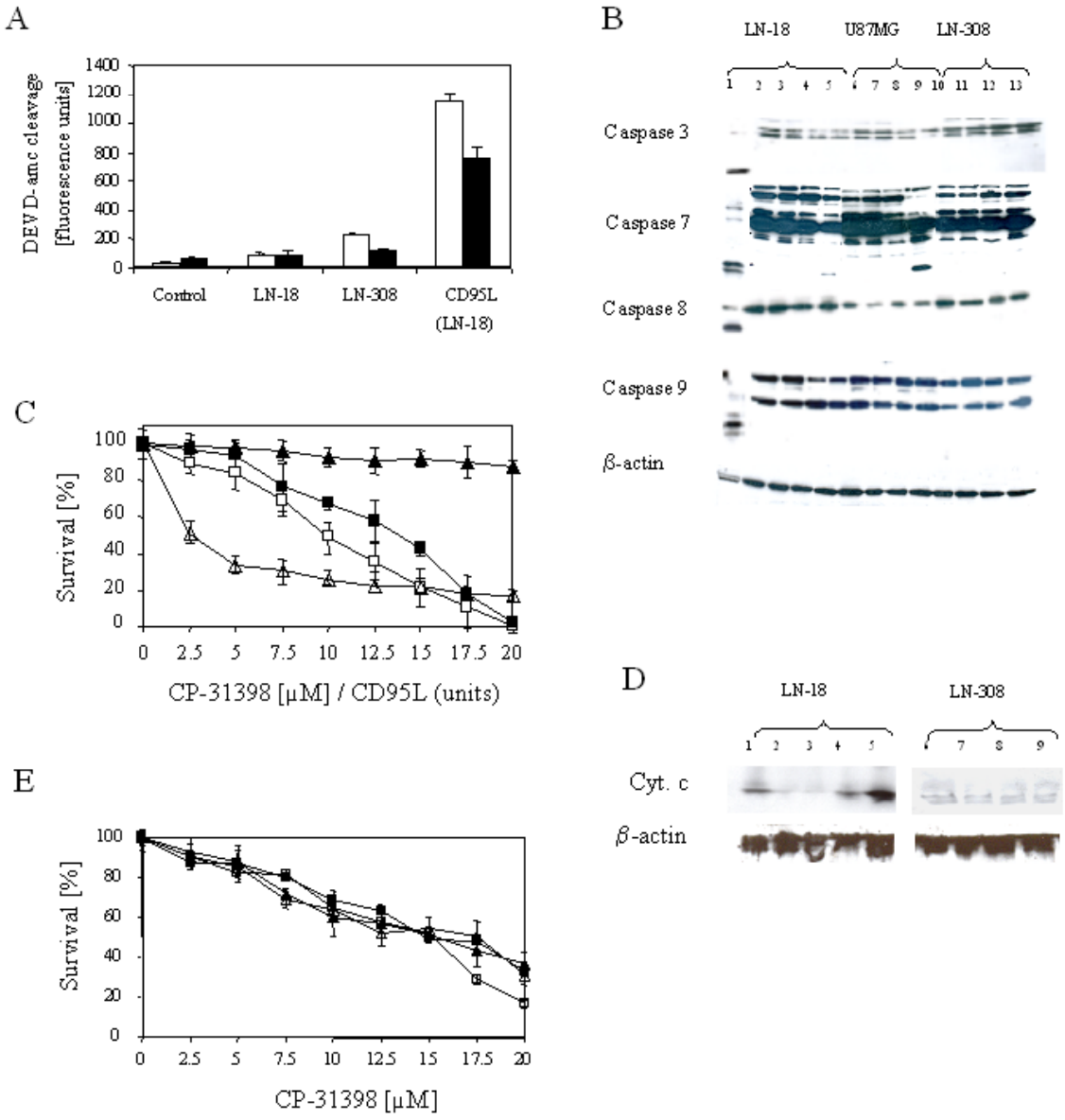

Fig. 2.4. **CP-31398-induced glioma cell death is largely caspase-independent.** A. DEVD-amc cleavage was assessed at 6 (open bars) and 18 h (filled bars) after treatment with CP-31398 at 12 μM (LN-18) or 36 μM (LN-308). CD95L (10 U/ml) in LN-18 cells was used as a positive control. B. LN-18, U87MG and LN-308 cells were treated for 16 h with CP-31398 (lanes 2-5: LN-18, lanes: 6-9 U87MG, lanes 10-13: LN-308, all treated with 0, 9, 18, 36 μM CP-31398). Lane 1 shows LN-18 cells treated with CD95L (10 U/ml) for 6 h as a positive control. Caspase cleavage was assessed by immunoblot. C. LN-18 cells were treated for 24 h with increasing concentrations of CP-31398 (squares) or CD95L (triangles) in the absence (open symbols) or presence (filled symbols) of zVAD-fmk (100 μM). D. LN-18 cells were treated for 6 h with CD95L (lane 1, 10 U/ml) or CP-31398 (lanes 2-5: 0, 9, 18, 36 μM). In lanes 6-9, LN-308 cells were treated with CP-31398 (0, 9, 18, 36 μM). Cytosolic fractions were assessed for cytochrome c (Cyt. c) and β-actin content by immunoblot. E. T98G neo (open squares), T98G Bcl-x_L (filled squares), LN-229 neo (open triangles) or LN-229 Bcl-x_L (filled triangles) cells were treated with CP-31398 for 24 h. Survival in C and E were assessed as in Fig. 2.2B.

Kinetic dissociation of p53-dependent and p53-independent effects of CP-31398

Cytotoxicity data for CP-31398 in all glioma cell lines are summarized in Table 1. The EC_{50} for the induction of cell death at 24 h ranged from 10-36 µM. Prolonged exposure for 72 h did not significantly alter these data except for a reduction of the EC_{50} to 19 µM in LN-308 cells ($p<0.05$, t-test). There was no correlation between the doubling times and the sensitivity to CP-31398 ($p>0.05$). Neither was there a difference in the sensitivity to CP-31398 of p53 mutant and p53 wild-type cell lines, defined genetically or functionally (Table 1). Also the expression level of p53 as determined by immunoblot and densitometric normalization to ß-Actin did not correlate with the sensitivity towards CP-31398-induced cell death. Although LN-308 cells, which lack p53 protein altogether, were the most resistant cell line, these cells were not fully resistant to CP-31398, clearly indicating that CP-31398 triggers a p53-independent cell death pathway. To confirm that part of the cytotoxicity of CP-31398 depends on p53, p53 synthesis was knocked down in the p53 wild-type cell line, LN-229, by siRNA technology. Transfection with pSUPERp53 encoding p53 siRNA (177) resulted in a massive down-regulation of p53 reporter gene activity (Fig. 2.5A) and protein level (Fig. 2.5B). No changes were observed in p63 or p73 protein levels (data not shown). Both assays showed that the suppression reached more than 98%. The p53-depleted cells were protected when exposed to moderate concentrations of CP-31398 (≤ 16 µM) for 24 h whereas no difference in sensitivity was observed at higher concentrations (Fig 2.5C). This apparently low specificity appeared to be difficult to reconcile with the reported (19) safety and anti-tumour specificity of the agent in animals.

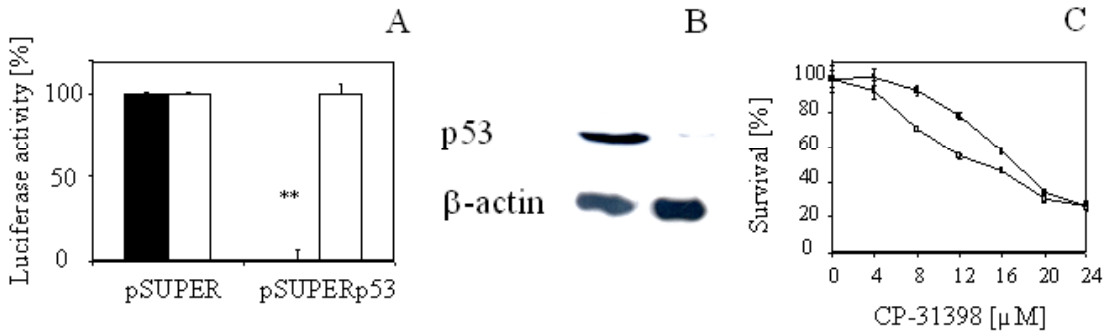

Fig. 2.5. **Knockdown of p53 in LN-229 cells.** A,B. LN-229 sublines bearing either a pSUPER control plasmid (left lane) or a pSUPERp53 construct (right lane) were generated. p53 expression and activity were determined by reporter gene assay (A, filled bars) and immunoblot (B). Equal loading was assessed by β-actin expression, luciferase production was further monitored by transfection with an NF-κB-Luc plasmid (A, open bars). C. LN-229 pSUPERp53 knock-down cells (filled squares) or LN-229 pSUPER control transfectants (open squares) were treated with CP-31398 for 24 h.

This led to the hypothesis that some non-specific effects occurred only with prolonged exposure not observed *in vivo* because of rapid metabolic clearing ($t_{1/2} \approx 2$ h in mice). Therefore compared the data obtained with continuous exposure was compared with data obtained in pulse assays where CP-31398 was removed after certain time periods, but survival still assessed at 24 h. Drug washout experiments revealed that p53-independent cytotoxicity, defined as the cytotoxicity observed in the p53 null cell line LN-308, did not become apparent until a minimum exposure of 6 h. In contrast, all p53 mutant and p53 wild type cell lines showed cytotoxic effects already at 1-2 h (Fig. 2.6A). Representative concentration curves for LN-18, U87MG, LN-229 and LN-308 cells are shown in Fig. 2.6B. Similar curves for LN-229 pSUPER control transfectants and LN-229 pSUPERp53 cells are shown in Fig. 2.6C. The protection conferred by suppression of p53 turned out to be much more prominent when the cells were pulse-treated for 4 h than when they were exposed continuously for 24 h. The EC_{50} values obtained in 4 h pulse assays ranged from 21.8 µM to 38.2 µM (Table 1). Importantly, these concentrations did not induce cell death in cultured postmitotic cerebellar granule neurons when CP-31398 containing medium was replaced by sister culture medium at 4 h (data not shown).

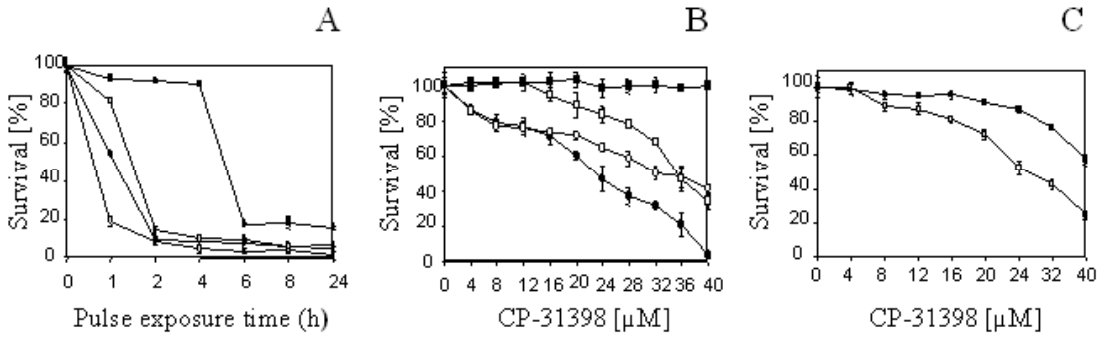

Fig. 2.6. **Pulse exposure to CP-31398 enhances the selectivity of the agent for p53-bearing cell lines.** A. Glioma cells (LN-18, filled circles; U87MG; open circles; LN-229, open squares; LN-308, filled squares) were pulse-treated with CP-31398 (48 µM). The agent was removed by washing at the indicated timepoints. B. The same cell lines were treated with different concentrations of CP-31398 for 4 h. Survival was assessed by crystal violet staining at 24 h. C. LN-229 pSUPERp53 cells (filled squares) or LN-229 pSUPER control transfectants (open squares) were treated and analysed as in B.

The modulation of p53 activity by CP-31398 was assessed by reporter assay. Fig. 2.7 shows that either prolonged exposure for 20 h, or a 4 h pulse exposure with subsequent washing and further culturing for 16 h induced considerable p53 reporter gene activity in all cell lines except LN-308. (The liabilities of the reporter used here will be referred to in the next section of this thesis.) The endogenous p53 activity of LN-229 cells reaches the upper limit of detection in the assay and can thus not be induced any further by CP-31398. Thus short-term exposure effectively induces p53 activity and cell death, but appears to lack the non-specific effects seen in LN-308 cells with prolonged exposure. Still zVAD-fmk, crm-A or Bcl-x_L were not protective even under the pulse assay conditions (data not shown).

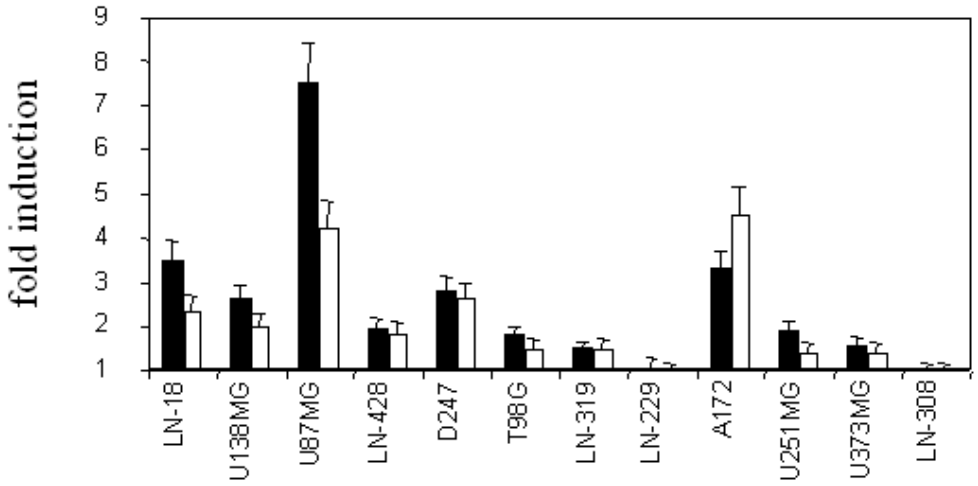

Fig. 2.7. **Induction of p53-like reporter gene activity by CP-31398.** p53 activity was determined by reporter gene assay and is given in % of the respective cell line cotransfected with pFC-p53 and the reporter gene (filled bars, cells treated with CP-31398 at 12 µM for 20 h; open bars, cells pulse-treated for 4 h at 18 µM and p53 reporter activity assessed 16 h later).

To further assess the role p53 plays in cell death induced by CP-31398, the murine $p53^{V135A}$ mutant was used. This mutant is temperature-sensitive, this is, silent and acting as a dominant-negative mutation at 38.5°C, but assuming wild-type conformation and generating transcriptional activity at 32.5°C. This mutant was expressed in LN-308 and U87MG cells (200). Reporter gene assays showed that $p53^{V135A}$ strongly decreased p53

activity in U87MG cells at 38.5°C, confirming its dominant-negative activity. At 32.5°C, $p53^{V135A}$ exhibited strong transcriptional activity in both cell lines, consistent with the assumption of wild-type conformation. Conversely $p53^{V135A}$ was not completely silent at 38.5°C in LN-308 cells (2% in $p53^{V135A}$-transfected LN-308 cells compared with essentially zero in hygro control transfectants) (Fig. 2.8A). CP-31398 (6 h, 36 μM) increased p53 activity in U87MG hygro cells at both temperatures, and in U87MG $p53^{V135A}$ and LN-308 $p53^{V135A}$ at 32.5°C. The apparent failure of response in the dominant negative mutants at 38.5°C may be due to the large excess of already misfolded p53 protein. Conversely the highest concentration of CP-31398 induced p21 in LN-308 $p53^{V135A}$ cells at 38.5°C (Fig. 2.8B), but not in LN-308 hygro control cells at either temperature (data not shown, see also Fig. 2.12). $p53^{V135A}$-transfected LN-308 cells shifted to 32.5°C revealed strong expression of p21 which was moderately increased by CP-31398.

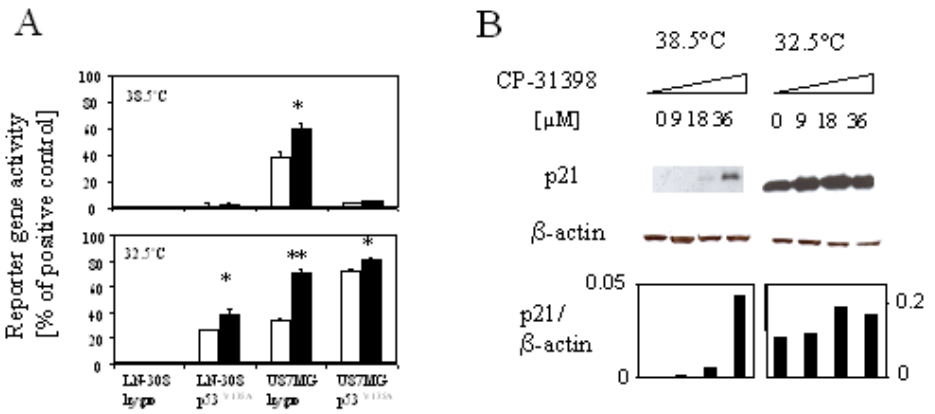

Fig. 2.8. **p53-dependent effects of CP-31398 in $p53^{V135A}$-transfected glioma cell lines.** A. LN-308 hygro control transfectants or $p53^{V135A}$-transfected LN-308 or U87MG cells were maintained at 38.5°C or shifted to 32.5°C for 24 h, and were then left untreated (open bars) or treated with CP-31398 (36 μM) for 6 h (filled bars). p53 activity was determined by reporter gene assay and is given in % of the respective cell line cotransfected with pFC-p53 and the reporter gene. B. p21 and β–actin levels were determined by immunoblot at 6 h after exposure of LN-308 $p53^{V135A}$ cells to increasing concentrations of CP-31398 at 38.5°C (left) or 32.5°C (right). Immunoblot bands were quantified and normalised to β-actin signal intensity.

Ectopic expression of $p53^{V135A}$ at mutant conformation (38.5°C) did not alter the sensitivity of LN-308 cells to CP-31398 (data not shown). In contrast, expression of $p53^{V135A}$ in wild-type conformation conferred sensitization to CP-31398 over a broad range of concentrations (Fig. 2.9A). In U87MG cells, which carry wild-type p53 alleles, $p53^{V135A}$ inhibited the cytotoxicity of CP-31398 at 38.5°C (Fig. 2.9B), but had no effect at 32.5°C (data not shown).

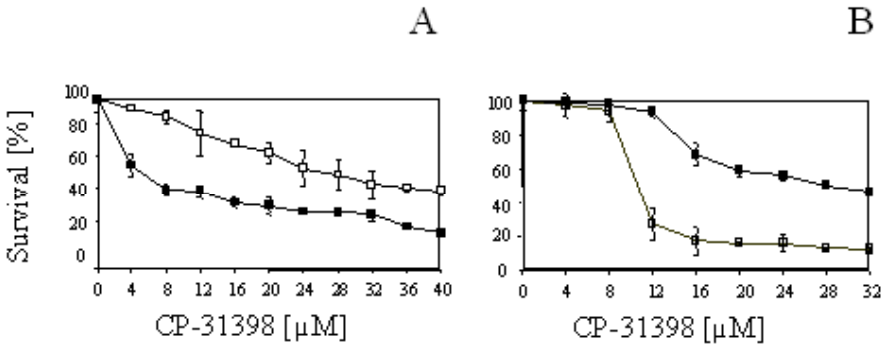

Fig. 2.9. **p53 gene transfer enhances CP-31398-induced cell death.** A. Hygro control (open circles) or $p53^{V135A}$-transfected LN-308 (filled squares) cells were shifted to 32.5°C for 24 h and then treated with CP-31398 for 24 h. B. Hygro control (open circles) or $p53^{V135A}$-transfected U87MG (filled squares) cells were treated with CP-31398 at 38.5°C for 24 h. Survival was assessed by crystal violet staining.

The kinetic difference between p53-dependent and p53-independent effects was confirmed in LN-308 $p53^{V135A}$ and LN-308 hygro cells in 4 h pulse assays. Whereas LN-308 parental or hygro control transfectants were resistant to CP-31398 in the 4 h pulse exposure assay, LN-308 $p53^{V135A}$ cells cultured at 32.5°C were sensitive to CP-31398 under these conditions (Fig. 2.10). Similarly, flow cytometry using AnxV-FITC/PI labelling showed a strong signal already at 6 h in U87MG, LN-18 and T98G cells, and also in LN-308 $p53^{V135A}$ cells at 32.5°C, whereas LN-308 hygro cells were still unresponsive at this time (data not shown).

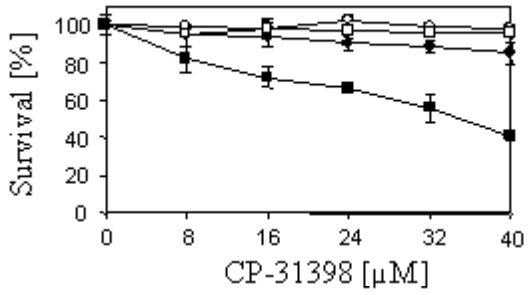

Fig. 2.10. **Short-term exposure of p53^{V135A}-transfected glioma cells to CP-31398.** Hygro control (open symbols) or p53^{V135A}-transfected LN-308 (closed symbols) cells were either maintained at 38.5°C (circles) or shifted to 32.5°C for 24 h (squares) and then pulse-treated (4 h) with CP-31398. Survival was assessed by crystal violet staining.

It has been suggested that CP-31398 cannot refold already misfolded mutant p53 proteins, but rather enforces the assumption of a wild-type conformation in newly synthesized p53 proteins (19). Hence inhibition of protein synthesis should specifically prevent the p53-dependent cytotoxic effects of CP-31398. As predicted, cycloheximide (CHX), an inhibitor of protein synthesis, inhibited the cytotoxic effects of CP-31398 in LN-18, U138MG, U87MG, T98G and LN-229, but not in LN-308 cells (Fig. 2.11A, data not shown). Since CP-31398-induced cell death in LN-308 cells is necessarily p53-independent, these data supported the idea that p53-dependent cell death induced by CP-31398 requires protein synthesis, most likely synthesis of p53 itself, whereas the p53-independent pathway can occur also in the presence of CHX. Consistent with this hypothesis, the sensitizing effects of p53^{V135A} in transfected LN-308 cells at 32.5°C were nullified by CHX, whereas CHX had no effect on CP-31398-induced cell death in hygro control cells treated at 32.5°C (Fig. 2.11B). Altogether these data suggested that p53-dependent effects of CP-31398 can be examined at timepoints up to 6 h where non-specific effects of the agent are still negligible or at least reversible.

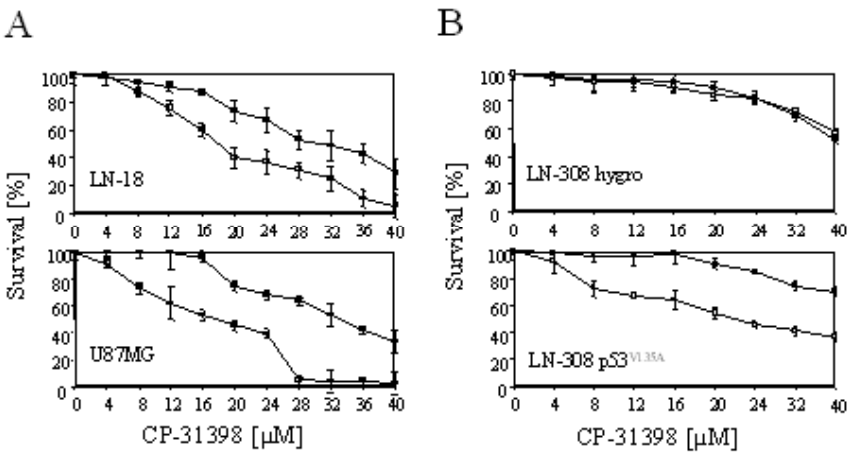

Fig. 2.11. **CP-31398-dependent cell death requires protein synthesis.** A. LN-18 or U87MG cells were treated for 16 h with CP-31398 in the absence (open squares) or presence (filled squares) of CHX (10 µg/ml). M. LN-308 hygro (upper panel) or LN-308 $p53^{V135A}$ (lower panel) cells were shifted to 32.5°C for 24 h and treated for 16 h with CP-31398 in the absence (open squares) or presence (filled squares) of CHX (10 µg/ml). Survival was assessed by crystal violet staining.

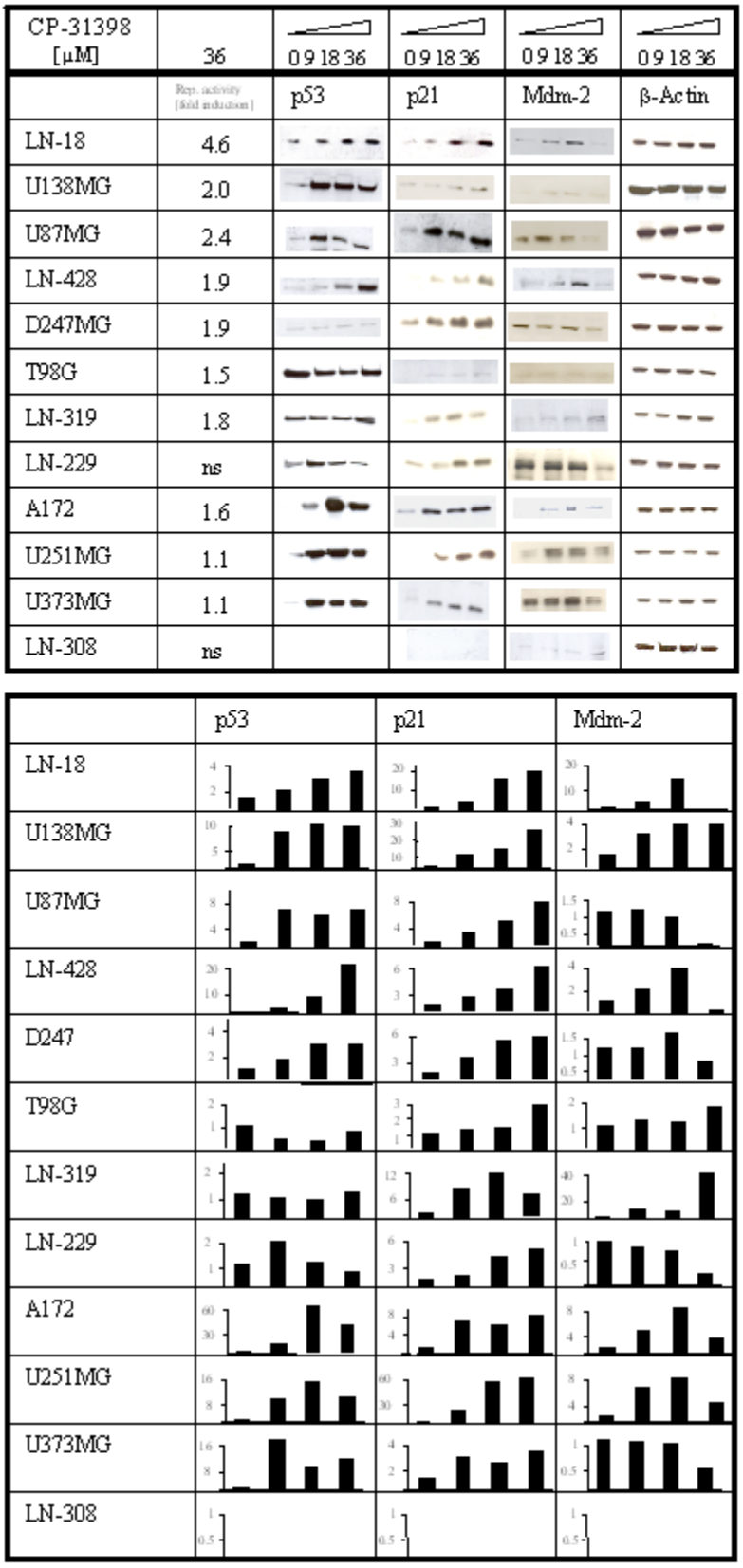

Figure 2.12.

Modulation of p53 reporter activity, and p53, p21 and Mdm2 protein accumulation by CP-31398. The cells were left untreated or treated with CP-31398 (36 µM) for 6 h and assessed for p53 reporter activity. Values are given as fold increase over background (for mutant cell lines) or constitutional activity (for p53 wild-type cell lines). Lysates from untreated cells or from cells treated with CP-31398 at 9, 18 or 36 µM for 6 h were assessed for the protein levels of p53, p21, Mdm2 and ß-Actin (upper panel). All signals were quantified, normalised to β-Actin content and expressed as fold increase over the respective untreated control (lower panel).

Next the effects of fixed concentrations of CP-31398 on p53 reporter activity and gene expression were compared in the panel of 12 glioma cell lines. CP-31398 induced changes in reporter gene activity at 6 h in all cell lines except LN-308 (p53 null) and LN-229 (maximal constitutive activity) (Fig. 2.12). The strongest effect of CP-31398 was seen in LN-18 cells which carry a mutation (Cys→Ser) in codon 238. T98G cells, which carry a Met→Ile mutation in the neighbouring codon, 237, showed low p53 activity in response to CP-31398. p53 activity was also induced in two other cell lines, LN-319 and LN-428, with mutations in codons 175 (Arg→His) and 173 (Val→Met) as well as 282 (Arg→Trp), respectively. The two cell lines mutated in codon 273 (Arg→His), U251MG and U373MG, remained almost silent. There was no correlation between the induced activity in the reporter assay and the sensitivity to CP-31398 defined by EC_{50} values over 24 h or in the 4 h pulse experiment (Table 2.1). Hence the type of p53 mutation may predict whether CP-31398 is able to induce p53 activity in a reporter assay, but not the cytotoxic effects of CP-31398. These data also indicate that some mutations within the DNA binding domain of p53, exemplified by U251MG and U373MG, are rather refractory to the action of CP-31398, as defined by p53 reporter assay.

Next, the correlation between the p53 reporter assay data and the stabilization of p53 as determined by p53 protein accumulation on immunoblot analysis was investigated. CP-31398 promoted the accumulation of p53 in all 5 cell lines retaining wild-type p53 activity (U138MG, U87MG, D247MG, LN-229, A172) and in 4 of 6 p53 mutant lines (LN-18, LN-428, U251MG, U373MG). T98G and LN-319 cells, which showed enhanced activity in the reporter assay, did not show p53 accumulation in response to CP-31398. Conversely, U251MG and U373MG, which developed low p53 activity in the reporter assay, nevertheless showed marked accumulation of p53 protein. Thus p53 stabilization and p53 activity in a reporter assay induced by CP-31398 do not necessarily coincide.

The accumulation of p21 as a major p53 response protein was also monitored. The stabilization of p53 and the accumulation of $p21^{WAF/CIP1}$ protein were concentration-dependent and occur roughly in parallel. All 5 p53 wild-type cell lines accumulated p21 in response to CP-31398. Similarly the 6 p53 mutant cell lines accumulated p21. LN-308 cells again failed to respond. Physiologically the up-regulation of p53 is limited by

the p53-mediated accumulation of Mdm2 which targets p53 for proteasome-dependent degradation. Mdm2 accumulation was observed in response to CP-31398 in LN-18, U138MG, LN-428, LN-319, A172 and U251MG cells, but not in U87MG, D247MG, T98G, LN-229, U373MG and LN-308 cells. At the highest concentration of CP-31398 used, Mdm2 levels decreased in all cell lines except U138MG, T98G, LN-308 and LN-319 which may in part be due to the stabilization of Mdm2 by $p14^{arf}$ (205). LN-319 and LN-308 cells are the only cell lines which show no deletion or mutation of the $p14^{arf}$ locus (15, 197). Thus in LN-319 cells the binding activity of $p14^{arf}$ may protect Mdm2 from proteasomal degradation. Further, Mdm2 may bind to p53 in the presence of CP-31398 while the ubiquitinylation and subsequent degradation of this complex are inhibited (206). Thus the effects seem to be complex and cell-type specific.

Modulation of proapototic p53 response gene expression by CP-31398

Changes in the expression of the proapototic p53-response genes NOXA (36) and PUMA (35, 207) were assessed by Northern blot. While the p53 null cell line LN-308 did not respond to treatment with CP-31398 with the up-regulation of either mRNA, both genes were induced in LN-18, U87MG and LN-229 cells (Fig. 4). Quantification of the signals revealed that LN-18 cells showed only a slight induction of NOXA while the mRNA levels for PUMA were strongly up-regulated. In U87MG cells, on the other hand, induction of NOXA was much stronger.

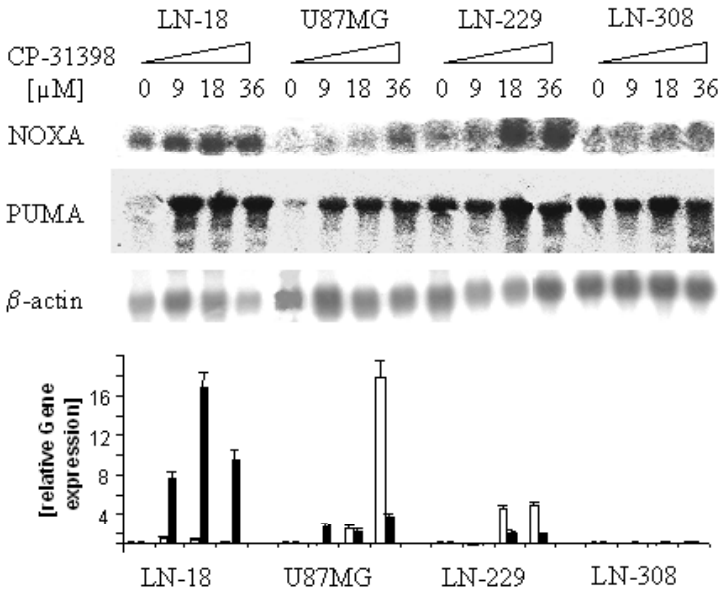

Figure 2.13. **Modulation of NOXA and PUMA expression by CP-31398.** LN-18, U87MG, LN-229 or LN-308 cells were untreated or treated with CP-31398 at 9, 18 or 36 µM for 6 h. Total cellular RNA was analysed for NOXA and PUMA expression by Northern blot. Signal intensities were quantified using a Fuji PhosphoImager and normalised to β-actin content. Gene induction is expressed as fold increase over the untreated control (open bars: NOXA, filled bars: PUMA).

Modulation of Bcl-2 family protein expression by CP-31398

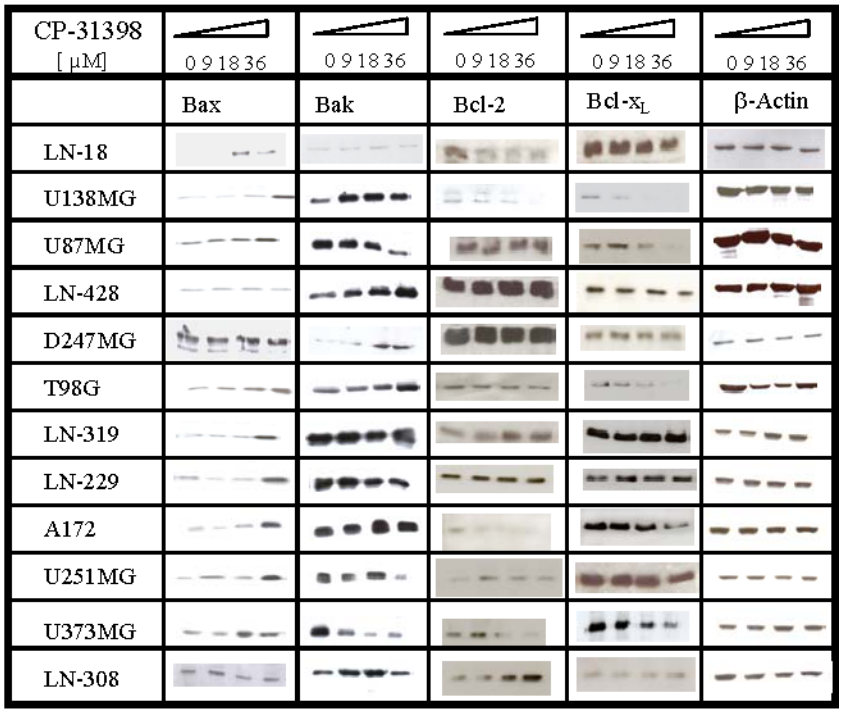

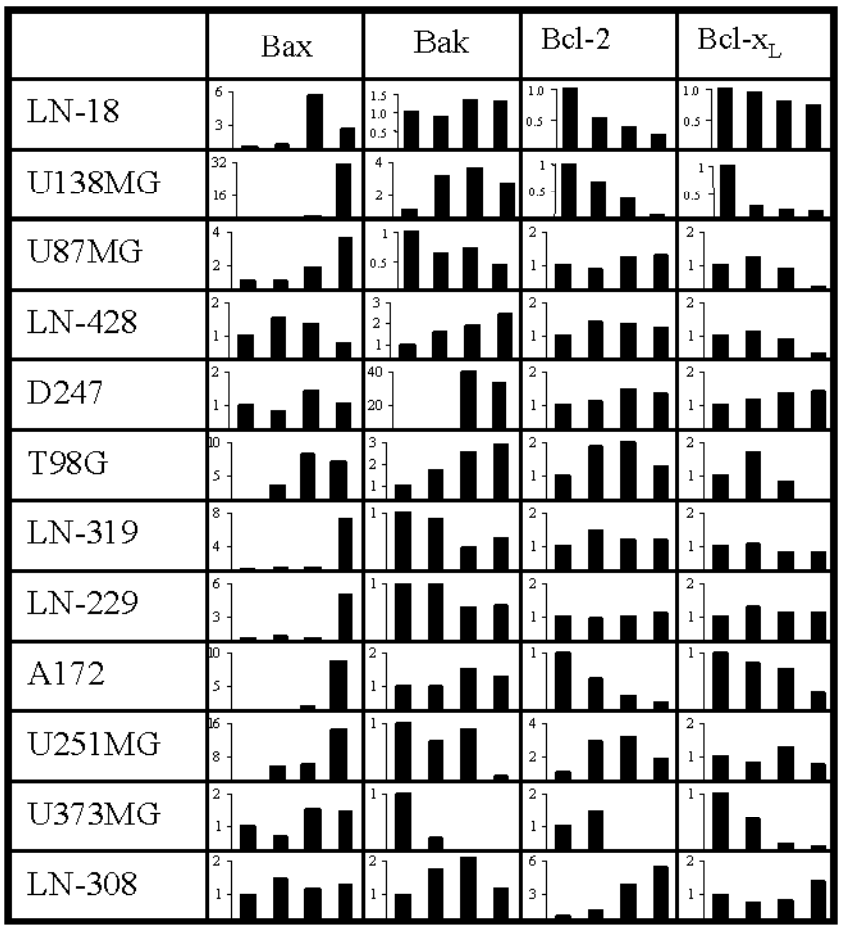

Figure 2.14. **Modulation of Bcl-2 family protein expression by CP-31398.** Lysates from untreated cells or cells treated with CP-31398 at 9, 18 or 36 µM for 6 h were assessed for the protein levels of Bcl-x_L, Bcl-2, Bax, Bak and ß-Actin (upper panel). All signals were quantified, normalised to β-Actin content and expressed as fold increase over the respective untreated control (lower panel).

Changes in the expression of Bcl-2 protein family members have been attributed an important role in mediating p53-dependent apoptosis (38). Such changes include enhanced expression of proapoptotic proteins such as Bax and decreased expression of antiapoptotic proteins such as Bcl-2. Exposure to CP-31398 increased the levels of proapoptotic Bax in 9 of 12 cell lines (LN-18, U138MG, U87MG, T98G, LN-319, LN-229, A172, U251MG and U373MG cells) (Fig. 2.14). Proapoptotic Bak levels increased in 4 of 12 cell lines (U138MG, LN-428, D247MG, T98G), but decreased in 4 cell lines (U87MG, LN-319, U251MG, U373MG). Antiapoptotic Bcl-2 levels decreased in response to CP-31398 in 4 of 12 cell lines (LN-18, U138MG, A172, U373MG), but increased in LN-319 and LN-308 cells. Antiapoptotic Bcl-x_L levels decreased in 6 of 12 cell lines (U138MG, U87MG, LN-428, T98G, A172, U373MG). These changes in Bcl-2 family protein favoured induction rather than prevention of apoptosis, but were too heterogeneous to account for the cytotoxic effects of CP-31398.

p53-independent CP-31398-induced cell death involves epiphenomenal free radical formation, is inhibited by aurintricarboxylic acid (ATA) and may be mediated by calcium cytotoxicity

Free radical formation has been linked to p53-dependent and p53-independent types of cell death (32, 39). CP-31398 induced free radical formation in a concentration- and time-dependent manner in LN-18, LN-229 and LN-308 cells (Fig. 2.15A,B, data not shown). The analysis of free radical formation in LN-229 pSUPER and LN-229 pSUPERp53 cells (Fig. 2.15C) as well as in LN-308 hygro and LN-308 $p53^{V135A}$ cells at 38.5°C or 32.5°C showed no difference between $p53^{V135A}$-transfected and hygro control cells (data not shown), suggesting that free radical formation induced by CP-31398 is p53-independent. Free radical formation was unlikely to be a mere indicator of cell death since it was observed as early as 30 min after exposure and since the increased CP-31398 sensitivity of LN-308 $p53^{V135A}$ cells compared with LN-308 hygro control cells at 32.5°C (Fig. 2.9A) did not translate into increased free radical formation. A peroxide assay performed with CP-31398 in medium or cell culture supernatant with various components being added (serum, Fe^{2+}, phenol red) excluded the possibility that free radicals were produced by chemical interactions with CP-31398 in a cell-free system (data not shown). Free radical formation thus appeared to be part of the p53-independent effects of CP-31398.

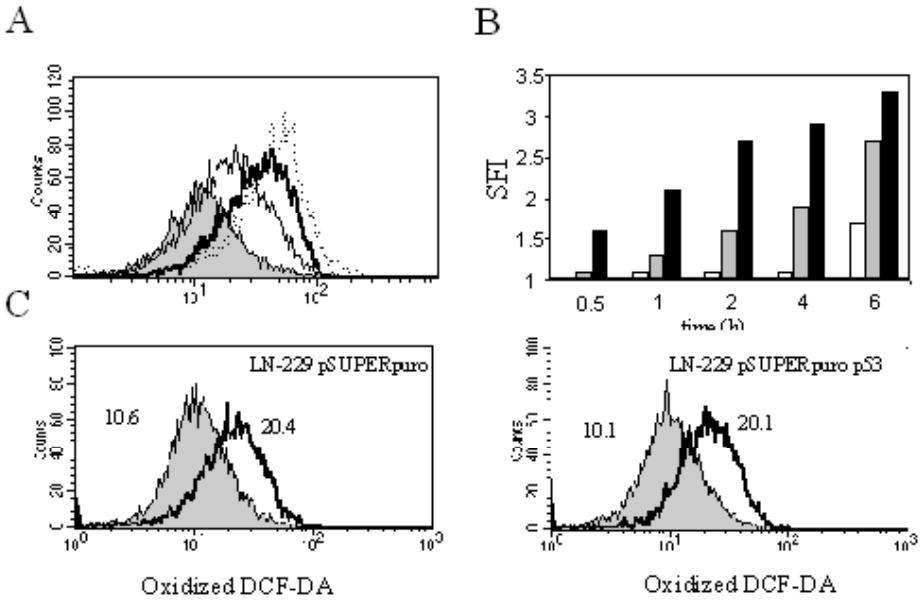

Fig. 2.15. **CP-31398 induces free radicals in a p53-independent manner.** A. LN-308 cells were treated for 4 h with increasing concentrations of CP-31398 (untreated, filled histogram; 9 µM, solid, thin line; 18 µM, solid, thick line; 36 µM, dotted line). The cells were loaded with the non-fluorescent dye DCFH-DA and analysed by flow cytometry. The fluorescence originating from the oxidized product DCF was recorded in channel Fl-1H. Dead cells were gated out by double staining with PI. B. Shifts in mean fluorescence (SFI values) were calculated at 0.5, 1, 2, 4 or 6 h (9 µM, open bars; 18 µM, grey bars, 36 µM, black bars). As a positive control, ethacrynic acid (100 µM) induced an SFI of 2.6 at 30 min. C. LN-229 pSUPERp53 transfectants (lower panel) or LN-229 pSUPER control transfectants (upper panel) were left untreated (filled histograms) or treated for 6 h with 18 µM CP-31398 (open histogram). Free radical formation was determined as in A, mean fluorescence values are indicated in the diagrams.

However, free radicals were not critical mediators of CP-31398-induced cell death since various antioxidants, including N-t-butyl-α-phenylnitrone (PBN) (1-100 µM) or N-acetylcysteine (NAC) (1-100 µM) failed to inhibit CP-31398-induced cell death in LN-18, T98G, LN-229, LN-308 hygro or LN-308 $p53^{V135A}$ cells (data not shown). As positive controls, the cytotoxic effects of ethacrinic acid (25 µM), cisplatin (50 µM) or betulinic acid (25 µM) were significantly reduced by PBN and NAC (208).

Excessive calcium influx, or its liberation from intracellular stores, may provide a second messenger signal for apoptosis and trigger caspase-independent pathways including the formation of superoxide species (209). All of three cell lines examined (LN-18, LN-229, LN-308) cells showed a marked increase in $[Ca^{2+}]_{free,\ cytosolic}$ at 6 h

after exposure to CP-31398. Down-regulation of p53 in LN-229 pSUPERp53 cells had no effect on calcium liberation (Fig. 2.16). Drug washout experiments revealed that the timepoint of calcium influx coincided with the onset of irreversible p53-independent effects (Fig. 2.6, data not shown). The increase in $[Ca^{2+}]_{free,\ cytosolic}$ was prevented by coexposure to ATA (20 µM) (Fig. 2.16A).

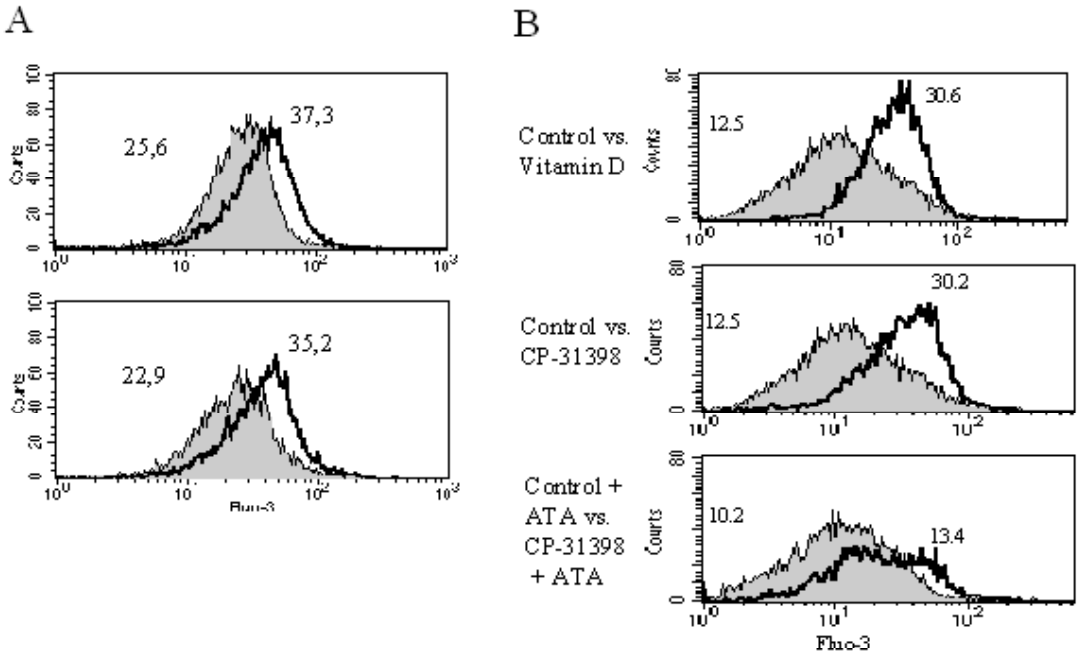

Fig. 2.16. **CP-31398-induced cell death is preceded by an increase in the intracellular Ca^{2+} level.**
A. Free cytosolic calcium concentrations were determined in pSUPERp53 transfectants (lower panel) or LN-229 pSUPER control transfectants (upper panel) by flow cytometry using the calcium-dependent fluorescent probe Fluo3-AM. Untreated controls are shown as filled histograms, open histograms were recorded after cells had been exposed to 18 µM CP-31398 for 6 h. Mean fluorescence values are indicated in the diagrams. B. LN-229 cells were treated for 6 h with vitamin D (25 µM), CP-31398 (36 µM), ATA (20 µM) or combinations thereof. Intracellular calcium liberation was determined as in A.

ATA also attenuated CP-31398-induced cell death in all 12 cell lines (Fig. 2.17, data not shown) while the induction of p53 reporter gene activity was not inhibited by ATA in either cell line (data not shown).

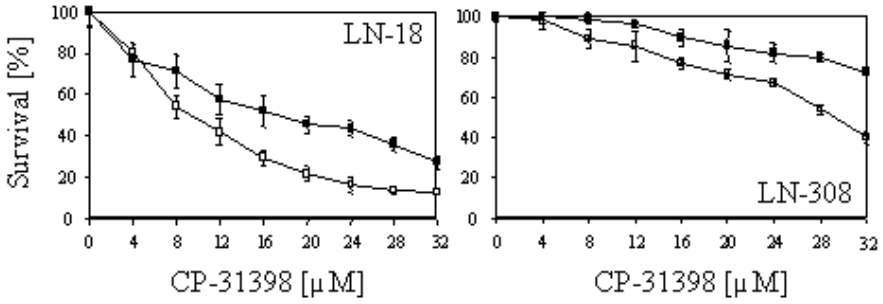

Fig. 2.17. **ATA protects against p53-independent effects of CP-31398.** LN-18 or LN-308 cells were treated with CP-31398 in the absence (open squares) or presence (filled squares) of ATA (20 µM) for 24 h. Survival was assessed by crystal violet staining.

To further assess which pathway triggered by CP-31398 was affected by ATA, LN-308 hygro and LN-308 $p53^{V135A}$ cells were compared at 38.5°C and 32.5°C. While CP-31398-induced cell death was strongly inhibited by ATA in LN-308 hygro cells maintained at both temperatures and in LN-308 $p53^{V135A}$ cells at 38.5°C, ATA had only minor effects in LN-308 $p53^{V135A}$ cells kept at 32.5°C (Fig. 2.18A). Accordingly ATA did not protect when LN-308 $p53^{V135A}$ cells were pulse-treated with CP-31398 whereas CHX (10 µg/ml) blocked cytotoxicity under these conditions (Fig. 2.18B).

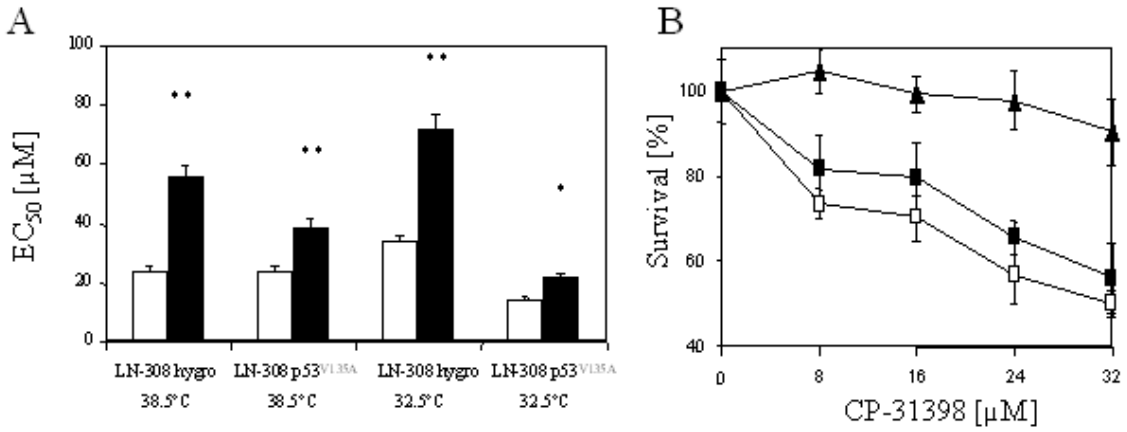

Fig. 2.18. **ATA does not prevent the p53-dependent effects of CP-31398.** A. LN-308 hygro or LN-308 $p53^{V135A}$ cells were treated with CP-31398 for 24 h in the absence (open bars) or presence (filled bars) of ATA (20 µM) at 38.5°C or 32.5°C. Data are expressed as EC_{50} and SEM at 24 h (**$p<0.01$, *$p<0.05$, t-test). B. LN-308 $p53^{V135A}$ cells were shifted to 32.5°C for 24 h and pulse-treated with CP-31398 for 4 h in the absence (open squares) or presence of ATA (20 µM, closed squares) or CHX (10 µg/ml, closed triangles). ATA was present during the whole course of the experiment whereas CHX was removed together with CP-31398.

Discussion

Pharmacological agents which specifically activate p53-dependent cell death pathways in mutant p53-accumulating cancer cells would represent a major advance in the therapy of human cancers characterized by p53 mutations. The first such molecule to be characterized was CP-31398 (19), a second one, PRIMA-1, has recently been described (20). Here is shown that none of 12 human malignant glioma cell lines resists the cytotoxic effects of CP-31398 (Fig. 2.2, Table 1), a small molecule discovered in a screening for compounds that force mutant p53 variants into assuming a wild-type conformation (19). At the molar level, the range of EC_{50} concentrations of 10-40 μM compares well with current cancer chemotherapeutics used in the treatment of malignant glioma (197). CP-31398-induced cell death had light microscopic and biochemical (AnxV-FITC staining, Fig. 2.3) features of apoptosis, but is an unusual type of apoptosis in that caspases appeared to play no role and in that Bcl-x_L was not protective (Fig. 2.4). The data summarized in Table 1 and Fig. 2.12 suggest that CP-31398 converts the mutant conformation of p53 into a functional one when the mutation is located in the central DNA binding region (175). The blunted response obtained with this mutant in the reporter assay in U251MG and U373MG cells might relate to the fact that residue 273 directly contacts the DNA. A conformational stabilization of the backbone of the protein may well optimize the conformation of this mutant and thus DNA binding while efficient transcription of the target genes is still not initiated (210). However, U251MG and U373MG cells nevertheless showed a strong accumulation of p21 when treated with CP-31398 (Fig. 2.12), suggesting that the reporter assay poorly reflects the transcriptional activation at least of the p21 gene. In this regard, gene chip analysis revealed that most, but not all, p53 response genes are induced when mutant p53 is stabilized through CP-31398 (211). Further, in analogy to the protein data shown here (Fig. 2.12), these authors observed a repression of Mdm2 mRNA expression by high concentrations of CP-31398. Further, they assumed that differential patterns of responses of various p53 target genes might be responsible for the biological activity of CP-31398 since pro-apoptotic p53 response genes were induced much more potently than p53 targets mediating cell cycle arrest, e.g. cyclin G2, or negative feed back loops, e.g. Mdm2-dependent, ubiquitin-mediated proteasomal degradation.

A comparative analysis of molecular events triggered by CP-31398 in different cell lines revealed at least two pathways of CP-31398-induced cell death, one being p53-

dependent and one being p53-independent. The p53-dependent killing pathway is triggered within few hours and depends on new protein synthesis, presumably of p53 itself (Fig. 2.6, 2.7, 2.11). The p53-independent pathway is associated with free radical formation, but free radical formation does not mediate cell death (Fig. 2.15). In contrast, p53-independent cell death involves delayed calcium release and is inhibited by ATA (Fig. 2.16-18), an agent that acts as a general inhibitor of Ca^{2+}-dependent endonucleases, amongst various other effects.

The specificity of these effects was ascertained both by p53 reconsitution (Fig. 2.8-11, Fig. 2.18) as well as by siRNA technology (Fig. 2.5,6,15,16). The relative resistance of p53 null LN-308 cells in the 4 h pulse assay (Fig. 2.10) indicates a central role for p53-mediated cell death in that paradigm. That LN-229 p53 knock-down cells were not fully protected (Fig. 2.6) may be due to some residual p53 activity as well as to effects of CP-31398 on other members of the p53 family, such as p63 or p73 (206). In fact, stabilization of p73 by CP-31398 was also detected (data not shown).

The proximate cause of CP-31398-induced cell death remains obscure and may in fact differ among cell lines. Although proapoptotic Bcl-2 family proteins were induced in many cell lines, caspases did not mediate cell death, and glioma cells may tolerate high level Bax expression under certain conditions (64). Further candidate mediators of cell death include NOXA and PUMA which were also differentially induced in response to CP-31398 (Fig 2.13). That transcription-independent effects of p53 were responsible for cell death cannot be excluded (212, 213), but seemed unlikely since at the time, when the experiments were performed, transcription-independent cell death had not yet been proven to occur with wild-type p53 or naturally occurring p53 mutants in intact cells. However, recent reports (172, 173) have shed a new light on this issue.

A p53-independent killing pathway triggered by CP-31398 had previously been discussed (214), but not studied at a molecular level. Surprisingly, these authors were unable to identify physico-chemical evidence for the interaction between CP-31398 and the isolated free core domain of p53. Instead they speculated that CP-31398 acts merely as a DNA intercalator. However, they could not exclude that CP-31398 acts in a chaperone-like manner on newly synthesized p53 protein. This, however, is the mode of action previously proposed for CP-31398 (19). Further support for a direct interaction of CP-31398 and p53 comes from EMSA studies showing restoration of the sequence-specific DNA binding ability of the 273 (Arg→His) p53 mutant by CP-31398 (206, 215).

The present study illustrates the difficult task to design and develop specific agents free of unexpected side effects. Conversely CP-31398 used in the p53-dependent pulse assays (Fig. 2.6, Fig. 2.18) induced cell death in some cell lines more efficiently than gene transfer-mediated overexpression of wild-type p53 (unpublished observations), suggesting that CP-31398 may not merely hit p53, but also p53-related proteins such as p63 or p73 (176). Similar to the synthetic p53 homolog, chimeric tumour suppressor 1 (CTS-1) (203), the p53-dependent cytotoxic effects of CP-31398 appeared not to be mediated by either death receptors, caspase activation or free radical formation. The proximate cause of death in glioma cells killed by p53-dependent pathways thus remains obscure. Future efforts of drug design aiming at optimizing CP-31398-related compounds will have to focus on the preservation of the p53-mediated effects, which are desirable and potentially therapeutic, and attenuation of p53-independent effects, a likely source of undesirable side effects.

III. p53 and its family members - reporter genes may not see the difference

A related manuscript has been published in Cell Death & Differentiation.

2004 Oct;11(10):1150-1152

Thanks go to Prof. Frank McKeon, PhD (Harvard Medical School, Cambridge, MA, USA) for providing p63 plasmids and antibody. All p73 reagents were kindly provided by Prof. Gerry Melino, PhD (Medical Research Council, Leicester, UK) who also made helpful suggestions concerning the discussion of the data.

Introduction

Luciferase-coupled reporter genes are widely used to investigate the activity of transcription factors. However, there is little awareness that the promoter sequences contained in these vectors are not always specific. This report shows that both p63 and p73 activate Stratagene´s p53 *PathDetect* reporter plasmid, one of the most commonly used reporter genes. Thus data obtained using this system (or any similar one) should be interpreted with caution because they may not actually reflect p53 activity, but rather provide an integrated signal derived from different members of the p53 family. In the absence of p53 signalling, this reporter gene may be useful for the analysis of effects that depend on p63 or p73.

Materials and Methods

Cell lines. The human malignant glioma cell lines, kindly provided by Dr. N. de Tribolet (Lausanne, Switzerland), have been characterized (15, 197). SV-FHAS non-neoplastic astrocytes were kindly provided by D. Stanimirovic (Institute of Biological Sciences, National Research Council of Canada, Ontario, Ottawa, Canada). The cells were cultured in Dulbecco`s modified Eagle medium (DMEM) containing 10% foetal calf serum, 2 mM glutamine and penicillin (100 IU/ml)/streptomycin (100 μg/ml).

Plasmids. The PathDetect® p53 cis-reporter gene plasmid, containing the p53-responsive enhancer element $(TGCCTGGACTTGCCTGG)_{15}$, was from Stratagene (La Jolla, Ca). pRL-CMV was obtained from Promega (Mannheim, Germany). pcDNA3-HA-p53, pcDNA3-HA-p73α, pcDNA3-HA-p73β, pcDNA3-HA-p73γ, pcDNA3-HA-p73δ, pcDNA3-HA-ΔNp73β, pcDNA3-HA-p73α^{A156V}, pcDNA3-HA-p73β^{A156V} pcDNA3-HA-p73χ^{A156V} and pcDNA3-HA-p73δ^{A156V} have been described (216). pcDNA3myc-TAp63α, pcDNA3myc-TAp63β, pcDNA3myc-TAp63γ, pcDNA3myc-ΔNp63α, pcDNA3myc-ΔNp63β and pcDNA3myc-ΔNp63γ have been described (Boston, MA, USA) (217).

p53 silencing. The p53 specific oligonucleotide sequences GATCCCC**GACTCCAG TGGTAATCTAC**ttcaagaga**GTAGATTACCACTGGAGTC**TTTTTGGAAA and TCGATTTCCAAAAA**GACTCCAGTGGTAATCTAC**tctcttgaa**GTAGATTACCAC TGGAGTC**GGG were obtained from Metabion (Munich, Germany) and cloned into Bgl II and Sal I-sites of the pSUPERpuro vector (177), generously provided by Dr. Reuven Agami (Amsterdam, NL). The p53-specific parts of the sequence are depicted in bold letters and underlined. The resulting pSUPERp53 plasmid was stably transfected (10:1) and puromycin-resistant bulk transfectants were generated. Control transfectants were generated by co-transfecting pSUPERpuro alone**.**

Immunoblot analysis. The general procedure has been described (200). Soluble protein levels were analysed using 20 μg of cellular lysate separated on 10-12% acrylamide gels (Biorad, Munich, Germany). After transfer to a PVDF membrane, the blots were blocked and incubated with murine anti-human p53 monoclonal antibody Bp53-12 (2

µg/ml), goat anti-mammalian β–actin polyclonal antibody I-19 (1 µg/ml) (both from Santa Cruz, Santa Cruz, CA), mouse anti-mammalian p63 4A4 (217) or rabbit anti-human p73 antiserum (Sanofi, Paris, France) (218). Visualization of protein bands was accomplished using horseradish peroxidase (HRP)-coupled IgG secondary antibody (Sigma) and enhanced chemiluminescence (ECL) (Amersham, Braunschweig, Germany). Quantification was performed by multiplying the respective signal area with its mean intensity using Corel Photo-Paint 11 software (Corel Corporation, Ottawa, CA).

p53 reporter gene assay. Glioma cells were seeded into 96 well plates (6 x 10^3cells/well) and left to adhere overnight, before they were co-transfected with 0.06 µg of the PathDetect® p53 cis-reporter gene plasmid, 0.03 µg of the respective activator plasmid (or irrelevant DNA) and 0.01 µg of pRL-CMV, using FuGene 6 (Roche, Mannheim, Germany). At 16 h after transfection, the cells were shifted to the respective temperature. Another 32 h later, the cells were washed and lysed using Reporter Lysis Buffer (Promega). The respective activities of firefly and renilla reniformis luciferase were determined sequentially using the firelite dual luminescence reporter gene assay (Perkin-Elmer, Rodgau-Jügesheim, Germany). Background was subtracted from all values and the counts obtained from the measurement of firefly luciferase were normalized with respect to pRL-CMV.

Results

To study effects caused by p53 mutations (219), resulting in loss of functional p53 activity (220, 221), and suppression of signalling from p53-related proteins such as p63 or p73 (222, 223), a stable subline of LN-18 glioma cells was generated where the expression of the endogenous mutant p53 (238 Cys → Ser) (224) was suppressed by more than 90% by pSUPER siRNA technology (177). RNA interference targeting p53 had no effects on the levels of p63 and p73 (Fig. 3.1 A). A transiently transfected pcDNA3-HA-p53 plasmid induced greater p53-Luc reporter gene activity in the p53-depleted cells than in the control transfectants, consistent with a dominant negative effect of the endogenous p53 mutant (Fig. 3.1 B).

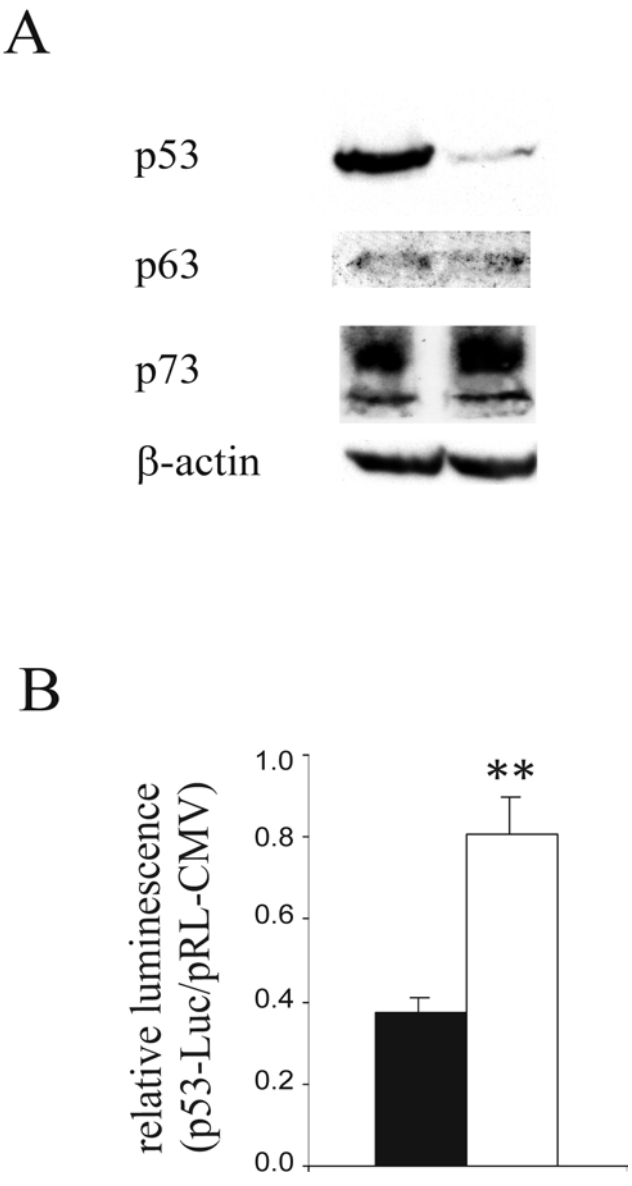

Figure 3.1: **siRNA-mediated downregulation of mutant p53 in LN-18 glioma cells.** A. LN-18 human malignant glioma cells were stably transfected with pSUPERpuro control (left) or pSUPERpuro p53 plasmid (right) and analysed for p53, p63, p73 or β-actin levels by immunoblot. B. LN-18 pSUPER puro control (left) or p53-knockdown cells (right) were seeded into 96 well plates (6 x 10^3cells/well) for 24 h and then co-transfected with 0.06 µg of the PathDetect® p53 cis-reporter gene plasmid, 0.03 µg of pcDNA3-HA-p53 and 0.01 µg of pRL-CMV. At 48 h after transfection, the cells were washed and lysed. The respective activities of *photinus pyrsalis* and *renilla reniformis* luciferase were determined sequentially. Background was subtracted from all values and the counts obtained from the measurement of firefly luciferase were normalized to pRL-CMV.

Surprisingly, the mutant p53-depleted cells provided a significantly (Student's t-test, $p<0.01$) increased p53-Luc signal (Fig. 3.2) even in the absence of wild-type p53 transfection which, by definition, could not be derived from wild-type p53 in this cell line.

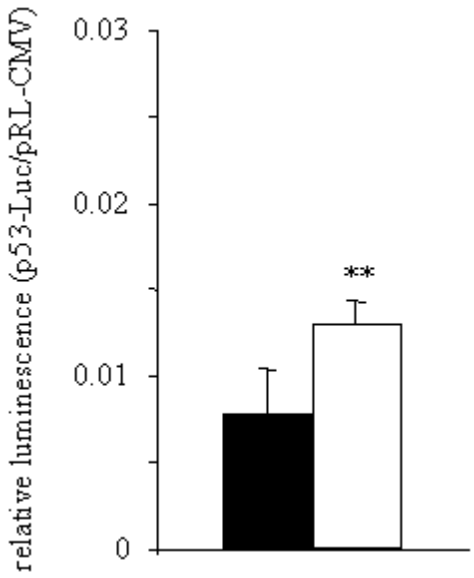

Fig. 3.2. **Induction of p53-like reporter gene activity by knock-down of mutant p53.** LN-18 pSUPER puro control (left) or p53-knockdown cells (right) were transiently co-transfected with p53-Luc and pRL-CMV alone. Luminescence was determined as in Fig.3.1B.

Since we had previously demonstrated the expression of p73 in LN-18 cells (225), this p53-like reporter gene activity could possibly be derived from the de-repression of p73 after the depletion of endogenous mutant p53. To assess whether the p53-luc reporter responds to p73, LN-308 cells which express neither p53 nor p73 (6,8) nor p63 by immunoblot (Fig. 3.3) were examined.

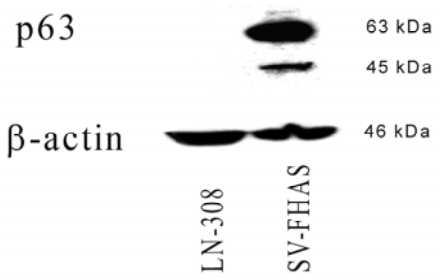

Fig. 3.3. **LN-308 glioma cells do not express p63 protein.** LN-308 glioma cells (left) and SV-FHAS non-neoplastic astrocytes (right) were analysed for p63 and β-actin levels by immunoblot. The size of the isoforms detected (corresponding to TAp63β and ΔNp63γ) is indicated.

Co-transfection assays revealed that the transcriptionally most active p73β isoform was even a stronger activator of the reporter plasmid than p53 itself. p73δ was approximately as effective as p53. p73α and p73γ gave weaker, but still significant signals. Only the truncated p73ΔNβ remained transcriptionally silent (Fig. 3.4).

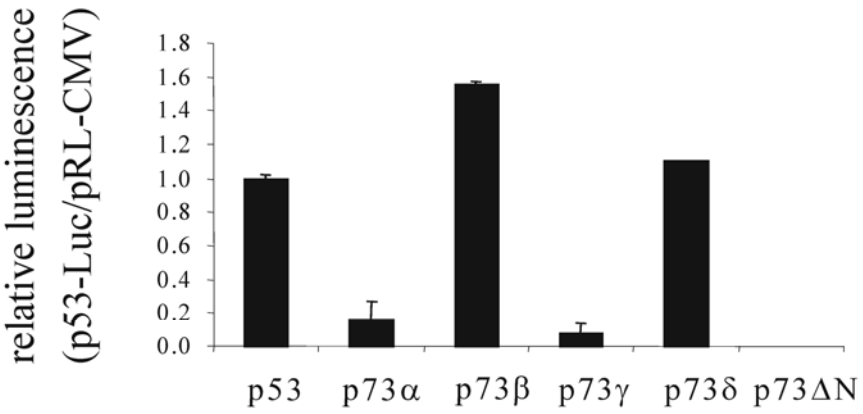

Fig. 3.4. **p53-like reporter gene activity can be induced by p73.** LN-308 cells were co-transfected with p53-Luc, pRL-CMV and plasmids encoding p53 or the different isoforms of p73 (pcDNA3-HA-p53, pcDNA3-HA-p73α, pcDNA3-HA-p73β, pcDNA3-HA-p73γ, pcDNA3-HA-p73δ, pcDNA3-HA-ΔNp73). *Photinus pyrsalis* and *renilla reniformis* luciferase activities were determined as in Fig. 1 and the values for p53-Luc/pRL-CMV are expressed relative to pcDNA3-HA-p53.

Similar experiments performed with p63 showed that TAp63β and TAp63γ were also strong inducers of reporter gene activity while TAp63α gave only a weak signal, most likely because of the rapid degradation of this isoform caused by the MDM-2 like activity of the α C-terminus (226). While the ΔNp63α and ΔNp63β isoforms remained transcriptionally silent, the ΔNp63γ isoform, which lacks the p53-homologous transcriptional activation domain at the N-terminus, induced strong reporter gene activity. This is consistent with this isoform being pro-apoptotic (217) and may be due to an additional C-terminal activation domain (227) which is repressed in the longer C-termini of other isoforms (Fig. 3.5). The use of p63 plasmids encoding the murine and not the human protein does not weaken the findings since p63 is more than 99% conserved between mice and men, with consensus sites being identical.

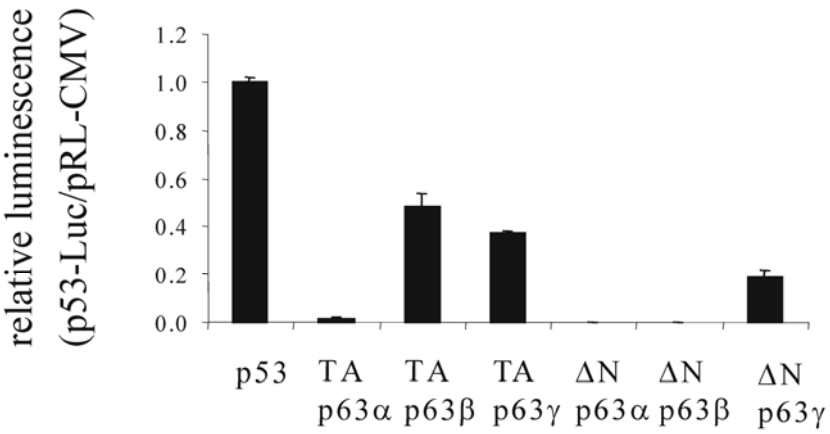

Fig. 3.5. **p53-like reporter gene activity can be induced by p63.** LN-308 cells were co-transfected with p53-Luc, pRL-CMV and plasmids encoding p53 or the different isoforms of p63 (pcDNA3myc-TAp63α, pcDNA3myc-TAp63β, pcDNA3myc-TAp63γ, pcDNA3myc-ΔNp63α, pcDNA3myc-ΔNp63β, pcDNA3myc-ΔNp63γ). *Photinus pyrsalis* and *renilla reniformis* luciferase activities were determined as in Fig. 1.

Temperature-sensitive mutants of p53 such as murine $p53^{V135A}$ are widely used for the study of p53 function. A screening of a comprehensive p53 missense mutation library has revealed a huge number of temperature-sensitive mutations that could become valuable tools (228). A set of similar mutants has been described for p73 (229). Reporter gene analysis is ideally suited to assess their transcriptional activity under various conditions. All $p73^{V156A}$ mutants, the functional analogs to murine $p53^{V135A}$ and human $p53^{V143A}$, were found to be highly temperature-dependent. While they were almost transcriptionally silent at 38.5°C, transcriptional activity increased by more than 20-fold when the temperature was shifted to 32.5°C (Fig. 3.6).

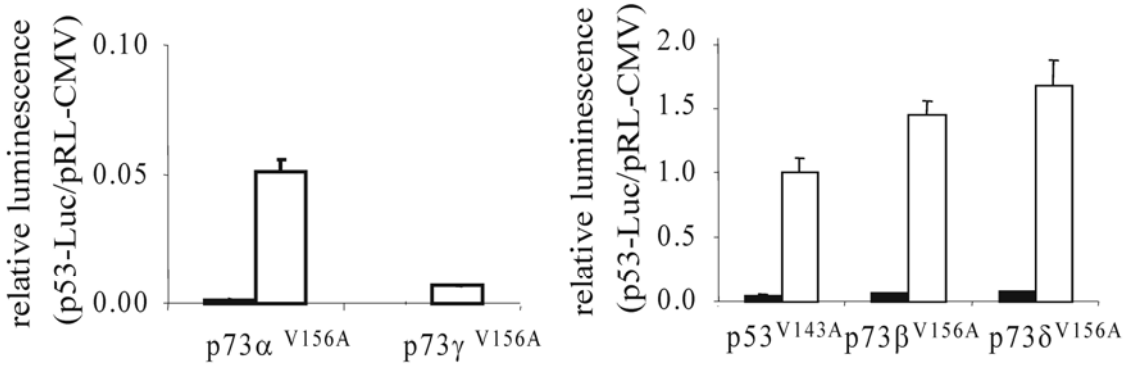

Fig. 3.6. **The $p73^{V156A}$ mutant is temperature-sensitive.** The cells were transfected as in A with the ^{V156A} mutants of p73 (pcDNA3-HA-$p73\alpha^{A156V}$, pcDNA3-HA-$p73\beta^{A156V}$ pcDNA3-HA-$p73\chi^{A156V}$ and pcDNA3-HA-$p73\delta^{A156V}$) or the human $p53^{V143A}$ mutant. At 24 h after transfection, the cells were shifted to 38.5°C (filled bars) or 32.5°C (open bars) and analysed 24 h later.

Finally, to confirm the inhibition of p63- and p73-induced p53-like reporter gene activity by mutant p53, the various p63 and p73 isoforms were transfected in pSUPER puro p53-transfected LN-18 cells or control transfectants. Overexpression of transcriptionally active plasmids reliably induced luciferase activity, suggesting that p63 and p73 signalling can occur in the presence of mutant p53 variants and may mainly depend on the relative abundance of p53-related transcription factors in the cell (230). Yet, when mutant p53 expression was suppressed by pSUPER puro p53, the signals obtained were up to ten-fold stronger than in the respective control cells. It should be noted that some residual mutant p53 was still present in the knock-down cell line (Fig. 1A). This may explain why p63α as well as the p73α and γ isoforms, which are weaker activators of the p53-Luc plasmid, are less well de-repressed from p53-mediated suppression than the p73β and p73δ isoforms (Fig. 3.7) which induce stronger p53-like transcriptional activity (Fig. 3.4). Further, it was found that the p53-like reporter gene activity observed in the p53 knock-down cell line was abrogated by the ΔNp63α, ΔNp63β and p73ΔNβ isoforms, confirming their dominant-negative action over the endogenous isoforms of p63 or p73.

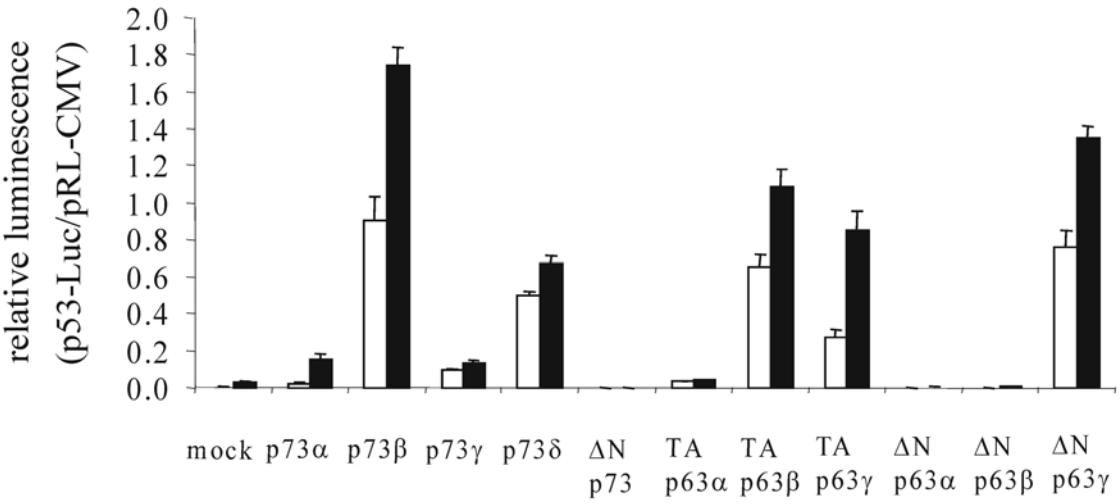

Fig. 3.7. **Presence of mutant p53 inhibits p63- and p73-dependent reporter gene activation.** LN-18 pSUPERpuro p53-transfected cells (filled bars) or control transfectants (open bars) were transiently co-transfected with p53-Luc, pRL-CMV and plasmids encoding the different isoforms of p63 and p73. Luciferase activities were determined as in Fig. 3.2 and are expressed relative to the activity induced by pcDNA-HA-p53 in LN-18 pSUPER puro p53 cells.

Discussion

These data demonstrate that the PathDetect® p53 cis-reporter gene plasmid, a typical reporter for the measurement of p53 transcriptional activity, is also activated by p63 and p73. This raises concerns about the specificity of p53-related data obtained by this and similar assays and suggests that often only integrated information on p53 and its family members is obtained. While several p53-dependent promoters including p21, bax, mdm2, gadd45 and cyclin G respond to p63 (231) and p73 (232) and thus resemble the artificial p53-responsive enhancer element $(TGCCTGGACTTGCCTGG)_{15}$ contained in the *PathDetect*® p53-Luc reporter, activation by all three family members is not a general characteristic of p53-dependent promoters. This is because only 6 of 36 p53-induced transcripts were upregulated by tetracycline-dependent induction of p73α in DLD-1 colon cancer cells (233). Other promoters are activated by p63 and p73 only (234). Thus, the relative activity of p53, p63 and p73 isoforms appears to be promoter-dependent, allowing for a finely differentiated cellular response. Further fine-tuning may occur in a cell-type specific way through the presence of co-factors like brn-3a, which shows synergy with p53 at the p21, but antagonism at the bax promoter (235). Other co-factors like MDM-2 (236), ASPP/iASPP (237) or PARC (238) show different (MDM-2) or yet unexplored interactions with the various p53 family members, adding further complexity.

IV. Death receptor-mediated apoptosis in human malignant glioma cells: modulation by the CD40/CD40L system

For help with this project I wish to thank Dr. Dagmar Schneider (at that time in Heinz Wiendl´s Neuro-Immunology group in the Department of General Neurology, Hertie Institute for Clinical Brain Research) who performed the immunohistochemical stainings. Prof. Richard Meyermann (Institute for Brain Research, University of Tübingen Medical School, 72076 Tübingen, Germany) helped with the assessment and photography of these stainings and provided the material. CD40L-transfected BHK and mock transfected BHK cell, as well as G28.5 antibody, were kindly provided by Dr. Hartmut Engelmann (Institute for Immunology, University of Munich, 80336 Munich, Germany). The bispecific antibody constructs used in this study were generated by Dr. Gundram Jung (Department of Immunology, Institute for Cell Biology, University of Tübingen, 72076 Tübingen).

Introduction

CD40 is a member of the TNFR family which has been assumed to chiefly mediate antiapoptotic signalling, proliferation and differentiation in B cells (239, 240). The cognate ligand, CD40L, is mainly expressed on activated T cells and platelets (241). CD40L expression has also been described on macrophages, smooth muscle and endothelial cells (242). CD40 contains a cytoplasmic motif reminiscent of the death domain which mediates TNF-R- and CD95-dependent apoptosis. Accordingly, CD40 mediates cell death in certain transformed cell lines, including neuroblastoma cells (243) and other tumour cells of mesenchymal and epithelial origin (244, 245). Given the lack of a proper death domain in CD40 homologous to that of CD95 or TNF-R, the mechanisms underlying the cytotoxic effects of CD40L mediated by CD40 ligation have not been resolved (246). It has been suggested that CD40 stimulation induces the production of membrane-anchored TNF-α which then engages TNF-R1 (p55) at the cell surface, thus triggering the death receptor-dependent pathway involving caspases 8 and 3 (247). The synergistic cytotoxic effects of CD40 and TNF-R1 (p55) activation (183, 245, 247, 248) as well as the protection from CD40L-induced apoptosis by antagonistic TNF-R1 (p55) antibodies (247) support this model. Alternatively, CD40 ligation may increase CD95L or TRAIL mRNA and protein levels (249, 250).

Initiation of apoptosis via death receptors such as TNF-R, CD95, DR4/TRAIL-R1 or DR5/TRAIL-R2 by recombinant ligands or agonistic antibodies is currently being explored as a therapeutic approach to malignant gliomas (67, 251-253). A potential modulation of the sensitivity of malignant glioma cells to cytotoxic cytokines by the CD40/CD40L system would therefore be of clinical interest.

Materials and Methods

Materials. Isoleucine zipper CD40L was generously provided by Immunex (Seattle, WN). Mouse monoclonal antibodies to human CD40 included mAb89 from Immunotech-Coulter (Marseille, France), 5C3 from BD Pharmingen (Heidelberg, Germany), HB14 from Caltag (Hamburg, Germany) and G28.5 (raised in the laboratory of H. Engelmann). Further antibodies were TRAP-1 mouse anti-human CD40L and 4C10-5 mouse anti-human PARP from BD Pharmingen, mouse anti-human caspase 3 and mouse anti human FADD (#C31720 and F33620, Transduction Laboratories, Lexington, KY), C5 and C15 mouse anti-human caspase 8 (generously provided by P.H. Krammer, Heidelberg, Germany), M3 mouse anti-human CD95 (American Type Culture Collection, Manassas, VA), goat anti-human Apo2L/TRAIL #AF-375 (R&D Systems, Wiesbaden, Germany), W27 mouse anti-human hsp-70 and rabbit anti-human CD95 FL-335 and C-20 (Santa Cruz, Santa Cruz, CA). Antibodies to TRAIL receptors 1-4 were generously provided by H. Walczak (Heidelberg, Germany). Anti-TNF-R1 (p55) antibody (H398) was generously provided by Dr. P. Scheurich (Stuttgart, Germany). The generation of the bispecific antibody constructs using switch variants of anti-human Apo-1 has been described (182). CHX was purchased from Sigma (St. Louis, MO), MG-132 and Bay 11-7082 from Calbiochem (Hamburg, Germany), PHA from Biochrom (Berlin, Germany) and zVAD-fmk and DEVD-amc from Bachem (Heidelberg, Germany). Human IFN-γ and TNF-α were obtained from Roche (Mannheim, Germany). Apo2L/TRAIL.0 was provided by A. Ashkenazi (Genentech, South San Francisco, CA). CD95L-containing supernatant was harvested from CD95L-transfected N2A neuroblastoma cells (254).

Cell lines. The human glioma cell lines, kindly provided by Dr. N. de Tribolet (Lausanne, Switzerland), have been characterized previously (197). The cells were maintained in DMEM containing 10% FCS and penicillin (100 IU/ml)/streptomycin (100 μg/ml). Primary human glioma cell lines were prepared from surgically obtained glioma specimens as described (253). The human ovary adenocarcinoma cell line EFO-27 was obtained from the German Collection of Microorganisms (Braunschweig, Germany). Cells were cultured in RPMI 1640 containing 2 mM L-glutamine, 1 mM sodium pyruvate and amino acids with addition of 20% FCS and penicilline (100 IU/ml)/streptomycine (100 μg/ml). The hepatocellular carcinoma cell line Hep-G2 was

from the American Type Culture Collection (Manassas, VA). CD40L-transfected BHK cells and the respective neo control transfectants have been described earlier (183). Before use, these cells were fixed in paraformaldehyde and washed thoroughly. For the generation of stable CD40 transfectants, the cells were transfected with a pcDNA3 control or a pcDNA3 CD40 plasmid generously provided by A. Eliopoulos (Birmingham, UK) (255). Transfection was carried out using FuGene transfection reagent (Roche). The cells were selected in medium containing 0.5 mg/ml neomycin (G418) (Calbiochem, Bad Soden, Germany).

RT-PCR. Total RNA was extracted using the RNeasy RNA purification system (Qiagen, Hilden, Germany). RT-PCR for the detection of CD40 mRNA expression was performed according to standard procedures. The following primers were used with an annealing temperature of 62°C: 5′-CTCGCTATGGTTCGTCTGCCTC-3′ (42-63), 5′-CTCCTGGGTGACCGGTTGGCA-3′ (839-818), 5′-CTGCCCAGTCGGCTTCTT CTC-3′ (482-502) and 5′-GAGAAGAAGCCGACTGGGCAG-3′ (502-482). CD95 was amplified at 59°C annealing using 5'-GAGACTCAGAACTTGGAAGGC-3' (133-153) and 5'-CTTTGCACTTGGTGTTG CTGG-3' (390-370). To test for expression of CD40L, 5′-CCATGAGCAACAACTTGGTAAC-3′ (479-500) and 5′-CACTTGGC TTGGATCAGTCAC-3′ (780-760) were used at 62°C annealing temperature. β-actin was amplified at 55°C using 5′-TGTTTGAGACCTTCAACACCC-3' (409-429) and 5'-AGCACTGTGTTGGCGTACAG-3' (937-918).

Northern blot. Denatured total RNA (10 µg) was loaded on a 1% agarose gel containing 6.7% formaldehyde. The RNA was separated at 100 V, transferred to a Hybond N+ membrane (Amersham, Freiburg, Germany) using capillary blotting and cross-linked in a UV stratalinker 1800 (Stratagene, La Jolla, CA) at 1200 J. Methylene blue staining was performed as a loading control. The membrane was preincubated for 2 h in Church buffer at 65°C. The probe was constructed by cutting CD40 or CD95, respectively, from expression plasmids. The CD95 plasmid was obtained from N. Itoh (Osaka, Japan). The full-length gene sequences were purified by gel extraction (Qiagen, Hilden, Germany) and labeled using 5 µl (~1.6 Mbq) dCTP and the Rediprime II random labelling system (Amersham). Filters were hybridized overnight at 65°C in a hybridization oven with a rotisserie device using Church buffer. Binding of radioactive probes was visualized

using a PhosphoImager (FujiBasReader 1500, Fuji, Kangawa, Japan). Loading was controlled by assessing ß-actin mRNA expression.

Immunoblot analysis. Cellular soluble proteins (20 µg/lane) were loaded on a 12% acrylamide gel (Biorad, Munich, Germany). Anti-TNF-R1 (p55) antibody H398 recognizes an epitope that is only present under non-reducing conditions, otherwise β-mercaptoethanol (5%) was added. After transfer to nitrocellulose (Biorad), the blots were blocked in PBS containing 5% skim milk and 0.05% Tween 20 and incubated overnight at 4°C with antibodies to CD40 (G28.5), CD95 (FL-335 and C-20), TNF-R1 (p55), caspase 3 or caspase 8 (2 µg/ml). Visualization of protein bands was accomplished using HRP-coupled secondary antibody (Sigma) and ECL (Amersham).

Immunoprecipitation. The cells (1.5 x 10^6/condition) were detached, washed in PBS and lysed for 30 min on ice in a buffer containing 10 mM Tris-HCl (pH 7.4), 150 mM NaCl, 1% NP40, 2 mM $MgCl_2$, 2 µM EDTA, 1 µM pepstatin, 1 µM leupeptin and 0.1 mM PMSF. Lysates were centrifuged and pre-cleared on a shaker using protein A/G Plus sepharose (Santa Cruz). Cleared lysates were then divided for either direct loading or immunoprecipitation with 2 µg of antibody (30 min, 4°C, constant agitation). For pull-down (4 h, 4°C, under shaking), protein A/G Plus sepharose was added. Precipitates were pelleted in a tabletop microcentrifuge. Pellets were washed three times in lysis buffer. Finally proteins were recovered by boiling for 5 min in 50 mM Tris-HCl, pH=6.8, 2% SDS, 0.1% bromphenol blue and 10% glycerol and loaded onto an agarose gel (12%).

Flow cytometry. The cells were treated as indicated, detached with cell dissociation buffer (Gibco, Karlsruhe, Germany) and resuspended in flow cytometry buffer (PBS containing 1% bovine serum albumin and 0.01% sodium azide). The cells were stained with CD40 or CD40L antibodies (10 µg/ml) or appropriate isotype control antibodies. The SFI was defined as the ratio of mean fluorescence obtained with specific antibody divided by mean fluorescence obtained with the isotype control antibody. Intracellular staining was performed with the Cytofix/Cytoperm^{TM} kit (BD Pharmingen). Alternatively the cells were permeabilized with ice-cold ethanol (70%) for 5 min.

Immunocytochemistry. The cells were seeded on coverslips (5 x 10^4 cells/well in a 24 well plate), allowed to adhere overnight and stimulated with CD40L or G28.5 agonistic anti-CD40 antibody for the indicated time intervals. Incubations were terminated on ice and all further steps were performed at 4°C. The cells were washed twice in PBS and once in blocking buffer (PBS with 2% goat serum) before FITC-conjugated goat anti-mouse secondary antibody (1:250, Sigma) was added. After three further washes, the cells were fixed in 4% ice-cold paraformaldehyde, mounted with Vectashield mounting medium (Vector Laboratories, Peterborough, UK), and analysed and photographed (at 40x magnification) on a Leica DM IRBE inverted microscope (Leica, Wetzlar, Germany).

For double-staining of CD40 and TNF-R1 (p55) the cells were fixed with 4% paraformaldehyde for 5 min, washed, blocked with normal goat serum (10% in PBS with 1% Triton X-100) and incubated for 2 h with antibodies against CD40 (G28-5, IgG1-κ, 5 µg/ml), TNF-R1 (p55) (H398, IgG2a, 5 µg/ml) or the respective isotype controls in PBS containing 1% serum and 0.1% Triton X-100. After washing with PBS visualization of bound antibodies was performed using isotype-specific goat anti-mouse IgG_1-PE and goat anti-mouse IgG_{2a}-Alexa Fluor 488 antibodies (Molecular Probes, Eugene, OR). Cross-reactivity was controlled by mismatched antibody pairing. Cells were analyzed by confocal laser scanning microscopy (LSM 510, Carl Zeiss, Jena, Germany).

Immunohistochemistry. Cryosections (10 µm) of human glioblastomas (WHO grade 4) were fixed in acetone, air-dried, washed with TBS and stained with G28-5 anti-CD40 antibody or control IgG_1-κ (20 µg/ml). Avidin biotin complex (ABComplex, Dakopatts, Glostrup, Denmark) consisting of biotinylated anti-mouse secondary antibody and HRP-conjugated avidin was used at 1:400. Stainings were developed for 1-2 min with diaminobenzidine. Nuclei were counterstained with haemalaun. Umbilical chord was taken as positive control. Normal human brain served as a negative control.

Viability assay. The cells were seeded in 96 well plates at 10^4 cells/well and allowed to attach for 24 h. CD40L was added in fresh serum-free medium for up to 72 h. In some experiments, the cells were pretreated with IFN-γ or cotreated with CHX for 16 h. Viable cell counts were obtained by crystal violet staining. When paraformaldehyde-

fixed BHK cells were used to deliver the apoptotic signal, the cells were removed by washing before the crystal violet stain was performed.

Proliferation assay. The cells were pulsed for 24 h with [methyl-^{3}H] thymidine (0.5 μCi, Amersham), lysed and harvested with a cell harvester (Inotech, Dottikon, Switzerland). Incorporated radioactivity was bound to a glass fibre filtermat (Wallac, Turku, Finland). The filtermat was wetted with Ultima Gold Scintillation Cocktail (Packard, Dreieich, Germany) and radioactivity was determined in a Wallac 1450 Microbeta Plus Liquid Scintillation Counter (Wallac, Turku, Finland).

DEVD-amc-cleaving caspase activity. The cells (0.5 x 10^4) were seeded in 96 well plates, treated as indicated, lysed in 25 mM Tris-HCl, pH 8.0, 60 mM NaCl, 2.5 mM EDTA, 0.25% NP40 for 10 min, and the substrate DEVD-amc was added at 12.5 μM. Caspase activity was assessed by fluorescence using a Millipore fluorimeter at 360 nm excitation and 480 nm emission wave lengths.

NF-κB and IL-8 reporter assay. The cells were transfected with the PathDetect® NF-κB cis-reporter gene plasmid (#219077 Stratagene) or with an IL-8-luc construct generously provided by M. Kracht (Hannover, Germany) (256). The NF-κB–responsive element is $(TGGGGACTTTCCGC)_5$. Transfection was performed using FuGene (Roche). Treatment with TNF-α (10 ng/ml, 6 h) (Roche) was used as a positive control. At 24 h after transfection, CD40L was added to some samples. Another 6 h later, the cells were washed and lysed using Reporter Lysis Buffer (Promega, Madison, WI). Following one freeze-thaw cycle, the lysates were transferred to a LumiNuncTM plate (Nunc, Roskilde, Denmark), Luciferase assay substrate (100 μl, Promega) was added automatically, and luminescence was measured in a LumimatPlus (EG&G Berthold, Pforzheim, Germany). The background was subtracted from all values.

TNF-α ELISA. TNF-α concentrations in cell lysates and supernatants were determined by ELISA (Endogen, Woburn, MA).

Generation of bispecific antibody fragments. Bispecific antibody fragments ($bsFab_2$) were prepared by selective reduction and reoxidation of hinge region disulfide bonds as described (257). The reaction conditions prevent the formation of homodimers and

allow almost complete hybridization of modified Fab fragments of the parental antibodies. For this study, the IgG2A variant of the Apo-1 antibody (to CD95) (258) generously provided by P.H. Krammer (Heidelberg, Germany) was hybridized to antibodies directed to CD20 (L3B3, provided by Baxter, Munich, Germany) or CD40 (G28.5).

Statistical analysis. Data are representative of experiments performed three times with similar results. Viability studies were performed using triplicate wells. Significance was assessed by t-test ($^{*}p<0.05$, $^{**}p<0.01$).

Results

CD40 expression in human glioma cell lines

CD40 mRNA expression was assessed in untreated or IFN-γ-stimulated (500 U/ml, 48 h) glioma cells by RT-PCR (Fig. 4.1A) and Northern blot (Fig. 4.1B). The levels of mRNA varied considerably, however, some signal was detected in all cell lines by both methods. Immunoblot revealed a rather homogenous expression among the cell lines, suggesting that the regulation of CD40 protein levels does not only depend on CD40 gene transcription, but is regulated posttranscriptionally as well (Fig. 4.1C).

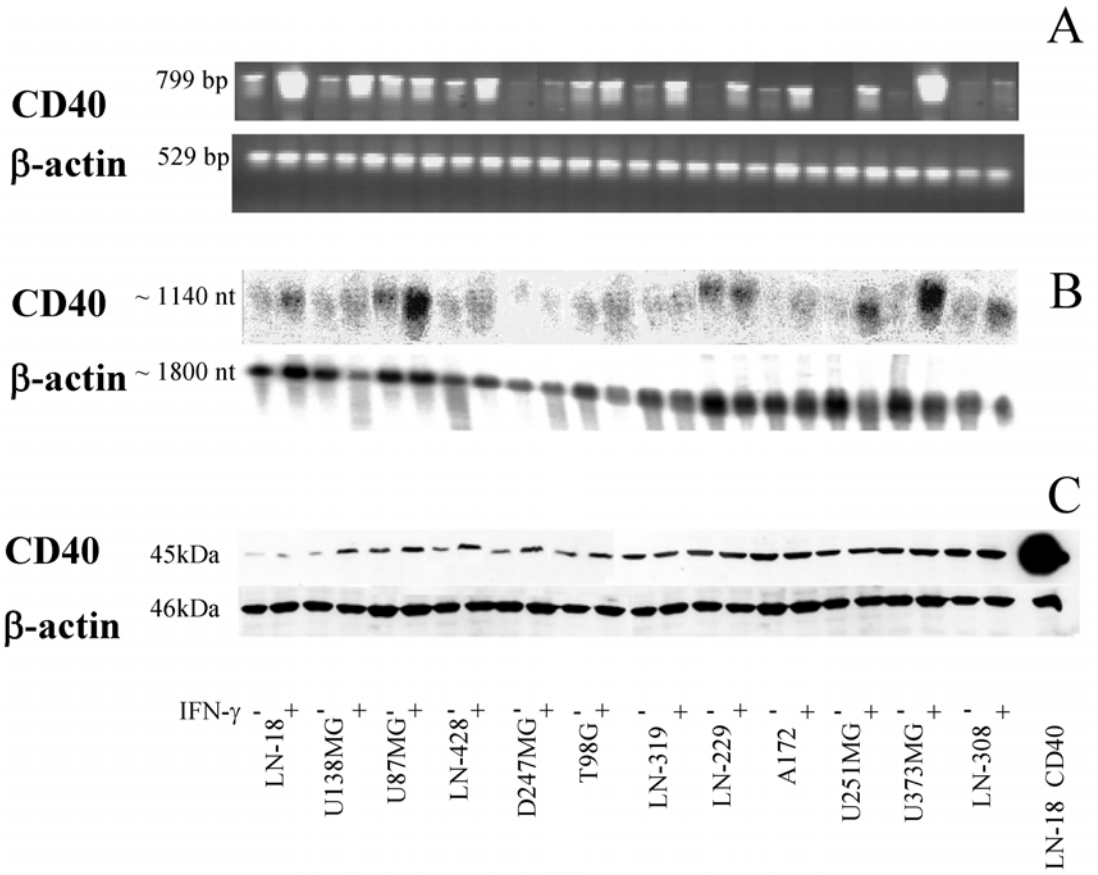

Fig. 4.1. **Constitutive and IFN-γ-inducible CD40 expression in human glioma cell lines.** The cells were untreated or treated with IFN-γ (500 U/ml) for 48 h. CD40 expression was analysed by RT-PCR (A), Northern blot (B) or immunoblot (C). The primers 5′-CTCGCTATGGTTCGT CTGCCTC-3′ (42-63) and 5′-CTCCTGGGTGACCGGTT GGCA-3′ (839-818) were used for RT-PCR for 28 cycles to allow for a semi-quantitative assessment.

Surprisingly flow cytometry (of unpermeabilized cells) revealed that only 1 of 12 glioma cell lines, U87MG, showed constitutive CD40 protein expression at the cell surface (Fig. 4.2A). Further, none of 5 primary polyclonal glioma cell cultures showed

constitutive CD40 expression at the cell surface (data not shown). The exposure to IFN-γ resulted in enhanced CD40 mRNA expression assessed by Northern blot in 11 of 12 cell lines (LN-18, U138MG, U87MG, LN-428, D247MG, LN-319, LN-229, A172, U251MG, U373MG, LN-308). At the total protein level determined by immunoblot, IFN-γ exposure increased CD40 levels in 5 of 12 cell lines (LN-18, U138MG, U87MG, LN-428, D247MG). The specificity of CD40 labelling was confirmed using lysates from CD40-transfected LN-18 glioma cells (Fig. 4.1C, right outer lane) and by competitive inhibition of labelling using lysates from CD40-transfected glioma cells (data not shown). At the cell surface, IFN-γ enhanced CD40 expression in U87MG cells, and induced low level CD40 expression in LN-18 and LN-229 cells (Fig. 4.2A,B).

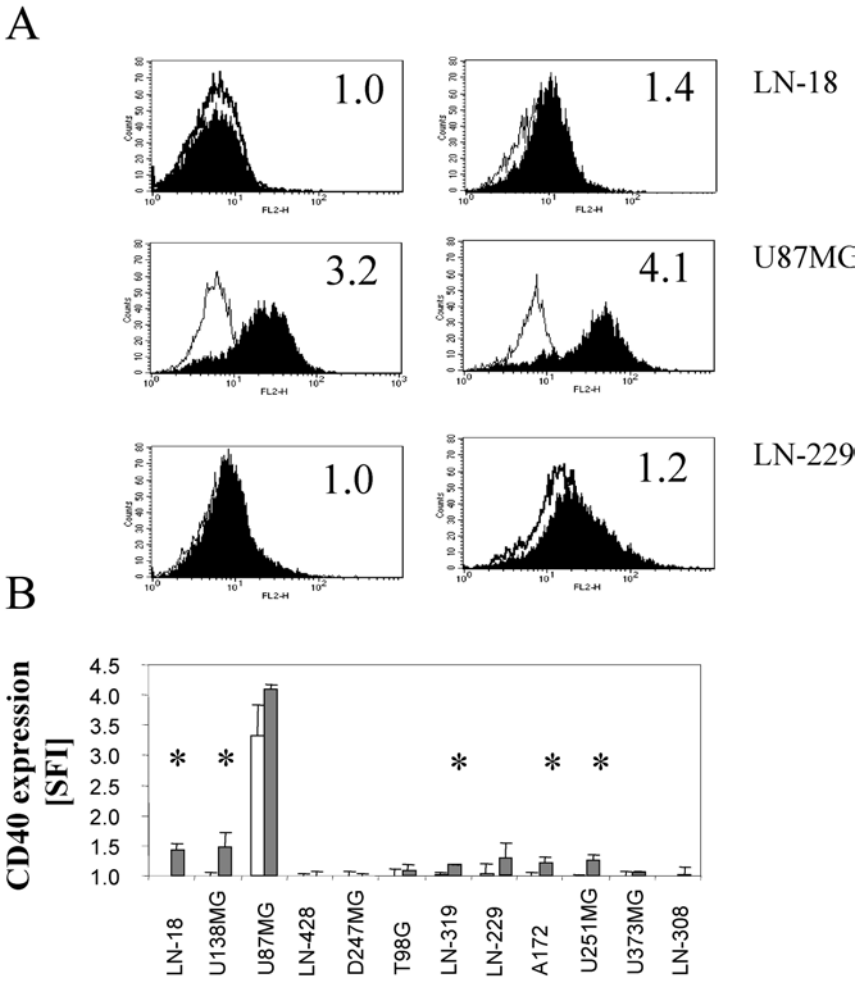

Fig.4.2 **CD40 surface expression in human gliomas is inducible by IFN-γ.** In A, LN-18, U87MG and LN-229 cells are shown untreated (left) or IFN-γ-treated (right). Filled curves indicate signal obtained with specific antibody, open curves indicate signal obtained with isotype control antibody. Specific fluorescence indexes (SFI) are indicated in the graphs. B. Synopsis of CD40 cell surface expression of untreated (open bars) or IFN-γ-treated (grey bars) glioma cells expressed as SFI. Note that a value of 1 indicates the absence of CD40 expression (*$p<0.05$, t-test, presence *versus* absence of IFN-γ).

To account for the discrepancy between the detection of CD40 in total cellular lysates, but not on the cell surface in most cell lines, several attempts were made to stain CD40 intracellularly using flow cytometry, but none of the available antibodies (G28.5, mAb89, 5C3 and HB14) gave a signal when used for the flow cytometric analysis of cells permeabilized with Cytofix/Cytoperm reagents or with ethanol. Further, the pretreatment of the cells with 0.1% acetic acid in 0.15 M NaCl, which has been reported to free antigens from bound ligands (259), did not result in the surface staining of otherwise negative cell lines (data not shown). The possibility that glioma cells might produce a soluble CD40 molecule lacking the transmembrane domain corresponding to amino acids 194-215 or nucleotides 629-694 or release full-length CD40 into the cell culture supernatant was also considered. However, immunoblot analysis of supernatant protein and a transmembrane region-spanning RT-PCR failed to support these possibilities (Fig. 4.1A). Instead, glioma cells appeared to express exclusively full-length CD40 while various alternatively spliced isoforms were detected in PBMC (260) (data not shown). CD40L RNA and protein were not detected in any glioma cell line as assessed by RT-PCR and flow cytometry, using PBMC as a positive control (see Table 1).

Table I. **Death ligand expression in human malignant glioma cells**

	TNF-α[a]	CD95L[b]	Apo2L/TRAIL[c]	CD27L[d]	CD40L[e]
LN-18	-	+	+	+	-
U138MG	-	+	+	+	-
U87MG	-	+	nd	+	-
LN-428	-	+	+	+	-
D247	-	+	nd	+	-
T98G	-	+	+	-	-
LN-319	-	+	+	+	-
LN-229	-	+	nd	+	-
A172	-	+	nd	+	-
U251MG	-	+	+	+	-
U373MG	-	+	+	+	-
LN-308	-	+	+	+	-

[a]ELISA and bioassay (261), [b]RT-PCR, immunoblot or flow cytometry (204, 262-264), [c]RT-PCR and immunoblot (265), [d]Northern blot, immunoblot and flow cytometry (261), [e]RT-PCR and flow cytometry (this study) (nd no data)

CD40 expression in primary human glioblastoma tissue

Cryosections from glioblastoma patients were stained for CD40 expression. While post mortem sections from patients with no reported neurological diseases or symptoms (further designated as normal brain tissue) showed no CD40 immunoreactivity (Fig. 4.3A), all glioblastoma samples showed CD40 expression ranging from scattered positive cells to over 30% of CD40-expressing cells (Fig. 4.3B). Both cell surface and intracellular staining was observed (Fig. 4.3C), suggesting that CD40 protein is not restricted to the outer cell membrane in glioma cells *in vivo* either. CD40-positive cells were identified as tumour cells by morphological criteria in all samples. Strong expression was also detected on tumour-associated blood vessels.

A

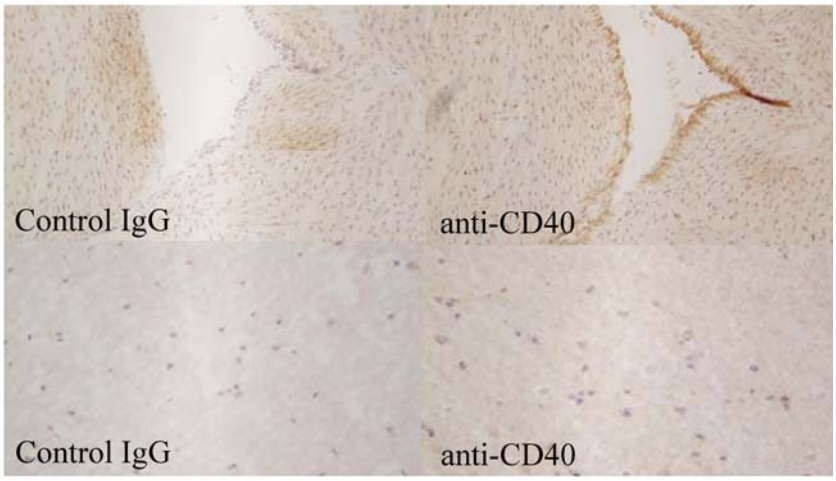

Fig. 4.3. **Human glioblastomas express CD40 *in vivo*.** Frozen tissue sections were immunostained with the CD40-specific mAb G 28.5 or isotype control. A. Umbilical cord (upper panel) and normal brain tissue (#636/02II, lower panel) (x200). Endothelial cells of blood vessels in the umbilical cord are CD40-positive (positive control).

B

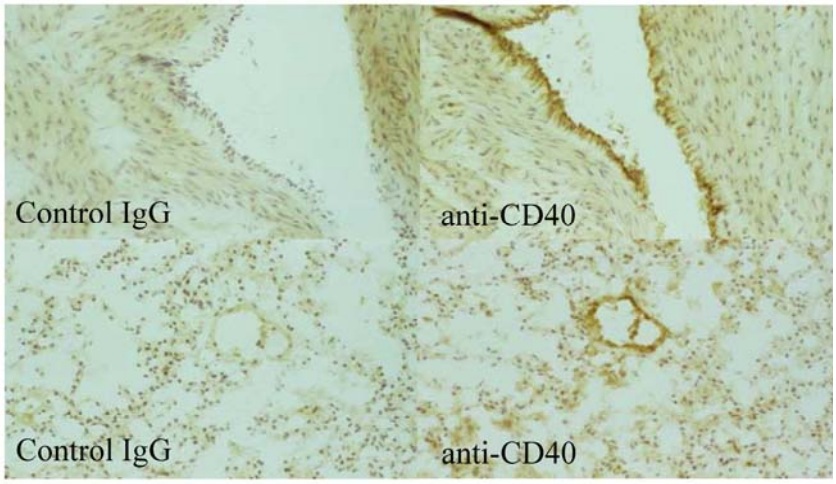

B. Umbilical cord (upper panel) and glioblastoma section (#551/02, lower panel) (x 200, overview).

C

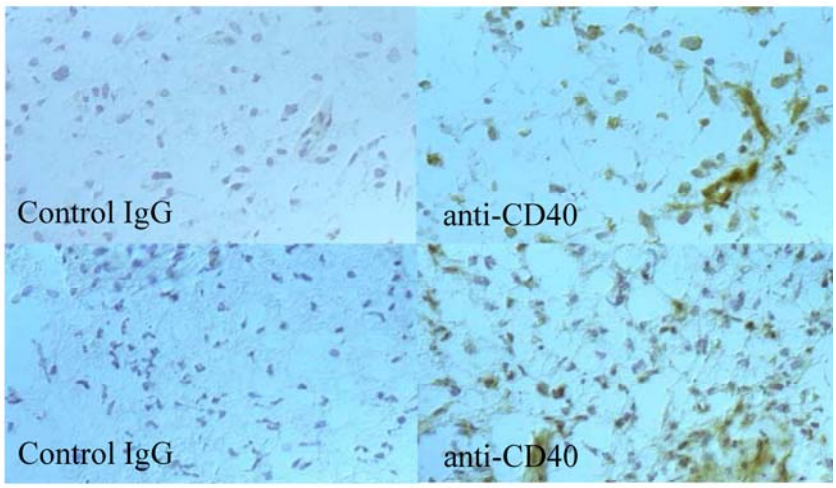

C. For better visualization of tissue structure, glioblastoma sections (#551/02, upper panel; #1110/02, lower panel) stained with the CD40-specific mAb G 28.5 or isotype control were photographed under polarised light (x400).

Human glioma cell lines are refractory to CD40L-mediated signalling

To assess the death signalling properties of CD40 expressed on glioma cells, untreated and IFN-γ-stimulated EFO-27 ovarian adenocarcinoma cells were treated with isoleucine zipper CD40L which is cytotoxic to lymphoma and epithelial ovarian carcinoma cells (266, 267). While unstimulated cells were almost unresponsive (a small effect was observed in a 72 h cytotoxicity assay – data not shown), cell death was readily induced in IFN-γ-pretreated EFO-27 and Hep-G2 cells (Fig. 4.4A and data not shown). Apoptosis was greatly enhanced by inhibition of protein synthesis with cycloheximide (10 μg/ml for 16 h) (Fig. 4.4A). However, U87MG glioma cells were refractory to soluble CD40L at concentrations up to 10 μg/ml (Fig. 4.4B). This resistance was not overcome when the cells were pretreated with IFN-γ, or cotreated with CHX, or both (Fig. 4.4C). CHX alone reduced cell density by about 20% within 16 h, due to growth arrest, but not cytotoxic effects as demonstrated by LDH release assays (data not shown). IFN-γ alone had no effect on cell density in these experiments. Neither did the pharmacological NFκB inhibitor, Bay 11-7082, sensitize U87MG cells to the cytotoxic properties of CD40L.

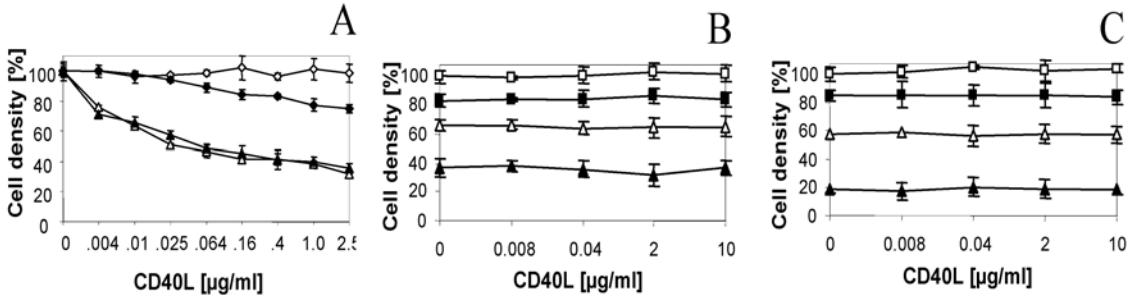

Fig. 4.4. **CD40-expressing glioma cells are refractory to CD40L-induced cell death.** A. Untreated (open symbols) or IFN-γ (48 h, 500 U/ml)-stimulated (closed symbols) EFO-27 cells (10^4/well) were treated with CD40L in the absence (rhomboids) or presence (triangles) of CHX (10 μg/ml). Cell density was assessed at 16 h by crystal violet staining. The data are expressed relative to cells exposed to vehicle, CHX, IFN-γ or their combination alone. B,C. Untreated (B) or IFN-γ (48 h, 500 U/ml)-stimulated (C) U87MG cells (10^4/well) were treated with CD40L in the absence (squares) or presence (triangles) of CD95L with (filled symbols) or without (open symbols) CHX (10 μg/ml). Cell density was assessed at 16 h by crystal violet staining and is expressed in % of the untreated control. Note that either CD95L or CHX, and both in synergy, reduced cell density, but that these effects were unaffected by CD40L.

Similarly, IFN-γ-treated LN-18 and LN-229 cells did not acquire sensitivity to CD40-mediated cell death (data not shown). Alternatively, CD40L-transfected BHK cells, or the respective neo control transfectants (183) were used to deliver a death signal to unstimulated or IFN-γ-stimulated glioma cells, in the absence or presence of CHX. However, membrane-bound CD40L was unable to induce apoptosis either. In IFN-γ-treated or untreated LN-18, U87MG or LN-229 cells, there was no synergy of CD40L with death ligands such as CD95L (Fig. 4.4B,C) or Apo2L/TRAIL (data not shown). Also the resistance of U87MG and LN-229 cells to TNF-α induced apoptosis was not overcome by CD40L (data not shown). Further, soluble or membrane-bound CD40L did not induce NF-κB or IL-8 reporter gene activity in naïve U87MG (Fig. 4.5B, data not shown) or in IFN-γ stimulated LN-18, U87MG or LN-229 cells (Fig. 4.5C, data not shown) whereas untreated or IFN-γ stimulated Hep-G2 cells responded readily (Fig. 4.5A). Treatment with TNF-α (10 ng/ml), on the other hand, resulted in a 4-10-fold activation of these reporter genes in all cell lines. Finally [methyl-^{3}H] thymidine incorporation by these cell lines was not altered by treatment with CD40L whereas the reagent induced massive B cell proliferation (data not shown).

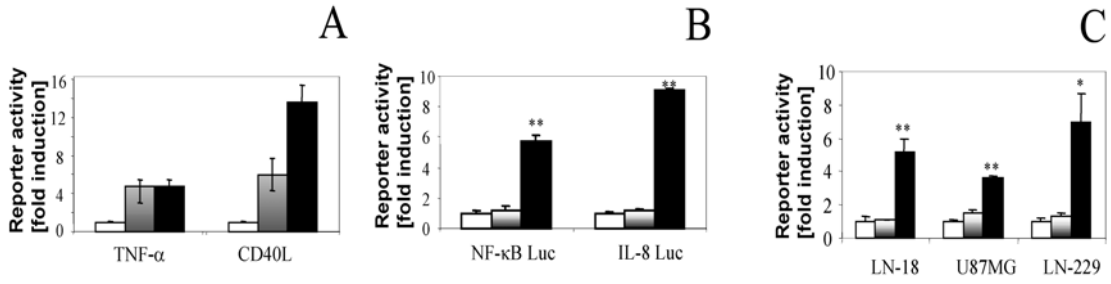

Fig. 4.5. **CD40-expressing glioma cells are refractory to CD40L-induced signalling** A. Untreated (shaded bars) or IFN-γ (48 h, 500 U/ml)-stimulated (filled bars) Hep-G2 cells (10^4/well) were treated with CD40L (1 μg/ml) or TNF-α (10 ng/ml) as a positive control. NF-κB reporter activity was assessed at 6 h. Data are expressed as fold induction compared with untreated control cells (open bars). B. NF-κB and IL-8 reporter activity were measured in untreated U87MG cells or cells treated with CD40L (1 μg/ml) (shaded bars) or TNF-α (10 ng/ml) (filled bars) for 6 h. Data are expressed as in A. In C, IFN-γ (48 h, 500 U/ml)-stimulated LN-18, U87MG and LN-229 cells were examined as in A for NF-κB reporter activity (*$p<0.05$, **$p<0.01$, t-test).

Gene transfer mediated overexpression of CD40 confers sensitivity to CD40L-induced cell death

Given these data, CD40 function or the signal transduction pathway triggered by CD40 may be disabled in glioma cell lines. Consequently it was attempted to generate U87MG and LN-18 sublines stably overexpressing CD40 using plasmid-mediated gene transfer. Whereas LN-18 CD40 transfectants showed high expression of CD40 (Fig. 4.6A), no stable overexpression was achieved in U87MG cells. Soluble and membrane-bound CD40L induced NF-κB and IL-8 reporter activity in CD40-transfected LN-18 cells (Fig. 4.6B, and data not shown), indicating that the signalling cascade was intact and that the physiological levels of CD40 expressed on naïve U87MG or IFN-γ-treated U87MG, LN-18 or LN-229 glioma cells were insufficient to transmit a signal. Further, CD40L was cytotoxic to CD40-transfected LN-18 cells, and its cytotoxicity was strongly enhanced by CHX (Fig. 4.6C).

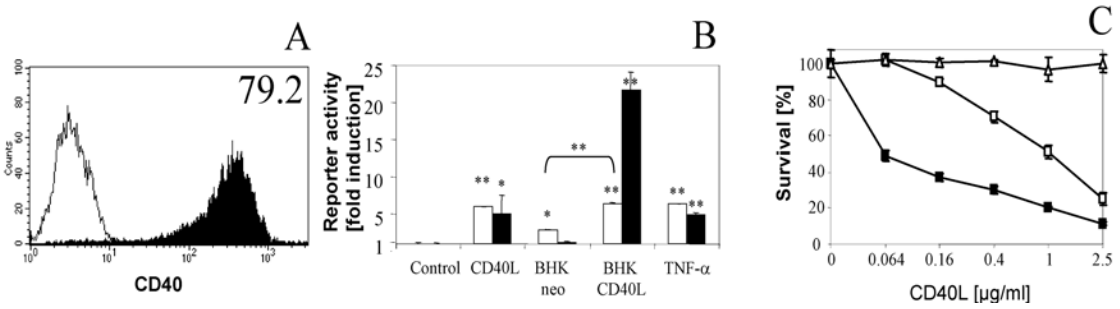

Fig. 4.6. **CD40-transfected LN-18 cells are susceptible to CD40L-induced apoptosis.** A. CD40 expression in CD40-transfected LN-18 cells was assessed by flow cytometry (see Fig. 1D for comparison). B. NF-κB (open bars) or IL-8 (filled bars) reporter gene activity were measured in CD40-transfected LN-18 cells after stimulation (6 h) with CD40L (1 µg/ml), BHK neo or BHK CD40L cells (at a 4:1 ratio of BHK:LN-18 cells) or TNF-α (10 ng/ml). C. CD40-transfected LN-18 cells (10^4/well) were treated with increasing concentrations of CD40L in the absence (open squares) or presence (filled squares) of CHX (10 µg/ml), or CHX and zVAD-fmk (50 µM) (open triangles) for 16 h. The data are expressed relative to cells exposed to vehicle, CHX, zVAD-fmk or their combination alone.

Since CD40 does not contain a proper death domain, CD40-dependent apoptosis has been attributed to the recruitment of other TNF family receptors. These receptors do not only need to trimerize, instead, super-aggregation induced by cross-linked ligands (268) may be required for the induction of apoptosis (269). Thus CD40-transfected LN-18 cells were examined for the "capping" of TNF receptor family members after

stimulation with trimeric CD40L or agonistic CD40 antibody (270). While no aggregation of TNF-R1 (p55), CD95 or TRAIL-R 1 or 2 was detected after treatment with CD40L (data not shown), clustering of CD40 itself was observed, beginning at 5 min after stimulation and peaking at 45-60 min (Fig. 4.7). In contrast to the cytotoxicity of CD40L in the absence or presence of CHX (Fig. 4.6C), CD40 clustering was insensitive to the pan-specific caspase inhibitor zVAD-fmk (data not shown).

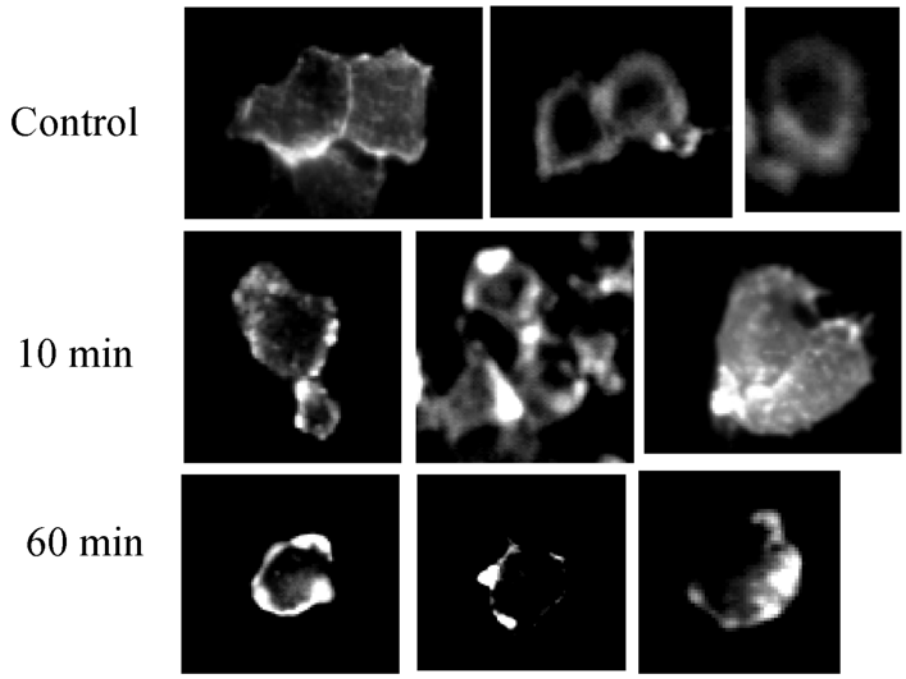

Fig. 4.7. **CD40L induces clustering of CD40 on LN-18 CD40 cells.** CD40-transfected LN-18 cells (5 x 10^4/well) were stimulated with agonistic G28.5 anti-CD40 antibody (10 µg/ml) for 0 min (top), 10 min (middle) or 60 min (bottom) before the cells were put on ice for life-staining using FITC-labeled goat anti-mouse secondary antibody. The cells were fixed for 5 min in 4% paraformaldehyde. Staining was visualized under a Leica DM IRBE microscope and photographed (40x).

The role of caspases in CD40L-induced cell death was further investigated using activity assays and immunoblot. There was a concentration-dependent induction of DEVD-amc cleavage at 6 h after exposure to CD40L in CD40-transfected LN-18 cells (Fig. 4.8A), but not in LN-18 neo cells, which, however, were sensitive to CD95L or

Apo-2L/TRAIL. Further, the processing of caspases 8 and 3 into the active fragments p18/caspase 8 and p17/caspase 3 and the cleavage of PARP into the 85 kDa and 25 kDa fragments characteristic for apoptosis was promoted by CD40L in CD40-transfected LN-18 cells but not in control transfectants (Fig. 4.8B and data not shown). Induction of apoptosis by TNF-α or TNF-α plus CD40L was included as a positive control.

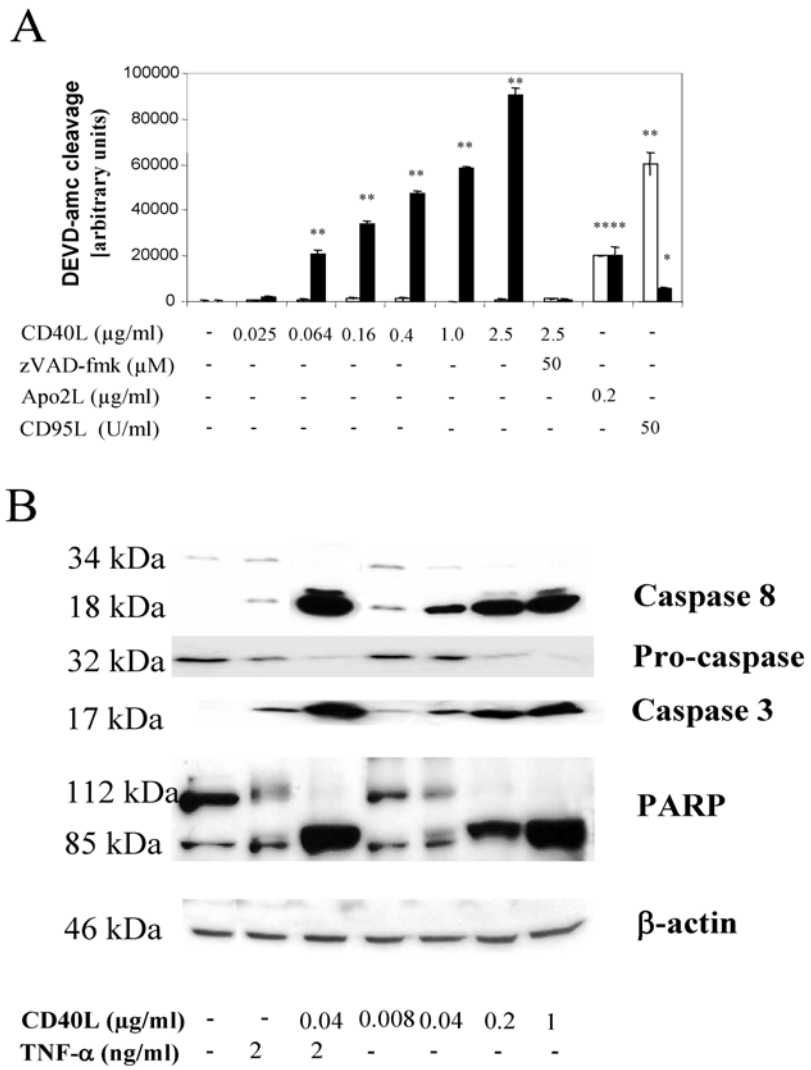

Fig.4.8. **CD40L-induced cell death is caspase-dependent.** A. DEVD-amc cleavage was assessed in lysates from CD40-transfected (filled bars) or mock-transfected (open bars) LN-18 cells at 6 h after treatment with CD40L. CD95L (50 U/ml) and Apo2L/TRAIL (0.2 µg/ml) were included as controls. B. The processing of caspases 8 and 3 and PARP was investigated at 6 h after treatment of CD40-transfected LN-18 cells with TNF-α (2 ng/ml) or CD40L (0.008, 0.04, 0.2, 1.0 µg/ml) alone or in combination (2 ng/ml TNF-α and 0.04 µg/ml CD40L). β-actin was included as a loading control.

Gene transfer mediated overexpression of CD40 confers resistance to CD95L-induced cell death

LN-18 is among the most sensitive cell lines to CD95-mediated apoptosis (253). Interestingly, CD95L-treated CD40-transfected LN-18 cells exhibited only little DEVD-amc cleavage (Fig. 4.8A) and did not respond with massive cell death (Fig. 4.9A). In contrast, their sensitivity towards Apo2L/TRAIL remained unaltered (Fig. 4.9B). A clonal artefact was excluded because bulk transfectants from three different transfections showed the same pattern of selectively induced resistance to CD95L, but not Apo2L/TRAIL (data not shown).

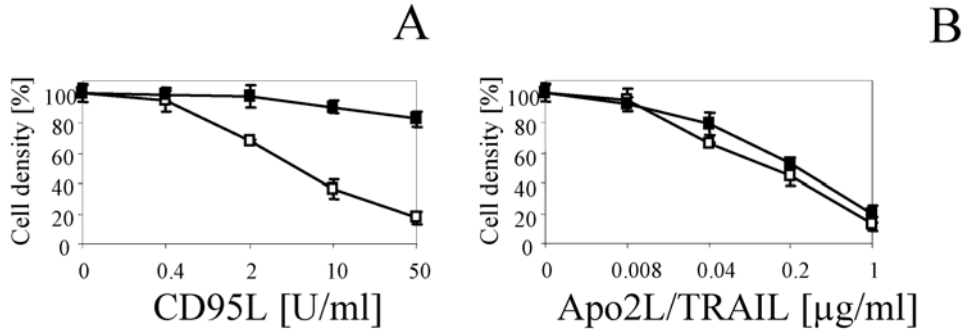

Fig. 4.9. **CD40 overexpression modulates CD95-mediated apoptosis.** LN-18 neo control (open squares) or CD40-transfected LN-18 cells (filled squares) were treated with CD95L (A) or Apo2L/TRAIL (B). Survival was assessed at 24 h by crystal violet staining.

Flow cytometry for CD95 and DR5 revealed a loss of CD95 expression whereas DR5 was still expressed at a rather high level (Fig. 4.10). The expression of the other Apo2L/TRAIL receptors remained also unchanged (data not shown).

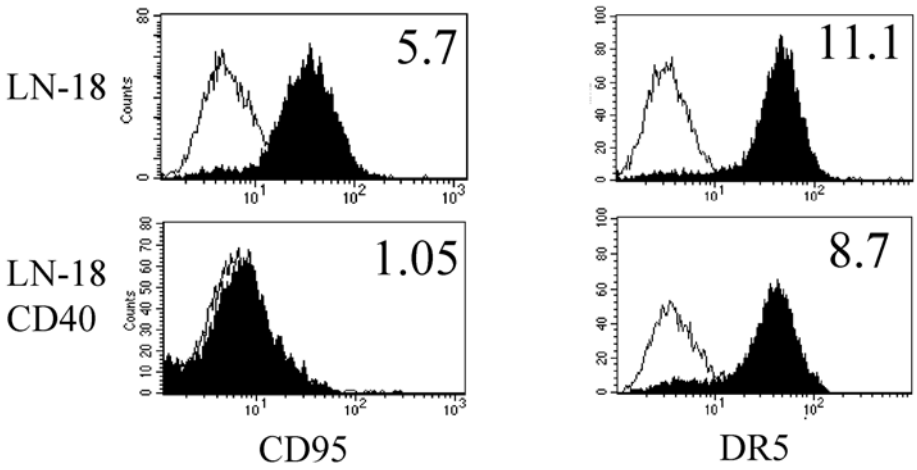

Fig. 4.10. **CD40 overexpression leads to decreased surface expression of CD95/Fas.** CD95 or DR5/TRAIL-R2 expression in LN-18 neo or CD40-transfected LN-18 cells were assessed by flow cytometry. SFI values are indicated.

This suggests that glioma cells were selected against high co-expression of CD95 and CD40. This issue was addressed by transient transfection assays using LN-18 and U87MG cells. Whereas the generation of stable CD40-overexpressing sublines had failed in U87MG cells, transient transfection was feasible: at 36 h after transfection, 60-70% of the cells showed enhanced CD40 expression at the cell surface. Interestingly, more than 50% of these cells had down-regulated CD95 expression (Fig. 4.11A). Coexposure to zVAD-fmk did not alter these results, indicating that cells expressing both receptors at high levels are not simply deleted by apoptosis (Fig. 4.11A, right panel). Similar results were obtained in LN-18 cells, and ectopic expression of the viral caspase inhibitor, crm-A, also failed to prevent the loss of CD95 at the cell surface of CD40-transfected LN-18 cells (data not shown). When cells from the same transfection were gated for CD40-overexpressing cells and for cells expressing CD40 at the endogenous level only, the groups showed prominent differences in CD95 expression, assessed either at the level of specific fluorescence index (SFI) values or of calculating the percentages of CD95-negative cells in the respective groups (Fig. 4.11B).

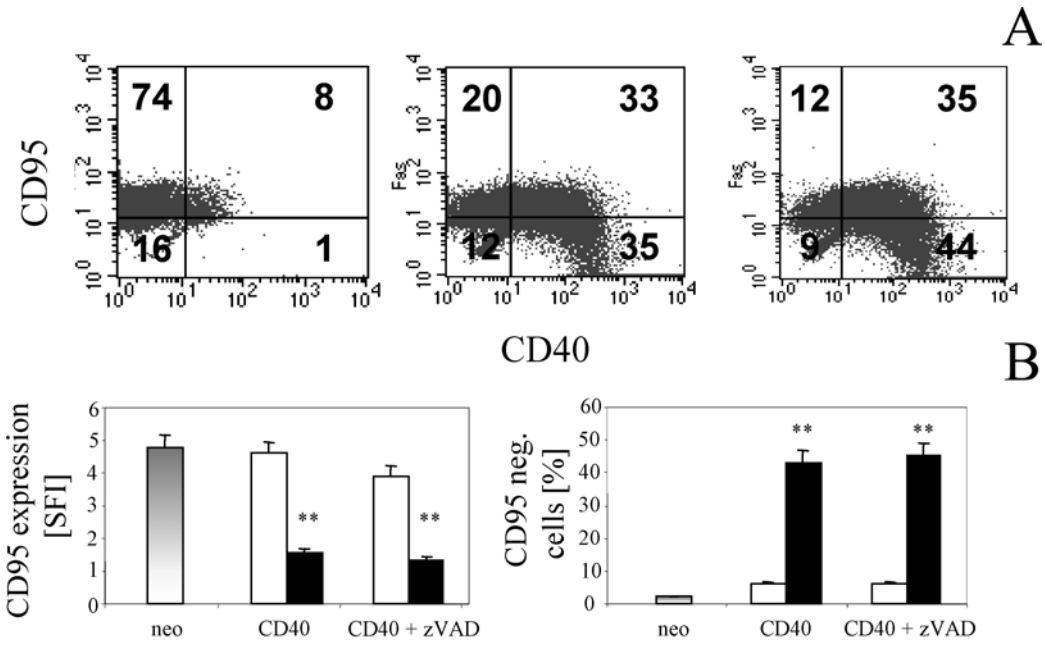

Fig.4.11. **Transient transfection with CD40 results in reduced CD95/Fas surface expression.** A. U87MG cells were transiently transfected with pcDNA3 neo (left panel) or pcDNA3-CD40 (middle and right panel). In the right panel, zVAD-fmk was added (100 μM). The cell surface expression of CD40 and CD95 was analysed at 36 h by flow cytometry. The percentages of cells in each quadrant are indicated in the graph. In the isotype controls, ≥ 97% of the cells were in the lower left quadrant (data not shown). B. U87MG cells from D were separately gated for non-transfected, this is, CD40-negative (open bars) and transfected cells (filled bars). U87MG control transfectants were also included as a pool (grey bars). CD95 expression was then quantified for the respective groups by histogram analysis. Data are expressed as SFI (left panel) or as percentages of CD95-negative cells (right panel) (*$p<0.01$, t-test).

To assess whether the protein level of CD95 was absolutely diminished in CD40-transfected LN-18 cells or whether the receptor was internalized, immunoblots for CD95 were also performed. Fig. 4.12A shows a striking reduction in total cellular CD95 levels in CD40-transfected LN-18 cells compared with LN-18 neo cells. In contrast, CD95 mRNA levels were unaltered (Fig. 4.12B), suggesting that CD95 protein levels were regulated at the posttranslational level. In fact, exposure to the proteasome inhibitor, MG-132, for 16 h almost restored CD95 protein levels in CD40-transfected LN-18 cells (Fig. 4.12C), suggesting that the forced expression of CD40 promoted the increased proteasomal degradation of CD95.

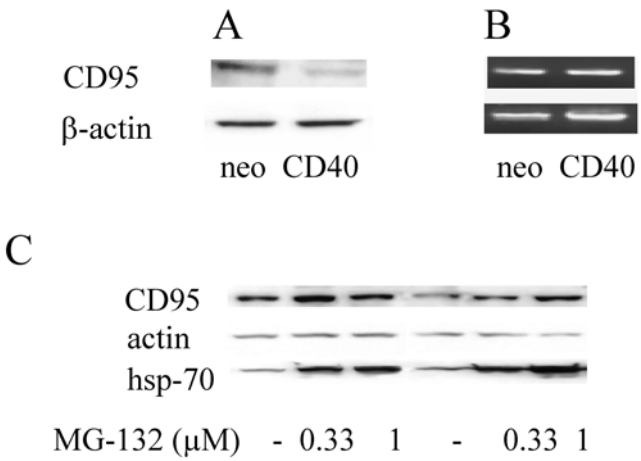

Fig. 4.12. **CD40-dependent down-regulation of CD95 expression is due to increased proteasomal degradation.** A,B. Total cellular levels of CD95 protein and mRNA in LN-18 neo or CD40 cells were determined by immunoblot using antibody FL-335 (A) or RT-PCR (B). β-actin expression was assessed as a loading control. C. Total cellular levels of CD95 were determined by immunoblot in LN-18 neo (left) or CD40-transfected LN-18 (right) cells after 16 h treatment with MG-132 at 0, 0.33 or 1 μM. Proteasome inhibition was verified by hsp-70 protein accumulation.

To exclude the possibility of CD95 mRNA being induced under conditions of proteasome inhibition (271), Northern blots were also performed to assess the CD95 mRNA levels in response to MG-132 (Fig. 4.12D). These actually showed a slight decrease in CD95 mRNA expression, quantified in Fig. 4.12E. Thus the accumulation of CD95 upon proteasome inhibition was most likely due to the prevention of proteasomal degradation.

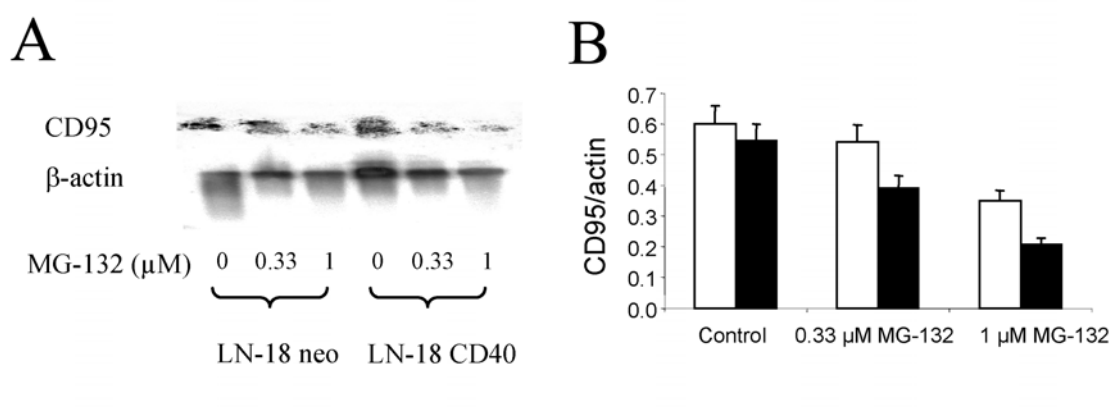

Fig. 4.13. **Proteasome inhibition does not increase CD95 mRNA expression.** A. CD95 mRNA levels were assessed by Northern blot in LN-18 neo (left) or CD40-transfected LN-18 (right) cells after 16 h treatment with MG-132 at 0, 0.33 or 1 μM. Total cellular β-actin mRNA levels were measured as a loading control (lower panel). B. CD95 mRNA levels from A were quantified using a PhosphoImager and normalized to β-actin mRNA signals.

CD40 interacts with TNF-α-dependent signalling

Proapoptotic effects of CD40L have been proposed to be mediated by CD95 (250) or TNF-R1 (p55) (247) in different cell types. The sensitivity of CD40-transfected LN-18 cells to TNF-*a* alone was unaltered. However, in contrast to the negative results for CD95L (Fig. 3A,B), coexposure revealed strong synergy between CD40L and TNF-*a* in CD40--transfected LN-18 cells, but not in the neo control transfectants (data not shown), both in the absence (Fig. 4.14A) and presence of CHX (Fig. 4.14B). The concentrations of CD40L required for this effect were subtoxic when applied on their own (see Fig. 4.6), and cell death was sensitive to zVAD-fmk (data not shown).

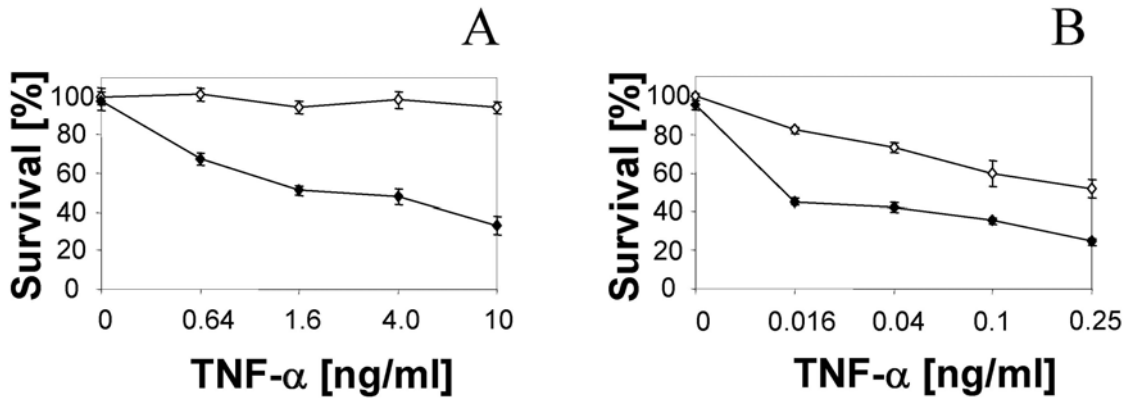

Fig. 4.14 **CD40L-mediated signaling affects TNF-R1-dependent cell death.** A,B. CD40-transfected LN-18 cells (10^4/well) were treated with TNF-α in the absence (open symbols) or presence (closed symbols) of subtoxic concentrations of CD40L (0.04 μg/ml in A, 0.0016 μg/ml in B). In B, CHX (10 μg/ml) was added to all wells. Survival was assessed at 16 h by crystal violet staining.

Ligation of CD40 did not trigger endogenous TNF-α production by glioma cells since ELISA did not reveal TNF-α in supernatants or lysates from treated CD40-transfected LN-18 cells, using PBMC stimulated with PHA (5 µg/ml) as a positive control (Table 1). Neither did blockade of TNF-R1 (p55) (247) or CD95 (250) or neutralization of TRAIL/Apo2L (248) confer protection against CD40L-induced cell death while apoptosis mediated by the respective ligands was blocked in CD40-transfected LN-18 cells (shown for TNF-α and CD95L in Fig. 4.15).

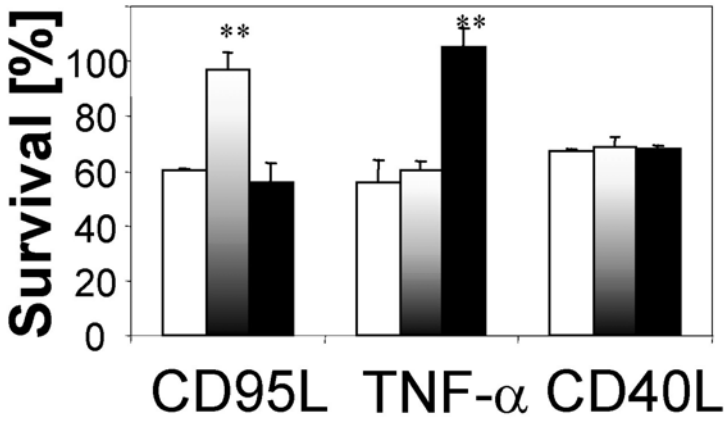

Fig. 4.15. **Blocking of TNF-related death receptors does not inhibit CD40-mediated apoptosis.** CD40-transfected LN-18 cells (10^4/well) were treated with CD95L (100 U/ml), TNF-α (1 ng/ml) or CD40L (1 µg/ml) in the presence of 10 µg/ml of either control antibody (open bars) or M-3 anti-CD95 (shaded bars) or H398 anti-TNF-R1 (p55) antibody (black bars). Survival was assessed by crystal violet staining at 24 h (**$p<0.01$, t-test).

The constitutive cell surface expression of TNF-R1 (p55) in CD40-transfected LN-18 cells was somewhat increased. Interestingly, however, TNF-R1 (p55) surface expression was down-regulated in CD40-transfected LN-18 cells after treatment with CD40L, but not in the neo control cells (Fig. 4.16). This effect was seen as early as 2 h after exposure. Accordingly, addition of TNF-α to LN-18 CD40 cells that had been pre-exposed to CD40L did not increase CD40-mediated cell death any further.

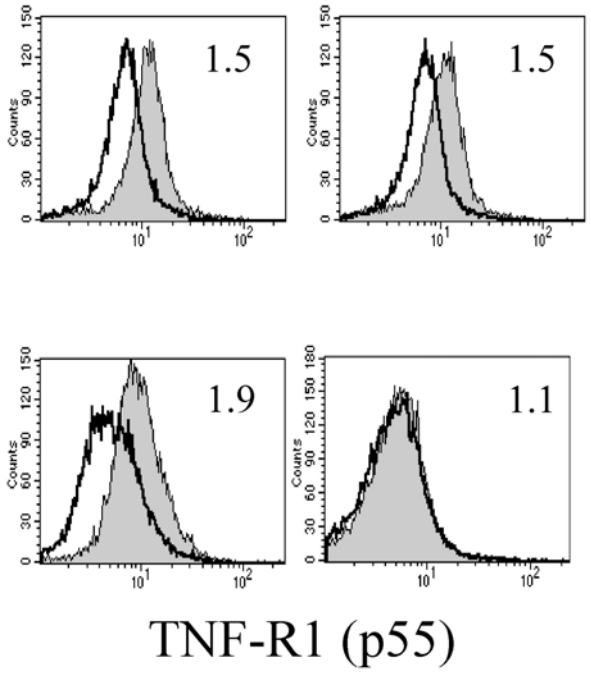

Fig. 4.16. **TNF-R1 surface expression is reduced after treatment with CD40L.** TNF-R1 (p55) expression levels at the cell surface were analysed by flow cytometry in LN-18 control transfectants (upper panel) and in CD40-transfected LN-18 cells (lower panel) before (left) or 6 h after (right) exposure to CD40L (0.5 μg/ml). The SFI values are indicated in the upper right.

Immunoblotting showed that the overall expression levels of TNF-R1 (p55) remained unchanged (Fig. 7E), suggesting that TNF-R1 (p55) was internalised rather than degraded (272). It should be noted that immunoblots for TNF-R1 (p55) commonly yield more than one band, probably due to glycosylation and ubiquitination (273).

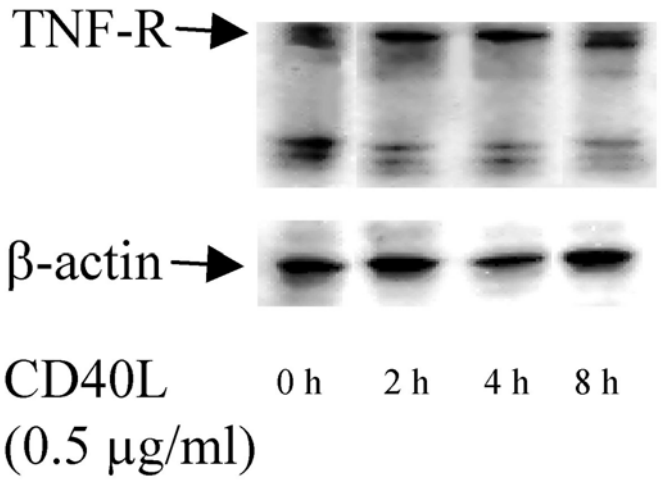

Fig. 4.17. **Total cellular TNF-R1 expression is unaltered after treatment with CD40L.** Total cellular TNF-R1 (p55) content was assessed in CD40-transfected LN-18 cells before (lane 1) or 2 h, 4 h or 8 h (lanes 2-4) after exposure to CD40L (0.5 μg/ml). β-actin was included as a loading control.

Immunocytochemistry showed co-localization of CD40 and TNF-R1 (p55) (Fig. 4.18).

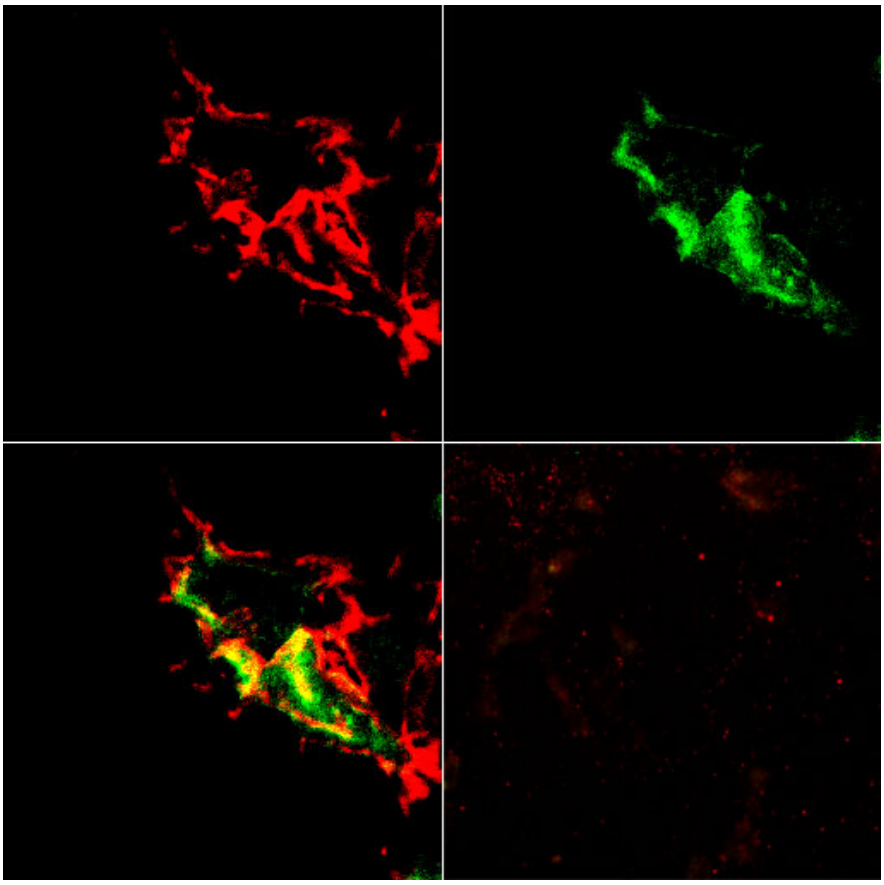

Fig. 4.18. **TNF-R1 (p55) and CD40 co-localize.** Untreated, paraformaldehyde-fixed CD40-transfected LN-18 cells were stained for both CD40 (red staining) and p55 TNF-R1 (green stain) and analyzed by confocal microscopy. Shown are stainings for CD40 (upper left), p55 TNF-R1 (upper right) and their respective overlay (lower left). Co-localization is indicated by yellow patches. A control staining with the respective isotype antibodies is shown in the lower right panel.

Further, CD40 and TNF-R1 (p55) could be co-immunoprecipitated (Fig. 4.19A). In contrast, no interaction of CD40 with CD95 was detected, neither in LN-18 neo control transfectants nor in unstimulated or CD40L-stimulated CD40-transfected LN-18 cells (Fig. 4.19B, data not shown). Yet, TNF-R1 (p55) was pulled down with anti-CD95 antibody in stimulated CD40-transfected LN-18 cells, suggesting that treatment with CD40L initiates some kind of crosstalk between TNF-R1 (p55) and CD95. Anti-FADD and anti-caspase 8 blots showed that these molecules form an integral part of the DISC formed after stimulation via CD95. However, small but detectable amounts of these molecules were also pulled down when the apoptotic process was triggered by CD40L.

The specificity of all signals was confirmed by IgG controls (data not shown) and immunoblots from the respective lysates. Due to the much lower amounts of specific protein contained in the lysates, exposure times were not always the same for the input and the precipitate, e.g. for TNF-R1 (p55) and CD95/Fas in Fig. 4.19B.

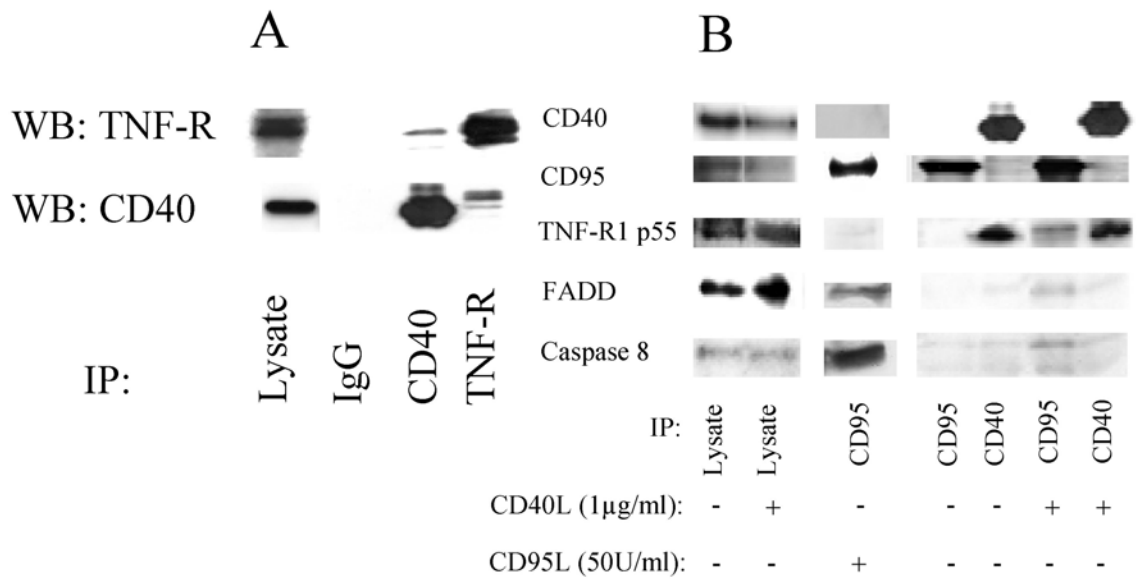

Fig. 4.19. **CD40 interacts with TNF-R1 (p55) and induces crosstalk between death receptors in CD40-transfected LN-18 cells.** A. The interaction of CD40 and TNF-R1 (p55) was analysed in CD40-transfected LN-18 cells by immunoprecipitation with anti-TNF-R1 (p55) (H-398) or anti-CD40 (G28.5) antibodies followed by immunoblot with either antibody. An IgG control was used to exclude non-specific pull-down or bands originating from antibody fragments. The respective lysates are shown on the left. B. The interactions of the TNF family receptors TNF-R1 (p55), CD95 and CD40 were further explored by immunoprecipitation using anti-CD95 (FL-335) or anti-CD40 antibodies and subsequent immunoblotting with anti-CD40 (G28.5), anti-CD95 (FL-335), anti-TNF-R1 (p55) (H398), anti-FADD (F33620) or anti-caspase 8 (C15) antibodies (lanes 4 and 5, CD40-transfected LN-18 cells; lanes 6 and 7, CD40-transfected LN-18 cells stimulated with 1 µg/ml CD40L for 1 h). Controls include lysates from unstimulated and stimulated CD40-transfected LN-18 cells (lanes 1 and 2) and immunoprecipitates from

An interaction between CD40 and TNF-R1 (p55) was also observed in U87MG cells. However, there was no interaction of CD40 or TNF-R1 (p55) with CD95 in this cell line, not even after stimulation (Fig. 8D). Accordingly, U87MG cells did not die in response to the treatment with TNF-α alone or TNF-α plus CD40L (Fig. 8E).

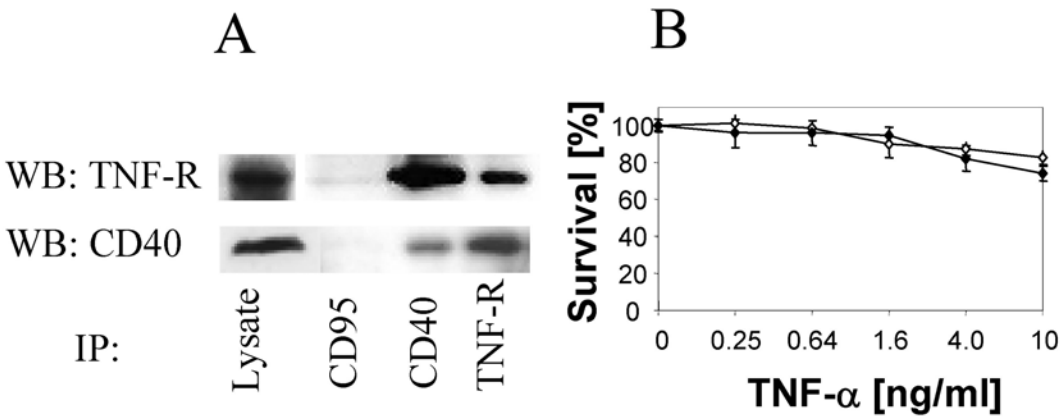

Fig. 4.20. **CD40 interacts with TNF-R1 (p55) and does not induce crosstalk in U87MG cells.** A. Immunoprecipitation was performed as in 4.19, using wild-type U87MG cells stimulated with CD40L (1 µg/ml, 1 h). B. U87MG cells (10^4/well) were treated with increasing concentrations of TNF-α in the absence (open symbols) or presence (closed symbols) of CD40L (1 µg/ml). CHX (10 µg/ml) was added to all wells. Survival was assessed at 16 h by crystal violet staining.

Bispecific CD40xCD95 antibodies promote cell death signalling in U87MG cells

A crosstalk between CD40 and CD95 was enforced in U87MG cells using a bispecific antibody to these two antigens. This antibody was cytotoxic to U87MG cells. A similar construct directed to CD20 and CD95 had no such effect. CD40xCD95 antibody-induced cell death was enhanced by CHX (Fig. 4.21A) and blocked by zVAD-fmk (data not shown). Addition of a five-fold excess of anti-CD95 Fab fragment, anti-CD40 or CD40L prevented cell death (data not shown). The construct was almost equally effective in IFN-γ-stimulated LN-18 cells which show lower expression of CD40, but are more susceptible to CD95-mediated apoptosis. In contrast, uninduced (CD40-negative) LN-18 cells were not killed by the CD40xCD95 antibody. Neither did the construct induce cell death in IFN-γ-stimulated LN-229 cells which are much less susceptible to CD95L-induced apoptosis than LN-18 cells (Fig. 4.21B).

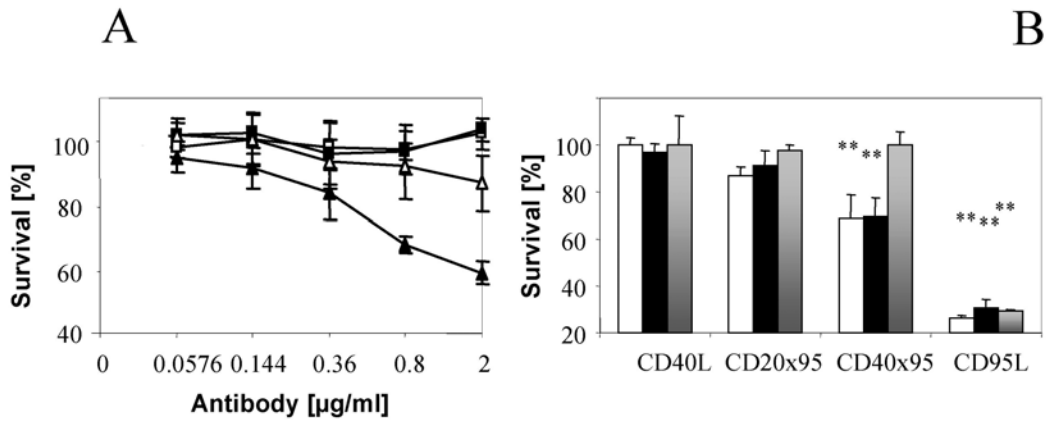

Fig. 4.21. **CD40/CD95 bispecific antibodies induce apoptosis in U87MG cells.** A. U87MG cells (10^4/well) were treated with CD20xCD95 (squares) or CD40xCD95 (triangles) bispecific antibodies in the absence (open symbols) or presence (filled symbols) of CHX (10 µg/ml) for 16 h. B. IFN-γ (48 h, 500 U/ml)-stimulated LN-18 (open bars), U87MG (black bars) or LN-229 (shaded bars) cells (10^4/well) were treated with CD40L, CD20xCD95 or CD40xCD95 antibodies (1 µg/ml), or with CD95L (50 U/ml), all in the presence of CHX (10 µg/ml), for 16 h.

Further, the CD40xCD95 antibody induced DEVD-amc cleavage in U87MG cells in a concentration-dependent manner, and this was blocked by zVAD-fmk (Fig. 4.22A). Immunoblot analysis also revealed the processing of caspases 8 and 3 in response to the antibody (Fig. 4.22B), showing that the bispecific CD40xCD95 antibody kills glioma cells in a fashion similar to the respective natural ligands.

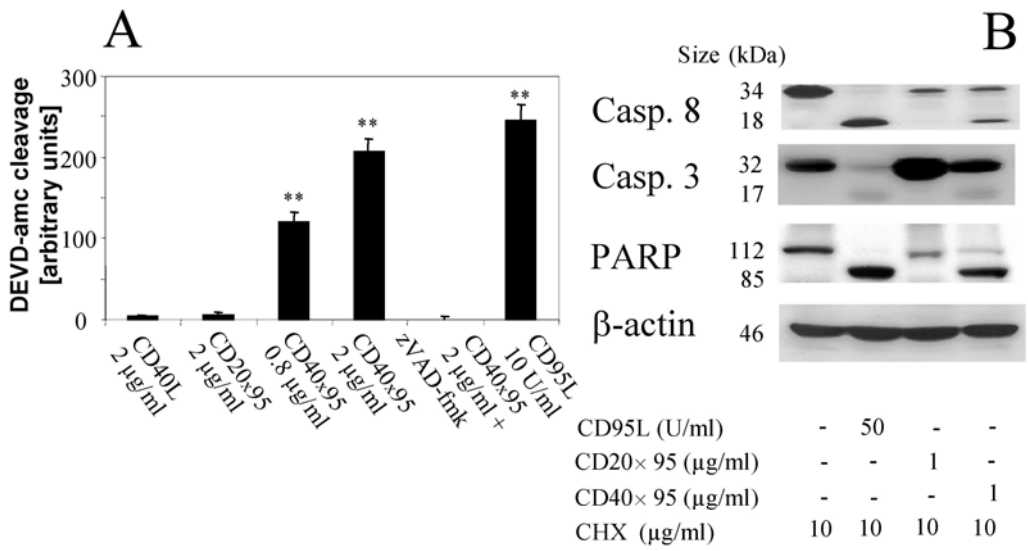

Fig. 4.22. **Apoptosis by CD40xCD95 bispecific antibody is caspase-dependent.** A. DEVD-amc cleavage was assessed in lysates from U87MG cells at 6 h after co-exposure to CHX (10 µg/ml) and CD40L (2 µg/ml), CD20xCD95 (2 µg/ml) or CD40xCD95 (0.8 µg/ml and 2 µg/ml, in the absence or presence of zVAD-fmk at 100 µM). CD95L (10 U/ml) was included as a positive control. In A-C, all values were normalised to control cultures containing vehicle or CHX alone. B. U87MG cells were treated for 6 h with CD20xCD95 (1 µg/ml) or CD40xCD95 (1 µg/ml) bispecific antibodies or with CD95L (50 U/ml) as a positive control in the presence of CHX (10 µg/ml). Cleavage of caspases 8 and 3 was assessed by immunoblot. Neither CHX alone nor CD40L nor any of the monospecific antibodies induced caspase 8 or 3 cleavage (data not shown).

Discussion

The TNF receptor family member, CD40, is thought to promote proliferation, survival and differentiation in B cells (239, 240). The survival-promoting activity of CD40 has been attributed to the transcriptional activation of c-IAP via TRAF 2-5 (274) and the NF-κB-dependent induction of c-FLIP (275) and A20 (244). In dendritic cells CD40 provides a strong stimulatory signal that may overcome a pre-induced tolerance to tumour antigens (276). Pro-apoptotic effects of CD40 signalling seem to be restricted to tumour cells (277).

The biological significance of aberrant CD40 expression in cancer cell lines has remained obscure and the mechanism of CD40 triggering the death receptor-dependent apoptotic pathway is still somewhat enigmatic (246). A role for CD40 in tumour cell survival, growth and neo-vascularization has been proposed for Kaposi sarcoma cells (278). CD40-expressing tumour cells have also been suggested to impair immune cell function (279). A role of CD40/CD40L interactions in normal or diseased human brain has not been clearly defined either. For instance, it has remained controversial whether mouse astrocytes can be induced to express CD40 (280) or not (160). T helper type 1 cells expressing CD40L may induce IL-12 release in CD40-expressing microglial cells in the mouse (281). CD40 expressed on neuronal cells has been suggested to mediate death in the absence of ligand binding, similar to TNF-R p75 (282). CD40 is also expressed by normal neurons of the adult mouse brain and, based on *in vitro* studies and analysis of CD40-deficient mice, may serve a protective function here (283).

The present study shows that CD40 is expressed by human glioma cells *in vitro* and *in vivo* (Fig. 4.1, 4.2, 4.3). In malignant glioma cell lines, CD40 is uniformly expressed at the RNA (Fig. 4.1 A,B) and protein level, as assessed by immunoblot (Fig. 4.1C). Interestingly, differences in CD40 mRNA levels did not translate into according differences in total CD40 protein, indicative of posttranslational regulation of protein levels, e.g. at the level of protein degradation. In contrast to the uniform CD40 expression in glioma cell lysates, flow cytometry showed that only one cell line (U87MG) expressed CD40 at the cell surface constitutively (Fig. 4.2A), and two more cell lines were induced to do so by IFN-γ treatment (Fig. 4.2B). There was no evidence for the release of soluble CD40 by the glioma cell lines. These data indicated that a possible function of CD40 in glioma cell lines would have to be largely a ligand-independent, intracellular one. Since CD40 contains a pre-ligand-binding assembly

domain (PLAD) (284), ligand-independent receptor assembly is likely to occur. It is, however, not clear whether this may result in ligand-independent signalling.

Under conditions where CD40 was expressed at the cell surface, several assays failed to document signal-transducing activity, including assessment of viability or NF-κB or IL-8 reporter gene activity in glioma cells exposed to soluble CD40L or CD40L-expressing effector cells (Fig. 4.4, 4.5, data not shown). In wild-type glioma cell lines, no indications for synergistic induction of apoptosis by CD40L and TNF-α, CD95L or Apo2L/TRAIL were found, nor was any modulation of the respective receptor levels observed (Fig. 4.4, data not shown). This was not only true for long-term established glioma cell lines, but also short passage polyclonal glioma cell cultures (data not shown). These negative data were confirmed when membrane-bound CD40L expressed on BHK cells was used instead of recombinant CD40L to trigger CD40. Still, it cannot be excluded that CD40 exerts effects on growth, apoptosis, and cytokine secretion *in vivo* that are rapidly lost when the cells are cultured *in vitro*. Such an effect has already been described for epithelial ovarian carcinoma cells (285).

To decide whether the level of CD40 was insufficient to transduce a signal or whether the signalling cascade triggered by CD40L was essentially disabled in glioma cells, LN-18 sublines expressing high levels of CD40 were generated (Fig. 4.6 A). These cells acquired sensitivity to CD40L-induced promoter activity and cell death (Fig. 4.6 B,C). Further, CD40L-induced cell death resembled death ligand-induced apoptosis of glioma cells in several ways: CHX-mediated inhibition of protein synthesis potentiated cell death (Fig. 4C), the broad spectrum caspase inhibitor, zVAD-fmk, was protective and cell death involved clustering of receptor (CD40) molecules (Fig. 4.7), the proteolytic activation of caspases 8 and 3 and PARP cleavage (Fig. 4.8).

Interestingly, forced expression of CD40 resulted in the loss of CD95 protein presumably *via* proteasomal degradation (Fig. 4.9, 4.10). A synergy of CD40 and CD95 in the induction of apoptosis has been reported (250). Thus the possibility of a negative selection pressure preventing co-expression of CD40 and CD95 at high levels was investigated. However, down-regulation of CD95 resulting from forced ectopic expression of CD40 occurred even in the presence of the broad-spectrum caspase inhibitor zVAD-fmk as well as in crmA-transfected glioma cells, strongly arguing against an apoptotic deletion of cells co-expressing both receptors at high level (Fig. 4.11). Further, earlier experiments had shown (204) that glioma cells are resistant to suicidal or fratricidal killing by glioma-cell bound CD95L. In any case, the loss of

CD95 in CD40-transfected cells with the concomitant resistance to CD95-dependent apoptosis renders the possibility of endogenous CD95 mediating CD40L-induced cell death unlikely. There were no such interactions with the Apo2L/TRAIL receptor system (data not shown).

Interestingly, exposure of CD40-transfected LN-18 cells to proteasome inhibitors restored CD95 protein levels to that found in control transfectant (Fig. 4.12). At the same time, CD95 mRNA levels were slightly diminished (Fig. 4.13). While the contribution of further mechanisms cannot be excluded, CD95 is likely to be subjected to increased proteasomal degradation when high levels of CD40 are present. This might be due to CD40 and CD95 competing for a rate-limiting step of receptor transport and integration into the cell membrane, thus redirecting CD95 to degradation.

In contrast, CD40L showed strong synergy with TNF-α in inducing apoptosis (Fig. 4.14). Since CD40 does not contain a death domain, a role for endogenous TNF-R mediating CD40-induced apoptosis has been proposed on the basis of the following observations: Both CD40 and TNF-R1 (p55) use common signalling pathways including TRAF-2, TRAF-6, p38-MAPK, NF-κB and AP-1. Further, co-exposure to CD40L and TNF-α synergistically induces apoptosis on various cell types whereas preexposure to either one induces resistance to further doses of TNF. Interestingly, CD40-transfected HeLa cells are protected from CD40L-induced apoptosis by neutralizing antibodies to TNF or TNF-R1 (p55). In this cell line, stimulation with CD40L even induced TNF-α mRNA synthesis and protein production (247). However, the authors also postulated a TNF-α-independent interaction between TNF-R1 (p55) and CD40.

A role for endogenous CD95 mediating CD40-induced apoptosis was also assumed since biliary epithelial cells upregulated CD95L mRNA in response to CD40L and were protected from CD40-dependent apoptosis by Nok-1 anti-CD95L antibody (249, 250). The same authors observed an up-regulation of TNF-α, CD95L and Apo2L/TRAIL mRNA and achieved various degrees of protection by neutralization of any of these cytotoxic ligands in CD40-transfected HeLa cells (248).

Our study of glioma cells does not support the model of a delayed and attenuated CD40-dependent apoptosis via the production of membrane-anchored cytotoxic ligands which then engage their respective receptors on the cell surface resulting, in autocrine or fratricidal apoptotic deletion. Apart from the absence of TNF-α and the failure of blocking experiments with TNF-, CD95- and Apo2L/TRAIL-specific antibodies (Fig.

4.15), the suggested mechanism requires synthesis of mRNA and protein. However, inhibition of protein synthesis by CHX led to a dramatic sensitization towards CD40-mediated apoptosis (Fig. 4.6C), even when the cells where pre-exposed to CHX (data not shown). Thus CD40-transfected LN-18 cells exposed to CD40L die through a mechanism that does not require protein synthesis and that is probably independent of other TNF-related ligands.

Concomitant with cell death, TNF-R1 (p55) expression at the cell surface decreased (Fig. 7D), presumably due to internalization (Fig. 4.17) which would be characteristic for TNF-R1 (p55)-mediated apoptosis (272). Immunoprecipitation studies demonstrated an interaction between TNF-R1 (p55) and CD40 both in control cells and in resting CD40-transfected cells (Fig. 4.19). While a direct physical interaction between these molecules seems unlikely, they may both be incorporated into a larger complex containing common adaptor molecules. Then stimulation of CD40 might lead to the removal of a protective protein from TNF-R1 (p55), thus enabling the formation of an activated TNF-R1 (p55) complex. Alternatively, following CD40 engagement, an adaptor protein might be recruited that organizes TNF-R1 (p55) aggregation. Finally, the clustering of CD40 itself will induce proximity of molecules that interact with CD40, including TNF-R1 (p55). Thus clustering of TNF-R1 (p55) by “induced proximity” is most likely to occur, but may have escaped detection due to the internalization of this receptor.

After stimulation, immunoprecipitation with anti-CD95 antibody also revealed an interaction with TNF-R1 (p55), suggesting an intracellular crosstalk between these two receptor complexes. Assuming that CD40 stimulation induces the formation of an activated TNF-R1 complex, an interaction with CD95 may then be mediated by some common adaptor molecules. While this is still speculative, the fact that TNF-R1 (p55) and CD95 use the same executors of cell death and some common adaptor molecules adds plausibility to this proposed crosstalk (286). In particular, FADD and caspase 8 are common to and essential for both the TNF-R1 (p55) and the CD95 signalling pathways (287, 288). TNF-R1 (p55) signalling even is promiscuous with regard to TRADD and FADD, including heterodimers of both, which may provide a molecular basis for the observed involvement of components from both the p55 TNF-R1 and the CD95 apoptotic pathways (289).

Interestingly, TNF-R1 does not directly interact with caspase 8 or FADD. Neither are caspase 8 and FADD incorporated into a membrane-bound, TNF-induced receptor

signalling complex (290). Instead, caspase 8 and FADD are recruited to a second, intracellular complex (187) that is formed after or upon dissociation from the internalized TNF-R1 (p55). This complex apparently contains most essential components of the CD95-related DISC apart from CD95 itself. Thus, already a weak interaction of this complex with CD95 could account for the small amounts of FADD and caspase 8 that were co-precipitated with CD95 from CD40-transfected LN-18 cells after stimulation with CD40L. Accordingly, a CD95-related DISC immunoprecipitation yielded much larger amounts of FADD and caspase 8. While the various complexes and potential intermediates involved in this signalling pathway clearly require further exploration, the involvement of both TNF-R1 (p55) and CD95 in a cell type-specific manner might reconcile the divergent observations concerning the further death receptors involved in CD40-mediated apoptosis.

Finally bispecific antibodies targeting CD95 and CD40 had specific activity against glioma cells that was not seen with a similar antibody targeting CD95 and CD20 and that required the expression of CD40 at the cell surface (Fig. 4.21, 4.22). These data indicate that endogenous CD40 expressed at the cell surface does participate in cell death signalling, albeit under specific circumstances. Further, these observations shed novel light on antibody-mediated triggering of receptors in that bispecific antibodies would a priori not be predicted to have the steric properties of activating death receptors at endogenous expression levels (48, 291). In view of the fact that glial cells or neurons of normal brain appear not to express CD40 (see Figure 4.3), a bispecific antibody would seem a reasonably safe way to activate the death receptor pathway on glioma cells in the absence of neurotoxicity. Thus, the demonstration of tumour cell cytotoxicity mediated by bispecific antibodies against a death receptor and a second antigen preferentially expressed on tumour cells opens up new perspectives for the development of innovative cancer therapies based on selective death receptor activation in tumour cells.

V. Identification of CD70-mediated apoptosis of immune effector cells as a novel immune escape pathway of human glioblastoma

A manuscript based on this project has been published in
Cancer Res. 2002 May 1;62(9):2592-9.

For help with this project, thanks go to Dr. Gundram Jung (Department of Immunology, Institute for Cell Biology, University of Tübingen, 72076 Tübingen) who introduced me to the immunological techniques employed in this project. Dr. Ivan Radovanovič (at that time in Adriano Aguzzi´s group in the Institute of Neuropathology, University of Zürich, 8091 Zürich, Switzerland) performed all immunohistochemical stainings. CD70 expression in glioma cells was found when Huatao Huang and Hiroko Ohgaki (International Agency for Research on Cancer, 69372 Lyon, France) performed a cDNA array using mRNA from untreated and irradiated glioma cells prepared by my colleague Andreas Rimner.

Introduction

Human glioblastoma is a highly lethal brain tumour which kills affected patients by local destructive growth. Although glioblastoma cells display virtually all features of aggressive neoplastic cells, including resistance to multiple apoptotic stimuli and strong migratory and invasive properties, these tumours hardly ever metastasize outside the central nervous system. This clinical observation, as well as ample evidence of altered immune function in glioblastoma patients, has raised the hope that immunological approaches may lead to a therapeutic breakthrough in the management of glioblastoma (155). Glioblastoma-mediated immunosuppression has been attributed to various mechanisms, including the release of immunosuppressive TGF-β (292), CD95L-dependent maintenance of immune privilege (63, 264, 293), interference with IL-2-mediated T cell activation (294) and the release of as yet unidentified soluble factors (295, 296).

CD70 (297), a cell surface protein, is the ligand for CD27, a type I glycoprotein and member of the TNF receptor family (298). CD70 is expressed by cells of the lymphoid lineage, notably activated B (299) and T cells (300, 301), but not resting lymphocytes. CD27 is expressed constitutively by T, B (302) and NK cells. A reciprocal expression pattern for CD27 and CD70 has been described (303). CD70/CD27 interactions may play an important role in the maturation and activation of B (304, 305), T (306) and NK (307) cells. CD8-positive T cells may be activated *via* CD70 whereas T helper cells remain largely unaffected (308). Direct inhibitory effects on the generation of plasma cells (309) and on T cell activation (310) have also been reported. CD27 costimulation may induce CD45 RA^+ $CD4^+$ T cells with regulatory function, resulting in a down-regulation of the immune response (311). CD27 can also mediate apoptosis (49). The immune system of CD27 knockout mice shows impaired T cell memory, but no further immunodeficiency (312). A more severe phenotype was observed in CD70-transgenic mice which show chronic T cell activation associated with depletion of the B cell compartment and of naive and CD27-positive T cells. When aged 6-8 months, CD70 transgenic mice die from T cell immunodeficiency (313, 314).

Some lymphoproliferative diseases are associated with reduced CD27 expression while CD70 expression is elevated (315, 316). CD27 was not detected on the affected CD3 cells in 20 of 21 patients suffering from lymphoproliferative disease of

granular lymphocytes whereas the nontransformed cells expressed CD27 constitutively (317). In contrast, CD70 was induced by malignant transformation in these patients. Here, the aberrant expression of CD70 by human malignant glioma cells is shown *in vitro* and *in vivo* and a role for CD70/CD27 interactions in mediating immune escape in this type of cancer is delineated.

Materials and Methods

Cell culture and reagents. The human malignant glioma cell lines LN-18, U138MG, U87MG, LN-428, D247MG, T98G, LN-319, LN-229 (the p53 wild-type subline), A172, U251MG, U373MG and LN-308, kindly provided by Dr. N. de Tribolet (Lausanne, Switzerland), and SKN-LE and SKN-BE human neuroblastoma cells (American Type Culture Collection, Rockville, MD) were cultured in 75 cm^3 Falcon plastic flasks using DMEM supplemented with 1% glutamine (Gibco Life Technologies, Paisley, Great Britain), 10% FCS (Biochrom KG, Berlin, Germany) and penicillin (100 IU/ml)/streptomycin (100 µg/ml). U87MG cells were transfected with the dominant-negative $p53^{V135A}$ mutant by electroporation (200). The CD70-transfected murine pre B-cell line 300-19 and control-transfected 300-19 B cells carrying a neo control plasmid, kindly supplied by Dr. S. Jacquot (Rouen, France), were maintained in RPMI 1640 (Gibco) with 10% FCS, G418 (250 µg/ml) and 15 µM β-mercaptoethanol. All cell lines were routinely tested for contamination with mycoplasma by DAPI staining (Sigma, Deisenhofen, Germany). Where indicated, the cells were irradiated while adherent using a Gammacell 1000 Elite (Nordion, Ontario, Canada). Radiation was applied as a single dose at a central dose rate of approximately 9 Gy/min. The pan-specific caspase inhibitor zVAD-fmk was purchased from Bachem (Heidelberg, Germany). Lomustine was kindly provided by Medac (Hamburg, Germany). Cycloheximide and propidium iodide were purchased from Sigma (St. Louis, MO). AnnexinV-FITC was obtained from Pharmingen (Heidelberg, Germany), human recombinant TNF-α from Roche (Mannheim, Germany). The following antibodies were used: M-T271 mouse anti-human CD27, FITC-labeled, and unlabeled BU69 mouse anti-human CD70 (Ancell, Bayport, MN), HNE.51 mouse anti-human CD70 (Dakopatts, Glostrup, Denmark), C-20 goat anti-human CD70 (Santa Cruz, Santa Cruz, CA), Ki-24 mouse anti-human CD70, NOK-1 mouse anti-human CD95L (Pharmingen) and MAB1835 mouse anti-human TGF-β (R&D Systems, Wiesbaden, Germany). All cell lines were tested for the cell surface expression of costimulatory molecules using FITC-labeled antibodies to CD40, CD80, CD86, and CD154 (Pharmingen). The cell lines were also analysed for HLA-A2 expression using the murine BB7.2 antibody raised in the laboratory of H.G.R.. Maxisorp plates used for antibody immobilization were obtained from Nunc (Roskilde, Denmark).

cDNA Array analysis. The Atlas Human Cancer 1.2 Arrays (Clontech, Palo Alto, CA, USA) were used to screen for alterations of gene expression by irradiation in U87MG and T98G cells. Details for cDNA probe synthesis, array hybridization and quantitation were described previously (318). The irradiated to control ratio of at least 1.5 in expression was considered as up-regulation and a ratio of less than 0.67 in expression was considered as down-regulation after irradiation.

Northern blot analysis. Total RNA was extracted using the RNeasy RNA purification system (Qiagen, Hilden, Germany). Denatured total RNA (10 µg) was loaded on a 1% agarose gel containing 6.7% formaldehyde. The RNA was separated at 100 V, transferred to a Hybond N+ membrane (Amersham, Freiburg, Germany) using capillary blotting, and cross-linked in a UV stratalinker 1800 (Stratagene, La Jolla, CA) at 1200 J. Methylene blue staining was performed as a loading control. The membrane was preincubated for 2 h in Church buffer at 65°C. The probe was constructed by PCR-amplifying nucleotides 192-535 from a human CD70 expression vector, kindly provided by M.R. Bowman (Cambridge, MA), using CD70-specific primers (5´-CTT GGT GAT CTG CCT CGT GG-3´ up and 5´-GCA GCA GGC TGA TGC TAC G-3´ down). Purified PCR product (40 ng) was labeled using 5 µl (~1.6 Mbq) dCTP and the Rediprime II random labelling system (Amersham). Filters were hybridized over night at 65°C in a hybridization oven with a rotisserie device using Church buffer. Binding of radioactive probes was visualized and quantified using a PhosphoImager (FujiBasReader 1500, Fuji). Signals were normalized to ß-actin mRNA expression. RNA from the 12 glioma cell lines under investigation was also probed for CD27 expression using a sCD27 probe amplified from human CD27 cDNA (ATCC, Manassas, VA). The primers used were 5´-GGG AAT TCT TGG AGG TGC TAA CT-3 up and 5´-ATG GGC CCC GAA TAA AAT CGG AGC-3 down (319).

Immunoblot analysis. CD70 protein levels were analysed by immunoblot using 20 µg of protein per lane on a 10% acrylamide gel (Biorad, Munich, Germany). After transfer to nitrocellulose (Biorad) the blots were blocked in PBS containing 5% skim milk and 0.05% Tween 20 and incubated overnight at 4°C with 2 µg/ml of CD70 antibody (C20). Visualization of protein bands was accomplished using horseradish

peroxidase-coupled anti-goat IgG secondary antibody (Sigma) and enhanced chemiluminescence (ECL) (Amersham).

Flow cytometry. Glioma cells were detached non-enzymatically using cell dissociation solution (Sigma). The cells were preincubated in PBS with 2% bovine serum albumin and incubated with FITC-labeled CD70 antibody (BU69, 20 µg/ml in PBS/BSA) or isotype-matched mouse IgG-FITC as a control. Fluorescence was measured in a Becton Dickinson FACScalibur (Heidelberg, Germany). Specific fluorescence indexes (SFI) were calculated by dividing mean fluorescence obtained with specific antibody by mean fluorescence obtained with control antibody. To validate the data, experiments were repeated with additional monoclonal CD70 antibodies (HNE.51 and KI-24). To examine the cells for CD27 expression, M-T271 antibody was used under the same conditions.

Immunohistochemistry. Cryosections (0.7 mm) of human gliomas were fixed in acetone and blocked with normal rabbit serum and bovine serum albumin. All samples were stained with three different CD70 antibodies (Dakopatts, Pharmingen, Santa Cruz) at dilutions of 1:25 to 1:100. All antibodies gave comparable results at all tested dilutions. A biotinylated anti-mouse or anti-goat secondary antibody (Zymed) was used at 1:150. Avidin biotin complex was added, and the staining was developed with diaminobenzidine. Human tonsils were taken as positive control. Normal human brain (temporal lobe) served as a negative control.

T cell reaction against allogeneic glioma cells. To suppress glioma cell proliferation, the cells were incubated in serum-free medium for 24 h, irradiated at 200 Gy and maintained in serum-free medium for another 24 h. Although doses in excess of 10 Gy are sufficient to suppress colony formation in all glioma cell lines examined here (131), the high dose of 200 Gy was necessary to prevent proliferation within the 1-5 days of the experiments and to suppress [methyl-^{3}H] thymidine incorporation in assays where this incorporation was used to assess immune cell proliferation in the presence of glioma cells. PBMC were isolated from healthy donors by density gradient centrifugation (Biocoll, Biochrom KG) and characterized for their HLA-A isotype. Monocytes were depleted by adhesion and differential centrifugation. To obtain purified T cells, the samples were depleted of B cells and monocytes using the

LymphoKwik T^{TM} reagent (One Lambda Inc., Canoga Park, CA). The purity of this population was controlled by flow cytometry using anti-human CD3-PE (Becton Dickinson). HLA-A2-negative T cells or PBMC (10^5/well) were cocultured with 10^4 irradiated HLA-A2-positive glioma cells in 96 well plates in triplicates. In order to minimize interference of CD70 antibody with CD70 expressed by activated immune cells, the glioma cells were preincubated with CD70 antibody for 2 h and washed twice with PBS. After 4 days, the cells were pulsed for 24 h with [methyl-^{3}H] thymidine (0.5 µCi, Amersham). The cells were harvested with a cell harvester (Inotech, Dottikon, Switzerland) and incorporated radioactivity was bound to a glass fibre filtermat (Wallac, Turku, Finland). The filtermat was wetted with Ultima Gold Scintillation Cocktail (Packard, Dreieich, Germany) and radioactivity was determined in a Wallac 1450 Microbeta Plus Liquid Scintillation Counter (Wallac, Turku, Finland).

Chromium release assay. The glioma cells were seeded into 25 cm^2 flasks such that the number of cells reached 10^6 per flask 24 h later. The cells were serum-deprived and irradiated at 200 Gy. After repeated washing and preincubation of the glioma cells with CD70 or control antibodies, 1.5 x 10^7 PBMC were added in 5 ml RPMI containing 10% FCS. The cells were cocultured for 5 days. PBMC from the same isolation were maintained in culture without glioma cells in parallel. On day 3, PHA (10 µg/ml) (Biochrom) was added to one group of PBMC. On day 5, PBMC were collected and counted. The supernatants were collected for cytokine measurements. Glioma cells were detached, suspended in medium (1 ml) and labeled by addition of 50 µCi ^{51}Cr (#NEZ147, NEN, Boston, MA). The PHA-stimulated PBMC were also labeled. The labeled allogeneic glioma cells (10^4 per well) were incubated either alone (spontaneous release) or with effector PBMC from the cocultures at effector:target ratios of 10:1, 20:1, 40:1 or 80:1. The maximum ^{51}Cr release possible was determined by addition of NP-40 (100% lysis). To determine autoreactivity, labeled activated PBMC (10^5 per well) were incubated with numbers of effector PBMC equivalent to those used for the lysis of the glioma cells. After 4 h, 50 µl of the supernatant were transferred to a Luma-Plate^{TM}-96 (Packard, Dreieich, Germany), dried overnight and measured. Lysis was calculated as [cpm (effector cells) - cpm (spontaneous)] / [cpm (NP-40) - cpm (spontaneous)] x 100%. To examine the killing of immune cells by glioma cells, 10^4 glioma cells were seeded in

a 96 well plate. One day later, 10^5 labeled PBMC were added. Both PHA-stimulated and non-stimulated PBMC were tested. Supernatants were collected 18 h later and assayed as above.

TNF-α bioassay. L-M cells (5 x 10^4 per well) were seeded in 96 well plates. One day later the serum-containing medium was replaced by 100 µl serum-free DMEM containing cycloheximide (20 µg/ml). The supernatants from PBMC or glioma cells or cocultures were diluted to a volume of 100 µl and added. Survival was assessed 16 h later by crystal violet staining. These data were confirmed by ELISA for human TNF-α (Endogen, Woburn, MA).

Determination of sCD27. Cell culture supernatants were analysed for sCD27 by sandwich ELISA (CLB, Amsterdam, Netherlands) according to the manufacturer's instructions.

Detection of DNA fragmentation and apoptosis. PBMC were stained with FITC-labeled antibodies to CD4, CD8, CD14, CD19 or CD56, fixed and permeabilized in ice-cold 70% ethanol. RNA was digested with RNase A (Gibco). DNA was stained with propidium iodide (50 µg/ml). FACScalibur settings were adjusted so that the G1-peak measured in channel Fl-2A moved to 200 relative fluorescence units. Cells to the left of this peak have less than 2n chromosomes signifying loss of DNA. Aggregated cells were detected in channel Fl-2W and gated out. Given the strong adherence of glioma cells and the excess of PBMC in these assays, contamination of PBMC populations with glioma cells was negligible as controlled by staining of lymphocyte subpopulations and size. PBMC apoptosis was also analysed by AnnexinV-FITC staining. The cells were collected, washed and resuspended in a buffer containing 10 mM HEPES/NaOH, pH 7.4, 140 mM NaCl and 2.5 mM $CaCl_2$. AnnexinV-FITC (1:100) and propidium iodide (50 µg/ml) were added. When analysis of lymphocyte subsets was desired, PBMC were first incubated with CD4-PE, CD8-PE, CD14-PE, CD19-PE or CD56-PE monoclonal antibodies.

Statistical analysis. Data are representative of experiments performed three times with similar results. Viability studies were performed using triplicate wells. Significance was assessed by t-test ($^{*}p<0.05$, $^{**}p<0.01$).

Results

Human malignant glioma cell lines express CD70 mRNA and protein in vitro and CD70 protein in vivo

U87MG and T98G cells were screened for changes in gene expression in response to irradiation. In U87MG cells, the Clontech Atlas cDNA array revealed that 42 genes were induced and 36 were down-regulated 1 h after irradiation. At 4 h after irradiation, 15 genes were up- and 10 down-regulated. In T98G cells, the expression of 27 genes was up-regulated and 66 genes were down-regulated 1 h after irradiation, while 6 genes were up- and 22 down-regulated at 4 h after irradiation. Genes known to be induced by irradiation, e.g. p21, were up-regulated in U87MG cells after 1 h (1.4-fold) and 4 h (2.6-fold) irradiation. T98G is a p53 mutant cell line and p21 levels did not change with irradiation in these cells. Surprisingly, CD70 antigen mRNA was found in both control and irradiated U87MG cells. Whereas no change in CD70 expression was observed at 1 h after irradiation, there was a 5.7-fold increase 4 h after irradiation (Fig.5.1). CD70 mRNA was not detectable in T98G cells with or without irradiation.

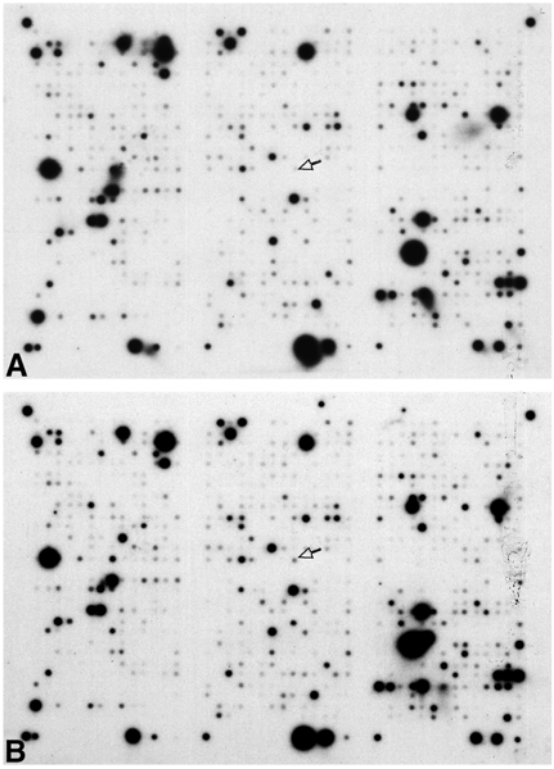

Fig. 5.1. **cDNA array autoradiographs showing up-regulation of CD70 in U87MG cells after irradiation.** Five μg of DNase-treated total RNA isolated from non-irradiated U87MG cells (A) and from U87MG cells 4 hrs after irradiation (6 Gy) (B), respectively, were reverse-transcribed into cDNA in the presence of [α-^{32}P]-dATP separately, and hybridized to Clontech Atlas Human Cancer 1.2 Arrays. Note that CD70 antigen (indicated by an arrow) expression was up-regulated 4h after irradiation.

Northern blot analysis revealed that 11 of 12 malignant glioma cell lines expressed CD70 mRNA (Fig. 5.2A). T98G cells were negative. High levels of CD70 mRNA were detected in U138MG, D247MG, LN-319 and U373MG cells. Immunoblot analysis confirmed that CD70 mRNA was translated into CD70 protein (Fig. 5.2B). Flow cytometry showed that the protein was expressed at the cell surface (Fig. 5.2C). Quantitative data for CD70 mRNA expression and CD70 protein levels are provided in Table I. There was strong correlation between CD70 mRNA expression and CD70 protein expressed at the cell surface ($r = 0.9594$, $p < 0.0001$). Two human neuroblastoma cell lines, SKN-BE and SKN-LE, did not show CD70 protein determined by flow cytometry and immunoblot analysis (data not shown).

Table 5.1. **CD70 expression in human glioma cell lines.**[a]

	CD70/ß-actin mRNA ratio	**CD70 protein [SFI]**
LN-18	**0.0146**	1.3
U138MG	0.1925	10.3
U87MG	0.0604	2.7
LN-428	0.0479	2.5
D247MG	0.0888	3.9
T98G	0.0048	1.1
LN-319	0.2747	15.5
LN-229	0.0317	1.9
A172	0.0288	1.5
U251MG	0.0479	6.4
U373MG	0.4613	31.7
LN-308	0.0167	3

[a]CD70 mRNA expression assessed by Northern blot analysis is expressed as ratios of optical density values normalized to ß-actin (Fig. 5.2A). CD70 protein quantified by flow cytometry is expressed as SFI values (Fig. 5.3B).

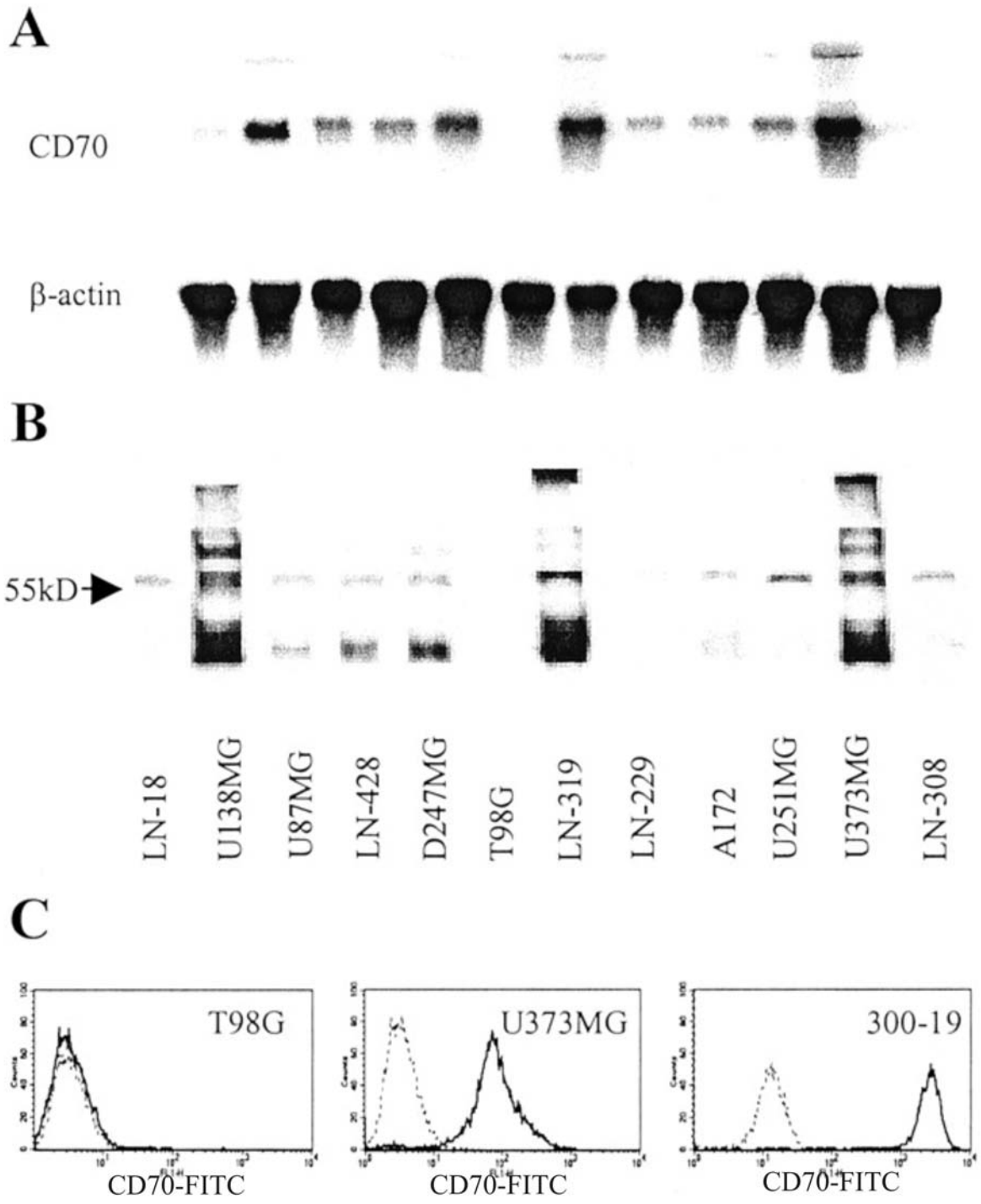

Fig. 5.2. **CD70 expression in human glioma cells.** (A). Total RNA was analysed for the expression of CD70 or ß-actin mRNA. B,C. CD70 protein levels were determined by immunoblot (B) and flow cytometry (C). B shows CD70 migrating at 55 kD. C shows representative flow cytometry profiles for CD70-negative T98G cells (left), CD70-positive U373MG cells (middle) and CD70-transfected 300-19 cells (right) (bold profile, CD70 antibody; dotted profile, control antibody) (see also Table 1, right column).

Among 12 human glioblastoma specimens, 5 were positive for CD70. A representative sample is shown in Fig. 5.3A. Among 4 anaplastic astrocytomas examined, 3 showed CD70 expression (Fig. 5.3B). Morphological features led to the identification of CD70-expressing cells as tumour cells rather than tumour-infiltrating host cells. Normal brain sections revealed no CD70-expressing cells (Fig. 5.3C).

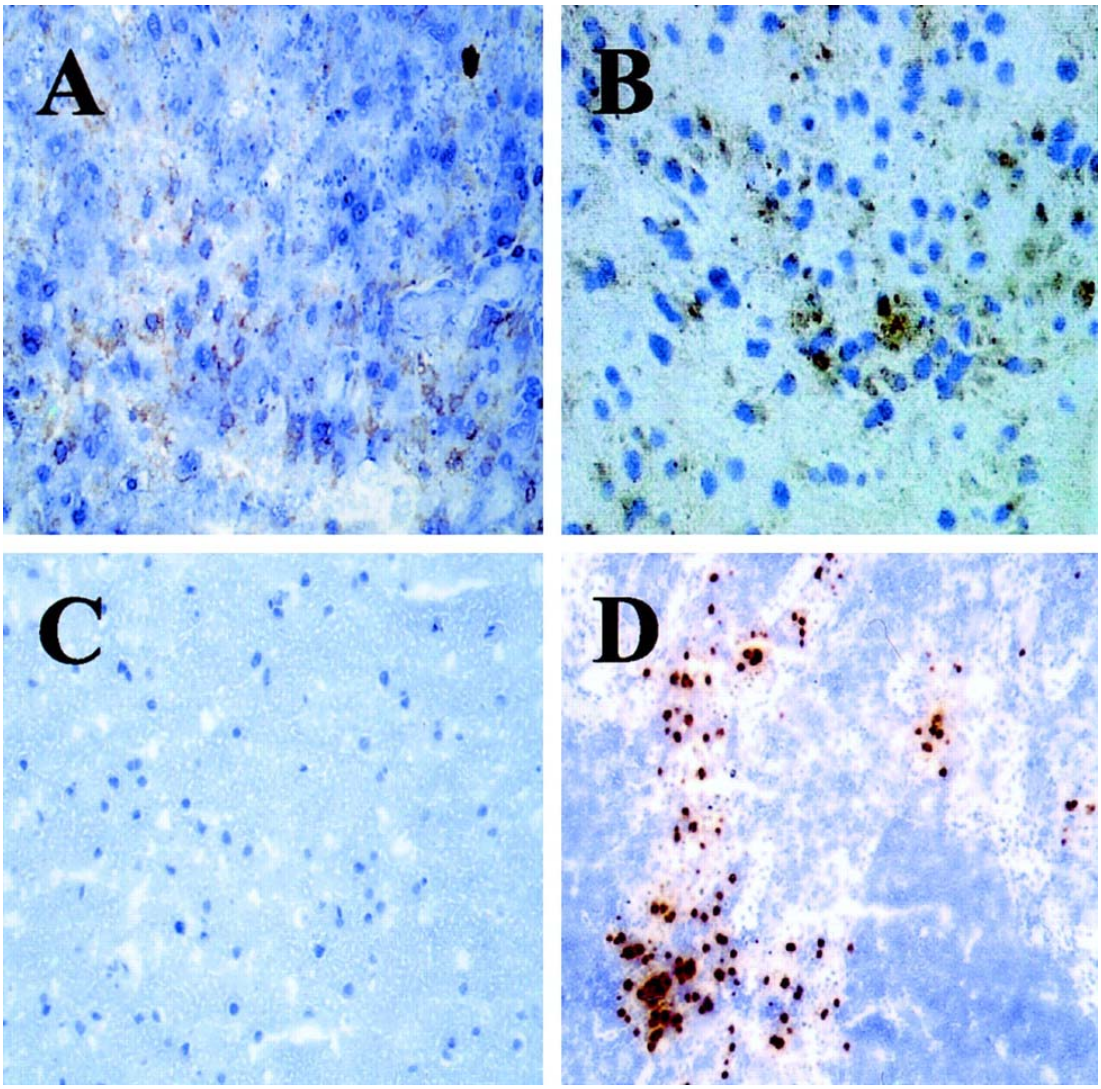

Fig. 5.3. **CD70 expression in human gliomas *in vivo*.** CD70 expression was assessed by immunocytochemistry in glioblastoma (A), anaplastic astrocytoma (B), normal brain (C) or tonsil, as a positive control (D, magnification 200x in A,B and 100x in C,D).

p53-independent modulation of CD70 expression in human malignant glioma cell lines by irradiation

Since irradiated glioma cells were used for the ensuing immunological studies, it was also determined whether radio-inducibility is a general feature of CD70 expression in human glioma cells. All 12 cell lines were irradiated at 6 Gy and assessed for CD70 mRNA and protein levels. CD70 mRNA levels increased in 8 cell lines, CD70 protein expression at the cell surface in 7 cell lines (Fig. 5.4). The increase in CD70 mRNA in LN-319 cells, which express high levels of CD70 constitutively, did not result in enhanced CD70 protein expression. The highest increase in CD70 protein expression was 89% in U87MG cells (Fig. 5.4C). Kinetic analyses in U87MG and LN-229 cells showed that the maximum cell surface expression was found at 6 h after irradiation.

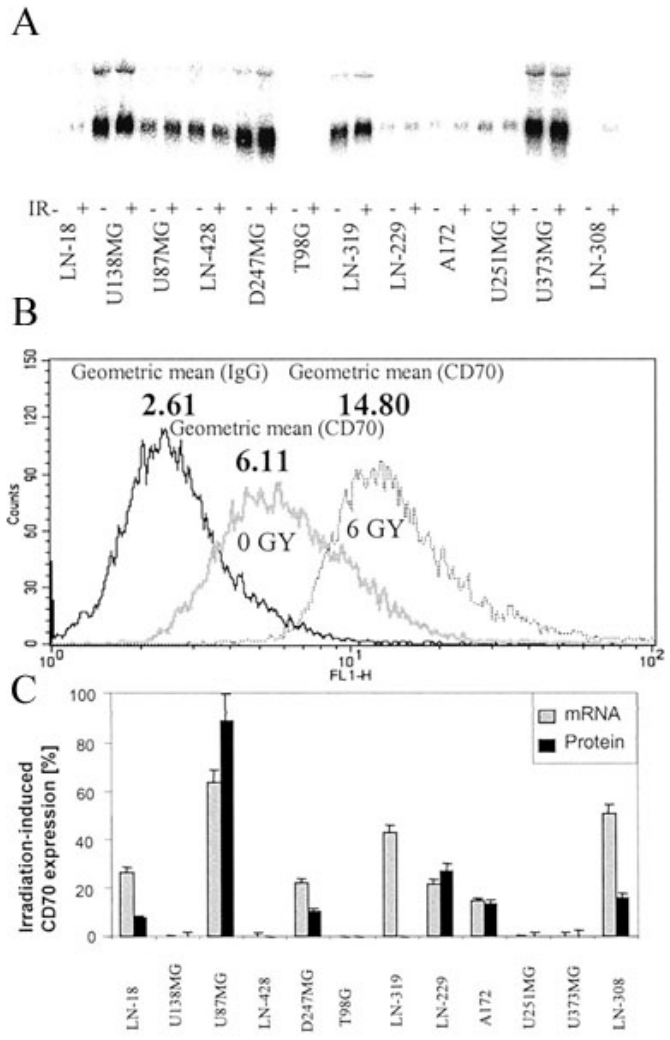

Fig. 5.4 **CD70 expression by glioma cells is enhanced by irradiation.** A. The cells were untreated or irradiated at 6 Gy. RNA was isolated 4 h later and CD70 mRNA levels were quantified by Northern blot. (B,C). CD70 protein in untreated or irradiated cells (6 Gy, 4 h) was quantified by flow cytometry, shown representatively in B for U87MG cells. The isotype control was not shifted after irradiation at 6 Gy. The numbers indicate the mean fluorescence values used to derive the SFI values. In (C), the induction of CD70 expression is expressed as percentages as determined by Northern blot analysis (relative intensities corrected for ß-actin) and flow cytometry ($SFI_{6Gy}/SFI_{0Gy} - 1$).

To assess whether CD70 is also induced at lower doses of irradiation, U87MG and LN-308 cells were irradiated at 1, 3 or 6 Gy. The SFI were 2.7 at 0 Gy, 3.6 at 1 Gy, 4.9 at 3 Gy and 5.1 at 6 Gy in U87MG cells, and 3.0 at 0 Gy, 3.4 at 1 Gy; 3.5 at 3 Gy and 3.5 at 6 Gy in LN-308 cells (data not shown). Irradiation of U373MG, U138MG or T98G at 200 Gy resulted in the same changes in CD70 expression detected by flow cytometry as irradiation at 6 Gy (data not shown). U87MG, the first cell line identified to respond to irradiation with enhanced CD70 expression, is wild-type for p53 (196). However, the irradiation-induced increase in CD70 expression was unaffected by ectopic expression of a dominant-negative p53 mutant, $p53^{V135A}$ (31), confirming that p53 does not mediate the induction of CD70 after irradiation. Conversely, the nitrosourea lomustine, a cytotoxic agent which induces p53 expression in U87MG cells, did not modulate CD70 expression, confirming that enhanced CD70 expression is not a nonspecific response to genotoxic stress (data not shown).

No autocrine effects of CD70 expression in human glioma cells

To investigate possible autocrine effects of the CD70/CD27 system (320) in glioma cells, the glioma cell lines were screened for the expression of CD27 mRNA using Northern blot, RT-PCR and flow cytometry. None of the methods revealed the expression of CD27 in either of the 12 cell lines, using PBMC as a positive control. Further, ligation of CD70 with specific antibody in LN-18, U138MG, U87MG, T98G or U373MG cells had no effect on the proliferation or survival of the glioma cells. These data remained negative, even with immobilisation of the CD70 antibody on a Nunc Maxisorp surface or crosslinking by a secondary antibody. These overall negative data (not shown) provided no evidence for autocrine or backward signalling of the CD70 system in human glioma cells.

CD70-mediated inhibition of alloreactivity by human glioma cells

None of the 12 glioma cell lines expressed B7.1 (CD80), B7.2 (CD86) or CD40L (CD154) (see also section 4 of this thesis). The cell lines used for the ensuing immunological experiments (T98G, U138MG, U373MG) were also negative for CD40 and MHC class II expression, but all three expressed the MHC class I molecule HLA-A2 at high levels. First the alloproliferative response of HLA-A2-negative PBMC or T cells to the glioma cells was examined. The Ki-24, HNE.51 and

BU69 antibodies to CD70 have all been described as blocking antibodies (Vth Workshop on Leucocyte Typing). When tested in parallel, these antibodies uniformly enhanced the alloproliferative response to the CD70-positive cell lines, U138MG and U373MG, but not the alloproliferative response to the CD70-negative cell line, T98G (Fig. 5.5A). Since the effects were most prominent with the Ki-24 antibody, an azide-free preparation of this antibody (10 µg/ml) was chosen for all ensuing functional experiments. Consistent with this inhibitory effect of CD70, PHA-induced T cell proliferation (Fig. 5.5B) or PBMC proliferation in a mixed lymphocyte reaction (MLR) (Fig. 5.5C), were inhibited much stronger by U138MG and U373MG cells than by T98G cells, and this inhibition was partly relieved by the CD70 antibody. The broad spectrum caspase inhibitor, zVAD-fmk, mimicked the effects of CD70 antibody in the MLR (Fig. 5.5C).

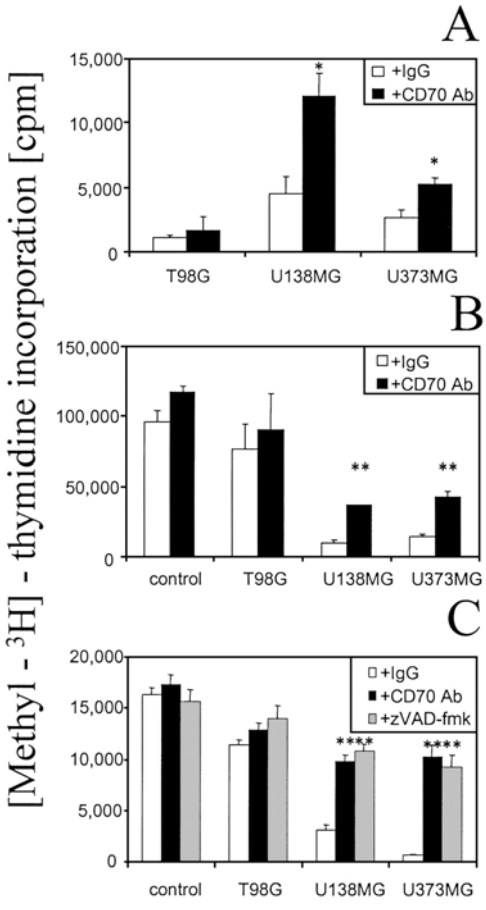

Fig. 5.5 **Modulation of alloreactivity to glioma cells by CD70.** (A-C). Irradiated glioma cells were preincubated with isotype control antibody (open bars) or CD70 antibody (Ki-24) (black bars) (10 µg/ml) for 2 h. In (A), the glioma cells were seeded in 96 well plates (10^4/well) and 10^5 T cells were added in a total volume of 150 µl RPMI containing 10% FCS. [Methyl-^{3}H] thymidine (0.5 µCi/well) was added on day 4 for 16 h. [Methyl-^{3}H] thymidine incorporation was measured by liquid scintillation counting. In (B), PHA (10 µg/ml) was added to all wells. In (C), 10^5 irradiated HLA-A2-positive stimulator PBMC were cocultured with 10^5 HLA-A2-negative responder PBMC and 10^4 irradiated glioma cells. Data in (A-C) are expressed as cpm determined by liquid scintillation counting (*$p<0.05$, **$p<0.01$, CD70 antibody or zVAD-fmk compared with isotype control antibody).

CD70-mediated induction of PBMC apoptosis by glioma cells

The number of viable PBMC was decreased by a factor of 1.8-2.6 after the coculture with U138MG and U373MG cells compared to T98G cells. This cell loss was prevented by CD70 antibody, by sCD27 or zVAD-fmk (Fig. 5.6 A). In PBMC cocultured with U138MG and U373MG cells, the number of AnnexinV-positive cells was significantly reduced by CD70 antibody or sCD27. No such effect was seen in PBMC cocultured with T98G cells (Fig. 5.6 B). Flow cytometry confirmed cell loss by apoptosis: the percentage of PBMC in the sub-G1-peak was significantly reduced by CD70 antibody and sCD27 after coculture with U138MG and U373MG cells, but not after coculture with T98G cells. zVAD-fmk (100µM) exerted a protective effect in cocultures with all three cell lines (Fig. 5.6 C). The protection afforded by CD70 antibody or sCD27 was similar to that achieved with zVAD-fmk.

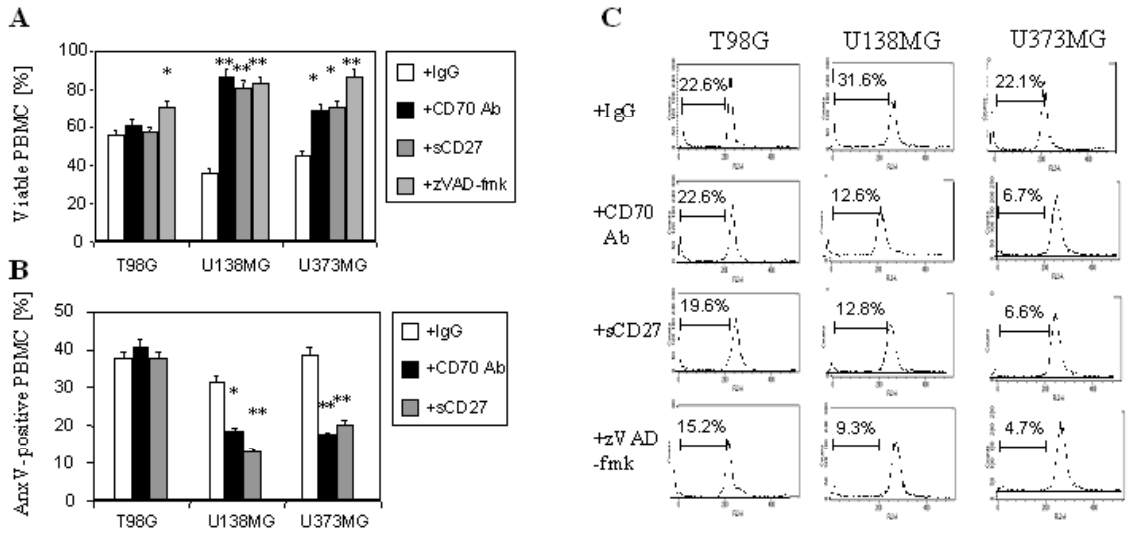

Fig. 5.6. **CD70-expressing glioma cells kill PBMC in a CD70-dependent manner.** (A) Irradiated (200 Gy) glioma cells were preincubated with isotype control antibody, CD70 antibody (10 µg/ml) or sCD27 (50 U/ml) for 2 h and washed twice in PBS before PBMC were added. Alternatively, zVAD-fmk (100 µM) was added at 0 h. The number of viable PBMC was assessed 5 days later by trypan blue exclusion. (B) The percentage of AnnexinV-positive PBMC was determined after coculture conditions as in (A). (C) After coculture with glioma cells, the PBMC were fixed, permeabilized and stained with propidium iodide. Cells to the left of the G_1-peak show loss of DNA indicative of apoptosis.

Induction of apoptosis was strong in CD4-positive and CD8-positive T cells, which constitute the major subpopulations after 5 day coculture, whereas no significant effect was found for CD56-positive cells. As expected, the effect was only apparent in the $CD27^+$ subset.

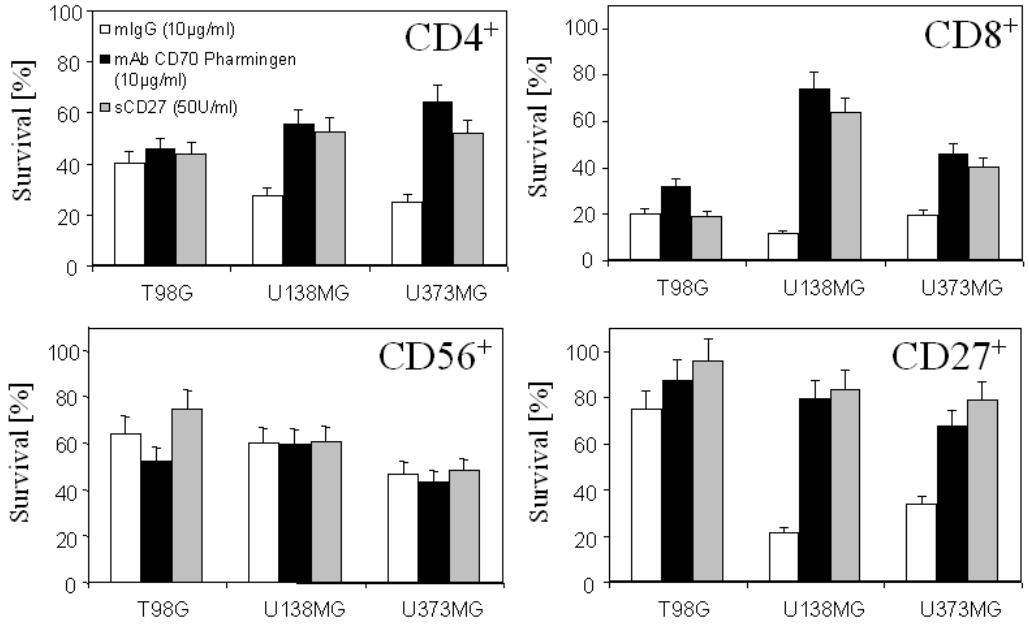

Fig. 5.7. **CD70-dependent apoptosis affects $CD27^+$ cells from the $CD4^+$ and $CD8^+$ subset.** Survival rates of $CD4^+$, $CD8^+$ T cells, of $CD56^+$ NK and NKT cells and of pooled $CD27^+$-lymphocyte subpopulations were determined by AnnexinV-FITC-staining following 5 days of coculture with irradiated glioma cells.

The hypothesis that glioma cells kill PBMC (reversed lysis) was confirmed in a redirected ^{51}Cr release assay. The coincubation of ^{51}Cr-labeled resting or PHA-stimulated PBMC with the glioma cells resulted in the release of ^{51}Cr. Lysis was much more prominent with U138MG and U373MG cells than with T98G cells. zVAD-fmk decreased the lysis of PBMC in cocultures with all three cell lines (Fig. 5.8 A). Similar results were obtained in PHA-activated PBMC (Fig. 5.8 B).

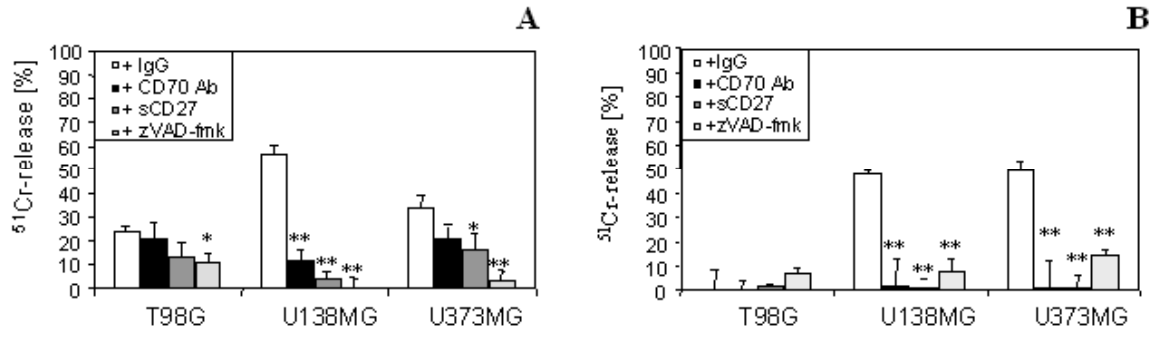

Fig. 5.8. **CD70-expressing glioma cells kill PBMC in a caspase- and CD70-dependent manner.**A. PBMC were labeled with ^{51}Cr. Following coculture with non-irradiated glioma cells (10^5 PBMC, 10^4 glioma cells/well) for 18 h, ^{51}Cr was determined in the supernatant. Assays were performed in the presence of an isotype-matched control antibody (10 µg/ml), Ki-24 CD70 antibody (10 µg/ml), sCD27 (50 U/ml) or zVAD-fmk (100 µM). (B) As in A, but PBMC (5 x 10^4) were activated by incubation with PHA (10 µg/ml) for 24 h (*p<0.05, **p<0.01, coculture in the presence of Ki-24 CD70 antibody, sCD27 or zVAD-fmk compared to coculture plus control IgG, t-test).

After longer stimulation with PHA (48 h), about 25% of all cells underwent spontaneous apoptosis which was prevented by zVAD-fmk. The spontaneous ^{51}Cr release by PHA-stimulated PBMC, but not by resting PBMC, in the absence of glioma cells was also reduced by CD70 antibodies or sCD27. These effects in the ^{51}Cr release assay may be mediated by interactions of the reagents (CD70 antibody, sCD27) with CD70 expressed on the activated immune cells.

In line with this concept, PHA stimulation greatly enhanced the cell surface expression of CD70 (Fig. 5.9 A). In contrast, the expression of CD27 remained largely unchanged for 24 h (data not shown), but was considerably decreased among CD4-, CD8- and CD56-positive cells after 48 h (Fig. 5.9 B). No cells expressed both CD27 and CD70.

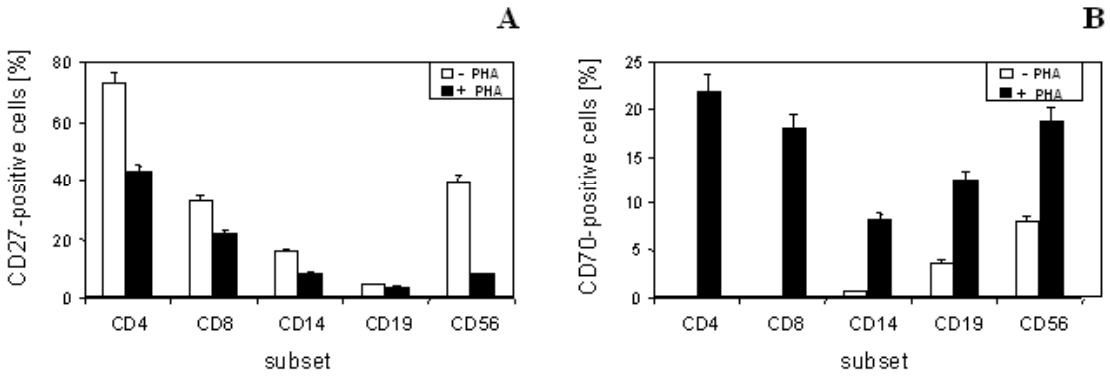

Fig. 5.9. **CD 27 and CD70 expression by lymphocyte subsets.** The expression of CD27 (A) and CD70 (B) by lymphocyte subsets (CD4-, CD8-, CD14-, CD19- and CD56-positive cells) under resting conditions (open bars) or 48 h after stimulation with 10 µg/ml PHA (filled bars) was assessed by double-staining with FITC- and PE-labeled antibodies.

Corresponding to the larger number of surviving PBMC, the number of remaining U138MG and U373MG stimulator cells determined by crystal violet staining was decreased by a factor of 1.7 to 2.5 after 5 days of cocultures when CD70 antibody or sCD27 were present (data not shown). However, Fig. 5.10 shows that the lytic activity of the surviving PBMC was unaffected by pre-exposure of the glioma cells to CD70 antibodies, demonstrating that PBMC surviving the challenge of glioma cell-induced CD70-mediated apoptosis were fully functional (Fig. 5.10).

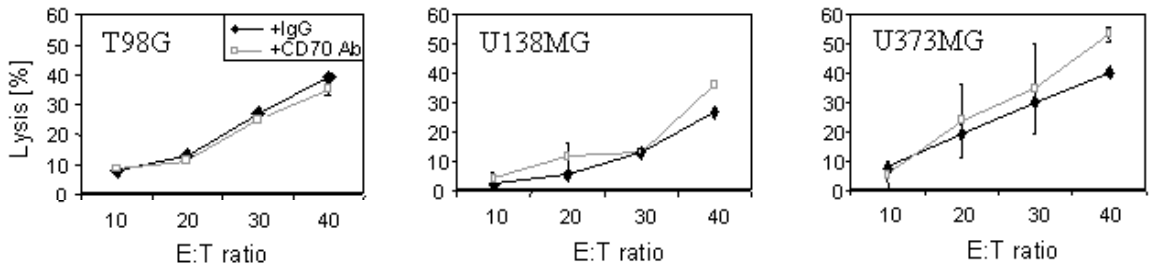

Fig. 5.10. **Surviving PBMC from co-cultures with glioma cells display CD70-independent lytical activity.** The lytic activity of PBMC stimulated with glioma cells was determined by ^{51}Cr release. Prior to the stimulation period (5 days), glioma cells were incubated with a non-specific isotype control antibody or Ki-24 CD70 antibody (10 µg/ml) for 2 h. During the effector period (4 h), no antibody was present. The lytic activity of the remaining viable PBMC is given for various effector:target (E:T) ratios with the number of ^{51}Cr-labeled target cells kept constant.

To further confirm the specificity of the effects mediated by CD70 expressed on glioma cells, similar experiments were performed in the absence of glioma cells, but in the presence of agonistic CD27 antibodies. These experiments revealed induction of apoptosis in resting PBMC and in the MLR, and apoptosis was blocked by zVAD-fmk (Fig. 5.11 A,B). The proportion of apoptotic PBMC detected by flow cytometric analysis of DNA content remained at an almost constant level for 5 days. Since apoptotic cells are likely to be cleared by macrophages in culture (321), the actual number of dying cells may be considerably higher than the level of approximately 20% found at a given time point. The amount of ^{51}Cr released by resting and activated PBMC was significantly increased by the CD27 antibody compared with an isotype control antibody (data not shown).

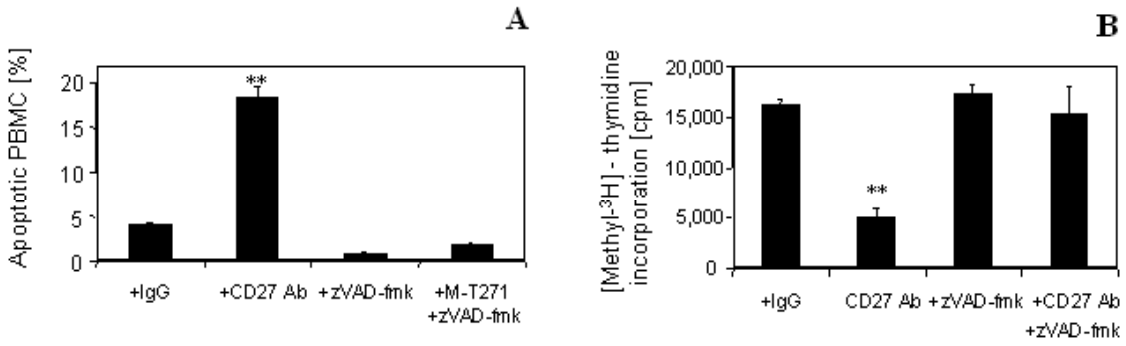

Fig. 5.11. **CD70-mediated apoptosis of PBMC cocultured with glioma cells is mimicked by agonistic CD27 antibody.** A. Resting PBMC were cultured in the presence of non-specific IgG or agonistic CD27 antibody (10 µg/ml), without or with zVAD-fmk (100 µM), for 48 h. Dead cells were quantified by flow cytometry as in Fig. 4C. In (B), 10^5 irradiated HLA-A2-positive stimulator PBMC were cocultured with 10^5 HLA-A2-negative responder PBMC and 10^4 irradiated glioma cells. On day 4, [methyl-^{3}H] thymidine (0.5 µCi/well) was added. [Methyl-^{3}H] thymidine incorporation was measured 16 h later by liquid scintillation counting.

Apoptotic PBMC detected by AnnexinV-FITC staining or DNA loss (sub G_0-peak) were further characterised by staining with specific antibodies. Subset analysis revealed that several CD27-positive subsets, in particular CD19-positive, CD4-positive and CD8-positive cells, were affected (data not shown).

Table 5.2. **TNF-α release by cocultures of PBMC and glioma cells.**[a]

	TNF-α [pg/ml]			
	PBMC alone	PBMC + T98G	PBMC + U138MG	PBMC + U373MG
Control antibody	160 ± 32	992 ± 49**	73 ± 74	152 ± 49
Ki-24 CD70 antibody	34 ± 86	947 ± 8**	665 ± 62**$^{++}$	615 ± 62**$^{++}$
sCD27	148 ± 111	894 ± 74**	714 ± 123**$^{++}$	652 ± 111**$^{++}$
zVAD-fmk	174 ± 37	1128 ± 37**$^{+}$	689 ± 49**$^{++}$	775 ± 62**$^{++}$

[a]PBMC (1.5 x 10^7) were cultured alone or cocultured with 1.5 x 10^6 irradiated T98G, U138MG or U373MG cells in 5 ml RPMI/10% FCS for 5 days. TNF-α release was determined by L-M bioassay (**$p<0.01$, coculture compared to PBMC alone; $^{++}p<0.01$, compared to coculture plus control IgG, t-test).

TNF-α release into the supernatant (Table II). TNF-α release was enhanced by CD70 antibody in cocultures containing U138MG and U373MG cells but not in cocultures containing T98G cells. The addition of zVAD-fmk levels elevated TNF-α under all conditions. There was no TNF-α release by glioma cells cultured in the absence of PBMC or in the presence of IFN-γ (100 U/ml) (data not shown). As in other experiments, PBMC from some donors were strongly activated by T98G cells whereas PBMC from other donors hardly responded to this cell line. This donor-specific variability was less pronounced with U138MG and U373MG cells. Importantly, TNF-α release from PBMC in cocultures with T98G was never affected by the addition of CD70 antibody or sCD27 whereas these reagents produced consistent effects in the other two cell lines. Appropriate control experiments revealed that CD70/CD27-mediated PBMC apoptosis was not mediated by CD95/CD95L interactions or TGF-ß since neutralizing antibodies to CD95L or TGF-ß failed to rescue the loss of PBMC in experiments corresponding to Figures 5.6 and 5.8. The antibodies were used at concentrations previously shown to block human CD95L (204) and TGF-ß (292).

CD70-expressing glioma cells induce the release of sCD27 from PBMC and decrease CD27 expression

The detection of sCD27 in normal human serum (322) indicates that this molecule may have immune regulatory properties. The PBMC preparations used here showed levels of 5 U/ml at day 5 as determined by ELISA. None of the 12 glioma cell lines produced sCD27 when cultured alone, consistent with the failure to detect CD27 mRNA by RT-PCR and Northern Blotting (see above). Coculture with U138MG or U373MG cells significantly enhanced the levels of sCD27 in the supernatant whereas no such effect was seen with T98G cells. CD70 antibody and zVAD-fmk inhibited this effect (Fig. 5.12A). sCD27 is generated by proteolytic cleavage of membrane-bound CD27 (323) after triggering of T cells by antigen (322, 324). Hence CD27 expression at the cell surface of the remaining PBMC was also investigated after 5 day coculture. While no change in CD27 expression resulted from coculture with T98G cells, the CD70-positive cell lines U138MG and U373MG induced a reduction of CD27 expression at the surface of the remaining PBMC. The number of PBMC with high CD27 expression decreased from 50.7% to 10.9% after coculture with U373MG cells, suggesting that, after contact with CD70-expressing

glioma cells, CD27 is cleaved, released and not re-incorporated into the cell membrane, providing another response of PBMC to CD70-expressing glioma cells, in addition to apoptosis (Fig. 5.12B).

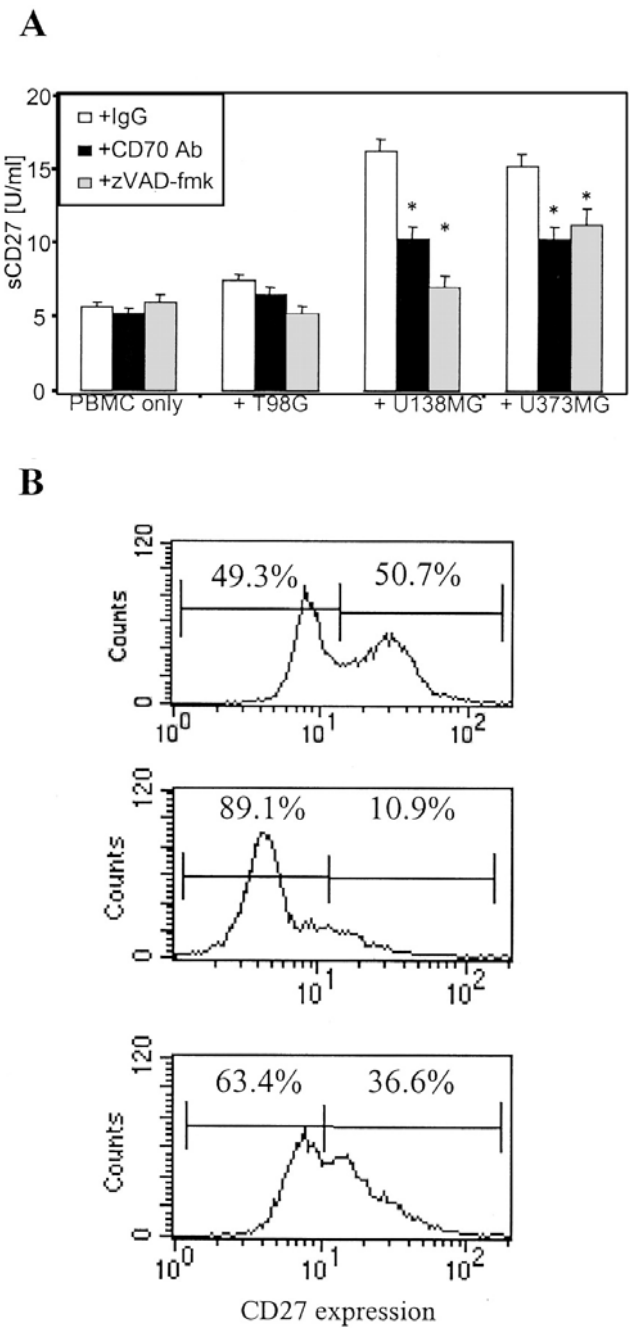

Fig. 5.12. **CD70-expressing glioma cells promote sCD27 release by PBMC.** (A) PBMC (1.5 x 10^7) were cultured alone or cocultured with 1.5 x 10^6 irradiated glioma cells for 5 days. Glioma cells were preincubated with control IgG or CD70 antibody (10 µg/ml) for 2 h; alternatively, zVAD-fmk (100 µM) was added during coculture. sCD27 levels in the supernatant were determined by ELISA ($^{*}p<0.05$, $^{**}p<0.01$, compared to control IgG). (B) CD27 expression was assessed by flow cytometry using M-T271 CD27 antibody: in PBMC cultured alone for 5 days (upper panel), cocultured with U373MG cells preexposed to control antibody (middle panel) or to CD70 antibody (lower panel).

Discussion

The present study identifies CD70 as a novel candidate molecule mediating immune escape of human malignant gliomas. The induction of CD70 expression by irradiation exemplifies how radiotherapy might suppress antitumour immune responses. This observation therefore has implications for the orchestration of multimodality cancer therapy in the clinic. Endogenous expression of CD70 had not been reported previously in nonlymphoid cancer cells, but has simultaneously been confirmed by another group (325). CD70 was identified as a radio-inducible gene in U87MG glioma cells (Fig. 5.1). CD70 expression turned out to be rather common among human malignant glioma cell lines (Fig. 5.2 A-C) Immunohistochemical stainings confirmed that CD70 was also expressed by neoplastic glial cells *in vivo* (Fig. 5.3). CD70 expression was specifically induced by irradiation in glioma cells (Fig. 5.4), but not in neuroblastoma cells. Irradiation-induced CD70 expression did not require wild-type p53 activity and was not merely a response to genotoxic stress since cytotoxic agents such as lomustine did not modulate CD70 expression. In contrast to the expected result, CD70 expressed by glioma cells induced immunosuppression rather than immune stimulation in alloreactivity assays *in vitro* (Fig. 5.5). Several lines of experimental evidence disclosed that CD70 expressed by glioma cells promoted apoptosis in the PBMC population (Fig. 5.6, 5.8, 5.11). The shedding of CD27 by PBMC may represent an escape mechanism from glioma cell-induced, CD70-dependent apoptosis (Fig. 5.12). The role for CD70/CD27 interactions in T, B and especially in NK cell activation has raised interesting perspectives for the immunotherapy of cancer (326, 327). For instance, virus-mediated CD70 gene transfer into mouse colon carcinoma cells enhanced T cell responses and induced antitumour immunity (328). Further, in a mouse model using CD70-transfected MHC class I-deficient RMA-S tumour cells, CD70 expression enhanced primary, NK cell-mediated tumour rejection *in vivo* as well as tumour-specific T cell memory against secondary tumour challenge (329). However, since all investigated glioma cell lines express large amounts of MHC class I (131), this NK cell-dependent response is likely to be inhibited. Further, T cell activation and apoptosis are complex processes that do not only depend on primary signals but also on secondary factors. This complex regulation seems to be necessary, given the need of rapidly controlling immune reactions under different and rapidly changing conditions (30). Many molecules can thus exert both stimulatory as well as proapoptotic effects on

the immune system (330). The costimulatory role of CD70 has been well characterized (331). However, CD70-induced apoptosis mediated by the proapoptotic protein Siva has also been demonstrated (49, 332). Recent findings suggest that Siva antagonizes the pro-survival function of Bcl-x_L and activates the mitochondrial (intrinsic) apoptosis pathway (333, 334). The present study provides ample evidence that CD70 expressed by glioma cells evokes immune inhibition rather than immune stimulation (Fig. 5.5-5.8) and thus contrasts with several previous studies aiming at exploiting immune stimulatory properties of CD70 (326-329). It is commonly assumed that cells undergoing malignant transformation can potentially be cleared by the immune system. In order to escape from the surveillance of the immune system, most tumours down-regulate costimulatory molecules and instead express molecules with immune inhibitory function, including TGF-β or CD95L. Such processes of selection *a priori* argue against a possible costimulatory role of CD70 expressed on glioma cells. It is well conceivable that (yet unidentified) immunosuppressive factors expressed by glioma cells interfere with CD27-mediated, NF-κB-dependent costimulatory signalling, while the apoptosis pathway via Siva may not be inhibited. Impaired CD70 signalling may occur when the level of sCD27 is abnormally high. This has been reported for the blood and cerebrospinal fluid of patients suffering from various autoimmune diseases (335-338). One might therefore speculate that high concentrations of sCD27 administered into a postsurgical glioma cavity might promote local antiglioma immunity.

Expression and functional activity of CD70 in a solid nonlymphoid tumour represents one of two novel and unexpected findings of this study. The second major observation was the radioinducibility of CD70 in glioma cells *in vitro* which led to its identification by cDNA array analysis. Human glioblastomas are commonly irradiated in 1.8-2 Gy fractions to a total dose of 54-60 Gy. Since single doses of 6 Gy were used here to assess the effects of irradiation in most experiments (Fig. 5.4), future studies will need to determine whether lower dose fractionated irradiation will also induce CD70 expression *in vitro* and whether similar effects can be demonstrated *in vivo*. This study defines a possible pathway by which fractionated radiotherapy may create a locally immunosuppressed environment in human glioblastomas. CD70 expression maintained by radiotherapy may thus interfere with immune responses to the tumour during the weeks of radiotherapy. It is tempting to speculate that irradiation-induced CD70

expression might be particularly counterproductive in human cancers known to be immunogenic, such as malignant melanoma or renal cell carcinoma.

VI. Expression of the non-classical MHC class I molecule HLA-G in human gliomas: an alternative strategy of immune escape

This work has been published in the Journal of Immunology 2002 May 1;168(9):4772-80.

This work is based on an idea from Dr. Heinz Wiendl (Group of Neuro-Immunology, Department of Neurology, University of Tübingen, Medical School, Tübingen) who also lead the project. The immunohistochemical stainings were performed by Dr. Antje Bornemann and Prof. Dr. Richard Meyermann in the Institute of Brain Research, University of Tübingen, Germany. Dr. Valeska Hofmeister and Prof. Dr. Elisabeth H. Weiss (Institute of Anthropology and Human Genetics, Ludwig Maximilians University, Munich, Germany) confirmed the expression of HLA-G by RT-PCR, Western and Northern Blotting. I generated the glioma cell transfectants (Fig. 6.5) that were used in this manuscript and guided the functional immunological experiments shown in Fig. 6.6, 6.7, 6.9, 6.10, 6.11, 6.12 that were largely carried out by Meike Mitsdörffer. Thanks also go to Drs. M. McMaster (University of California, San Francisco) and D. Geraghty (Fred Hutchinson Cancer Research Center, Seattle) for kindly providing anti-HLA-G mAbs.

Introduction

The escape from immune surveillance is thought to be a prerequisite for the development of clinical cancer. A failure of the immune system to recognize and eliminate tumour cells may be caused by the absence of tumour antigens and by the non-reactivity or non-recognition of tumour antigens because of insufficient costimulation, anergy, tolerance or immunosuppression. Human glioblastoma is a highly lethal tumour which is paradigmatic for its ability to suppress effective antitumoral immune responses. Two pathways of glioblastoma associated-immune suppression that have attracted a lot of attention are the release of the immunosuppressive cytokine TGF-β (155) and the expression of CD95L (253), both acting on lymphoid cells (reviewed in (63)).

Major histocompatibility complex (MHC) class Ia expression is frequently altered in a variety of malignancies. These alterations may have a decisive influence on the immune response and on the metastatic capacity of the tumours (e.g. (339)). HLA-G is a ”nonclassical” MHC class I molecule (class Ib) structurally related to classical MHC class Ia (HLA-A, -B, -C) which – in contrast to class Ia molecules – exhibits a limited tissue distribution: first detected on extravillous cytotrophoblast cells (340), it has now been recognized that HLA-G is also expressed by thymic epithelial cells (341), cytokine-activated monocytes (342), inflamed muscle and myoblasts (343) and some tumours (e.g. (344)).

In contrast to HLA class Ia molecules, HLA-G is characterized by a limited polymorphism and the transcription of alternatively spliced mRNAs that encode at least seven different isoforms, including membrane-bound HLA-G1, -G2, -G3, -G4 and soluble HLA-G5 (formerly HLA-sG1), -G6 (formerly HLA-sG2), -G7 proteins (reviewed in (190)). HLA-G binds CD8 and a restricted repertoire of peptides and might therefore act as a peptide-presenting molecule (345-348). However, HLA-G has so far chiefly been regarded as a mediator of immune tolerance because it protects target cells from NK cytolysis through direct or indirect interaction with several inhibitory receptors expressed on NK cells (349-351). Further, HLA-G can also modulate antigen-specific lysis through interaction with surface molecules expressed on cytotoxic CD8 T cells (352, 353). Expression of HLA-G has therefore been proposed to allow immune escape in tumours.

In this section, the expression and functional activity of HLA-G in glioblastoma cells is reported. The negative immune regulatory effects of HLA-G on different effector lymphocyte populations studied here in models of primary and secondary immune responses supports the idea of HLA-G-dependent suppression of T cell responses representing a novel immune escape pathway of human glioblastoma.

Material and Methods

Antibodies and reagents

The following antibodies were used: 87G (IgG2b, anti-HLA-G1; kindly provided by D. Geraghty), 4H84 (mIgG1, anti-HLA-G; kindly provided by M. McMaster); MEM-G/9 (mIgG1, anti-HLA-G; Exbio, Prague, Czech Republic); BFL1.1.2 (mIgG2b, anti-HLA-G; Immunotech, Marseille, France); W6/32 (mIgG2a, anti-HLA-A, -B, -C, -C, -G, -E and β_2 microglobulin (β_2m); Biozol, Eching, Germany); L243 (mIgG2a, anti-HLA-DR), BB7.2 (mIgG2b, anti-HLA-A2; ATCC; Rockville, MD); RPA-T4 (mIgG1κ anti-CD4 FITC- and PE-labeled), HIT8A (mIgG1κ, anti-CD8 PE-labeled), AnnexinV-FITC (Pharmingen, Heidelberg, Germany); B9.11 (mIgG1, anti-CD8 FITC-labeled) N901 (NKH-1; mIgG1, anti-CD56 PE-labeled) (Immunotech); goat anti-mouse F(ab)$_2$ fragment (Dianova, Hamburg, Germany), peroxidase (hrp)-labeled rabbit anti-human $\beta_2$microglobulin (DAKO Diagnostika, Hamburg, Germany). The antibodies were titrated for flow cytometry and used at concentrations indicated (usually 20 μg/ml) in the functional assays. Soluble CD95L was obtained from CD95L-transfected murine N2A neuroblastoma cells (354). Propidium iodide was purchased from Sigma (St. Louis, MO).

Cell culture

The human malignant glioma cell lines LN-18, U138MG, U87MG, LN-428, D247MG, T98G, LN-319, LN-229, A172, U251MG, U373MG and LN-308, kindly provided by Dr. N. de Tribolet (Lausanne, Switzerland), and SV40 FHAS non-neoplastic astrocytes (kindly provided by A. Muruganandam, Ottawa, Canada) were cultured in 75 cm^3 Falcon plastic flasks using DMEM supplemented with 1% glutamine (Gibco Life Technologies, Paisley, Great Britain), 10% foetal calf serum (FCS) (Biochrom KG, Berlin, Germany) and penicillin (100 IU/ml)/streptomycin (100 μg/ml) (Gibco). The JEG-3 human choriocarcinoma cell line and the K-562 human erythroleukemia cell line (ATCC) were maintained in RPMI 1640 supplemented with 1 mM sodium pyruvate, penicillin (100 IU/ml)/streptomycin (100 μg/ml) and 10% FCS. Cells were routinely tested for contamination with mycoplasma. Where indicated, the cells were irradiated using a Gammacell 1000 Elite (Nordion, Ontario, Canada).

Immunohistochemistry

Tumour biopsy specimens were surgically removed from 4 patients with glioblastoma (grade IV WHO) (male, age range 32-64 y, mean 46y) and one patient with anaplastic oligo-astrocytoma (grade III WHO) (female, 42 y). Frozen sections 10 μm thick were cut, fixed in

acetone, and immunostained with anti-HLA-G antibody (87G, BFL1.1.2). The reaction product was visualised with the streptavidin-biotin method (reagents from DAKO) using diaminobenzidine (Serva, Heidelberg, Germany) as an electron donor. As control tissue placenta was used.

HLA-G transfectants

HLA-G transfectants were obtained as described elsewhere (352, 355). In brief, HLA-G1 (encoding the full-length HLA-G transcript) and HLA-G5 (coding for the secreted HLA-G heavy chain) plasmids were generated by cloning HLA-G1 and HLA-G5 cDNAs into a GFP vector (pIRES2-pEGFP; Clontech, Palo Alto, CA). GFP vector transfectants (pIRES2-pEGFP) were used as controls. Transfection was done using Effectene® transfection reagent (Qiagen, Hilden, Germany). Cells were selected in media containing 0.5 mg/ml neomycin (G418, Calbiochem, Germany). The following transfectants were used in the study: K-562-HLA-G1, U87MG-pIRES2-EGFP (referred to as U87MG-pEGFP), U87MG-HLA-G1, U87MG-HLA-G5.

Peripheral blood mononuclear cells (PBMC) and purified lymphocyte populations

PBMC were isolated from the peripheral blood of normal healthy volunteers by density gradient centrifugation using Biocoll Separating Solution (Biochrom KG). Cells were analyzed for their HLA-A2 isotype by flow cytometry. CD4 and CD8 T cells were purified by positive selection with CD4 or CD8 Microbeads (Miltenyi Biotec, Bergisch Gladbach, Germany). NK cells were isolated by an NK cell-negative isolation kit (Dynal, Biotech, Hamburg, Germany). The purity of the isolated subpopulations used in the experiments was > 95% as determined by flow cytometry.

Flow cytometry

Adherent cell lines were collected after treatment with cell dissociation buffer (Gibco) at 37°C for 5 min. JEG-3, K-562-HLA-G1 or K-562 cells were used as positive and negative control cell lines for HLA-G or MHC expression when indicated. Cells were washed with PBS containing 0.1% bovine serum albumin (BSA) and 0.1% sodium acide and blocked with human immunoglobulins (Alphaglobin, Grifols, Langen, Germany) for 10 min at 4°C. After one washing step, the unlabeled first antibody was added at the final concentration. Isotype control monoclonal antibodies (mAbs) were used at the same concentration as the primary antibody. Incubation was done on ice for 30 min, followed by two washes. Goat anti-mouse

IgG ($F(ab)_2$-PE (5 µg/ml, Sigma) or IgG ($F(ab)_2$- di-chlorotriazinyl-fluoresceine (DTAF) (10 µg/ml, Dianova) were used as secondary antibodies. After washing, propidium iodide (PI) was added to the cells at a final concentration of 0.02 µM. PI-positive (nonviable) cells were excluded from analysis. Specific fluorescence indexes (SFI) were calculated by dividing mean fluorescence obtained with specific antibody by mean fluorescence obtained with isotype control antibody. Analysis of PBMC and lymphocyte subsets was performed similarly. Cells were blocked with human immunoglobulins and stained either with directly labeled antibodies or the respective combinations of an unlabeled first antibody and a fluorescent secondary antibody. Flow cytometry was performed using a FACSCalibur (Becton Dickinson, Heidelberg, Germany).

Detection of apoptosis by AnnexinV binding

PBMC or purified lymphocyte subsets undergoing apoptotic cell death were analysed by staining with FITC-labeled AnnexinV (Pharmingen). After various incubation times with the glioma cells, lymphocytes were collected, washed with PBS and resuspended in a buffer containing 10 mM HEPES/NaOH, pH 7.4, 140 mM NaCl and 2.5 mM $CaCl_2$. Then AnnexinV-FITC and PI were added. Following incubation for 30 min the cells were analysed by flow cytometry. When analysis of lymphocyte subsets was desired, PBMC were first incubated with respective PE-labeled cell surface antibodies (CD4-PE, CD8-PE, Pharmingen, CD56-PE; Imunotech) before the AnnexinV staining was performed.

Primary alloreactive proliferation

To suppress the proliferation of stimulator cells, glioma cells were incubated in serum-free medium for 24 h, irradiated at 50 - 200 Gy and maintained in serum-free medium for another 24 h. Cells were detached using cell dissociation solution (Gibco), counted and seeded in RPMI medium. HLA-A2-mismatched responder PBMC (10^5) were coincubated with 10^4 irradiated glioma cells in a total volume of 100 µl. The assay was performed in 96-well plates in triplicates. PBMC without glioma cells, glioma cells without PBMC, and PHA-stimulated PBMC (10 µg/ml) were used as controls. After 4 days, the cells were pulsed for 24 h with 0.5 µCi of [methyl-^{3}H] thymidine (Amersham-Pharmacia Biotech, Freiburg, Germany). Cells were harvested with a cell harvester (Inotech, Dottikon, Switzerland) and the incorporated radioactivity was bound to a glass fibre filtermat (Wallac, Turku, Finland). The filtermat was wetted with Ultima Gold Scintillation Cocktail (Packard, Dreieich, Germany) and radioactivity was determined in a Wallac 1450 Microbeta Plus Liquid Scintillation Counter.

Secondary alloreactive immune response (^{51}Cr release assay)

To test for lytic activity of primed cytotoxic T cells after coculture with HLA-A2-mismatched glioma cells (U87MG-pEGFP, U87MG-HLA-G1, U87MG-HLA-G5) for 5 days, a ^{51}Cr release assay was performed. Growth-suppressed glioma cells were seeded into 25 cm^2 flasks to a density of 10^6 cells. HLA-A2-mismatched PBMC (1.5 x 10^7) were added in 5 ml RPMI containing 10% FCS. Cells were cocultured for 5 days. Glioma cells (10^6) were labeled by addition of 100 µCi ^{51}Cr (#NEZ147, NEN, Boston, MA) in 1 ml and 10^4 labeled glioma cells were seeded as target cells in a U-shaped 96-well plate. Primed alloreactive cytotoxic lymphocytes obtained after 5 days of coculturing were removed and added to the labeled target cells at different effector:target ratios (ranging from 10 to 80) in a volume of 100 µl. After coincubation for 4 h, 50 µl of the supernatant were transferred to a Luma-PlateTM-96 (Packard), dried overnight and measured. To correct for spontaneous release of ^{51}Cr, a control of labeled target cells in medium only was included (0% specific lysis). The maximum ^{51}Cr release possible was determined by addition of NP-40 (100% lysis). Lysis was calculated as [cpm (effector cells)-cpm (spontaneous)]/[cpm (NP-40)-cpm (spontaneous)] x 100%.

Primary alloreactive lysis (^{51}Cr release)

Primary alloreactive lytic damage of glioma target cells by HLA-A2-mismatched lymphocytes was measured in a ^{51}Cr release assay. Target glioma cells were radioactively labeled and seeded into 96-well U-bottom wells as described above. For blocking experiments, glioma cells or HLA-G transfectants were preincubated with specific antibodies or the corresponding isotype control antibodies. After incubation for 1 h at 37°C, crosslinking by a secondary antibody (goat anti-mouse F(ab)$_2$ fragment, 10 µg/ml, Dianova) was performed to immobilize the antibody on the glioma cells. Effector cells (PBMC, CD4, CD8, NK cells) were added at effector:target ratios ranging from 1 to 100 in a total volume of 100 µl. After coincubation for 8 h, 50 µl of the supernatant were transferred to a Luma-PlateTM-96 (Packard), dried overnight and measured. In experiments using purified NK cells, incubation was done for 4 h. To correct for spontaneous ^{51}Cr release, a control of labeled target cells in medium only was included (0% specific lysis). The maximum ^{51}Cr release possible was determined by addition of NP-40 (100% lysis).

Soluble HLA-G (sHLA-G) ELISA.

Secreted HLA-G molecules were measured as total soluble HLA-class I molecules in the culture supernatants. MHC class I antibody (W6/32, concentration 5 µg/ml, volume 100µl) was coated onto a 96-well microtiter plate (Nunc) and incubated over night at 4°C. After three washes with PBS containing 0.05% Tween 20 (PBS-Tween), the plate was saturated with 250 µl of PBS containing 2% BSA. After incubation for 2 h at 37°C, the plate was washed three times with PBS-Tween. Cell culture supernatants (100 µl) were added to each well at various dilutions and incubated for 2 h at 37°C. Plates were washed another three times with PBS-Tween and hrp-labeled rabbit anti-mouse β_2m antibody (dilution 1:500, volume 100 µl) was added. After incubation for 1 h at 37°C and washing three times with PBS-Tween, 100 µl of ortho-phenyl-diamine peroxidase substrate was added (Abbott Diagnostics, Wiesbaden-Delkenheim, Germany) for 30 min at room temperature avoiding exposure to light. The reaction was stopped by addition of 50 µl of 2 M H_2SO_4. The concentration was estimated from the absorption measured at 490 nm (triplicate wells) on a ELISA microplate reader (Wallac).

Reverse transcription and amplification

First strand DNA synthesis of 1 µg total RNA primed with oligo(dT)$_{12-18}$ (Amersham Pharmacia Biotech) and Expand^{TM} Reverse Transcriptase (Boehringer, Mannheim, Germany) was done according to the manufacturer's recommendations (356). One µl of cDNA was amplified using the following primer pairs which coamplify the HLA-G isoforms HLA-G1, -G2/4, and –G3: Ex1 (5‘-CAAGGATGGTGGTCATGGCG-3‘) and Ex6/3‘UT (5‘-CAGCTGTTTCACATTGCAGCCTG-3‘), 60°C annealing temperature, 40 cycles. PCR products were analyzed on 1.5% agarose gels containing ethidium bromide or on 8% native polyacrylamide gels followed by silver staining (357).

DNA probes and Northern blot analysis

RNA was isolated with the TriPure Isolation reagent (Boehringer, Mannheim). 20 µg of total RNA were separated on 1.2% formaldehyde agarose gels, transferred to Hybond-N$^+$ membrane (Amersham Pharmacia Biotech) in 20x SSC over night and cross-linked by baking at 80°C for 2 h. The filters were hybridized with 10 ng/ml specific digoxigenin-labeled probe and detected as described (355). Hybridization probes specific for HLA-G transcripts were derived from the 3'- untranslated regions and were generated by PCR and incorporation of digoxigenin-labeled dideoxyuridine triphosphate (Boehringer Mannheim). The 486 bp HLA-

G probe was labeled from a subcloned 287 bp amplificate with the primers M13 (-20) and M13 reverse. The 440 bp HLA-B probe was generated from the subcloned 3‘UT Pvu II/Pst I fragment using SP6 and T7 primers. To detect HLA-G transcripts in HLA-G transfectants, a 787-bp HLA-G4 probe was generated by PCR using the primer pair Ex1 and Ex6/3'UT (358).

Immunoblot analysis

Cells were lysed for 30 min at 4°C in lysis buffer (20 mM Tris-HCl pH 7.5, 1% Triton X100, 2% trasylol) (Bayer, Leverkusen, Germany), 1 mM phenylmethyl sulfonylfluoride (PMSF, Sigma). After removal of cellular debris by centrifugation, protein content of the lysates was quantified using a Micro-Bradford assay (24). Lysates equivalent to 100 µg of protein were separated by 10% SDS-PAGE and transferred onto nitrocellulose membranes (Schleicher and Schuell, Dassel, Germany) using standard blotting techniques. HLA-G heavy chains were detected with the mAb 4H84 and the ECL Western blotting analysis system (Amersham Pharmacia).

Statistical analysis

All data are representative of experiments performed at least three times with similar results. Significance was assessed by two sided t-test (*$p<0.05$, **$p<0.01$).

Results

HLA-G expression in human glioma cell lines

Twelve human glioma cell lines were tested for HLA-G mRNA expression in the absence or presence of IFN-γ by Northern blotting using a probe specific for all HLA-G isoforms (Fig. 6.1). Six glioma cell lines transcribed HLA-G constitutively (U251MG, U373MG, D247MG, T98G, LN-428, A172). The presence of different alternative splicing patterns were confirmed by RT-PCR specific for transmembraneous and soluble isoforms of HLA-G (data not shown). After stimulation with IFN-γ, HLA-G transcripts became detectable in 10 of the 12 glioma lines (Fig. 6.1). Only U87MG and LN-308 cells were refractory to IFN-γ-mediated induction of HLA-G expression. PCR analysis paralleled these observations, confirming strong up-regulation of different HLA-G isoforms after IFN-γ induction (data not shown).

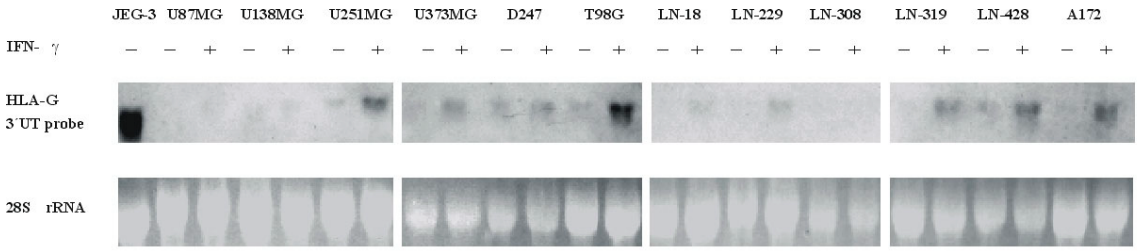

Fig. 6.1: **Human glioma cells express HLA-G mRNA.** HLA-G mRNA levels were assessed by Northern blot analysis. A total of 20 µg of total RNA from untreated (-) or IFN-γ- treated (+) cells (500 U/ml; 48h) (12 different glioma cell lines) was separated on a formaldehyde agarose gel and hybridized with HLA-G specific probes. The amount of RNA loaded is visualized by ethidium bromide staining of the 28S rRNA (lower panel). The human choriocarcinoma line JEG-3 was used as a positive control.

To test whether the transcripts detected were translated into protein, flow cytometry was performed using the anti-HLA-G mAbs 87G and MEM-G/9. A weak membrane expression of HLA-G was observed in 4 of 12 untreated glioma cell lines (U373MG, LN-319, T98G, A172) (Fig. 6.2). After stimulation with IFN-γ, HLA-G membrane expression increased and was detectable in 8 of the 12 tested glioma cell lines, using a cutoff SFI value of 1.3 (Fig. 6.2).

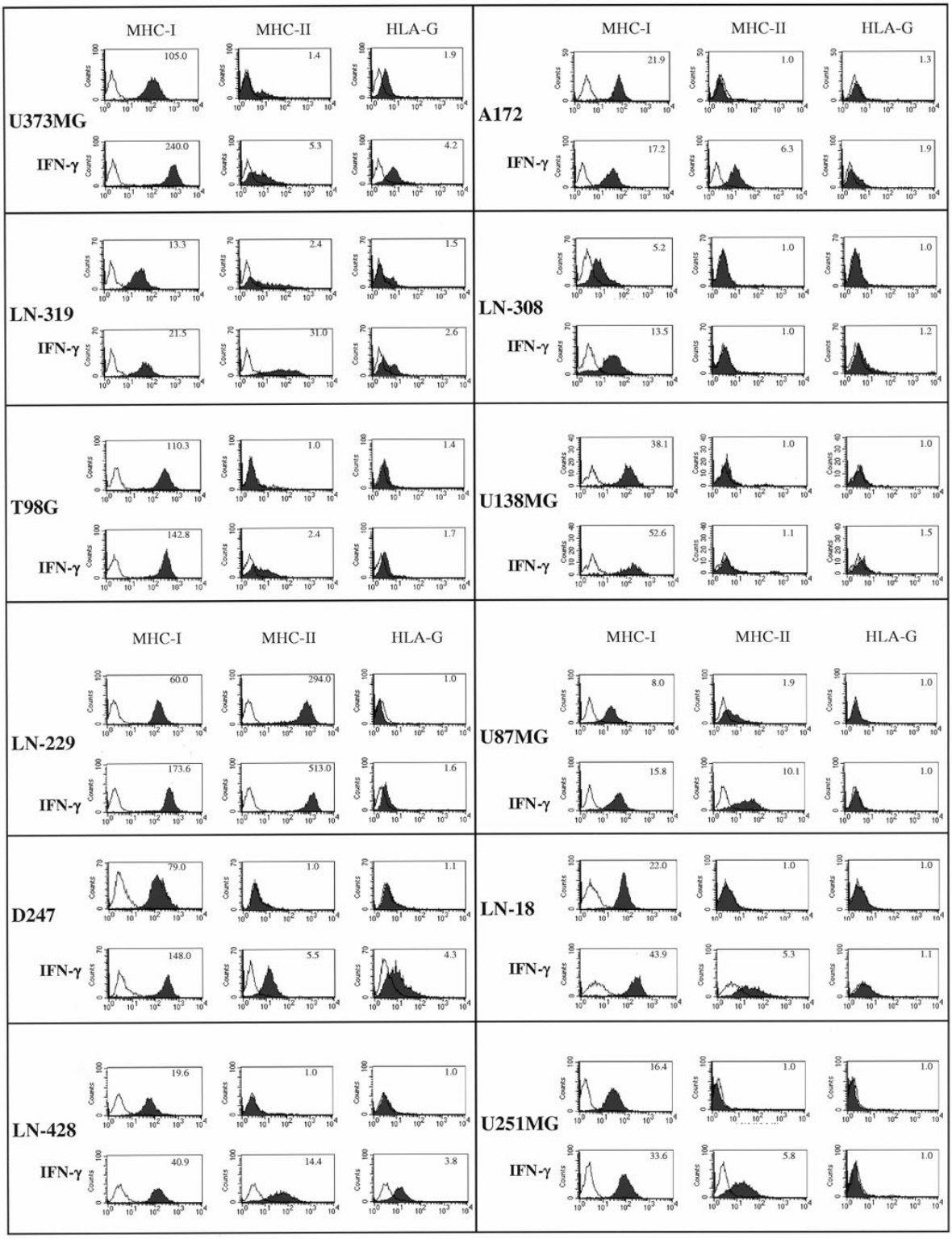

Fig. 6.2. **Human glioma cells express HLA-G protein.** MHC class I, class II and HLA-G expression by human glioma cell lines in the absence or presence of IFN-γwas determined by flow cytometry. The cell lines were incubated for 48 h with or without IFN-γ (500 U/ml), stained either with the MHC-class I reactive mAb W6/32 (HLA-A,-B,-C,-G,-E+$ß_2$-m), the MHC-class II reactive mAb L243 (HLA-DR) or the HLA-G specific mAb 87G (HLA-G1). JEG-3 choriocarcinoma were used as positive control, K-562 as negative control (not shown). The numbers in the upper right corner indicate SFI values. A SFI value of 1.3 was considered positive. Data are representative of 4 independent experiments with similar results.

The expression of class I (HLA-A, -B, -C mAb W6/32; HLA-A2 mAb BB7.2) and class II (HLA-DR; mAb L243) molecules was assessed in parallel, showing that all glioma cells expressed HLA-class I molecules constitutively. IFN-γ enhanced the surface expression of MHC class I in all cell lines except A172. The MHC class II DR-molecule was expressed constitutively in 4 of 12 glioma cell lines. IFN-γ induced HLA-DR in all except 2 cell lines (LN-308, U138MG). The human SV40-transformed astrocytic cell line SV40-FHAS did not show HLA-G RNA or protein expression in the absence or presence of IFN-γ (data not shown).

HLA-G expression in human brain tissue

Immunohistochemistry detected HLA-G expression in 4 of 5 brain tumours. Up to 50% of tumour cells expressed HLA-G in 3 of the 4 tested glioblastomas and in one anaplastic oligo-astrocytoma (Fig. 6.3; staining shown here with mAb BFL1.1.2 and mAb 87G). Positive cells were evenly scattered throughout the specimens. One glioblastoma was negative for HLA-G with all tested antibodies.

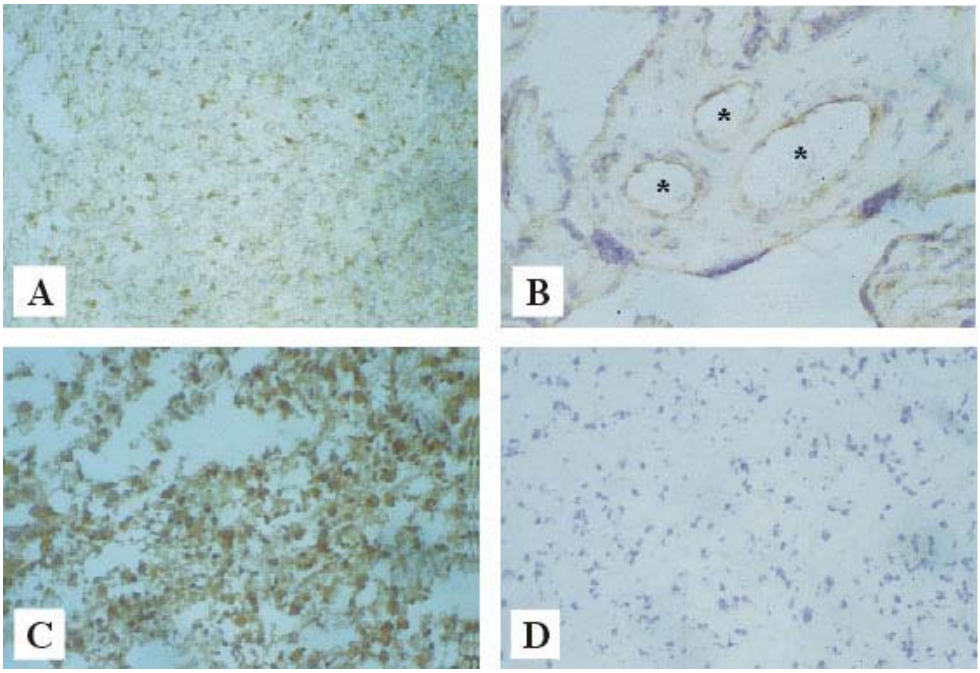

Fig. 6.3: Analysis of HLA-G expression *in vivo*. Frozen tissue sections of a glioblastoma (A, C and D) and term placenta as control (B) were immunostained with the HLA-G-specific mAb BFL1.1.2. (A, B), mAb 87G (C) or IgG-isotype control (D) About 50% of tumor cells expressed HLA-G (glioblastoma, 32 year old male, A magnification x 185, C, magnification x 420). Positive cells were evenly scattered throughout the specimen. Isotype control (D) of glioblastoma is shown at magnification x 420. Endothelial cells of three blood vessels (asterisks) in placenta control tissue are HLA-G-positive (B, magnification x 395).

Expression of HLA-G in glioma cells protects from alloreactive lytic killing

To elucidate the functional relevance of constitutive and inducible HLA-G expression by glioma cells, different alloreactivity assays were performed. Freshly isolated PBMC were used as effector cells and incubated with HLA-A2-mismatched glioma targets that had previously been cultured in the absence or presence of IFN-γ. The relevance of HLA-G molecules for the protection of glioma cells from alloreactive lysis was shown by preincubating glioma cells with HLA-G specific antibody 87G (Fig. 6.4). HLA-G expressed on U373MG and T98G participated in the protection of glioma cells against direct cytolytic activity of PBMC as recorded in a 8 h ^{51}Cr-release assay. The MHC class I specific antibody W6/32 was used as a control. Although W6/32 blocks alloreactive lysis by MHC class I restricted CD8 T cells, the observed net effect on PBMC lysis in the presence of W6/32 was an increase in specific lysis. MHC class I expression regulates NK cell lysis via interaction with killer inhibitory receptors, therefore blocking MHC class I might have facilitated lysis by NK cells present within the PBMC population. Since W6/32 crossreacts with HLA-G and the negative immune regulatory molecule HLA-E part of the observed effects of this antibody on lysis may have been mediated by an interaction with HLA-E. In U87MG, a glioma cell line lacking HLA-G expression, neutralization with 87G had no significant influence on lysis by alloreactive PBMC (data not shown).

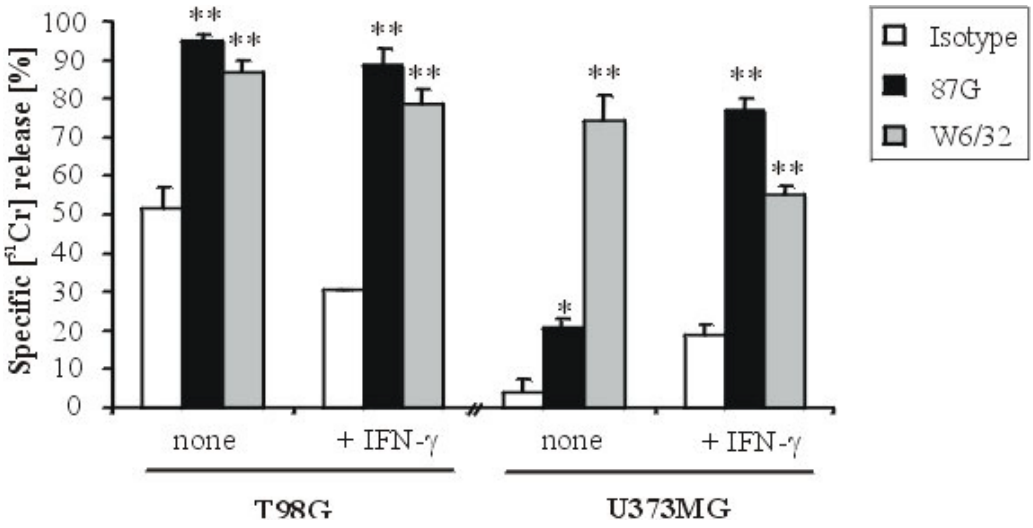

Fig. 6.4: **HLA-G expressed on human glioma cells inhibits lysis by alloreactive PBMC**. T98G or U373MG glioma cells were cultured in the absence or presence of IFN-γ (500 U/ml) for 48 h and used as targets. Target cells were preincubated either with 87G, W6/32 or isotype control antibody for 1 h. Freshly purified HLA-A2-mismatched PBMC were added as effector cells at different effector:target (E:T) ratios (shown 50:1). Data are expressed as percentages of specific lysis recorded in a 8 h ^{51}Cr-release assay (*$p<0.05$, **$p<0.01$ compared with isotype control antibody). Data are representative of 3 independent experiments with similar results.

Gene transfer of HLA-G1 or -G5 into HLA-G negative glioma cells

To elucidate the effects of the 2 major isoforms HLA-G1 and HLA-G5 on antitumoral immune responses, HLA-G transfectants of a HLA-G-negative glioma line (U87MG) were generated. Transfectants showed high levels of HLA-G expression as documented by immunoblot, flow cytometry, and ELISA for soluble HLA-G (Fig. 6.5). The forced expression of HLA-G isoforms did not alter the expression levels or inducibility by IFN-γ of classical MHC class I or MHC class II molecules as determined by flow cytometry (data not shown).

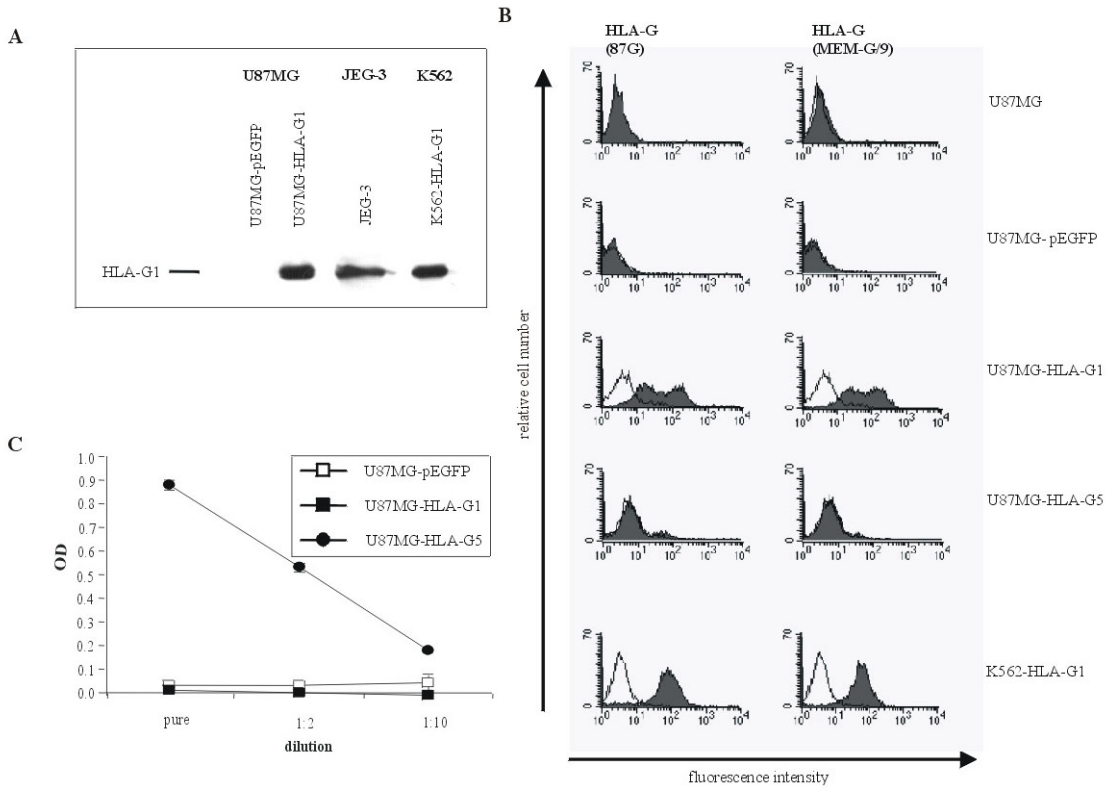

Fig. 6.5: **Expression of HLA-G1 and HLA-G5 after gene transfer into U87MG glioma cells.** A: The transfectants were examined by immunoblot analysis using the 4H84 mAb specific for the denatured HLA-G heavy chain. JEG-3 choriocarcinoma cells and K-562-HLA-G1 were used as positive controls. The HLA-G protein migrates at 39 kDa. B: Cell surface expression of HLA-G1 protein in the HLA-G transfectants was assessed by flow cytometry using the HLA-G specific antibodies 87G (left) and MEM-G/9 (right) and BFL1.1.2 (not shown). Filled profiles indicate specific fluorescence, open profiles correspond to the isotype control (IgG2b) for HLA-G. C: Levels of sHLA-G released into the supernatant by U87MG, U87MG-HLA-G5 and U87MG-HLA-G1 transfectants were determined by ELISA. Data are expressed as arbitrary units corresponding to the optical density measured at 490 nm. Data are representative of at least 3 independent experiments with similar results.

Gene transfer of HLA-G1 or -G5 into U87MG glioma renders glioma cells resistant to primary alloreactive lysis

Gene transfer of HLA-G1 and HLA-G5 rendered U87MG cells less susceptible to direct alloreactive lytic killing by HLA-A2-mismatched PBMC as assessed by ^{51}Cr-release of the target population (Fig. 6.6).

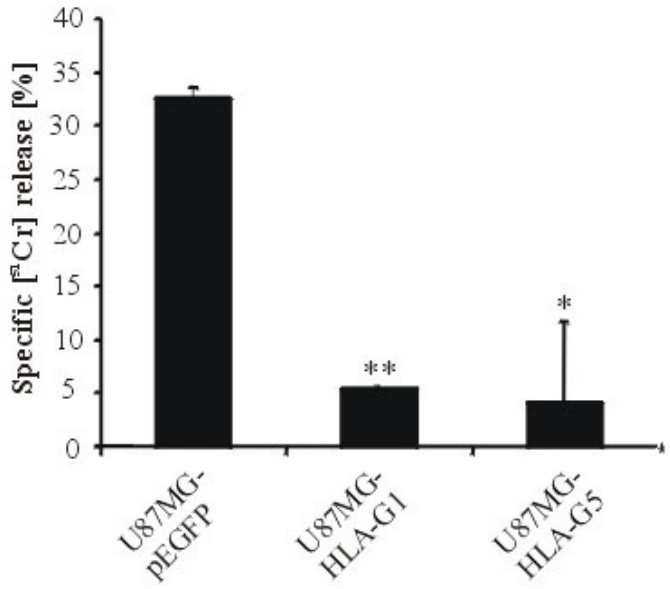

Fig. 6.6: **Inhibitory effects of HLA-G in U87MG glioma cell transfectants on different subsets of immune effector cells under primary alloreactive coculture conditions.** U87MG-pEGFP, U87MG-HLA-G1, or U87MG-HLA-G5 cells were used as targets in cocultures with freshly isolated HLA-A2-mismatched PBMC at different effector:target (E:T) ratios (shown 100:1). Data are expressed as percentages of specific lysis recorded in a 8-h ^{51}Cr-release assay (*$p<0.05$, **$p<0.01$ compared with U87-pEGFP).

Glioma cell death was also monitored by fluorescence microscopy. Modulation of glioma cell lysis after incubation of tumour targets with PBMC is demonstrated by the significantly higher survival rates of the HLA-G transfectants compared with the vector control transfectants at 48 h (Fig. 6.7).

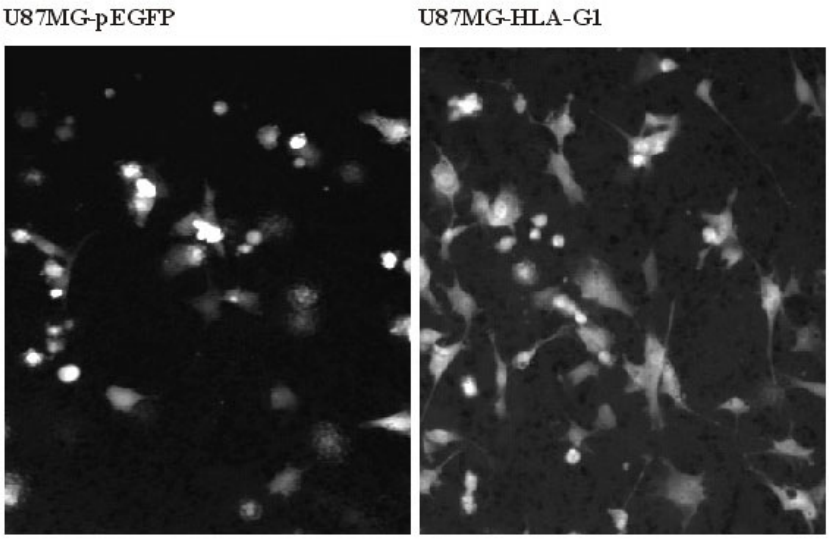

Fig. 6.7: **HLA-G overexpression protects glioma cells against immune-mediated lysis.** U87MG-pEGFP or U87MG-HLA-G1 were cocultured in 6-well culture plates with HLA-A2-mismatched PBMC for 48 h. Visualization over time was performed by fluorescence microscopy.

To further characterize the effector populations inhibited by HLA-G expressed on U87MG cells, primary alloreactivity assays were performed with purified lymphocyte subpopulations (CD56, CD4, CD8). U87MG parental cells showed resistance to NK cell lysis (Fig. 6.8).

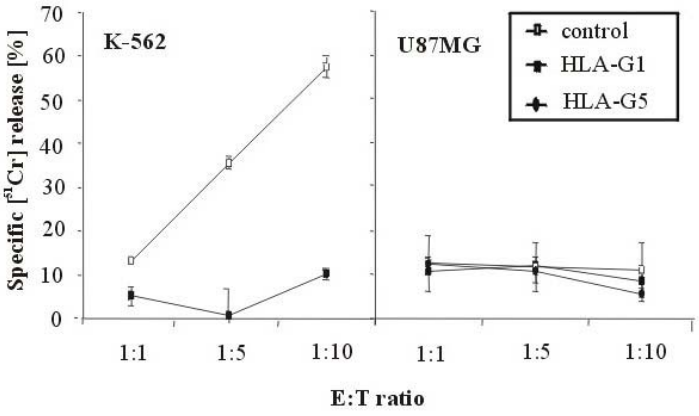

Fig. 6.8: **U87MG glioma cells are resistant to lysis by primary alloreactive NK cells.** CD56-positive NK effector cells were added to U87MG-pEGFP, U87MG-HLA-G1, or U87MG-HLA-G5 target cells at the indicated effector:target ratios. As a positive control, the MHC class I-negative K-562 and K-562-HLA-G1-transfectants were used.

Therefore effects of ectopic HLA-G expression could not be attributed to NK cell inhibition. In contrast, MHC class I-negative K-562 cells were clearly protected from NK lysis by the expression of HLA-G1. Unexpectedly, lytic assays with CD8 and CD4 effector cell subsets demonstrated that HLA-G1 directly inhibited lysis mediated by alloreactive CD4 and CD8 effector cell populations (Fig. 6.9).

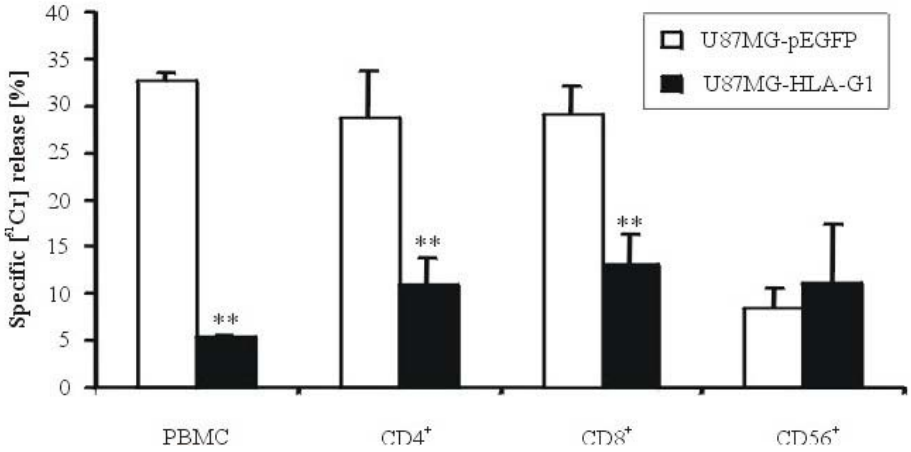

Fig. 6.9. **HLA-G overexpression protects glioma cells against killing by alloreactive T cells.** Freshly isolated, HLA-A2-mismatched PBMC or purified CD4, CD8, or CD56 subsets were incubated with U87MG-pEGFP or U87MG-HLA-G1 target cells at different E:T ratios (shown 80:1) for 8 h and specific lysis of the target glioma cells was quantified by release of ^{51}Cr (**$p<0.01$ compared with U87-pEGFP vector control cells). Data are representative of at least 3 independent experiments with similar results.

HLA-G gene transfer inhibits alloproliferation and prevents effective priming of antigen-specific cells

To study the effects of HLA-G on the generation of primary and secondary immune responses, first the primary proliferative response of HLA-A2-mismatched responder PBMC against growth-arrested glioma cells (U87MG-pEGFP, U87MG-HLA-G1 or U87MG-HLA-G5) was quantified by measuring [methyl-^{3}H] thymidine incorporation. The proliferative response towards glioma cells was significantly suppressed by U87MG-HLA-G1 and U87MG-HLA-G5 cells (Fig. 6.10).

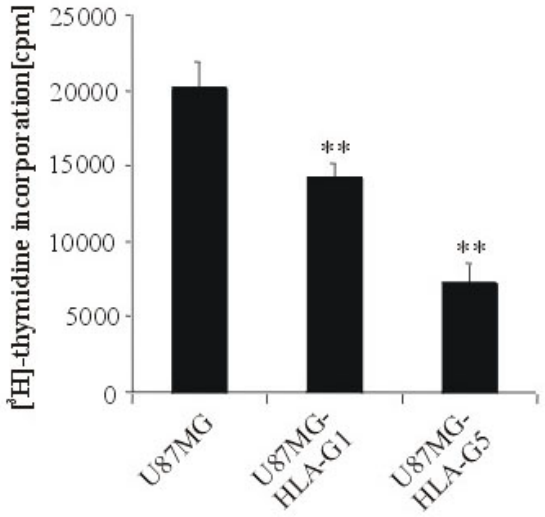

Figure 6.10. **HLA-G inhibits primary alloproliferative responses.** A: PBMC were cultured for 5 days in the absence or presence of growth-arrested stimulator cells (U87MG-pEGFP, U87MG-HLA-G1, U87MG-HLA-G5). Primary alloproliferation of the HLA-A2-mismatched responder population was determined by [^{3}H]-thymidine incorporation added for the last 24 h of coculture. Data are expressed as mean cpm ± SD of triplicate cultures (**p<0.01 compared with U87MG control cells).

To assess whether induction of apoptosis in the effector cells (19) contributes to these inhibitory effects, the cellular viability within the effector cell population was assessed during coculture of freshly isolated lymphocyte subpopulations (CD8, CD4) with U87MG-pEGFP, U87MG-HLA-G1 or U87MG-HLA-G5 transfectants. HLA-G1 did not induce apoptosis in the effector cell populations as detected by AnnexinV staining up to 72 h after coincubation of freshly isolated and not previously stimulated PBMC or lymphocyte subsets with target cells (Fig. 6.11). As a positive control for the induction of apoptosis, PHA-stimulated PBMC were treated with CD95L.

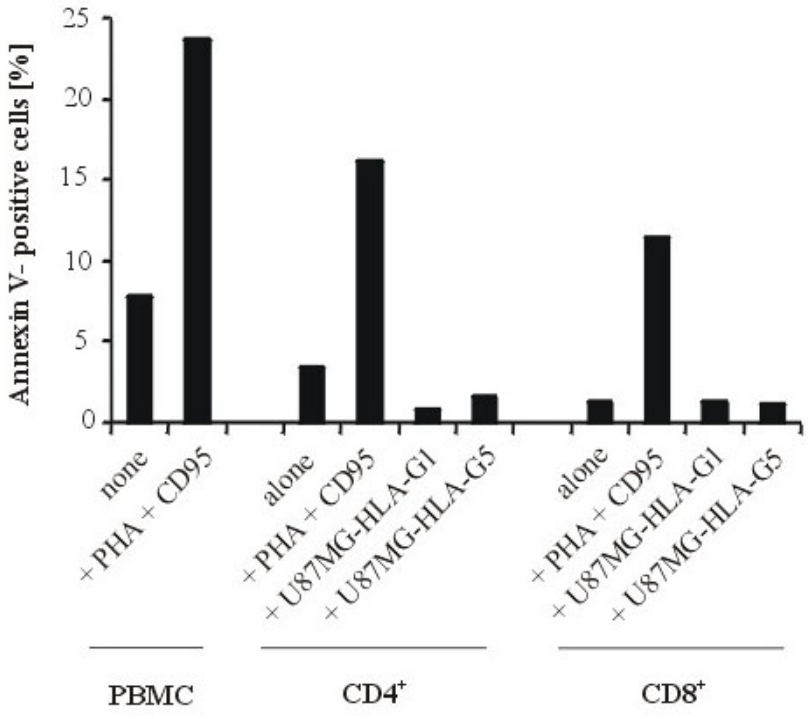

Fig. 6.11. **HLA-G expressed by human glioma cell lines does not induce apoptosis in immune effector cell population.** U87MG-pEGFP or U87MG-HLA-G1 cells were cocultured with HLA-A2-mismatched PBMC, CD4 or CD8 T cells and the amount of apoptosis in the lymphocyte population was quantified by AnnexinV-FITC at 48 h. As a positive control for apoptosis induction, PHA-stimulated PBMC treated with CD95L are shown.

Next the effect of HLA-G1 on the mounting of secondary immune responses was investigated. Antigen-specific cytotoxic lymphocytes were generated by coculturing U87MG-pEGFP or U87MG-HLA-G1 target cells with HLA-A2-mismatched PBMC for 5 days. After transferring primed effector cells, specific killing of parental U87MG target cells was assessed by ^{51}Cr release at different E:T ratios. The expression of HLA-G1 in the priming phase abrogated antigen-specific lysis by cytotoxic T cells (Fig. 6.12A). The protective effect of HLA-G against specific killing by cytotoxic effector cells depended on the presence of HLA-G in the priming phase. When HLA-G was present in the target population after antigen-specific cells had been primed against U87MG-pEGFP control cells, subsequent lysis of U87MG-pEGFP cells was not significantly different from U87MG-HLA-G1 (Fig. 6.12B). Similar results were obtained for U87MG transfectants expressing soluble HLA-G (U87MG-HLA-G5; data not shown).

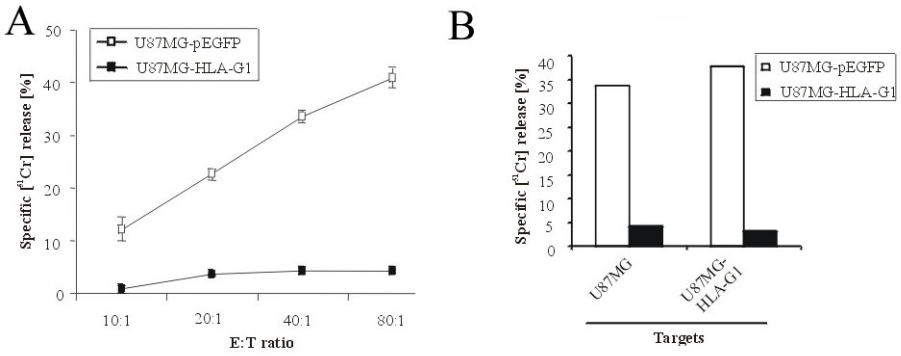

Fig. 6.12. **HLA-G overexpression prevents the priming of alloreactive, antigen-specific T cell responses.** A. Antigen-specific cytotoxic T cells were generated by coculture of HLA-A2-mismatched PBMC with U87MG-pEGFP or U87MG-HLA-G1 target cells for 5 days. Primed effector cells were removed and incubated with ^{51}Cr-labeled U87MG-pEGFP target glioma cells at the indicated E:T ratios. Data are expressed as percentage of specific lysis recorded in an 8 h [^{51}Cr]-release assay. B: Antigen-specific cytotoxic T cells were generated by coculturing HLA-A2-mismatched PBMC with U87MG-pEGFP (open bars) or U87MG-HLA-G1 (black bars) as described in A. After removing primed lymphocytes from the cultures, effector cells were incubated with either U87MG-pEGFP or U87MG-HLA-G1 as targets. Data are expressed as percentage of specific lysis recorded in an 8 h [^{51}Cr]-release assay. Data are representative of at least 3 independent experiments with similar results.

Few HLA-G-positive cells are sufficient to inhibit alloreactive lysis of HLA-G-negative glioma cells

To assess the possible immune modulatory effects of a minor population of glioma cells expressing HLA-G within a given tumour cell population, ^{51}Cr-labeled U87MG-HLA-G1 cells were mixed with ^{51}Cr-labeled vector control U87MG-pEGFP cells, and lysis of targets was assessed after incubation with alloreactive, HLA-A2-mismatched PBMC. Significant inhibition of lysis was observed when 10% or more of the target cells expressed HLA-G (Fig. 6.13A). To delineate whether the release of soluble HLA-G as a result of shedding into the supernatant might account for this effect, the levels of soluble HLA molecules in the supernatants were quantified by ELISA. However, the levels of sHLA-molecules (classical and non-classical MHC molecules absorbed by W6/32 mAb) in the supernatant of HLA-G1 cells were unaltered upon coincubation of PBMC with U87MG-HLA-G1 (Fig. 6.13B).

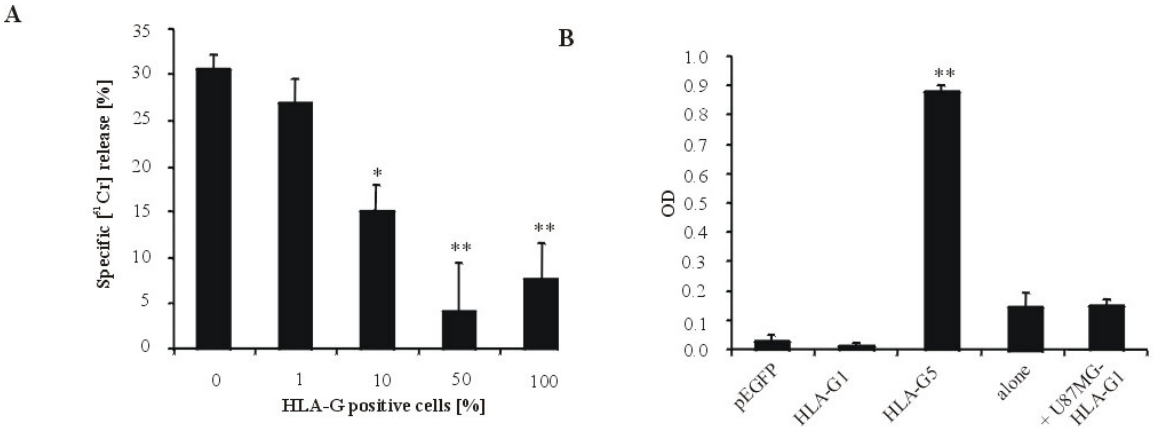

Fig. 6.13: **Single HLA-G-expressing tumor cells convey immune inhibitory effects.** A*:* U87-HLA-G1 cells were mixed with U87MG-pEGFP cells and used as target cells. After coincubation with HLA-A2-mismatched PBMC, the percentage of specific lysis was recorded in a 8-h [^{51}Cr]-release assay. Significant protection was observed, when 10% or more percent of the cells expressed HLA-G (**p<0.01, *p<0.05 compared with U87MG-pEGFP control cells) B: The levels of soluble HLA molecules were measured by ELISA in the supernatants of PBMC alone, U87MG-pEGFP, U87MG-HLA-G1, U87MG-HLA-G5 or U87MG-HLA-G1 coincubated with PBMC for 48 h. Levels of sHLA molecules were unaltered during coculture of PBMC and U87MG-HLA-G1 (**p<0.01 compared with PBMC). Data are representative of at least 3 independent experiments with similar results.

Discussion

In order to investigate the role of HLA-G in glioma immunobiology, the expression of HLA-G in human glioma was characterized *in vitro* and *in vivo* and the functional properties of the 2 major isoforms HLA-G1 and HLA-G5 in modulating primary and secondary immune responses were studied. HLA-G mRNA-transcripts were detected in 6 of 12 untreated glioma cell lines and in 10 of 12 cell lines after IFN-γ stimulation (Fig. 6.1).
A weak constitutive surface expression of HLA-G protein was observed in 4 cell lines (U373MG, LN-319, T98G, A172), cell surface expression of HLA-G protein was detected in 8 of 12 cell lines after IFN-γ stimulation (Fig. 6.2). These data confirm and extend a previous report (359) which provided the first evidence of HLA-G expression in two glioma cell lines (T98G, N59).

The expression of HLA-G rendered glioma cells less susceptible to alloreactive cytolytic killing as demonstrated by blocking experiments using a HLA-G-specific neutralizing monoclonal antibody (87G) in U373MG and T98G, two cell lines which constitutively express HLA-G at the cell surface (Fig. 6.4). Exposure to neutralizing HLA-G antibodies in U87MG, a glioma cell line which does not express HLA-G mRNA or protein (Fig. 6.1, 6.2), had no such effect.

To further corroborate these results and to delineate the contribution of the two major HLA-G isoforms HLA-G1 (HLA-G1) and HLA-G5 (HLA-G5) to immunoregulatory properties of glioma cells, gene transfer studies were performed in the MHC-class I positive, HLA-A2 positive glioma cell line, U87MG. This cell line lacks baseline or inducible expression of HLA-G (Fig. 6.1, 6.2). Gene transfer of HLA-G1 and –G5 rendered these glioma cells resistant to primary and secondary antitumoral immune responses under three different assay conditions: i) HLA-G directly inhibited alloreactive lysis (Fig. 6.6), ii) HLA-G inhibited the primary proliferative response to U87MG stimulator cells (Fig. 6.7), and iii) HLA-G prevented efficient priming of cytotoxic effector cells and protected glioma cells from lytic killing by antigen-specific cytotoxic lymphocytes (Fig. 6.9).

The first descriptions of HLA-G tissue distribution were suggestive of a limited expression on extravillous cytotrophoblast cells (340) suggesting an important role in foetal semi-allograft reaction (360). Therefore, HLA-G functional studies were mainly carried out using HLA class I negative cell lines such as LCL 721.221 or K-562 that were protected from NK cell-

mediated cytolysis when transfected with HLA-G (351). HLA-G was shown to interact with several receptors on NK cells, namely KIR2DL4, ILT-2, ILT-4, and putatively others (349-351). The hypothesis of HLA-G expression as a possible tumour immune escape mechanism has recently been demonstrated in melanoma cells, where HLA-G surface expression was shown to inhibit antitumoral NK cell lysis (344). These data demonstrate that the immune-paralytic effects of HLA-G expressed on glioma cells are NK cell independent (Fig. 6.8). HLA-G1 conveys immunoprotection by direct interaction with CD8 and CD4 alloreactive T cells (Fig. 6.9). Furthermore, HLA-G expressed on tumour cells inhibits primary proliferation in the effector population and prevents efficient priming of antigen-specific cytotoxic T cells (Fig. 6.10 and 6.12). Since human glioma cell lines constitutively express MHC class I, and some cell lines also MHC class II on the cell surface (Fig. 2), this study provides further evidence for an important immunoregulatory role of HLA-G coexpressed in the presence of MHC class I and class II (361). The effects can be attributed to HLA-G rather than being indirectly mediated by upregulation of other inhibitory molecules like HLA-E since lysis inhibition conveyed by the HLA-G transfectants was reversed by adding a neutralizing HLA-G antibody (87G) (data not shown). These observations therefore extend the hypothesis that HLA-G is capable of modulating antigen-specific (352, 362, 363) as well as non-antigen-specific cytotoxic T cell responses (353). HLA-G1 and HLA-G5 display similar immune-inhibitory effects in the experiments performed here. One possible explanation would be binding to common receptor(s) expressed on different lymphocyte subsets.

HLA-G1 as well as HLA-G5 inhibited the primary alloproliferative response in the responder population but did not render effector cells apoptotic (Fig. 6.11). Previous studies have suggested that soluble HLA-G molecules induce apoptosis in CD8 T cells (353), extending observations of such an effect of soluble HLA molecules in general (364). However, PBMC in those studies had already been prestimulated before encountering the soluble HLA-G molecules. The results obtained here from coincubation of unstimulated responder cells with HLA-G favour the mechanism of an HLA-G induced cell cycle arrest as possible explanation for the effect on effector cells. Of note, proliferative allogeneic responses in a mixed lymphocyte reaction induce soluble HLA-G production by CD4 T cells (365), an observation that underscores that the immune regulatory capabilities of HLA-G are broader than previously assumed.

In order to address the question what frequency of HLA-G expressing tumour cells might be relevant for a down-regulation of antitumoral immune responses, mixing experiments were

performed *in vitro*. The resulting data indicate that a low number of HLA-G-positive glioma cells in a population of glioblastoma cells may be sufficient for an effective suppression of an antitumoral immune response *in vivo* (Fig. 6.13A). A direct interaction of HLA-G with certain receptors on immune effector cells is assumed to be the predominant pathway of HLA-G action. Shedding of HLA-G into the cell suspension would be a possible explanation for some of these observations. However, no release of soluble HLA-G by the HLA-G1 transfectants was detected, making that possibility rather unlikely (Fig. 6.13B). This surprising observation could be interpreted as a ”negative bystander” effect: few HLA-G positive cells render neighbouring HLA-G-negative cells ”resistant” to immune-mediated killing or induce non-reactivity in cytotoxic cells. However, the molecular explanation for this phenomenon remains to be clarified. Whereas high levels of HLA-G in the transfected glioma cells are possibly required to directly suppress T cell responses, low levels or HLA-G as expressed constitutively by some tumour cells might modulate immune responses through other mechanism(s).

Expression of HLA-G *in vivo* was demonstrated in 4 out of 5 brain tumour specimens (Fig. 3), thus strongly corroborating the functional *in vitro* observations in glioma. Although to date ectopic expression of HLA-G has been demonstrated in some tumours (366-370), the overall relevance of this molecule as an alternative principle of tumour immune escape remains controversial (371-374), an issue which is further complicated by the limitations of available antibodies to detect HLA-G expression *in vivo* (375, 376).

The results outlined here provide the first functional analysis of HLA-G in human gliomas *in vitro* and *in vivo*. In summary these data support an important role of this molecule in the immune escape mechanisms of human gliomas. HLA-G displays its negative immunomodulatory effects severalfold on primary and secondary immune reactions: i) it directly interacts with alloreactive CD4 and CD8 cytotoxic T cells, ii) it prevents efficient antigenic priming of antitumoral cytotoxic effector cells, and iii) efficiently inhibits alloreactive proliferation without inducing apoptosis. Since minor portions of HLA-G expressing cells within a population of HLA-G negative cells are sufficient to convey relevant immune regulatory effects, expression of this molecule may have major implications also in other sites of desirable and undesirable immune reactions.

VII. SD-208, a novel TGF-β receptor I kinase inhibitor, inhibits growth and invasiveness and enhances immunogenicity of murine and human glioma cells *in vitro* and *in vivo*

A related manuscript has been accepted by Cabcer Research.

This project was a collaborative effort of Scios Inc., Fremont, CA and our laboratory. Scios scientists (Ramona Almirez, Ruban Mangadu, Yu-Wang Liu, Alison Murphy, Darren H. Wong and Linda S. Higgins) developed the drug and characterized it for receptor kinase specificity and bioavailability. In our laboratory, most experiments were carried out by Dr. Martin Uhl who is also the first author of a submitted manuscript based on this project. Dr. Markus Weiler performed the migration studies, Dipl.-Biochem. Steffen Aulwurm helped with the animal experiments and functional immunological assays. My contribution involved experiments on TGF-β signal transduction in glioma and primary immune effector cells, including phosphorylation-specific immunoblotting and reporter gene assays.

Introduction

The cytokine TGF-β, by virtue of its immunosuppressive and promigratory properties, has become a major target for the experimental treatment of human malignant gliomas (155). Experimental anti-TGF-β strategies including antisense approaches (377), gene transfer of TGF-β antagonists such as decorin (378), inhibition of TGF-β-processing proteases of the furin family (292) or drugs such as tranilast (379) have already shown that the specific deficits observed in the cellular *ex vivo* immune responses of glioma patients (294) may be relieved by antagonizing TGF-β signalling. Unlike other immunosuppressive molecules expressed by gliomas, which include prostaglandins (380), IL-10 (381), CD70 (261) and HLA-G (382), TGF-β also assumes a critical role in migration and invasion of glioma cells (383). This study investigates a novel therapeutic principle of TGF-β antagonism in malignant glioma, defined by SD-208, a pharmacological agent which blocks TGF-βRI signalling. Given the poor results obtained in glioma patients with the standard treatment of surgery, radiotherapy and nitrosourea-based chemotherapy (6), an orally available inhibitor of TGF-β mediated immunosuppression, migration and invasion could significantly improve the clinical management of gliomas.

Materials and Methods

Materials and cell lines. PHA was from Biochrom (Berlin, Germany). [Methyl-^{3}H] thymidine was obtained from Amersham (Braunschweig, Germany). ^{51}Cr was purchased from New England Nuclear (Boston, MA). Human recombinant TGF-β_1, TGF-β_2 and mouse IL-2 were obtained from Peprotech (London, UK). Neutralizing pan-anti-TGF-β antibody was purchased from R & D (Wiesbaden, Germany). The human malignant glioma cell line LN-308 was kindly provided by N. de Tribolet (Lausanne, Switzerland). The murine glioma line SMA-560 was a kind gift of D.D. Bigner (Durham, NC). CCL64 mink lung epithelial cells were obtained from the American Type Culture Collection (Rockville, MD).

Cell culture. The glioma cells and CCL64 cells were maintained in DMEM supplemented with 2 mM L-glutamine (Gibco Life Technologies, Paisley, UK), 10% FCS (Biochrom) and penicillin (100 IU/ml)/streptomycin (100 µg/ml) (Gibco). Growth and viability of the glioma cells were examined by crystal violet staining, LDH release (Roche, Mannheim, Germany) and trypan blue dye exclusion assays. For crystal violet staining, the cell culture medium was removed and surviving cells were stained with 0.5% crystal violet in 20% methanol for 10 min. The plates were washed extensively under running tap water, air-dried and optical density values were read in an ELISA reader at 550 nm wave length. Human PBMC were isolated from healthy donors by density gradient centrifugation (Biocoll, Biochrom). Monocytes were depleted by adhesion and differential centrifugation to obtain PBL. To obtain purified T cells, PBMC were depleted of B cells and monocytes using LymphoKwik T^{TM} reagent (One Lambda Inc., Canoga Park, CA). The purity of this population was > 97%, as verified by flow cytometry using anti-human CD3-PE antibody (Becton Dickinson, Heidelberg, Germany). Human polyclonal NK cell populations were obtained by culturing PBL on irradiated RPMI 8866 feeder cells for 10 days (384). Murine NK cells were prepared from splenocytes from VM/Dk mice by positive selection using DX5 monoclonal antibody-coupled magnetic beads with the corresponding column system (Miltenyi Biotech, Bergisch Gladbach, Germany) and cultured with mouse IL-2 (5000 U/ml) for at least 10 days before use. The human polyclonal NK cell cultures, PBL, T cells and mouse NK cells were grown in RPMI 1640 supplemented with 10% FCS, 2 mM L-glutamine, 1 mM sodium pyruvate, 50 µM β-mercaptoethanol and penicillin (100 IU/ml)/streptomycin (100 µg/ml).

Characterization of SD-208. SD-208 is a TGF-βRI kinase inhibitor developed by Scios Inc. (Fremont, CA). To assess the specificity of SD-208 for TGF-βRI, various kinase activities were assayed by measuring the incorporation of radiolabelled ATP into a peptide or protein substrate. The reactions were performed in 96 well plates and included the relevant kinase, substrate, ATP and appropriate co-factors. The reactions were incubated and then stopped by the addition of phosphoric acid. Substrate was captured onto a phosphocellulose filter which was washed free of unreacted ATP. The counts incorporated were determined by counting on a microplate scintillation counter (TopCount, Perkin Elmer Corporation, Boston, MA). The ability of SD-208 to inhibit the respective kinase was determined by comparing counts incorporated in the presence of compound to those incorporated in the absence of compound.

TGF-β bioassay. The levels of bioactive TGF-β were determined using the CCL64 bioassay. Briefly, 10^4 CCL64 cells were adhered to 96 well plates for 24 h and then exposed to recombinant TGF-β_1, TGF-β_2 or glioma cell culture SN diluted in complete medium for 72 h. Growth was assessed by crystal violet staining at 72 h. Glioma cell SN were harvested from subconfluent cultures maintained for 48 h in serum-free medium and heat-treated (5 min, 85°C) to activate latent TGF-β (292).

TGF-β reporter assays. Intracellular TGF-β signalling was assessed by reporter assays using pGL2 3TP-Luc (385) or pGL3 SBE-2 Luc (386) reporter gene plasmids kindly provided by J. Massagué (New York, NY) and B. Vogelstein (Baltimore, MD). The pGL2 3TP-Luc construct contains a synthetic promoter composed of a TGF-β-responsive plasminogen activator inhibitor 1 promoter fragment inserted downstream of three phorbol ester-responsive elements. The pGL3 SBE-2-Luc reporter contains two copies of the Smad-binding element GTCTAGAC. LN-308 and SMA560 cells were transfected using FuGene (Roche). At 24 h after transfection the cells were pretreated in serum containing medium with SD-208 for 12 h (1 μM). TGF-β_1 (5 ng/ml) was then added for another 16 h. The cells were lysed and transferred to a LumiNuncTM plate (Nunc, Roskilde, Denmark) and luminescence was measured in a LumimatPlus (EG&G Berthold, Pforzheim, Germany), using Luciferase assay substrate (Promega, Mannheim, Germany). For T cell assays, 5 x 10^6 freshly isolated PBL were co-transfected with 4.5 μg pGL2-3TP-Luc or pGL3-SBE-2 Luc reporter gene plasmid and 0.5 μg pRL-CMV (Promega), using the Nucleofector™ device and the cell type-specific human T cell nucleofector™ kit (Amaxa, Cologne, Germany). IL-2 (50 U/ml) was added 4 h after nucleofection and the cells were pretreated with SD-208 for 1 h before TGF-β_1 (5 ng/ml)

was added for another 16 h. The respective activities of firefly and renilla reniformis luciferase were determined sequentially using the firelite dual luminescence reporter gene assay (Perkin-Elmer, Rodgau-Jügesheim, Germany). Counts obtained from the measurement of firefly luciferase were normalized with respect to pRL-CMV. NK cell assays were performed accordingly, using the NK cell nucleofector^{TM} kit (Amaxa).

Immunoblot analysis. p-Smad2 levels in glioma cells were analyzed by immunoblot using 20 µg protein per lane on 12% SDS polyacrylamide gels. PBMC were analysed using 120 µg per lane and 10% gels. After transfer to a polyvinylidene difluoride membrane (Amersham), the blots were blocked in PBS containing 5% skim milk and 0.05% Tween 20, and incubated overnight at 4°C with p-Smad2 antibody (2 µg/ml) (Cell Signalling Technology Inc., Beverly, MA). Visualization of protein bands was accomplished using horseradish peroxidase-coupled secondary antibody (Sigma, Taufkirchen, Germany) and enhanced chemiluminescence (Amersham). Total Smad2/3 levels were assessed using a specific Smad2/3 antibody (1 µg/ml) (Becton Dickinson).

Matrigel invasion assay (Boyden Chamber). Invasion of glioma cells was measured by the invasion of 10,000 cells through Matrigel-coated transwell inserts (Becton Dickinson). Briefly, transwell inserts with 8 µm pore size were coated with Matrigel and preincubated SMA-560 cells were applied to the upper wells and allowed to transmigrate through the membrane towards conditioned medium derived from NIH-3T3 fibroblasts which was added to the lower wells. Migrated cells on the lower side of the membrane were fixed, stained in toluidine blue solution (Sigma) and counted in five microscopic high power fields using a microgrid.

Spheroid collagen invasion assay. Multicellular SMA-560 glioma cell spheroids were cultured in 25 cm^2 culture flasks base-coated with 1% Noble Agar (Difco Laboratories, Detroit, MI). Briefly, 4 x 10^5 cells were suspended in 10 ml medium, seeded onto 1% agar plates and cultured until spheroids had formed. Spheroids of about 200 µm diameter were selected for the experiments. Preincubated spheroids were seeded into collagen I and fibronectin containing wells. Spheroid radius, which is determined by the invasion of single cells into the matrix (387), was analyzed by morphometry using the MCID digitalization system (IMAGING Research Inc., Ontario, Canada) after 24, 48 and 72 h.

Lysis assay. HLA-A2-mismatched PBL or T cells (10^7/25 cm^2 flask) were cocultured with 10^6 irradiated (30 Gy) LN-308 glioma cells for 5 days. Glioma cell targets were labeled using ^{51}Cr (50 µCi, 90 min) and incubated (10^4/well) with effector PBL harvested from the cocultures at E:T ratios of 100:1 to 3:1. The maximum ^{51}Cr release was determined by addition of NP40 (1%) (Sigma). After 4 h the SN were transferred to a Luma-Plate TM-96 (Packard, Dreieich, Germany) and measured. The percentage of ^{51}Cr release was calculated as follows: 100 x [experimental release – spontaneous release]/[maximum release – spontaneous release].

Cytokine release. IFN-γ, TNF-α and IL-10 release by immune effector cells was assessed by Elispot assay in multiscreen-HA 96 well plates (Millipore, Eschborn, Germany) coated with corresponding anti-human capture antibodies (Becton Dickinson). Briefly, 5 x 10^4 glioma cells were cocultured for 24 h with 10^5, 2.5 x 10^5 or 5 x 10^5 HLA-A2-mismatched, prestimulated (5 days) PBL. The cells were removed using double-distilled water and captured cytokines were visualized using biotinylated antibodies and streptavidin-alkaline phosphatase (Becton Dickinson). Spots were counted on an Elispot reader system (AID, Straßberg, Germany).

p-Smad2/3 ELISA. Male mice (BALB/c, Jackson Labs, BarHarbor, ME) were studied in 6 groups of 8 animals each. For each drug group, a single volume of SD-208 was administered by oral gavage 1 h prior to dosing with TGF-β_1 (R&D Systems, Minneapolis, MN) diluted in 100 µl 0.1% BSA / 4 mM HCL/PBS by i.v. injection. The mice were sacrificed by cervical dislocation 1 h later. Tissues were removed and lysed in 20 mM Tris, pH 7.5, containing 1 mM EDTA, 0.5% TX-100, 0.5% NP-40, 150 mM NaCl and 1x protease inhibitor cocktail (Roche) and 1x phosphatase inhibitor cocktail set II (Calbiochem, San Diego, CA). Tissue was homogenized using an Ultra-turrax T8 (Reyom Instruments, Brabcova, Czech Republic). Tissue homogenates were clarified by centrifugation and the supernatant fraction was collected. Protein concentrations were determined with a BCA protein assay (Pierce, Rockford, IL). The levels of p-Smad were determined by sandwich ELISA. Briefly, 96 well ELISA plates were coated with an anti-Smad2/3 monoclonal antibody (100 ng/well, Becton Dickinson) for 18 h at 4°C. Excess antibody was removed and the wells were treated with blocking buffer (0.3% BSA/PBS) for 2 h at room temperature. Tissue lysates (125-150 µg total protein) were added to each well and incubated overnight at 4°C. Wells were rinsed before adding a polyclonal anti-p-Smad 2/3 antiserum diluted in 2% BSA/0.5% Tween-20/PBS. Following a 2 h incubation at room temperature, the wells were washed and

secondary antibody was applied (horseradish peroxidase-conjugated goat-anti-rabbit IgG, Southern Biotech, Birmingham, AL). After 1 h the wells were developed with TMB (Sigma). The plate was incubated 5-30 min before the reaction was stopped with 0.5 N H_2SO_4 and read at 450 nm in a SpectraMax 250 plate reader (Molecular Devices, Sunnyvale, CA).

Survival studies in vivo. VM/Dk mice were purchased from the TSE Research Centre (Berkshire, UK). Mice of 6-12 weeks of age were used for the survival experiments. The experiments were performed according to the German animal protection law. Groups of 8 mice were anesthesized before all intracranial procedures and placed in a stereotaxic fixation device (Stoelting, Wood Dale, IL). A burr hole was drilled in the skull 2 mm lateral to the bregma. The needle of a Hamilton syringe (Hamilton, Darmstadt, Germany) was introduced to a depth of 3 mm. Five x 10^3 SMA-560 cells (388) resuspended in a volume of 2 µl PBS were injected into the right striatum. Three days later the mice were allowed to drink SD-208 at 1 mg/ml in deionized water. The mice were observed daily and, in the survival experiments, sacrificed when developing neurological symptoms.

Statistical analysis. The experiments were usually performed at least three times with similar results. Significance was tested by Student's t-test. P values are derived from two-tailed t-tests.

Results

SD-208 is a functional TGF-β_1 and TGF-β_2 antagonist in vitro.

The initial characterization of SD-208 in cell-free assays led to its identification as a potent inhibitor of TGF-βRI. SD-208 exhibited an *in vitro* specificity for TGF-βRI kinase of >100-fold compared with TGF-βRII kinase and at least 20-fold over members of a panel of related protein kinases (Table I).

Table 7.1. **Specificity of SD-208 for TGF-βRI kinase activity**[1]

TGF-βRI	0.048
TGF-βRII	> 50
Epidermal growth factor receptor	68%
mutant Drosophila p38-α	0.867
p38 kinase γ	> 50
c-jun N-terminal kinase	> 50
Extracellular signal-regulated kinase-2	> 50
Mitogen-activated protein kinase-activated protein-2	87%
Mitogen-activated protein kinase kinase 6	> 50
Protein kinases A and C	> 50
Protein kinase D	70%

[1]Data are expressed as EC_{50} [μM] or percentage inhibition at 5 μM SD-208 in cell-free systems *in vitro*

CCL64 mink lung epithelial cells were sensitive to the growth inhibitory effects of human TGF-β_1 and TGF-β_2 at EC_{50} concentrations of 0.5 ng/ml. The inhibitory effects

of recombinant TGF-β as well as those of TGF-β-containing glioma cell SN were abrogated by specific TGF-β antibodies (11) (data not shown). The CCL64 bioassay was used here to verify the TGF-β-antagonistic properties of SD-208. SD-208 rescued the inhibition of growth mediated by TGF-β_1 or TGF-β_2 (10 ng/ml) or diluted SMA-560 (not shown) or LN-308 glioma cell SN in a concentration-dependent manner, with an EC_{50} concentration of 0.1 μM (Fig. 7.1). When these bioassays were performed in the absence of serum in the CCL64 medium, the EC_{50} for SD-208 was 0.03 μM (data not shown), corresponding to the data in Table I.

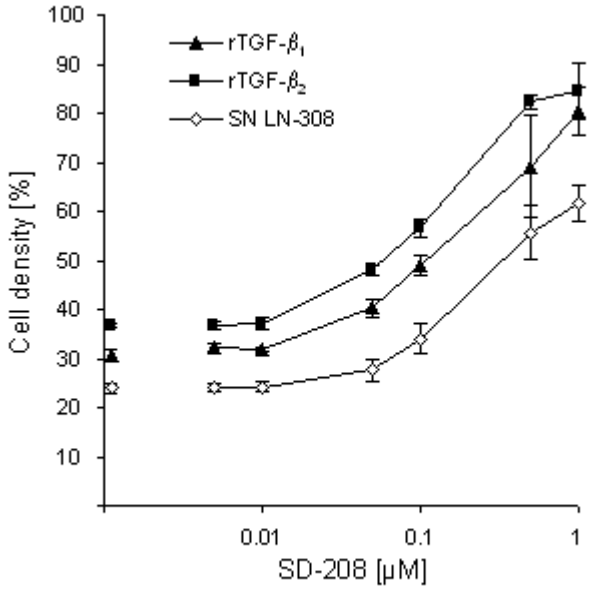

Fig. 7.1. **Prevention of the growth inhibitory effects of recombinant and glioma-derived TGF-β_1 and TGF-β_2 by SD-208.** CCL64 cells were exposed to human recombinant TGF-β_1 (filled triangles), TGF-β_2 (filled squares) (10 ng/ml) or heat-activated glioma cell SN (1:2) (open rhomboids) in the absence or presence of increasing concentrations of SD-208 for 72 h. Cell density was assessed by crystal violet assay (mean and SD, n=3).

SD-208 abrogates autocrine TGF-β-dependent signal transduction in glioma cells.

We next examined the biological effects of SD-208 on murine and human glioma cells *in vitro*. The concentrations required to block the growth inhibitory effects of TGF-β in the CCL64 bioassay had no effect on the proliferation of either cell line. SD-208 did not reduce proliferation assessed by [methyl-^{3}H] thymidine incorporation or viability assessed by LDH release or trypan blue dye exclusion assays at concentrations up to 1 μM for 72 h (data not

shown). The inhibition of signalling transduced by endogenous or exogenous TGF-β was ascertained by demonstrating that SD-208 interfered with Smad2 phosphorylation without altering total cellular Smad2/3 levels (Fig. 7.2 A). Similarly, two different reporter assays revealed a strong inhibition of TGF-β signalling when the glioma cells were treated with SD-208 (Fig. 7.2 B).

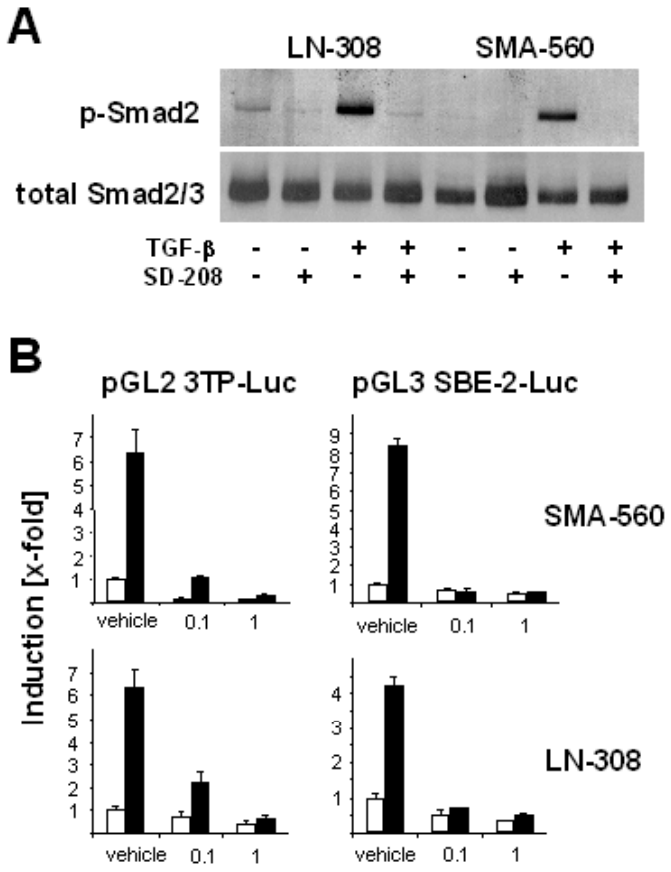

Fig. 7.2. **Abrogation of TGF-β signaling in glioma cells by SDD-208.** A. Lysates from untreated glioma cells or cells preexposed to SD-208 (1 μM) for 24 h or exposed to TGF-β_2 (5 ng/ml) for 1 h or both were assessed for the levels of p-Smad2 or total Smad2/3. Note that the antibodies are specific for p-Smad2 and total Smad 2 and 3, respectively. B. The cells were untreated (open bars) or treated with TGF-β_1 (5 ng/ml, filled bars) for 16 h in the absence or presence of SD-208 at 0.1 or 1 μM and assessed for TGF-β reporter activity in serum-containing medium.

SD-208 inhibits constitutive and TGF-β-evoked migration and invasion.

We next examined the biological effects of SD-208 on SMA-560 cells in two independent migration and invasion paradigms in vitro. SD-208 reduced the invasion of glioma cells from a spheroid into a three dimensional collagen I gel and also the transmigration of glioma cells in a Boyden chamber assay. Moreover, the proinvasive effect of exogenous TGF-β was neutralized by SD-208 in either assay (Fig. 7.3 A,B).

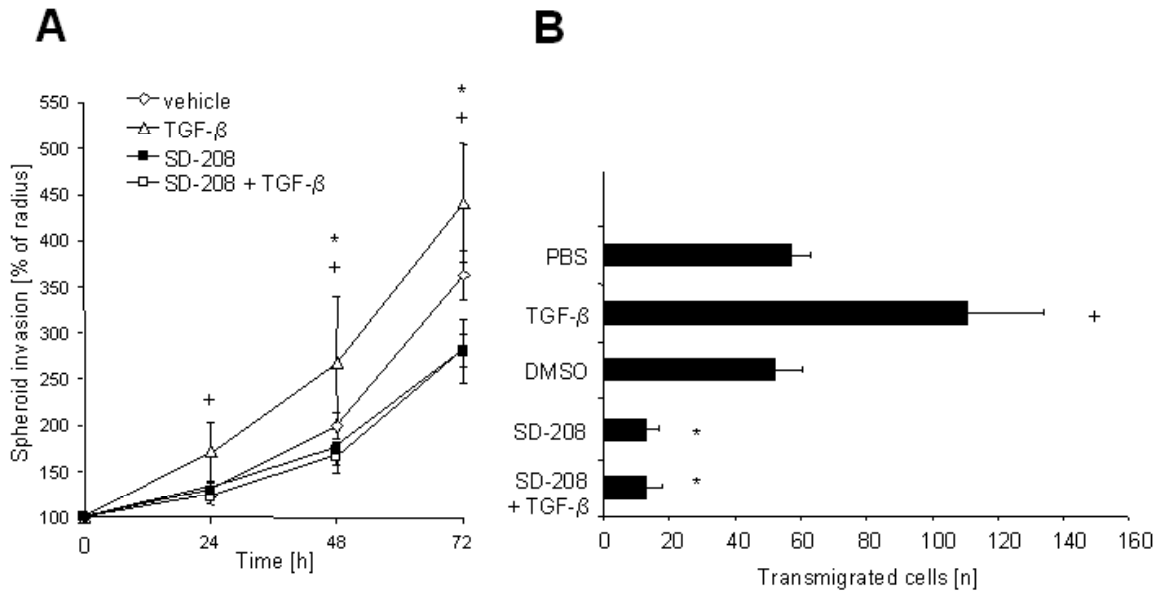

Fig. 7.3. **Inhibition of constitutive and TGF-β-induced invasion of glioma cells by SD-208**. A. SMA-560 spheroids were untreated or treated with SD-208 (1 μM), TGF-β_2 (5 ng/ml) or both for 24 h prior to placement into the collagen I gel and during the experiment and spheroid diameter was determined every 24 h. Data are expressed as mean radius in percent of the spheroid radius at 0 h set to 100% (n=3, *$p<0.05$, t-test, effect of SD-208; $^{+}p<0.05$, t-test, effect of TGF-β_2). The concentration of DMSO required to dissolve SD-208 had no effect in this assay. B. Invasion was analyzed with matrigel-coated membranes in a Boyden chemotaxis chamber assay applying 10,000 SMA 560 cells, control-treated or treated with SD-208 (1 μM), TGF-β_2 (5 ng/ml) or both for 24 h prior to and during the experiment, in the upper chamber. Invaded cells were counted at 24 h. Data are expressed as mean cell counts (n=3, *$p<0.05$, t-test, effect of SD-208, $^{+}p<0.05$, t-test, effect of TGF-β_2).

SD-208 enhances allogeneic immune responses to glioma cells in vitro.

Consistent with the effects of SD-208 on TGF-β-mediated signalling in glioma cells (Fig. 7.2 A,B), immunoblot analysis and reporter assays also revealed a strong resistance to TGF-β signalling in the presence of SD-208 in immune cells (Fig. 7.4 A,B,C).

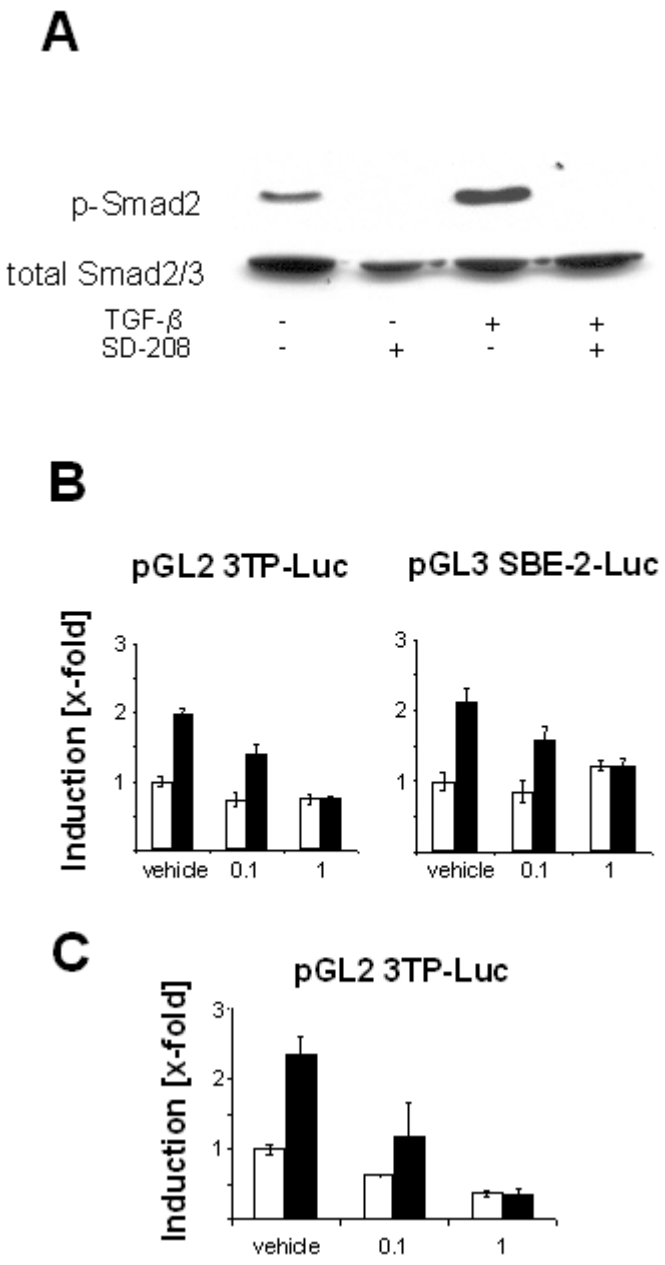

Fig. 7.4. **SD-208 inhibits TGF-β signaling in immune effector cells.** A. PBMC were treated with TGF-β_1 (5 ng/ml) in the absence or presence of SD-208 (1 μM) for 60 min and then subjected to immunoblot analysis for Smad2 phosphorylation (upper panel). Total Smad2 expression was assessed as a loading control (lower panel). B and C. PBL (B) or NK cells (C) were untreated or pretreated with SD-208 (0.1, 1 μM) for 1 h and then untreated (open bars) or treated with TGF-β_1 (5 ng/ml) (filled bars) for 16 h and subjected to the firelite reporter assay.

The next series of experiments was designed to examine whether SD-208 restores allogeneic immune cell responses to cultured human glioma cells. When HLA-A2-mismatched PBL or purified T cells were cocultured with irradiated glioma cells in the absence or presence of SD-208, their lytic activity in a subsequent 4 h ^{51}Cr release assay was significantly enhanced by a preexposure to SD-208 (Fig. 7.5). Similar effects were obtained using neutralizing TGF-β antibodies (10 μg/ml, added every two days) (data not shown**).**

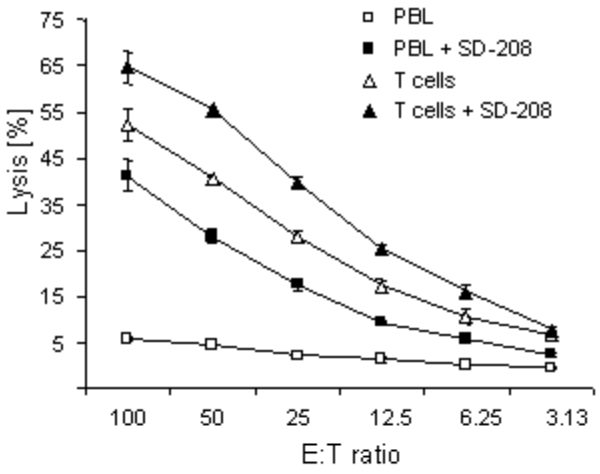

Fig. 7.5. **Modulation of alloreactive lysis of glioma cells by SD-208.** The lytic activity of PBL (squares) or purified T cells (triangles) preincubated with irradiated LN-308 cells in the absence (open symbols) or presence (filled symbols) of SD-208 (1 μM) was determined in ^{51}Cr release assays using LN-308 cells as targets ($^{+}p<0.05$, t-test, effect of SD-208 on PBL; *$p<0.05$, t-test, effect of SD-208 on T cells).

The release of IFN-γ by HLA-mismatched PBL was strongly inhibited when the priming had taken place in the presence of glioma cells. SD-208 restored the IFN-γ release to levels comparable to PBL pre-cultured in the absence of LN-308 cells (Fig. 7.6A). Similar results were obtained for TNF-α (Fig. 7.6B). In contrast, IL-10 release was stimulated after coculturing with LN-308 cells, and SD-208 reduced the release of IL-10 by immune effector cells generated both from unstimulated and glioma cell-primed cultures (Fig. 7.6C).

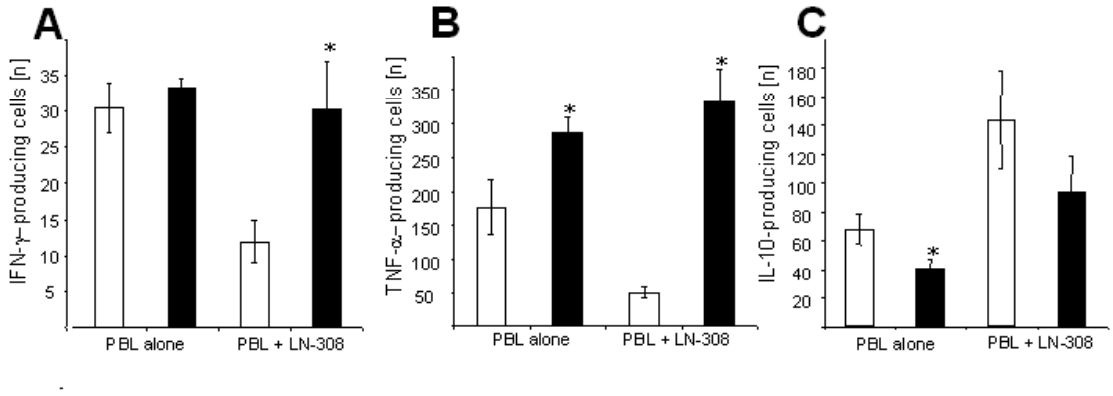

Fig. 7.6. **Modulation of allogeneic anti-glioma immune responses by SD-208.** PBL were cultured in the absence (left) or presence (right) of irradiated LN-308 cells for 5 days. The cultures contained SD-208 (1 μM) (filled bars) or not (open bars). Subsequently these effector cells were cocultured for 24 h with fresh non-irradiated LN-308 cells in the absence of SD-208. The release of IFN-γ (A), TNF-α (B) or IL-10 (C) was assessed by Elispot assay. Data are expressed as cytokine-producing cells per 5 x 10^5 effector cells (n=3, *$p<0.05$, t-test, effect of SD-208).

The lytic activity of polyclonal NK cells against LN-308 targets was inhibited by exogenous TGF-β, and TGF-β-mediated inhibition was relieved by SD-208 (Fig. 7.7A). Similarly, LN-308 SN inhibited NK cell activity, and this inhibition was also blocked by SD-208 (Fig. 7.7B) or neutralizing TGF-β antibodies (data not shown). Note that while the absolute lytical activity was donor-specific, the effect of SD-208 was consistent through all experiments.

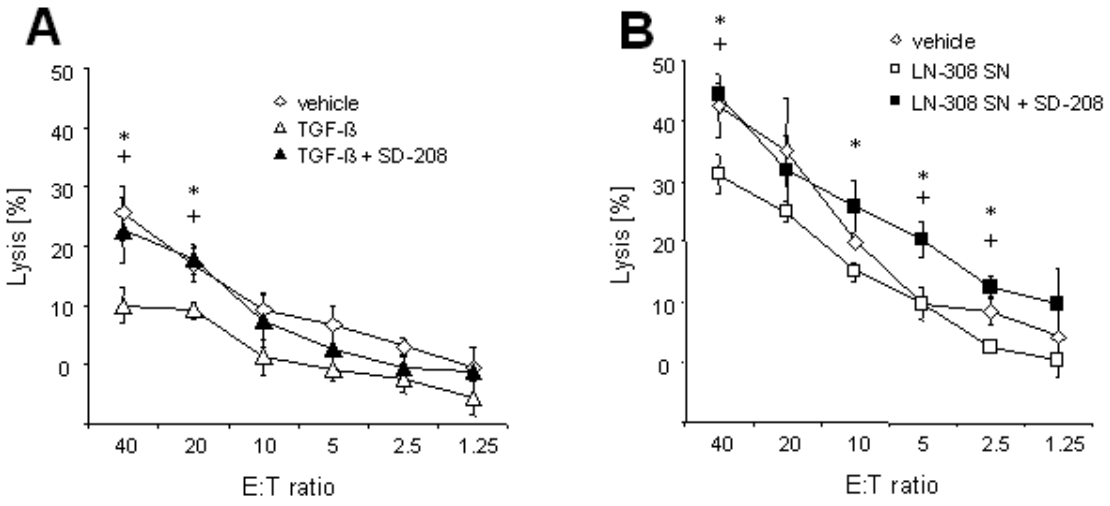

Fig. 7.7. **Modulation of NK cell-mediated lysis of glioma cells by SD-208.** Polyclonal NK cell cultures were exposed to TGF-β_1 (5 ng/ml) (A) or diluted (1:4) glioma cell SN (B) without or with SD-208 (1 μM) for 48 h and subsequently used as effectors in ^{51}Cr release assays using LN-308 cells as targets. SD-208 alone or TGF-β antibody alone had no effect on NK cell activity in these assays (data not shown, E: $^{+}p<0.05$, t-test, effect of TGF-β; *$p<0.05$, t-test, effect of SD-208; F: $^{+}p<0.05$, t-test, effect of glioma SN; *$p<0.05$, t-test, effect of SD-208).

SD-208 prolongs the survival of SMA-560 intracranial experimental glioma-bearing syngeneic mice.

To verify the bioavailability of orally administered SD-208, inhibition of TGF-β-dependent *in vivo* phosphorylation of Smad2/3 by SD-208 was ascertained in spleen and brain (Fig. 7.8 A,B). Exogenous TGF-β was a more potent inducer of Smad2/3 phosphorylation in spleen than brain, but that SD-208 was an equally effective antagonist of TGF-β in both tissues.

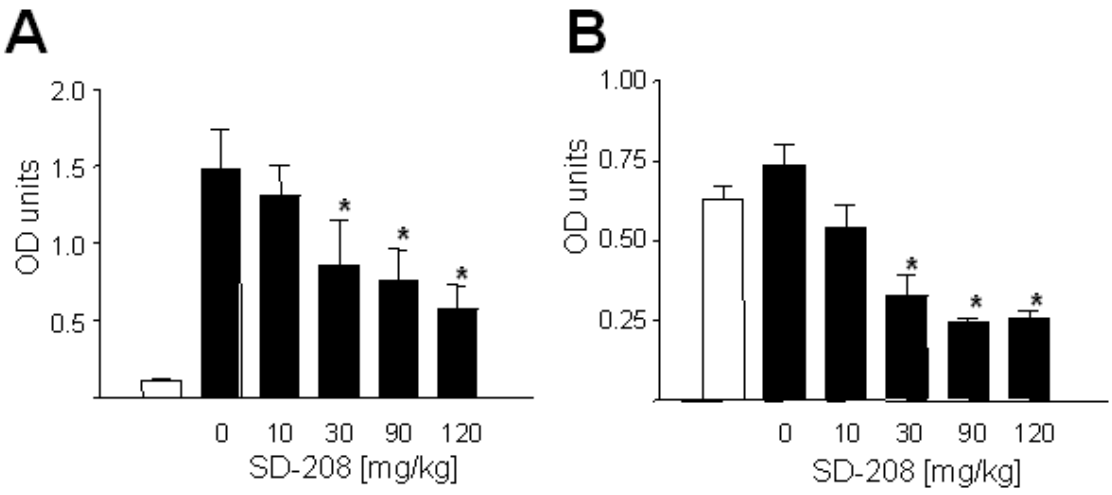

Fig. 7.8. **SD-208 blocks TGF-β signaling in the brain.** The animals were untreated (open bars) or treated with 150 ng TGF-β_1 i.v. (filled bars) at 1 h after oral exposure to SD-208 at increasing doses. The mice were sacrificed 1 h later and analyzed for Smad2/3 phosphorylation by ELISA in spleen (A) or brain (B) (*$p<0.01$, Bonferroni´s test, effect of SD-208 on TGF-β).

The therapeutic effects of SD-208 administered via the drinking water (1 mg/ml) were assessed in the syngeneic SMA-560 mouse glioma paradigm. The development of neurological symptoms was delayed by SD-208-treated mice and the mean survival was prolonged to 25.1±6.5 days (median 23) compared with 18.6±2.1 days (median 18) in vehicle-treated animals (Fig. 7.9) ($p=0.004$, t-test). The survival rate at 30 days was 29% in SD-208-treated animals, but 0% in control animals. Preliminary evidence also indicated that SD-208 modulated the immune response of the glioma-bearing animals. Elispot assays for IFN-γ release by splenocytes harvested at day 7 after the initiation of SD-208 treatment revealed an increase over background in 3 of 5 SD-208-treated animals, but only in 1 of 5 control animals (data not shown).

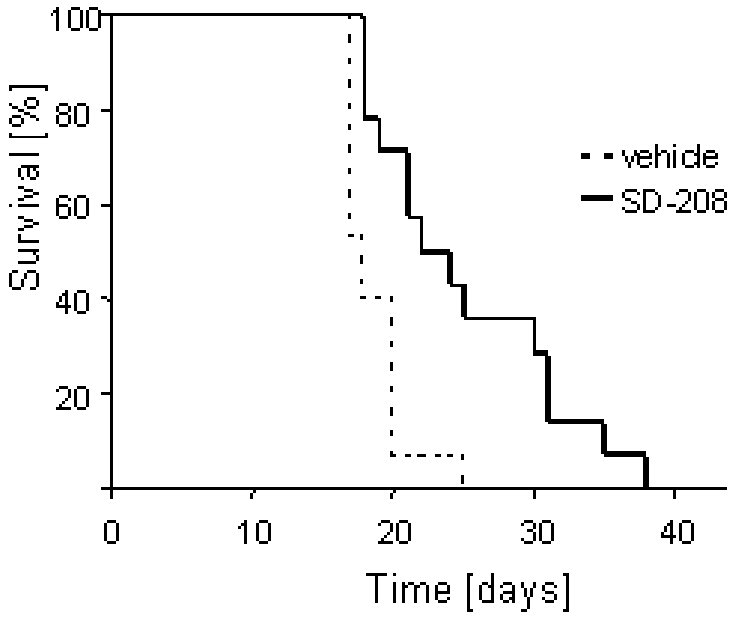

Fig. 7.9. **SD-208 blocks inhibits the growth of syngeneic SMA-560 experimental gliomas *in vivo*.** VM/Dk mice received an intracranial injection of 5 x 10^3 SMA-560 cells. Three days later SD-208 treatment was initiated, and survival was monitored.

Discussion

Antagonizing the biological effects of TGF-β has become a very attractive experimental strategy to combat various types of cancer including malignant gliomas. Current rationales for anti-TGF-β strategies include its putative role in migration and invasion (383), metastasis (389) and tumour-associated immunosuppression (155, 390). All of the TGF-β-based therapeutic approaches evaluated in experimental gliomas so far appear to have limitations with regard to their transfer into the clinic. Antisense oligonucleotides pose severe problems in terms of delivery to the desired site of action. The same applies to gene therapy strategies based e.g. on the transfer of the decorin gene (378). Inhibition of furin-like proteases aiming at limiting TGF-β bioactivity at the level of TGF-β processing (292) may not be achieved with acceptable specificity at present since a whole variety of molecules require processing by such enzymes (391). More specificity may result from the use of soluble TGF-β receptor fragments which act to scavenge bioactive TGF-β before it may reach the target cell population (389, 392). However, this approach may find its limits in the complex pathways of storage and activation of TGF-β. These considerations suggest that specific small molecules designed to protect cells from the actions of TGF-β at the level of receptor-dependent intracellular signal transduction are a particularly promising alternative for antagonizing TGF-β.

Here the activity of one such candidate agent, SD-208, against murine and human glioma cells is characterized *in vitro* and *in vivo*. Human LN-308 cells were chosen because they are paradigmatic for their prominent TGF-β synthesis (292, 393). SMA-560 cells transplanted in syngeneic VM/Dk mice represent the best model for the immunotherapy of rodent gliomas (388). The data outlined in this section show that SD-208 is a potent TGF-βRI kinase inhibitor (Table I) which blocks the biological effects of TGF-β_1 and TGF-β_2 as well as glioma cell SN in the CCL64 mink lung epithelial assay (Fig. 7.1). Since SD-208 did not modulate glioma cell proliferation at concentrations up to 1 μM (data not shown), a negative growth regulatory effect of TGF-β on SMA-560 cells was not confirmed (394). Smad2 phosphorylation is induced by TGF-β in a SD-208-sensitive manner (Fig. 7.2A), indicating that TGF-β signalling is not abrogated constitutively in glioma cells, but may not play a role in the modulation of glioma cell proliferation. Moreover, as expected (383), the antagonism of autocrine and paracrine

signalling by TGF-β in SD-208-treated glioma cells, as confirmed by reporter assay (Fig. 7.2B) resulted in a potent inhibition of migration and invasion (Fig. 7.3) (383).

We then focused on the desired immune modulatory effect of SD-208 which were expected to result in an enhanced immunogenicity of glioma cells as a consequence of reduced TGF-β bioactivity. As predicted, human PBL and purified T cells developed enhanced lytic activity against LN-308 glioma cell targets when prestimulated with glioma cells in the presence of SD-208 (Fig. 7.5). This was paralleled by an enhanced release of proinflammatory cytokines such as IFN-γ and TNF-α and a reduced release of the immunosuppressive cytokine IL-10 in SD-208-treated cells (Fig. 7.6). Similarly SD-208 restored the lytic activity of polyclonal NK cell cultures cocultured with TGF-β or LN-308 SN (Fig. 7.7).

The strong reduction of Smad phosphorylation in the unlesioned mouse brain indicates that SD-208 may reach sufficient levels beyond the intact blood brain barrier to counteract the biological effects of tumour-derived TGF-β (Fig. 7.8). Accordingly, SD-208 prolonged the median survival of SMA-560 glioma-bearing mice significantly (Fig. 7.9). No dose-limiting toxicity was reached in these experiments, but higher doses could not be administered by the drinking water because of poor solubility of SD-208, suggesting that the therapeutic effect of SD-208 or related agents might even be improved in that glioma model. The therapeutic effect of SD-208 might be mediated by the inhibition of glioma cell migration and invasion (383) (Fig. 7.3) or the promotion of anti-glioma immune responses (155) (Fig. 7.5 – 7.7).

The present data strongly suggest a role for SD-208 or related molecules in the treatment of gliomas. Such a systemic treatment with TGF-βRI kinase inhibitors might well be combined with local approaches to limit the bioavailability of TGF-β, e.g., TGF-β antisense oligonucleotides which are already evaluated clinically.

VIII. Transforming growth factor-β suppresses NKG2D-mediated anti-tumour immune responses and enhances tumour migration and invasiveness

A related manuscript has been accepted by Cancer Research.

This project is based on previous work from my colleague Dr. Manuel Friese (131) who also carried out most of the experiments. Dr. Alexander Steinle generated and supplied MICA and MICB-specific antibodies, Dr. Markus Weiler helped in characterizing the effect of TGF-β suppression on migration and invasiveness of glioma cells and Dr. Günter Eisele analyzed the expression of matrix metalloproteinases and UL-16 binding proteins (ULBP) in these cells. Yasmin Breithardt and Brigitte Frank provided expert technical assistance. I designed and cloned the constructs for the siRNA-mediated knock-down of TGF-β_1 and TGF-β_2, generated LNT-229 TGF-β_{si} glioma cells, characterized together with Manuel Friese and Günter Eisele the resulting immunological effects and was involved in the overall conception of the project.

Introduction

NKG2D is a C-type lectin-like homodimeric receptor, first identified as activatory receptor on natural killer (NK) cells where it mediates responses to stress-induced ligands (94). Further, NKG2D has been shown to exert additional roles in innate immunity by activating macrophages (395) and γδ T cells (396), and in adaptive immunity by providing costimulatory signals to $CD8^+$ αβ T cells (131, 397). NKG2D interacts with ligands that are not constitutively, but inducibly expressed by cell stress. In humans these are MHC class I-chain related molecules A (MICA) and MICB (398-401) and UL16-binding proteins (ULBP) 1, 2, 3, and 4 (95, 402). The human NKG2D ligands (NKG2DL) are well conserved within families (~55% identity among the ULBPs and ~84% between MICA and MICB alleles) and more distantly related between families in terms of sequence and structure (23-27% identical). The various NKG2DL have distinct patterns of expression, indicating that they cannot be considered simply redundant in function. Generally normal cells in adults show absent or low level NKG2DL expression, with the exception of intestinal epithelia, where NKG2DL may be induced as a consequence of stimulation by the neighbouring bacterial flora (399). In pathological conditions, however, NKG2DL expression is often upregulated, as described for epithelial tumours, gliomas and cells infected by HCMV or *Mycobacterium tuberculosis* (131, 396, 397, 399, 403-405). The molecular mechanisms underlying this induction of NKG2DL are still unclear. Heat-shock transcription elements have been implicated in the promoters of the MIC genes (399), however, neither MIC nor ULBP promoter regions have been characterized to date.

Engagement of NKG2D can initiate perforin-mediated cytolytic responses (406) by providing an activatory signal to NK cells and a co-stimulatory signal to antigen-specific T cells. NKG2D ligands (NKG2DL) are therefore induced self ligands and represent molecular markers which flag stressed, transformed, or infected cells for killing by NK and $CD8^+$ T cells (89). Thus, NKG2D is a potent mediator of antiviral and antitumour immune surveillance (131, 407-409).

Unfortunately, since gliomas grow progressively and eventually kill their host, the immune system clearly fails to mount an effective immune response against these tumours. Evasion from NKG2D-mediated tumour immunosurveillance has been attributed to proteolytical shedding of MIC molecules (410, 411). The binding of soluble MIC (sMIC) has been reported to induce the endocytosis and degradation of cell surface NKG2D, causing impairment of the responsiveness of tumour antigen-specific effector T cells (410). This systemic immune

deficiency is associated with circulating tumour-derived sMICA encompassing the three extracellular domains which is released by tumour cells at high levels into the sera of cancer patients (410-412). The release of MICA from tumour cells is blocked by the inhibition of MMP, resulting in the accumulation of MICA at the cell surface (411). MMP are proteolytic enzymes which shape the cellular microenvironment. Compared to normal tissue, their expression and activation is increased in almost all human cancers (413). Particularly MMP-2 and -9 are highly expressed in human gliomas (414).

This high expression of MMP-2 and -9 in glioma cells has been found to depend on TGF-β (415). Some aspects of the immune-modulatory properties of TGF-β have already been described in the previous chapter and are well-documented in the literature (155). TGF-β inhibits the maturation and antigen presentation by dendritic cells as well as the activation of T and NK cells (416). Accordingly, TGF-β production is associated with the growth and malignant progression of a large variety of tumours (292, 417, 418). A novel aspect of TGF-β as a central mediator of immune evasion by glioma cells is its influence on NKG2D-mediated antitumour responses. The data presented here demonstrate that TGF-β promotes immune escape and motility of human glioma cells by (i) down-regulating NKG2D expression in $CD8^+$ T and NK cells, (ii) (selectively) down-regulating NKG2DL gene expression in glioma cells, and (iii) mediating loss of cell surface MICA expression and (iv) enhanced motility, both in a MMP-dependent manner, in glioma cells.

Materials and Methods

Patient characteristics. PBMC were from patients with glioblastoma (5 males, 2 females, median age: 56 years, range: 48-71 years) who had not received radiotherapy, chemotherapy or glucocorticoids for 12 weeks. The glioma patients were compared with a group of 17 age- and sex-matched healthy donors (controls) without neurological or any other known disease. CSF was obtained from glioma patients or patients with other neurological diseases as part of the routine diagnostic work-up. The study was performed according to a protocol approved by the University of Tübingen Medical School Ethics Committee (#131/99).

Monoclonal antibodies and flow cytometry. Neutralizing pan-anti-TGF-$\beta_{1,2,3}$ mAb (1D11, IgG_1) was from R&D Systems (Wiesbaden, Germany). The following mAbs were used for the assessment of cell surface expression or the blocking of NKG2D, NKG2DL, CD3 and CD56: M585 IgG_1 anti-NKG2D (kindly provided by Amgen, Thousand Oaks, CA), MAB 139 IgG_1 anti-NKG2D (R&D Systems, Wiesbaden, Germany), BAMO1 IgG_1 anti-MICA/B, BAMO3 IgG_1 anti-MICA/B, AMO1 IgG_1 anti-MICA, BMO2 IgG_1 anti-MICB, AUMO1 IgG_1 anti-ULBP1, BUMO1 IgG_1 anti-ULBP2, CUMO1 IgM anti-ULBP3 (405), HIT3a IgG_{2a} anti-CD3-FITC (BD Pharmingen, Heidelberg, Germany), HIT8a IgG_1 anti-CD8-PE (BD Pharmingen) and B159 IgG_1 anti-CD56-PE (BD Pharmingen). Biotin-conjugated rabbit anti-mouse IgG (Dako, Hamburg, Germany), streptavidin-APC (BD Pharmingen) and PE-conjugated goat anti-mouse IgG (Sigma, Deisenhofen, Germany) were used for detection. Conjugated and unconjugated IgG_1 and IgG_{2a} isotype-matched mAbs were used as controls (BD Pharmingen). Staining for intracellular NKG2D was done after the cells had been fixed and permeabilized (Cytofix/Cytoperm Plus kit, BD Pharmingen). PBL, or glioma cells detached using Accutase (PAA, Wien, Austria), were preincubated in PBS with 2% BSA and incubated with the specific mAb or matched mouse Ig isotype (5 µg/ml) for 30 min on ice. Where specified, immune cells were acid-washed in 150 mM NaCl and 0.1% acetic acid to strip ligands from cell surface receptors (259). Specific binding was detected with the specific conjugate or by using a secondary conjugated antibody. Fluorescence was measured in a Becton Dickinson FACScalibur. Specific fluorescence indexes (SFI) were calculated by dividing mean fluorescence obtained with specific antibody by mean fluorescence obtained with control antibody.

Production of soluble murine NKG2D in insect cells. Recombinant soluble murine NKG2D lacking the amino-terminal cytoplasmic region and transmembrane domain was produced in Sf9 insect cells (Invitrogen, Karlsruhe, Germany) using the BAC-to-BAC system (Gibco Life Technologies, Paisley, UK). The expression construct included an amino-terminal FLAG/hexahistidine (401).

Purification of PBL and isolation of NK and T cells. PBL were prepared by density gradient centrifugation (Biocoll, Biochrom KG, Berlin, Germany) and depletion of plastic-adherent monocytic cells. PBL were cultured on irradiated RPMI 8866 feeder cells (384) to obtain polyclonal NK cell populations. To further enrich NK cells, PBL were sorted by immunomagnetic depletion using Dynabeads (NK Cell Negative Isolation Kit, Dynal, Oslo, Norway). $CD3^-CD56^+$ cells were used for cytotoxicity assays. To obtain purified $CD8^+$ T cells, fresh PBL were sorted by immunomagnetic CD8 MACS beads (Miltenyi Biotec, Bergisch Gladbach, Germany).

MICA/B ELISA. Glioma cell SN generated in the absence of FCS were concentrated with the Centriplus centrifugal filter device YM-3 (3000 Da cut-off; Millipore, Eschborn, Germany). The mAb AMO1 and BAMO3 were used in a sandwich ELISA for sMICA, and the mAb BAMO1 and BMO2 for sMICB as described (412).

Cell lines and transfectants. The human SV-FHAS astrocytic cell line was provided by D. Stanimirovic (Ottawa, Canada). The human malignant glioma cell lines were provided by Dr. N. de Tribolet (Lausanne, Switzerland). Unlike LN-229 cells grown in other laboratories, our LN-229 cell line still harbours wild-type p53 (224) and is therefore also referred to as LNT-229 (T for Tübingen, since 03/2004). Primary glioblastoma cells were established from freshly resected tumours, cultured in monolayers and used between passages 4 and 9 (419). The cells were maintained in DMEM medium supplemented with 2 mM L-glutamine (Gibco Life Technologies, Paisley, UK), 10% FCS (Biochrom KG, Berlin, Germany) and penicillin (100 IU/ml)/streptomycin (100 µg/ml) (Gibco). NKL cells, kindly provided by M. J. Robertson (Indianapolis, IN) (420), and YAC-1 cells (ATCC, Rockville, MD) were grown in RPMI 1640 medium supplemented with 15% FCS, 2 mM L-glutamine, 1 mM sodium pyruvate and penicillin (100 IU/ml)/streptomycin (100 µg/ml). The MMP inhibitor o-phenanthroline (oPA) was obtained from Sigma.

Adenoviral construct and transduction. The generation of adenoviruses encoding MICA has been described (131).

TGF-β siRNA. The human TGF-β_1-specific oligonucleotide sequences GATCCCCGACTATCGACATGGAGCTGttcaagagaCAGCTCCATGTCGATAGTCTTTTT GGAAA and TCGATTTCCAAAAAGACTATCGACATGGAGCTGtctcttgaa CAGCTCCATGTCGATAGTCGGG and the TGF-β_2-specific oligonucleotide sequences GATCCCCTGCCAACTTCTGTGCTGGAttcaagagaTCCAGCACAGAAGTTGGCATTTTT GGAAA and TCGATTTCCAAAAATGCCAACTTCTGTGCTGGAtctcttgaa TCCAGCACAGAAGTTGGCAGGG were obtained from Metabion (Munich, Germany) and cloned into the pSUPER vector (421), generously provided by Dr. Reuven Agami (Amsterdam, NL). The TGF-β-specific parts of the sequence are depicted underlined. A puromycin resistance cassette was cloned into the pSUPER vector before cloning to obtain stable transfectants. LNT-229 cells were stably cotransfected using a five-fold excess of pSUPER-TGF-β_1 over pSUPER-puro-TGF-β_2, using FuGENE 6 (Roche, Mannheim, Germany). Control transfectants were generated by transfecting pSUPER-puro into LNT-229 cells**.**

Immunoblot. Cell culture SN generated in the absence of FCS were concentrated with the Centriplus centrifugal filter device YM-3 (3000 Da cut-off; Millipore, Eschborn, Germany). Cell lysates were prepared in 50 mM Tris-HCl (pH 8) containing 120 mM NaCl, 5 mM EDTA, 0.5% NP-40, 2 μg/ml aprotinin, 10 μg/ml leupeptin and 100 μg/ml PMSF. Aliquots of concentrated SN or cell lysates were electrophoresed on 8-12% SDS-PAGE gels under reducing conditions and transferred to nitrocellulose (Schleicher & Schuell, Dassel, Germany). The lysates and SN were assessed at 10 μg total protein per lane. Equal protein loading was ascertained by Ponceau S staining. After blocking nonspecific binding sites with 5% (w/v) dried milk in PBS for 30 min, the filters were incubated with specific mAbs overnight at 4°C, washed and incubated with peroxidase-conjugated goat anti-rabbit or goat anti-mouse IgG (diluted 1:3000) (Santa Cruz Biotechnology, Santa Cruz, CA) for 3 h at 22°C. The mAbs BAMO1 anti-MICA/B, M585 anti-NKG2D, sc-146 goat anti-TGF-β_1 (Santa Cruz Biotechnology, Santa Cruz, CA), sc-90 goat anti-TGF-β_2 (Santa Cruz Biotechnology), Ab-3 mouse anti-MMP-2 (Oncogene, San Diego, CA), Ab-7 mouse anti-MMP-9 (Oncogene) or 113-5B7 mouse anti-MT1-MMP (Oncogene) were used at 1 μg/ml in PBS containing 0.05%

Tween 20 and 1.3% skim milk. Labelling was visualized using enhanced chemiluminescence (ECL, Amersham, Braunschweig, Germany).

Zymography. The activities of MMP-2 and MMP-9 were analyzed using SDS-PAGE gels containing 0.1% gelatine (wt/vol) and 10% polyacrylamide (wt/vol) (Biorad, Munich, Germany). Coomassie brilliant blue staining and subsequent destaining with glacial acid results in decreased staining at the level of electrophoretic migration of MMP-2 and MMP-9.

Real time PCR. Total RNA was prepared using RNAeasy (Quiagen, Hilden, Germany) and transcribed according to standard protocols. cDNA amplification was monitored using SYBRGreen chemistry on the ABI PRISM 7000 Sequence Detection System (Applied Biosystems, Weiterstadt, Germany). The conditions for all PCR reactions were: 40 cycles, 95°C for 15 s and 60°C for 1 min, using the following specific primers (forward, reverse): 18S: 5′-CGGCTACCACATCCAAGGAA-3′ (450-469), 5′-GCTGGAATTACCGCGGCT-3′ (636-619); MICA: 5′-CCTTGGCCATGAACGTCAGG-3′ (518-537), 5′-CCTCTGAGGCCTCGCTGCG-3′ (694-676); MICB: 5′-ACCTTGGCTATGAACGTCACA-3′ (483-503), 5′-CCCTCTGAGACCTCGCTGCA-3′ (661-642); ULBP1: 5′-GTACTGGGAACAAATGCTGGAT-3′ (584-605), 5′-AACTCTCCTCATCTGCCAGCT-3′ (730-710); ULBP2: 5′-TTACTTCTCAATGGGAGACTGT-3′ (579-600), 5′-TGTGCCTGAGGACATGGCGA-3′ (687-668); ULBP3: 5′-CCTGATGCACAGGAAGAAGAG-3′ (594-614) 5′-TATGGCTTTGGGTTGAGCTAAG-3′ (672-651); ULBP4: 5′-CTGGCTCAGGGAATTCTTAGG-3′ (573-593), 5′-CTAGAAGAAGACCAGTGGATATC-3′ (665-643). Data analysis was done using the $\Delta\Delta C_T$ method for relative quantification. Briefly, threshold cycles (C_T) for 18S rRNA (reference) and NKG2DL (sample) were determined in duplicates. The values obtained for untreated cells were arbitrarily defined as the standard value (100%) and determined the relative change (rI) in copy numbers according to the formula $rI = 2^{-[(C_T\text{Sample} - C_T\text{Reference}) - (C_T\text{Standard Sample} - C_T\text{Standard Reference})]}$.

TGF-β bioassay. Levels of bioactive TGF-β were determined using a modification of the CCL64 bioassay (378). Briefly, 10^3 CCL64 cells were adhered to 96 well plates for 24 h. After removal of regular medium, the cells were exposed to glioma cell SN, serum or CSF

from glioma patients or normal controls diluted in serum-free medium for 72 h. Viable cell counts were obtained by crystal violet staining.

TGF-β reporter assays. Intracellular TGF-β signalling was assessed by reporter assays using pGL2 3TP-Luc (385) or pGL3 SBE-2 Luc (386) reporter gene plasmids kindly provided by J. Massagué (New York, NY) and B. Vogelstein (Baltimore, MD). The pGL2 3TP-Luc construct contains a synthetic promoter composed of a TGF-β-responsive plasminogen activator inhibitor 1 promoter fragment inserted downstream of three phorbol ester-responsive elements. The pGL3 SBE-2-Luc reporter contains two copies of the Smad-binding element GTCTAGAC. For assessment of TGF-β_1 transcription, a pGL3b-TGF-β_1-Luc construct, containing the TGF-β_1 5'-flanking sequence (from -453 to +11 bp) (422) was used (a generous gift from C. Weigert, Tübingen). Cells were co-transfected with a ten-fold excess of the specific reporter over a pRL-CMV plasmid (Promega, Madison, WI), using FuGENE (Roche, Mannheim, Germany). At 32 h after transfection, TGF-β_1 (5 ng/ml) or SD-208 (1 μM, see previous section) was added or not for 16 h. The respective activities of firefly and renilla reniformis luciferase were determined sequentially in a LumimatPlus (EG&G Berthold, Pforzheim, Germany) luminometer, using the firelite dual luminescence reporter gene assay (Perkin-Elmer, Rodgau-Jügesheim, Germany). Background was subtracted from all values and the counts obtained from the measurement of firefly luciferase were normalized with respect to pRL-CMV.

T cell co-stimulation assay. T cell proliferation was measured using freshly isolated peripheral blood $CD8^+$ T cells after activation with plate-bound mAbs. mAb were plate-bound overnight in 96 well flat-bottomed MaxiSorp plates. T cells were stimulated with solid-phase anti-CD3 (OKT3, G. Jung, Tübingen, Germany) with or without anti-CD28 (9.3, G. Jung, Tübingen, Germany), anti-NKG2D (M585) or control IgG (2 μg/ml). Cultures were pulsed with [methyl-^{3}H] thymidine (1 μCi, Amersham) on day 3 and collected 16 h later using a cell harvester (Tomtec, Hamden, CT). Incorporated radioactivity was determined in a Wallac 1450 Microbeta Plus Liquid Scintillation Counter.

Cytotoxicity assay. Cytotoxicity was assessed in 4 h ^{51}Cr release assays in the absence or presence of various mAb or soluble mNKG2D. The concentrations for the masking experiments were 10 μg mAb/ml and 20 μg/ml for soluble mNKG2D. NK cells were pretreated with normal human IgG to prevent antibody-dependent cellular cytotoxicity.

Effector and ^{51}Cr-loaded target cells were incubated at various effector:target (E:T) ratios for 4 h. Spontaneous ^{51}Cr release was determined by incubating the target cells with medium alone. Maximum release was determined by adding NP-40 (2%). The percentage of ^{51}Cr release was calculated as follows: 100 x ([experimental release – spontaneous release]/[maximum release – spontaneous release]).

Glioma spheroids. Multicellular glioma spheroids were obtained by seeding glioma cell transfectants ($4x10^4$ cells/ml) in 96 well plates that were base-coated with 1.0% Noble Agar (Difco Laboratories, Detroit, MI) prepared in DMEM and culturing for 4-5 days until spheroids had formed. The extracellular matrix gel was prepared by mixing collagen I solution (Vitrogen 100, Cohesion, Palo Alto, CA) and modified Eagle´s medium (MEM) at a 8:1 ratio at 4°C, supplementing fibronectin to a final concentration of 10 µg/ml and adjusting the pH by addition of NaOH/$NaHCO_3$. This solution (400 µl) was added into 24-well plates and spheroids of defined size were implanted into the gel in triplicate. After gelation at 37 °C, the gel was overlayed with 400 µl complete medium and cultured in a humidified atmosphere (37°C; 5% CO_2). Photographs of each spheroid were taken after 0, 24, 48, 72 and 96 h. For quantification, the mean radial distance of 10 randomly selected glioma cells that had migrated from the tumour spheroid into the gel matrix was measured every 24 h, and expressed in relation to the mean radial distance at 0 h.

Matrigel invasion assays. Invasion *in vitro* was measured in Boyden chamber assays according to the manufacturer's recommendations (BD Biosciences, Heidelberg, Germany). Briefly, glioma cells were harvested in enzyme-free cell dissociation buffer (Gibco Life Technologies, Karlsruhe, Germany). 200 µl of cell suspension (2.5×10^5 cells/ml) per condition were added in triplicates to each Matrigel-coated transwell insert. 500 µl NIH 3T3-conditioned medium was used as a chemoattractant in the lower wells. Following a 20 h incubation period, cells on the lower side of each membrane were fixed in methanol at 4°C, stained with toluidine blue and sealed on slides. Photographs of representative microscopical fields were taken at 200-fold magnification. Quantification of cell invasion was expressed as the mean count of stained cells in five random fields of each membrane.

Mice and animal experiments. Athymic CD1 nude mice were purchased from Charles River Laboratories (Sulzfeld, Germany). Mice 6-12 weeks of age were used in all experiments. The experiments were performed according to NIH guidelines "Guide for the Care and Use of

Laboratory Animals" and to the German animal protection law. Groups of 4-6 mice were injected subcutaneously in the right flank with transfected LNT-229 cells in 0.1 ml of PBS, as indicated. Mice were examined regularly for tumour growth using a metric caliper and killed when tumours reached >12 mm diameter. Mice were anesthetized by an intraperitoneal injection of 7% chloral hydrate before all intracranial procedures. For intracranial implantation the mice were placed in a stereotactic fixation device (Stoelting, Wood Dale, IL) and a burr hole was drilled in the skull 2 mm lateral to the bregma. The needle of a Hamilton syringe (Hamilton, Darmstadt, Germany) was introduced to a depth of 3 mm. Five x 10^4 LNT-229 glioma cells in a volume of 2 µl PBS were injected into the right striatum. The mice were observed daily and sacrificed when developing neurological symptoms.

Mouse lymphocyte isolation. Murine NK cells were prepared from splenocytes of CD1-nude mice by positive selection using DX5 mAb-coupled magnetic beads with the corresponding column system (Miltenyi Biotech, Bergisch Gladbach, Germany) before use in cytotoxicity assays.

Statistics. Where indicated, analysis of significance was performed using the two-tailed Student's t-test with $P<0.05$ considered significant and $P<0.01$ considered highly significant (Excel, Microsoft, Seattle, WA). Evaluation of survival patterns in mice bearing intracerebral gliomas was performed by the Kaplan Meier method (423) and *P* values were evaluated by the Mantel log-rank test (424).

Results

Reduced NKG2D expression on CD8+ T and NK cells from glioma patients.

The constitutive presence of MIC at the surface of fresh primary human glioma cells (131) in the apparent absence of relevant tumour immunity suggests that MIC expressed on glioma cells or NKG2D expressed on immune cells might be functionally impaired in glioma patients. Therefore NKG2D expression was examined on $CD8^+$ T ($CD3^+CD8^+$) and NK ($CD3^-CD56^+$) cells from peripheral blood of glioma patients (n=7) and controls (n=17). NKG2D expression levels were significantly lower in $CD8^+$ T and NK cells of untreated, steroid-free glioma patients than of controls (mean $CD8^+$: 11.8 vs. 21, P=0.004; mean NK: 12 vs. 16.5, P=0.02) (Fig. 8.1).

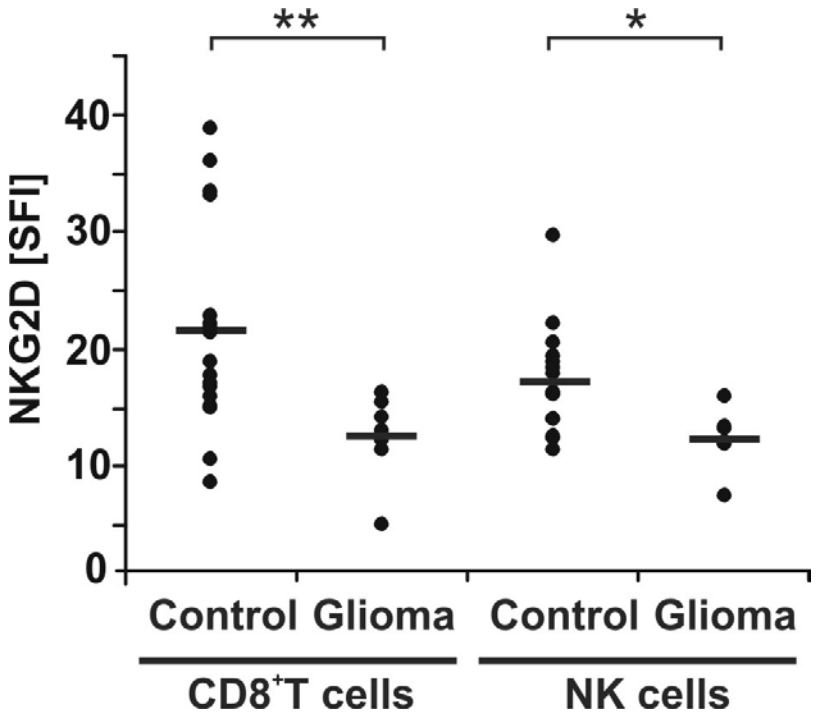

Fig. 8.1. **Downregulation of NKG2D on lymphocyte subsets from glioma patients.** Freshly isolated PBL from glioma patients (n=7) or controls (n=17) were examined for NKG2D expression at the cell surface by three-color flow cytometry with gating on $CD3^+CD8^+$ ($CD8^+$ T cells) or $CD3^-CD56^+$ (NK cells). Data are expressed as individual SFI values (∗P<0.05, ∗∗P<0.01, t-test).

Glioma cell lines release sMICA.

Immunoblot analysis was used to assess whether fresh primary polyclonal glioma cell cultures and long-term glioma cell lines release MICA into the cell culture supernatant (SN). sMICA (~57 kDa) was detected in the SN of 3 of 4 primary glioma cell cultures and in all 12 glioma cell lines, but not in the non-neoplastic astrocyte cell line, SV-FHAS. sMICB (~48 kDa) probably represents the smaller band in TU132 and TU140 cells (Fig. 8.2, A, B and C).

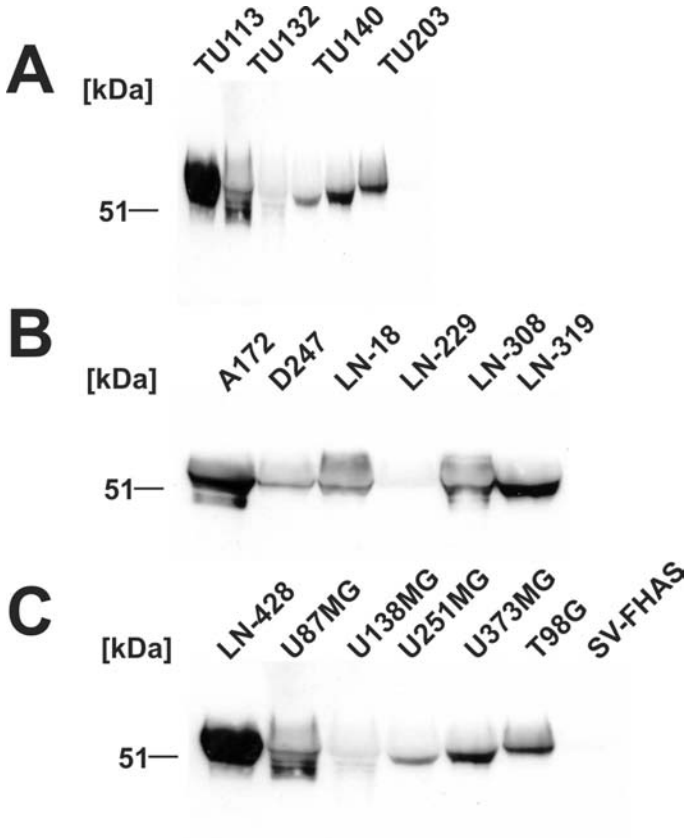

Fig. 8.2. **Glioma cells release sMICA/B.** The presence of sMIC in concentrated SN of primary glioma cell cultures (A) or glioma cell lines (B) and (C) was assessed by immunoblot using anti-MICA/B mAb BAMO1.

Apparent discrepancies in sMICA levels between immunoblot and ELISA might be due to the different antibodies used which might detect different allelic variants of MICA preferentially. A comparison of immunoblots of cell lysates and concentrated SN of 4 cell lines showed that the MICA protein in the SN was ~10 kDa smaller than the MICA protein in the cell lysates, suggesting proteolytic cleavage (Fig. 8.3).

Fig. 8.3. **Comparison of soluble and membrane-bound MICA/B.** SN and cell lysates of corresponding glioma cell lines were compared.

sMIC levels were also quantified by ELISA (Table 1).

Table 1. **Release of sMICA and sMICB by human glioma cell lines in 48 h SN.**

Cell line	sMICA (ng MICA / mg protein)	sMICB (ng MICB / mg protein)
A172	1.2	ND[a]
D247	2.0	0.2
LN-18	2.0	0.4
LN(T)-229	1.0	ND
LN-308	0.7	ND
LN-319	1.8	ND
LN-428	12.6	0.2
T98G	3.9	0.5
U87MG	0.4	ND
U138MG	1.0	ND
U251MG	0.7	ND
U373MG	1.3	ND
SV-FHAS	ND	ND
TU113	ND	ND
TU132	0.13	ND
TU140	ND	ND
TU203	ND	ND

sMIC concentration was determined by ELISA and normalized to the protein content of concentrated glioma cell SN ([a]ND=not detectable).

To investigate whether glioma-associated MIC is released into the cerebrospinal fluid (CSF) or serum, the levels of sMICA and sMICB were measured in sera and CSF from glioma patients (n=10) and control patients with lumbar disc prolapse, lumbar stenosis or normal pressure hydrocephalus (n=10) by ELISA and immunoblot. There were no detectable levels (≥ 0.1 ng/ml) of sMICA or sMICB in any of the investigated samples (data not shown), using serum samples from leukaemia patients as a positive control (412).

Glioma cell supernatants down-regulate NKG2D expression in immune cells in a sMICA-independent manner.

To investigate whether sMICA in the SN of glioma cells down-regulates NKG2D expression levels (410), freshly isolated and untreated PBL or NKL cells were incubated with glioma cell SN and then subjected to flow cytometry. LN-308 SN markedly reduced NKG2D expression on fresh $CD8^+$ T ($CD3^+CD8^+$) and NK cells ($CD3^-CD56^+$) (Fig. 8.4).

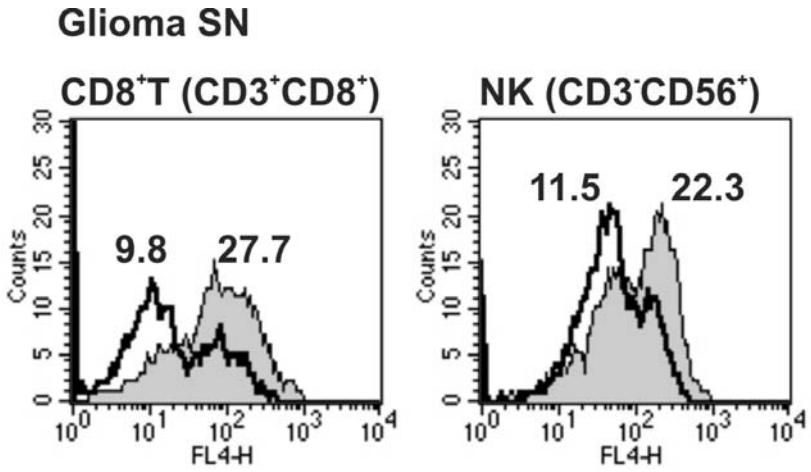

Fig. 8.4. **Downregulation of NKG2D on lymphocytes exposed to glioma cell SN.** Freshly isolated PBL were untreated (filled profiles) or exposed to LN-308 glioma cell SN (Glioma SN) (dilution 1/4) (open profiles) for 48 h and analyzed for NKG2D expression on $CD8^+$ T ($CD3^+CD8^+$) or NK ($CD3^-CD56^+$) cells. The SFI values for NKG2D expression are indicated.

Further, glioma SN reduced NKG2D expression in isolated $CD8^+$ T and NKL cells in a concentration-dependent manner (Fig. 8.5). A decreased binding of anti-NKG2D mAb due to masking of NKG2D by sMICA was excluded by demonstrating that the SFI values remained unaltered when potential ligands were stripped off cell surface receptors by an acid wash (data not shown).

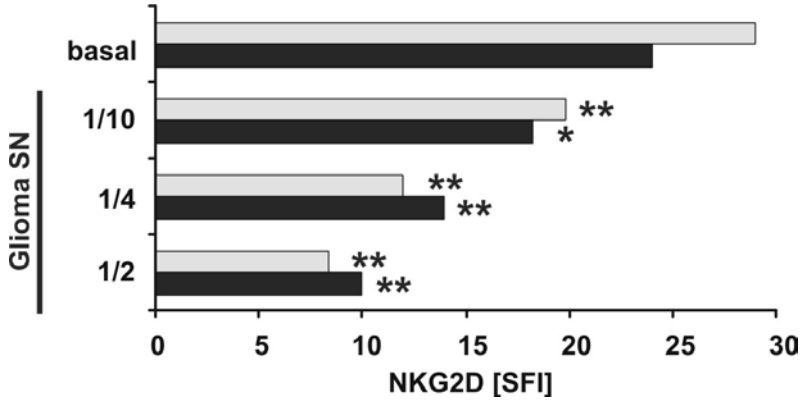

Fig. 8.5. **Downregulation of NKG2D on CD8$^+$ T cells exposed to glioma cell SN.** CD8$^+$ T cells freshly isolated by MACS beads (grey bars) or NKL cells (black bars) were examined accordingly, using increasing SN concentrations.

Surprisingly, the down-regulation of NKG2D mediated by glioma cell SN was not blocked by anti-MICA mAb or soluble NKG2D (Fig. 8.6A). The biological activity of either reagent was ascertained by their inhibition of MICA-mediated immune cell activation (131). It was confirmed that, in contrast to sMICA, membrane MICA down-regulates NKG2D expression levels. This was accomplished using adenoviral MICA gene transfer which resulted in high level MICA expression at the cell surface of glioma cells (131). The coincubation of transduced glioma cells with NKL cells strongly down-modulated NKG2D expression in NKL cells. The effect of adenoviral MICA gene transfer on NKG2D expression was nullified by anti-MICA (Fig. 8.6B). Moreover, the SN of Ad-MICA-infected cells, which contains high sMICA levels (23 ng/ml by ELISA), did not down-regulate NKG2D expression to a greater extent than the SN of Ad-dE1-infected or uninfected cells (both < 0.1 ng/ml by ELISA), and anti-MICA had again no effect (Fig. 8.6C).

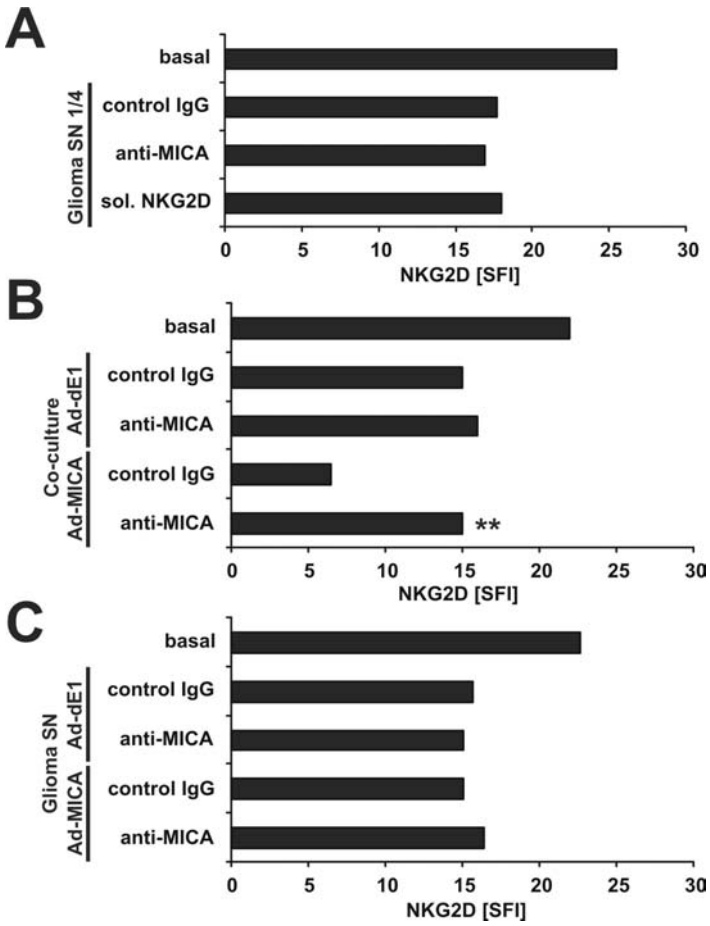

Fig. 8.6. **Downregulation of NKG2D on NKL cells by glioma cell SN depends on membrane-bound, but not on soluble MICA.** A. NKL cells were incubated with LN-308 SN in the presence of control IgG or anti-MICA (BAMO1) (10 μg/ml) or soluble murine NKG2D (20 μg/ml). B. NKL cells (3 x 10^5) were co-cultured with LN-308 glioma cells (1 x 10^5) infected with Ad-MICA or Ad-dE1 (300 MOI) in the presence of control IgG or anti-MICA (BAMO1) (10 μg/ml). C. The SN of Ad-MICA- or Ad-dE1- (300 MOI) infected glioma cells were incubated with NKL cells for 48 h in the presence of control IgG or anti-MICA (∗P<0.05, ∗∗P<0.01, t-test). Data are expressed as individual SFI values.

Glioma-derived TGF-β_1 and TGF-β_2 down-regulate NKG2D at the transcriptional level.

In the context of further efforts to elucidate the mechanism of glioma-induced loss of NKG2D expression on immune cells, it was noted that TGF-β_1 and TGF-β_2 down-regulate NKG2D expression in freshly isolated $CD8^+$ T and NK cells as well as in NKL cells (Fig. 8.7, A, B and C) (194). In contrast, IL-10 had no such effect (data not shown).

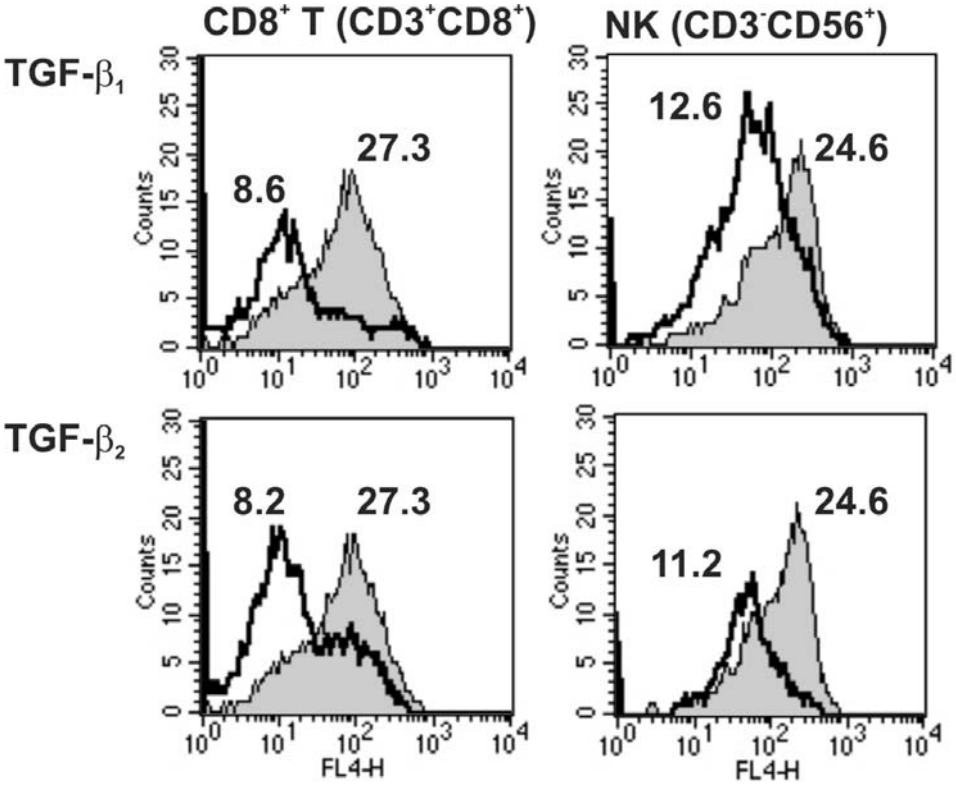

Fig. 8.7. **Downregulation of NKG2D on lymphocyte subsets by TGF-β.** Freshly isolated PBL were untreated (filled profiles) or treated with TGF-β_1 or TGF-β_2 (10 ng/ml) for 48 h (open profiles) and subjected to flow cytometry analyzing NKG2D expression on gated $CD3^+CD8^+$ T or $CD3^-CD56^+$ NK cells. The SFI values for NKG2D expression are indicated.

TGF-β-mediated down-regulation of NKG2D expression was concentration- and time-dependent (Fig. 8.8, A, B and C).

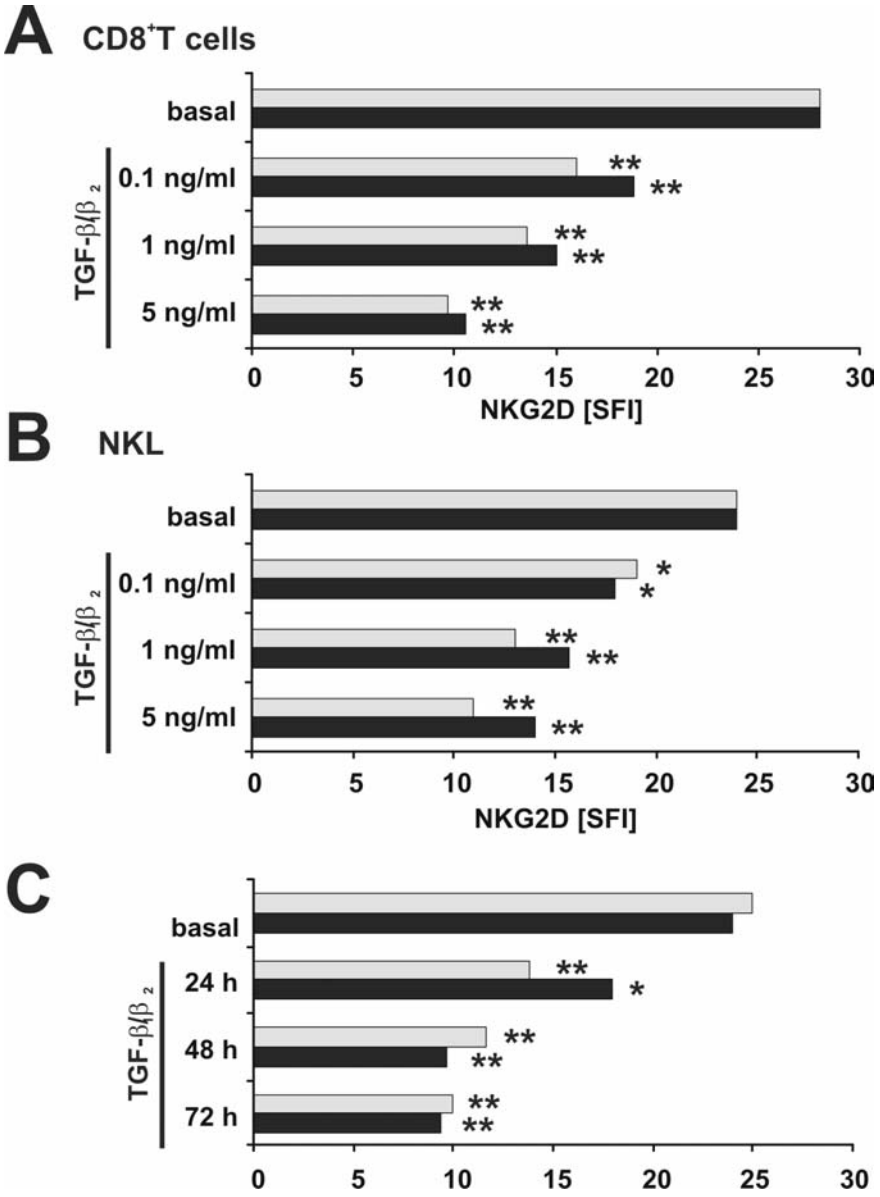

Fig. 8.8. **TGF-β-mediated downregulation of NKG2D is time- and dose-dependent.** Freshly isolated $CD8^+$ T cells (A) or NKL cells (B,C) were treated with TGF-β_1 (grey bars) or TGF-β_2 (black bars) at increasing concentrations for 48 h (A,B) or (C) lengths of time (NKL) at 10 ng/ml.

Since glioma cell SN, notably from LN-308 cells, contains large amounts of TGF-β_1 and TGF-β_2 (292), the next step was to investigate whether TGF-β mediated the effects of glioma SN on NKG2D expression. Anti-TGF-β mAb nullified the inhibitory effects of glioma cell SN on NKG2D expression, indicating that TGF-β is the principle soluble factor which reduces NKG2D levels at the surface of immune effector cells (Fig. 8.9).

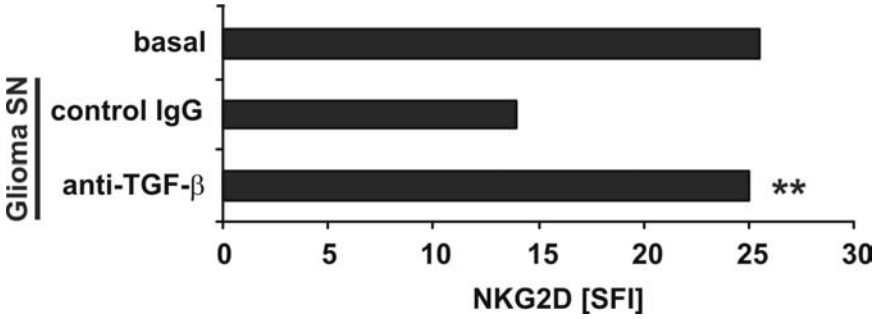

Fig. 8.9. **Anti-TGF-β antibody prevents downregulation of NKG2D by glioma cell SN.** NKL cells were incubated with LN-308 SN in the presence of control IgG or anti-TGF-β mAb (10 μg/ml).

The reduced signal for NKG2D at the cell surface was not due to receptor internalization or failure to translocate NKG2D to the cell membrane since TGF-β decreased the NKG2D levels in permeabilized cells (data not shown). Further, real time PCR analysis showed a reduction of NKG2D mRNA levels in NKL cells at 48 h after exposure to glioma cell SN, TGF-β_1 or TGF-β_2 (Fig. 8.10).

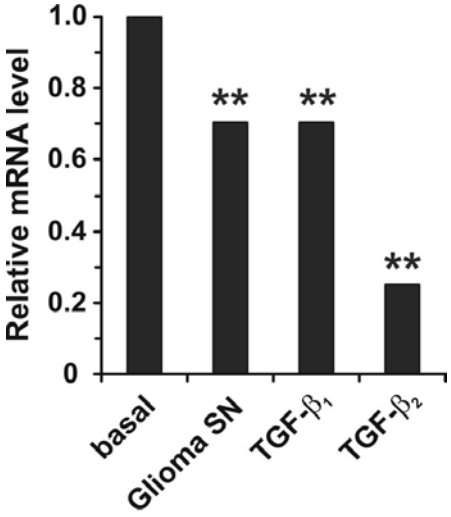

Fig. 8.10. **Transcriptional downregulation of NKG2D by TGF-β.** NKG2D mRNA expression was assessed in NKL cells exposed to LN-308 glioma SN (dilution 1/4) or TGF-β_1 and TGF-β_2 (10 ng/ml) for 48 h.

Further evidence for a decisive role of TGF-β was gained from the co-incubation of NKL cells with sera or CSF samples from glioma patients. Sera and CSF, as mentioned previously, showed no detectable sMICA levels by ELISA or immunoblot, but both body fluids reduced NKG2D expression in NKL cells. The inhibition of NKG2D expression by paired serum (20 ng/ml) and CSF (22 ng/ml) samples from a glioma patient was reversed by pan anti-TGF-β (Fig. 8.11). The restoration of NKG2D expression was incomplete in serum, suggesting the presence of other modulators of NKG2D expression in these samples (425).

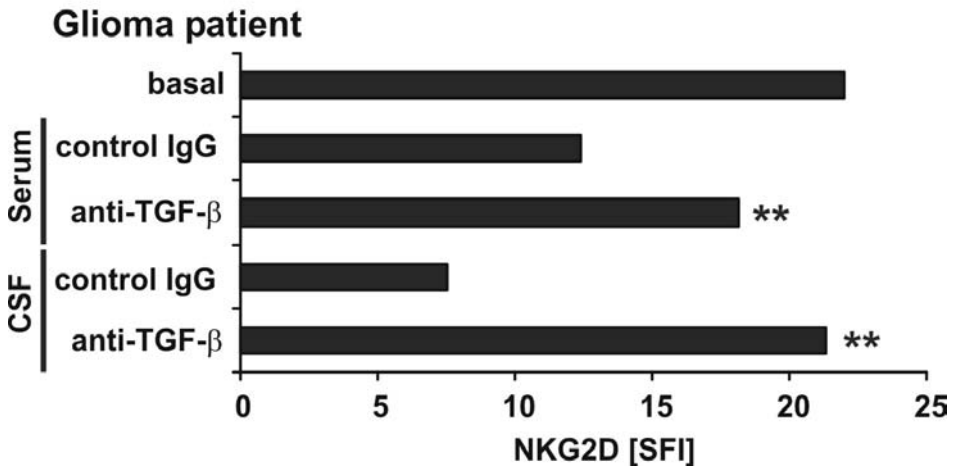

Fig. 8.11. **The effect of glioma patient serum or CSF on NKG2D expression can be blocked by anti-TGF-β antibody.** Diluted serum (1/4) or CSF (1/4) from a glioma patient was added to NKL cells for 48 h in the presence of control IgG or anti-TGF-β (10 μg/ml) (∗P<0.05, ∗∗P<0.01, t-test).

TGF-β-regulated MMP expression mediates MICA shedding.

Since TGF-β modulates MMP expression in glioma cells (415), the next question to be addressed was whether MMP mediates MICA release by glioma cells and whether this activity of MMP depends on TGF-β. MMP-2 levels were increased by TGF-β and reduced by neutralizing TGF-β mAb whereas MMP-9 levels showed no consistent change in response to altered TGF-β availability. Zymography, an assay based on the digestion of gelatine by electrophoretically separated MMP-2 and MMP-9, showed that MMP-2 (72 kDa) activity was enhanced by TGF-β and reduced by anti-TGF-β treatment. The effect of exogenous TGF-β was blocked in the presence of the MMP inhibitor oPA (Fig. 8.12A). Exposure to oPA, previously shown to reduce MMP activity in glioma cells (415), reduced the release of MICA in a concentration-dependent manner. In parallel, the expression levels of MICA at the cell surface increased (Fig. 8.12B). oPA did not alter the levels of TGF-β release by glioma cells (data not shown).

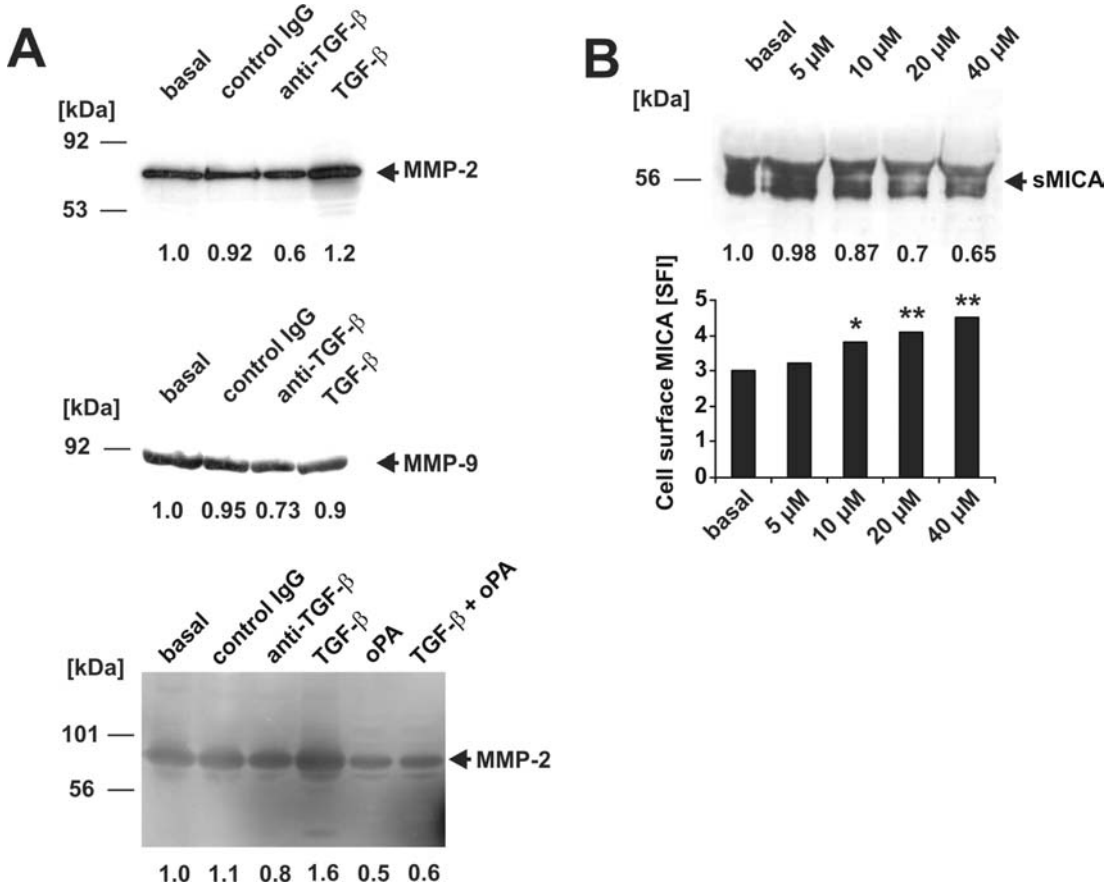

Fig. 8.12. **MMP, that cleave MICA, are induced by TGF-β.** A. The release of MMP-2 or MMP-9 by T98G cells that were untreated or treated for 48 h with control IgG or anti-TGF-β (10 μg/ml), or recombinant TGF-β_2 (10 ng/ml), was monitored by immunoblot. MMP-2 (72 kDa) and MMP-9 (92 kDa) activity in the SN of T98G were assessed by zymography (lower panel). Cells were treated as previously or with oPA (20 μM) or oPA (20 μM) plus TGF-β_2 (10 ng/ml). The numbers indicate relative densitometry units. B. sMICA levels in the SN of T98G cells exposed to increasing concentrations of oPA for 48 h were analyzed by immunoblot using mAb BAMO1. MICA levels at the cell surface were determined by flow cytometry in parallel.

However, neutralizing TGF-β mAb reduced sMICA release by 63% and exogenous TGF-β increased the levels of sMICA in the SN (Fig. 8.13A). Accordingly, anti-TGF-β mAb or oPA alone increased the expression of MICA at the cell surface (Fig. 8.13B). oPA antagonized the loss of MICA induced by exogenous TGF-β, but not to the full extent, indicating another mechanism of MICA suppression by TGF-β (Fig. 8.13B).

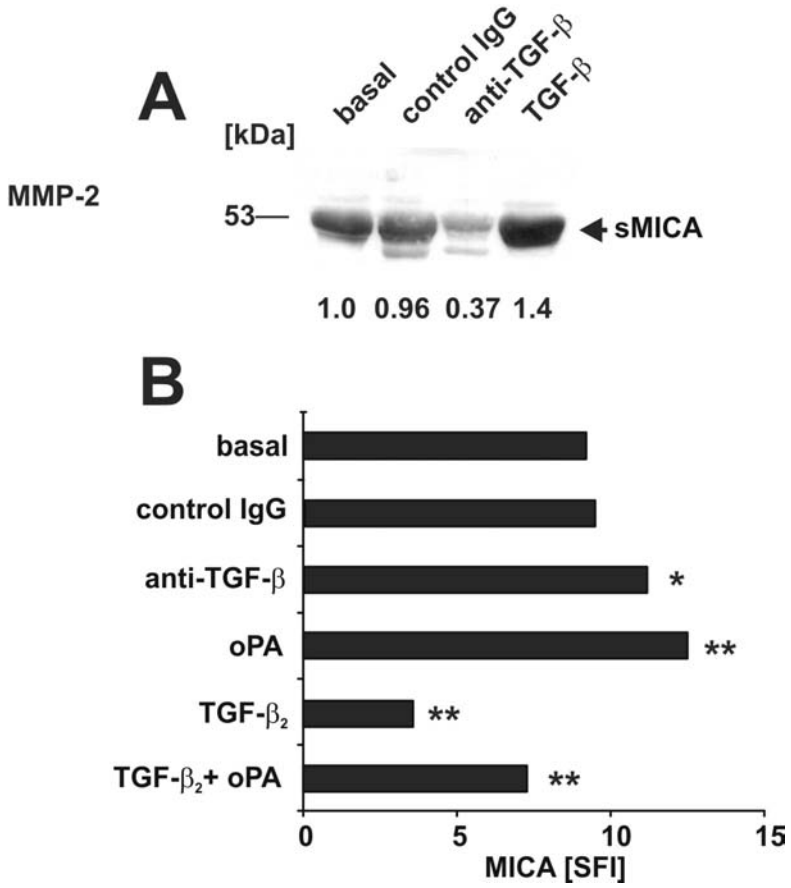

Fig. 8.13. **The levels of soluble and membrane-bound MICA are inversely correlated.** A. The release of sMICA by T98G cells that were untreated or treated for 48 h with control IgG or anti-TGF-β (10 μg/ml), or recombinant TGF-β_2 (10 ng/ml), was monitored by immunoblot. B, MICA expression at the cell surface of T98G cells cultured for 48 h in the presence of control IgG (10 μg/ml), anti-TGF-β (10 μg/ml), oPA (20 μM) or TGF-β (10 ng/ml) or both was assessed by flow cytometry (∗P<0.05, ∗∗P<0.01, t-test).

TGF-β and MMP activity inhibit NK cell-mediated glioma cell killing and T cell co-stimulation.

The relevance of the TGF-β-mediated reduction of NKG2D expression in NK cells and the TGF-β-mediated increase in MICA shedding by glioma cells were functionally investigated in ^{51}Cr release assays using immune effector cells pretreated with TGF-β or target glioma cells pretreated with oPA. MMP inhibition by oPA, which increases MICA expression at the surface of glioma cells, enhanced the NK cell-dependent killing of glioma cells. This was attenuated by coincubation with anti-MICA mAb. Other NKG2DL and activating molecules might also be regulated by MMP activity, explaining the incomplete blocking of lysis by anti-MICA in oPA-treated glioma cells (Fig. 8.14A). Exogenous TGF-β treatment of the NK effector cells had no effect on the lysis of control-transfected LN-229 cells, but markedly

reduced the specific lysis of stable LN-229.MICA (131) transfectants, indicating a specific effect on NKG2D-mediated glioma cell killing (Fig. 8.14B).

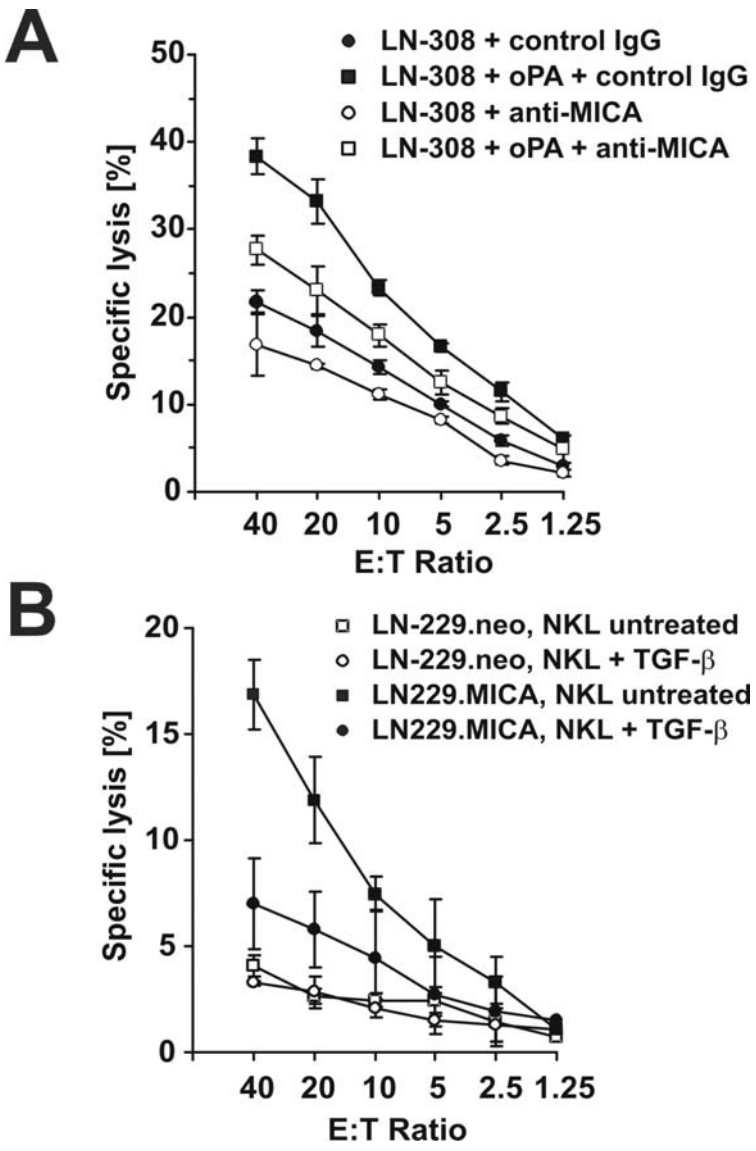

Fig. 8.14. **Immune-mediated lysis of glioma cells is MICA-dependent and sensitive to TGF-β.** A. LN-308 glioma cells untreated or treated with oPA (20 μM) or anti-MICA (BAMO1) (10 μg/ml) or both were used as target cells in a standard 4 h ^{51}Cr release assay using polyclonal NK cells as effectors. Data are expressed as specific lysis at different E:T ratios. In B, NKL cells untreated or pretreated with TGF-β (10 ng/ml) were used in a standard 4 h ^{51}Cr release assay, using LN-229.MICA stable transfectants or mock transfectants (LN-229.neo) as target cells.

To evaluate the significance of TGF-β for NKG2D-mediated CD8$^+$ T cell co-stimulation, purified human CD8$^+$ T cells were stimulated with anti-CD3 mAb in combination with NKG2D mAb or CD28 mAb in the presence or absence of TGF-β. While anti-CD3 mAb alone induced a moderate T cell response, significant increases in T cell proliferation were

observed by inclusion of NKG2D mAb. This effect, however, was less potent than that of anti-CD28 mAb. The co-stimulatory activity of anti-NKG2D was reduced by TGF-β treatment of $CD8^+$ T cells whereas anti-CD28 stimulation was less affected by TGF-β, showing a prominent effect of TGF-β on NKG2D-mediated activation (Fig. 8.15).

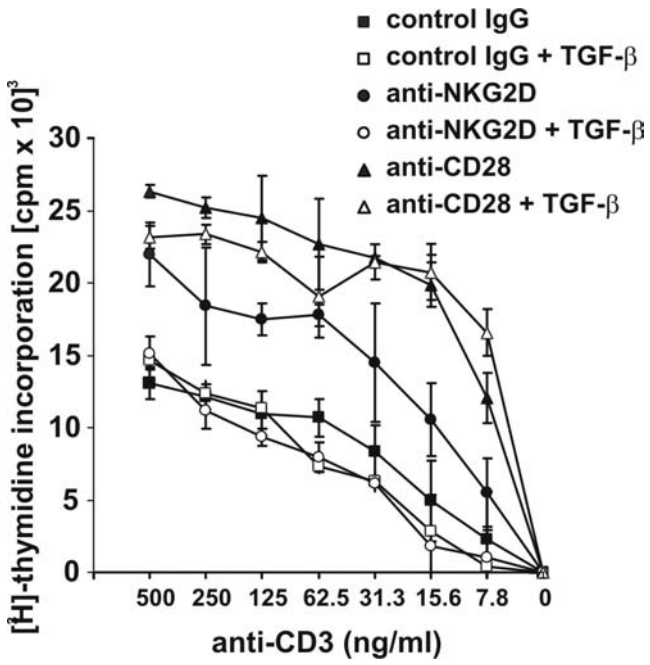

Fig. 8.15. **NKG2D-mediated co-stimulation is sensitive to TGF-β.** Purified $CD8^+$ T cells were cultured with precoated CD3 mAb (OKT3) at different concentrations and immobilized control IgG, NKG2D mAb or CD28 mAb (2 μg/ml) and in the absence or presence of TGF-β_2 (10 ng/ml) for 96 h. Cultures were pulsed with [methyl-^{3}H]-thymidine for the last 16 h. Data are expressed as mean cpm ± SD.

TGF-β knock-down in glioma cells: in vitro phenotype.

Pursuing a possible therapeutic perspective, siRNA technology was used to knock-down TGF-β_1 and TGF-β_2 expression in LNT-229 glioma cells. TGF-β_1 protein was stably reduced by 95% and TGF-β_2 by 99% with a combined approach using TGF-β_1 and -β_2 siRNA target sequences (Fig. 8.16A). TGF-β_1 siRNA only targeted TGF-β_1 but not TGF-β_2 and *vice versa* (data not shown). Accordingly, reporter gene assays using p3TP-Luc (Fig. 8.16B) or SBE2-Luc (Fig. 8.16B) confirmed that intracellular TGF-β signalling was repressed in TGF-$\beta_{1/2}$ siRNA cells compared to mock transfectants (controls). This effect was reversed (or, in the case of SBE2-Luc, diminished) by addition of exogenous TGF-β_1. The TGF-β receptor I kinase inhibitor SD-208 reduced reporter gene activity in the control transfectants, but not in TGF-$\beta_{1/2}$ siRNA cells. Further, the transcription of TGF-β_1 itself was not impaired in the

TGF-$\beta_{1/2}$ siRNA cells, consistent with posttranscriptional mRNA degradation triggered by siRNA (Fig. 8.16D).

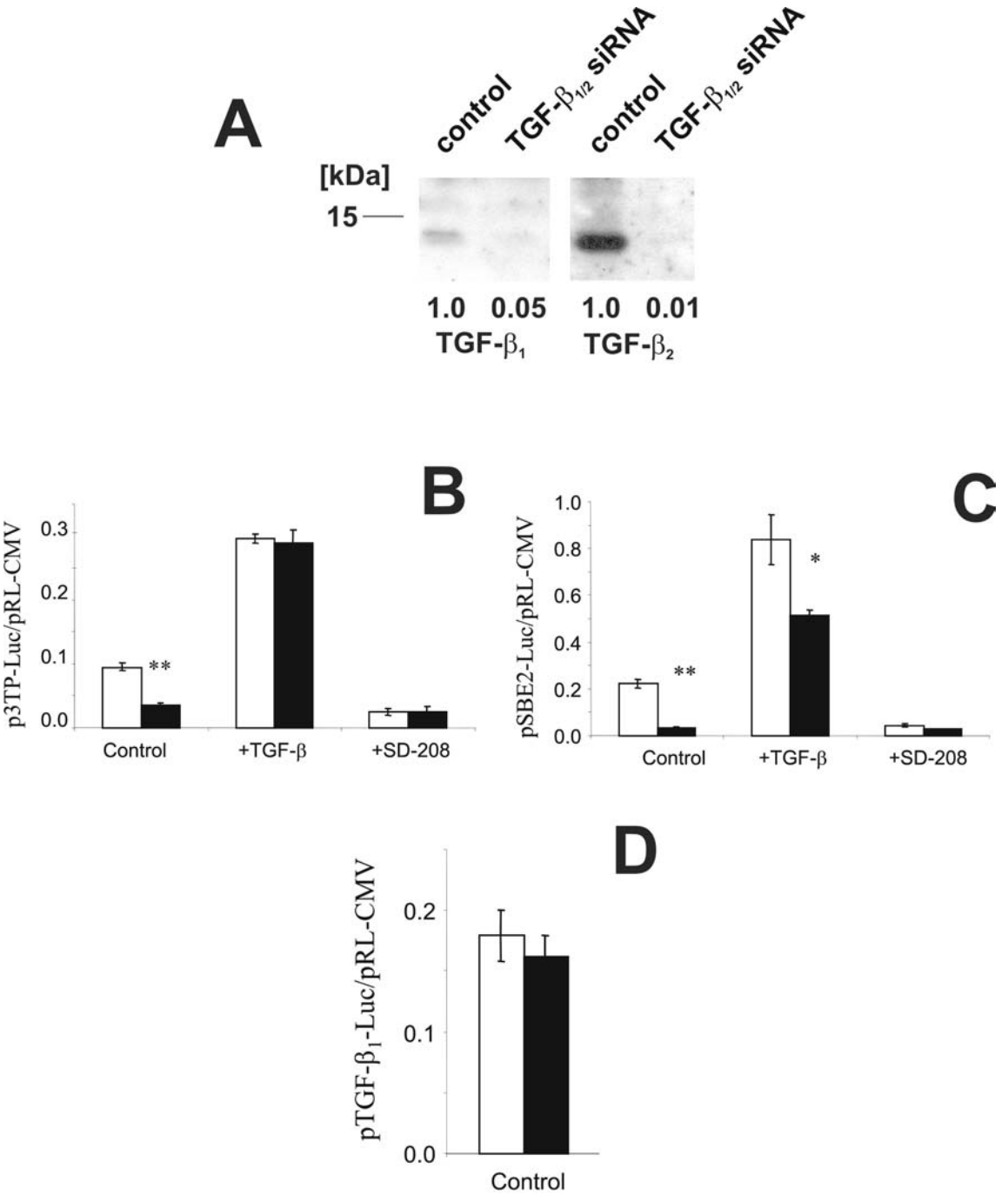

Fig. 8.16. **Downregulation of TGF-$\beta_{1/2}$ in LNT-229 TGF-$\beta_{1/2}$ siRNA cells.** A. The release of TGF-β_1 and TGF-β_2 in SN of pSUPER-puro-TGF-β_1 and- TGF-β_2 stably transfected LNT-229 cells (TGF-$\beta_{1/2}$ siRNA) or mock transfectants (control) was monitored by immunoblot. B-D. Intracellular TGF-β signalling was assessed in untreated or TGF-β_1 (5 ng/ml, 16 h) or SD-208 treated control cells (white columns) and TGF-$\beta_{1/2}$ siRNA cells (black columns). Luminescence counts for pGL2-3TP-Luc (B), pSBE2-Luc (C) and pGL3b-TGF-β_1-Luc (D) were divided by the counts obtained from co-transfected pRL-CMV. Their ratio is given as relative luciferase activity (mean ± SD, t-test, $*P<0.05$ $**P<0.01$).

The expression of MMP-2 and MMP-9 was suppressed in TGF-$\beta_{1/2}$ siRNA cells (Fig. 8.17), resulting in a 64% reduction in MMP activity by zymography (Fig. 8.17). No such effect was observed for MT1-MMP (data not shown).

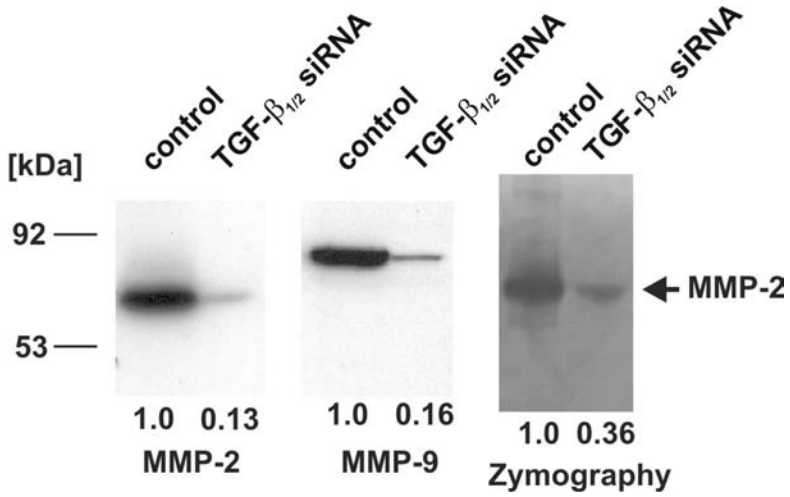

Fig. 8.17. **Downregulation of MMP expression in TGF-$\beta_{1/2}$ siRNA cells.** MMP-2 (72 kDa) and MMP-9 (92 kDa) expression in the SN of control cells and TGF-$\beta_{1/2}$ siRNA were assessed immunoblot and specific activity by zymography.

SN of control transfectants down-regulated NKG2D expression in NKL cells whereas the SN of TGF-$\beta_{1/2}$ siRNA cells left NKG2D levels unaltered (Fig. 8.18).

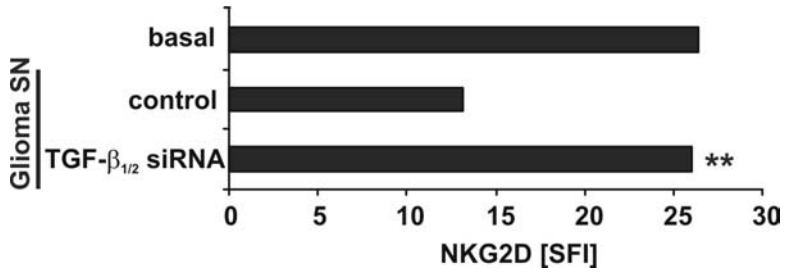

Fig. 8.18. **SN from LNT-229 TGF-$\beta_{1/2}$ siRNA cells does not affect NKG2D expression on NKL cells.** NKL cells were incubated with glioma cell SN (Glioma SN 1/4) of control or TGF-$\beta_{1/2}$ siRNA cells for 48 h and analyzed for NKG2D expression by flow cytometry.

MICA levels were also investigated by immunoblotting using lysates from untreated and treated LN-229 control or TGF-$\beta_{1/2}$ siRNA cells (Fig. 8.19).

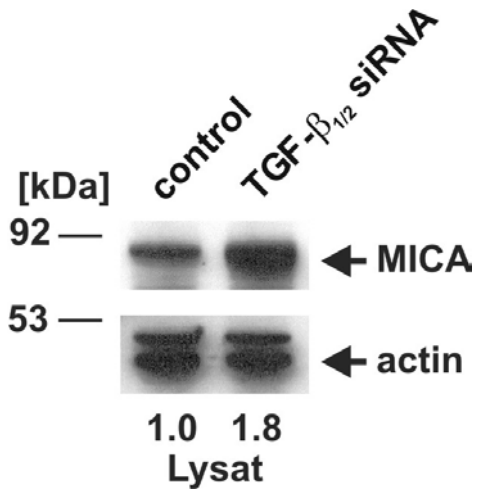

Fig. 8.19. **MICA protein expression is enhanced in lysates from TGF-$\beta_{1/2}$ siRNA cells.** The expression of MICA in cell lysates of LNT-229 control or TGF-$\beta_{1/2}$ siRNA cells was monitored by immunoblot. An actin control was included to verify equal amounts of loaded protein for the cell lysates.

Furthermore, MICA and ULBP2 expression were markedly increased on the cell surface of TGF-$\beta_{1/2}$ siRNA cells by flow cytometry, while MICB, ULBP1 and 3 showed no change in their surface expression levels (Fig. 8.20). A specific mAb against ULBP4 is currently not available, therefore this NKG2DL could not be investigated on protein level.
Importantly, the effects could be diminished by addition exogenous TGF-β_2 (10 ng/ml, 7d), confirming the specificity of the observation (see Fig. 8.20B and data not shown).

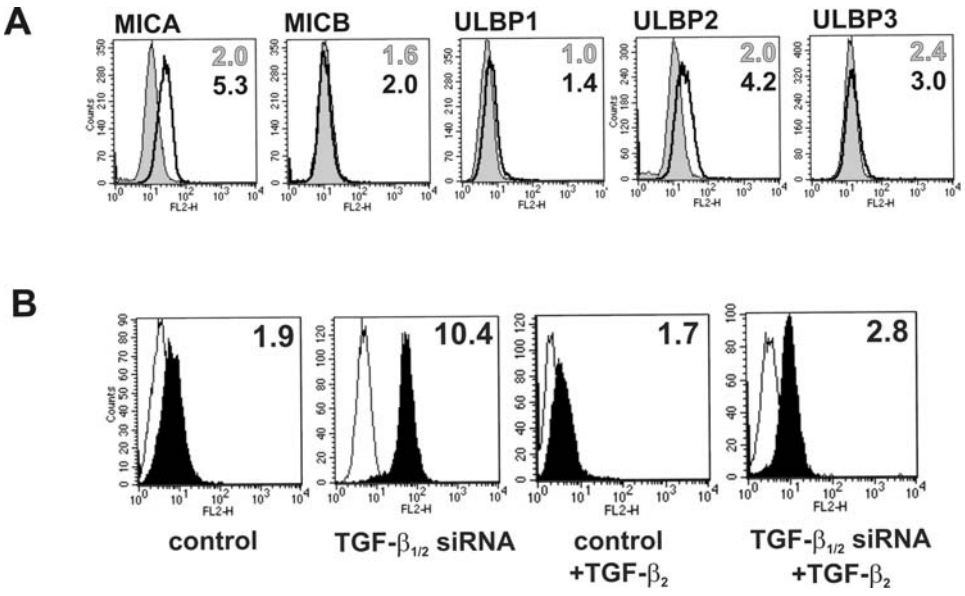

Fig. 8.20. **MICA and ULBP2 surface expression is increased in LNT-229 TGF-$\beta_{1/2}$ siRNA cells.** A. MICA, MICB, ULBP1, 2 and 3 expression at the cell surface of control (closed profiles) and TGF-$\beta_{1/2}$ siRNA cells (open profiles). B MICA expression at the cell surface of control, TGF-$\beta_{1/2}$ siRNA cells untreated or treated with TGF-β_2 (10 ng/ml) for 7 days were analyzed by flow cytometry. SFI values are indicated in the upper right corner.

Real time PCR analysis showed a marked induction of MICA, ULBP2 and ULBP4 mRNA levels in TGF-$\beta_{1/2}$ siRNA cells (Fig. 8.21A). This effect of the knock-down was again reversed by exogenous TGF-β_2 (Fig. 8.21B).

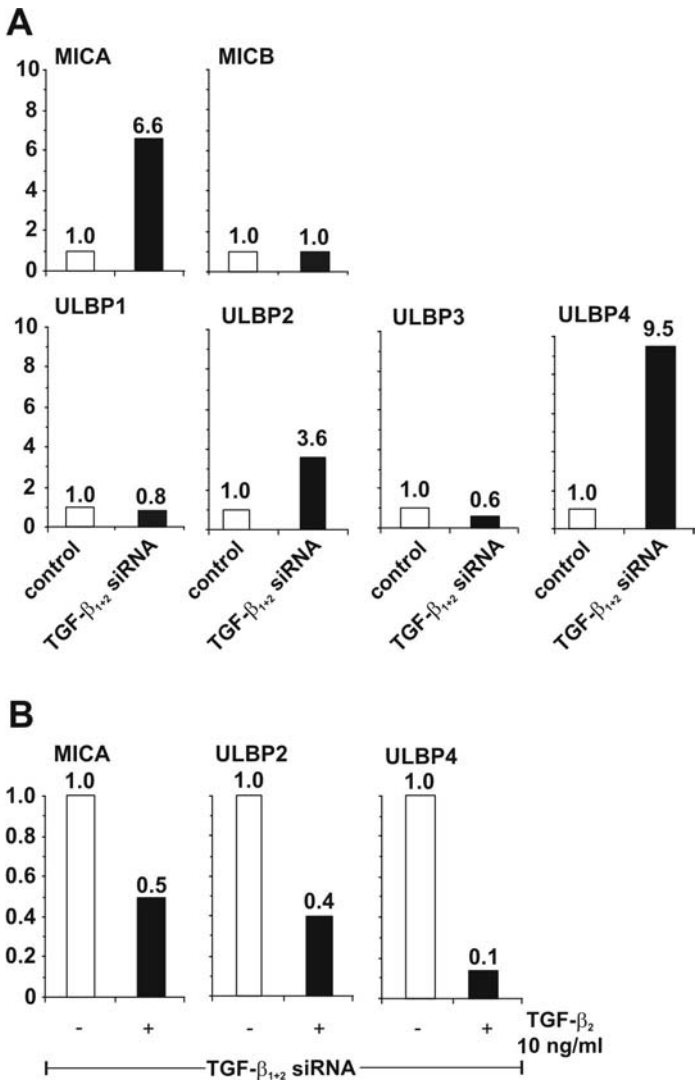

Fig. 8.21. **LNT-229 TGF-$\beta_{1/2}$ siRNA cells shown increased mRNA expression of MICA, ULBP2 and ULBP4.** A. MICA, MICB, ULBP1, 2, 3 and 4 mRNA expression were assessed in control or TGF-$\beta_{1/2}$ siRNA cells by real-time RT-PCR. B. TGF-$\beta_{1/2}$ siRNA cells were treated with TGF-β_2 (10 ng/ml) for 48 h and assessed for MICA, ULBP2 and ULBP4 mRNA expression. Data are expressed as the relative gene expression compared with control transfectants in A or untreated TGF-$\beta_{1/2}$ siRNA cells in B.

The changes in the expression of NKG2D, MICA and ULBP2 resulted in the expected increase in the lysis of TGF-$\beta_{1/2}$ siRNA cells by NKL (data not shown) or polyclonal NK cells (Fig. 8.22). This enhancement of immune-mediated lysis through TGF-$\beta_{1/2}$ "knockdown" could be diminished by blocking antibodies against MICA, ULBP2 or NKG2D or by a

soluble NKG2D receptor. The effects of masking MICA and ULBP2 were found to be additive and to equal the effect achieved by blocking the receptor. Importantly, addition of TGF-β during the 4 h effector phase of the lysis experiment had no significant effect (data not shown).

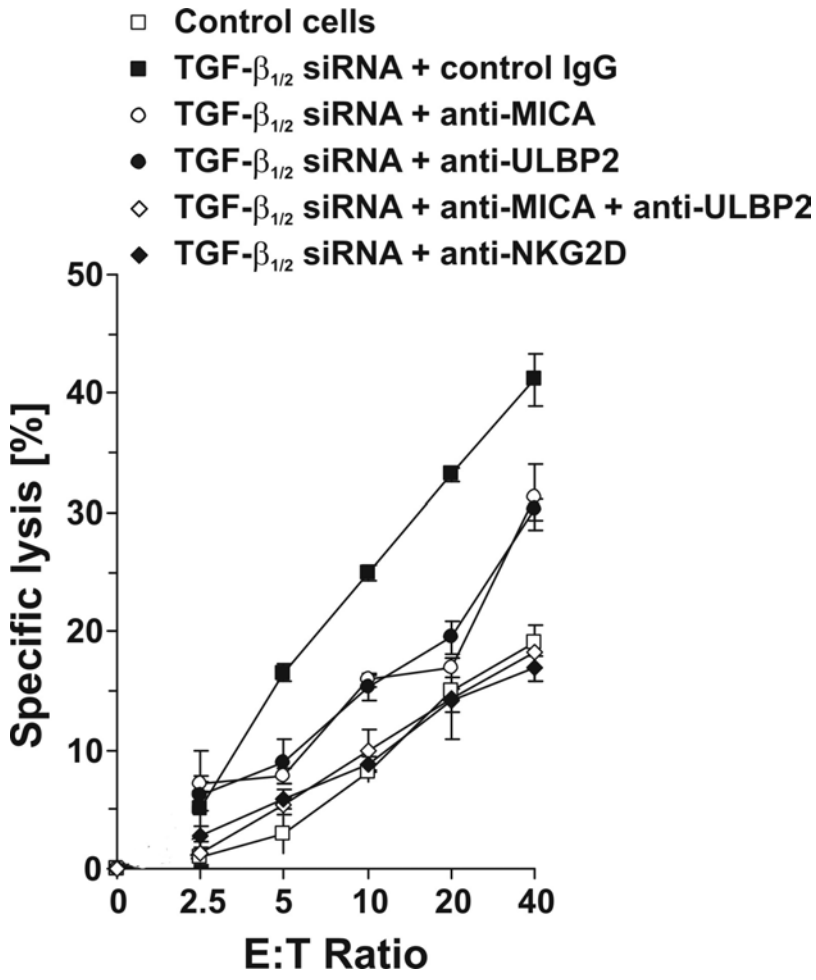

Fig. 8.22. **LNT-229 TGF-$\beta_{1/2}$ siRNA cells are more susceptible to lysis by NK cells.** Control or TGF-$\beta_{1/2}$ siRNA cells (10^4 cells/well) untreated or treated with anti-MICA (AUMO1), anti-ULBP2 (BUMO1) or anti-NKG2D (MAB 139) (10 μg/ml) were used as target cells in a standard 4 h ^{51}Cr release assay using polyclonal NK cells as effectors. Data are expressed as specific lysis at different E:T ratios.

The TGF-β siRNA cells did not only exhibit enhanced immunogenicity, but also an altered intrinsic tumour cell phenotype. Proliferation experiments showed a significant reduction in [^{3}H] thymidine uptake as a measure of proliferation in the TGF-$\beta_{1/2}$ siRNA cells *in vitro* (Fig. 8.23A). Furthermore, migratory and invasive properties were markedly impaired in TGF-$\beta_{1/2}$ siRNA transfectants (Fig. 8.23B).

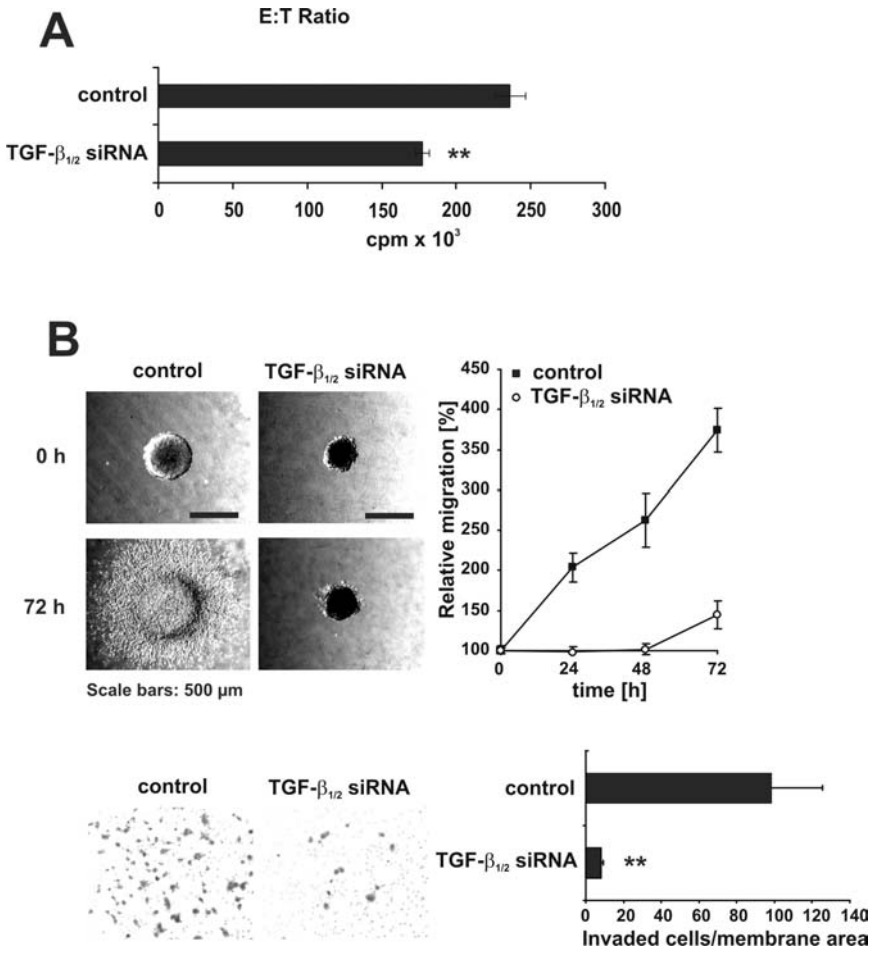

Fig. 8.23. **LNT-229 TGF-$\beta_{1/2}$ siRNA cells proliferate and migrate more slowly than LNT-229 control cells.** A. The growth of control or TGF-$\beta_{1/2}$ siRNA cells was assessed by [^{3}H]-thymidine incorporation, measured in 96 well plates (5000 cells/well) after 48 h (cpm ± SD). B. The migratory and invasive characteristics of LN-229 control and TGF-$\beta_{1/2}$ siRNA cells were examined in a glioma spheroid model (upper panel) and in matrigel invasion assays (lower panel).

TGF-β knock-down in glioma cells: in vivo phenotype.

Subcutaneous and intracerebral glioma xenograft models were used to assess a modulation of the tumorigenicity in TGF-$\beta_{1/2}$ knock-down cells. LNT-229 cells were injected subcutaneously in nude mice which possess NK cells, but lack T cells, and the tumour sizes were measured every two days. Mock transfectants grew rapidly to form compact tumours whereas TGF-$\beta_{1/2}$ siRNA transfectants did show tumour growth between day 3 and 7 before the tumours were rejected (Fig. 8.24).

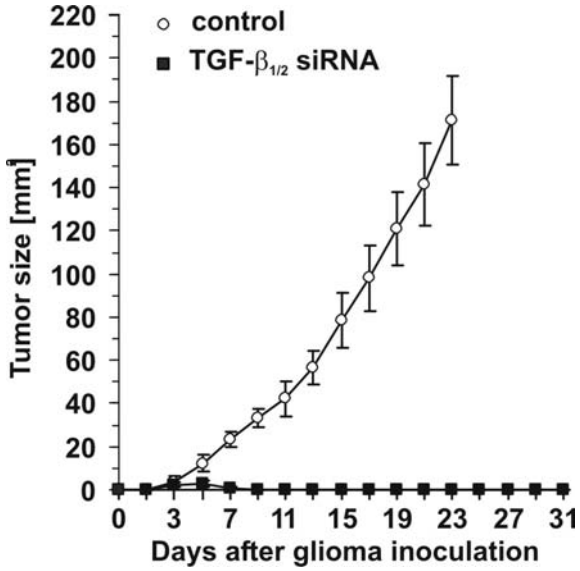

Fig. 8.24. **LNT-229 TGF-$\beta_{1/2}$ siRNA cells do not grow in the periphery of nude mice.** The growth of subcutaneous LNT-229 mock transfectants (control) (open symbols) or TGF-$\beta_{1/2}$ siRNA tumors (black symbols) was monitored every 2 days (mean ± SD, t-test, $*P<0.05$, $**P<0.01$).

When LNT-229 cells were implanted stereotactically into the brains of nude mice, animals carrying mock transfectants developed neurological symptoms and had to be sacrificed at days 34-41. In contrast, animals carrying TGF-$\beta_{1/2}$ siRNA transfectants showed no neurological symptoms after 90 days (Fig. 8.25) (log-rank test, $P<0.01$).

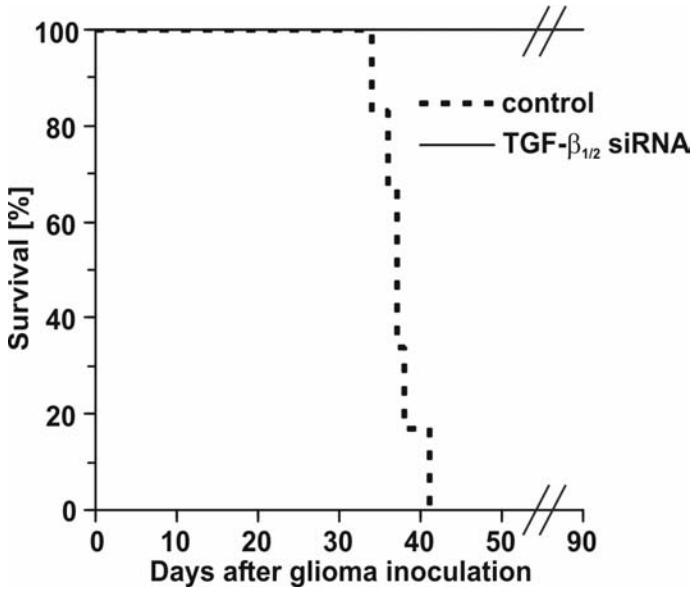

Fig. 8.25. **LNT-229 TGF-$\beta_{1/2}$ siRNA cells are not tumorigenic in nude mice.** LNT-229 control (broken line) or TGF-$\beta_{1/2}$ siRNA cells (solid line) (5×10^4) were inoculated intracerebrally in CD1 nude mice. Survival data for six animals per group are shown, evaluated by the Kaplan-Meier method (log-rank test, $P<0.01$).

NK cells isolated from mice inoculated with the TGF-$\beta_{1/2}$ siRNA-transfected glioma cells showed a substantially enhanced cytotoxic activity against YAC-1 target cells compared with NK cells from animals receiving mock transfectants (Fig. 8.26), suggesting altered NK cell reactivity as a contributing mechanism mediating the anti-tumorigenic effects of RNA interference against TGF-β.

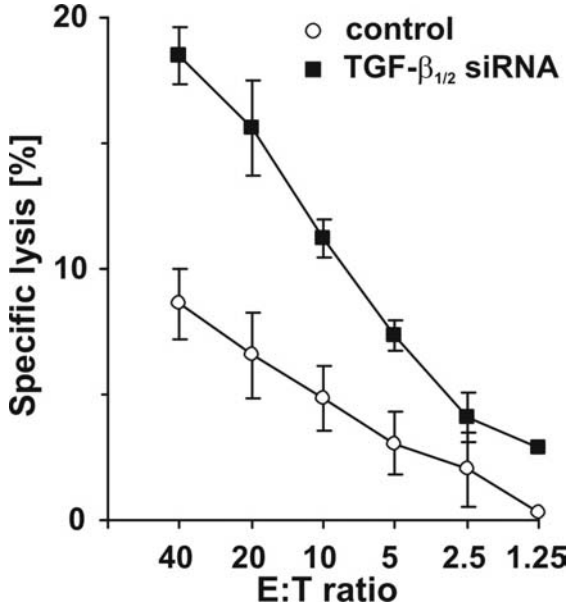

Fig. 8.26. **Inoculation with LNT-229 TGF-$\beta_{1/2}$ siRNA cells enhances NK cell activity in nude mice.** LNT-229 control (broken line) or TGF-$\beta_{1/2}$ siRNA cells (solid line) (5 x 10^4) were inoculated intracerebrally in CD1 nude mice. At day 5, splenocytes were recovered from the differently treated animals. NK cells were isolated and used as effector cells in a ^{51}Cr release assay using YAC-1 cells as targets.

Discussion

Among solid tumours, glioblastoma is paradigmatic for its immune inhibitory properties which involve the expression of cell surface molecules such as HLA-G and CD70 as well as the release of soluble molecules such as TGF-β (155, 261, 382). TGF-β has been considered central to the malignant progression of glial tumours and to the immune dysfunction in human glioblastoma patients (155). Here a novel pathway of immunosuppression mediated by TGF-β is delineated. This involves (i) the down-regulation of NKG2D expression in $CD8^+$ T and NK cells, (ii) the selective down-regulation of NKG2DL MICA, ULBP2 and ULBP4 expression in glioma cells and (iii) the enhanced shedding of the cognate ligand, MICA, from the cell surface in a MMP-dependent manner. By promoting the reduction of NKG2D on immune cells paralleled by the reduction of cell surface MICA expression through enhanced shedding and decreased transcription, glioma cells may efficiently escape innate immune recognition by reducing an induced-self danger signal (89, 426).

The present study builds upon our prior observation of NKG2DL expression by freshly isolated primary glioma cells and of an enhanced immunogenicity of MICA-transduced glioma cells (131) and the novel finding of reduced NKG2D expression in $CD8^+$ T and NK cells of human glioblastoma patients *in vivo* (Fig. 8.1). Although primary glioma cells and long-term glioma cell lines released sMICA into the cell culture SN (Fig. 8.2, 8.3 and Table 1), the sMICA levels in patient sera or CSF were below the detection limit of the ELISA used here. Glioma cell SN was shown to reduce the expression of NKG2D at the surface of $CD8^+$ T and NK cells (Fig. 8.4 and 8.5). However, this effect was not mediated by sMICA released by glioma cells, e.g., via NKG2D binding and subsequent internalization. Importantly, membrane-bound MICA was shown to down-regulate NKG2D expression (Fig. 8.6).

In experiments similar to those excluding a role for sMICA in down-regulating NKG2D expression, recombinant TGF-β mimicked the effects of glioma cell SN on NKG2D expression. Blocking experiments confirmed that TGF-β was the principle molecule within the glioma cell SN mediating the loss of NKG2D in immune cells. Real time PCR indicated that the reduction of NKG2D mediated by TGF-β involved the level of NKG2D gene transcription (Fig. 8.7).

Importantly, the disruption of the MICA/NKG2D recognition system by TGF-β does not only involve the loss of NKG2D expression in effector cells, mediated in a paracrine fashion, but also an autocrine effect of TGF-β on the expression of the cognate ligand, MICA, on the glioma cells. This is because the shedding of MICA from the surface of glioma cells is

mediated by MMP which in turn are under the control of TGF-β. However, suppression of MICA surface levels by TGF-β was not completely antagonized, when MMP activity was inhibited (Fig. 8.13). This may be due to a TGF-β-mediated decrease of MICA mRNA levels (Fig. 8.21). Inhibition via siRNA technology leads to an increase in MICA, ULBP2 and ULBP4 transcription, and suppression in MMP activity, leading to an increase in surface MICA and ULBP2 levels (Fig. 8.17, 8.19 and 8.20). A specific mAb against ULBP4 is currently not available, therefore this NKG2DL could not be investigated on protein level. Interestingly, TGF-β does not impair MICB, ULBP1 and ULBP3 mRNA and cell surface expression (Fig. 8.20 and 8.21). Blocking experiments using polyclonal NK cells as effectors and LNT-229 control or TGF-$\beta_{1/2}$ siRNA transfectants show that MICA and ULBP2 have additive functions in triggering NKG2D, indicating that an anti-tumour immune response depends on the expression level of each NKG2DL at the cell surface of transformed or infected cells. Importantly, the effect of blocking both MICA and ULBP2 equalled that of blocking the receptor (Fig. 8.22). Further, blocking of MICA also inhibited lysis by NKL cells (data not shown). These observations suggest a prominent role for the NKG2DL, MICA and ULBP2 in glioma immune surveillance, while the other ligands may exert their immune-stimulatory functions under different conditions.

SN of TGF-$\beta_{1/2}$ siRNA transfectants does not confer down-regulation of NKG2D in immune effector cells, supporting the importance of TGF-β in down-regulating NKG2D (Fig. 8.18). Consequently, either reducing TGF-β bioavailability, or MMP expression or activity, or their combination are suitable means to enable the immune cell-mediated lysis of glioma cells. An inhibition of MMP activity by TGF-β antagonism does also interfere with other aspects of malignancy such as proliferation, migration and invasiveness (Fig. 8.23) (427). Altogether, the significance of these biological effects of TGF-β were corroborated by the observation of a loss of tumorigenicity *in vivo* and enhanced NK cell activation when TGF-β_1 and TGF-β_2 gene expression were impaired using siRNA technology (Fig. 8.24-26).

The general importance for TGF-β as a mediator of impaired antitumour immune surveillance is no more disputed. The analysis of T cells expressing a dominant negative TGF-β-RII transgene confirmed an inhibitory role of TGF-β in the generation of antitumour $CD8^+$ T cell responses (428). Such mechanisms might involve effects of TGF-β on co-stimulatory signals using NKG2D as the target molecule (Fig. 8.15). Of note, the highly lethal nature of glioblastoma suggests that the levels of NKG2D expressed by immune cells or of activating NKG2DL expressed by glioma cells in the current clinical setting are too low to induce anti-

tumour immunity. Previous studies had already indicated that the activation potential for immune cells depends on the level of NKG2DL expression on glioma cells (131). Further, the inhibitory receptor CD94/NKG2A is induced by TGF-β and may thus potentiate the NK and $CD8^+$ T cell inhibition by glioma cells (429). TGF-β also reduces the expression of the NK cell activatory receptor, NKp30 (194). Collectively, these observations confirm that TGF-β is central to the malignant progression of glial tumours and a principle target for the treatment of gliomas (155). Anti-TGF-β therapies may therefore not only relieve the immune dysfunction in human glioblastoma patients, but also inhibit MMP-activity and restore MICA, ULBP2 and ULBP4 expression to the levels required for an effective anti-glioma immune response.

Summary

Our improved understanding of cancer biology has helped to establish criteria that appear to be prerequisites for tumour formation by transformed cells (430). Cancer cells must (i) be able to grow autonomously, (ii) develop insensitivity to negative growth regulation, (iii) display unlimited replicative potential, (iv) develop the capacity for angiogenesis, (v) develop competence for invasive growth and metastasis and (vi) evade intrinsic apoptotic signals. A further emerging precondition for the malignant phenotype *in vivo* is the capacity of a malignant cell to evade the extrinsic tumour suppressor functions of the immune system (154).

Glioma cells display all of these "hallmarks of cancer". Their intrinsic resistance to apoptosis and their immunosuppressive properties (**chapter 1**) have been analyzed in our laboratory (155, 431) and were also the main topics explored in my Ph.D. work.

p53 is a potent activator of the intrinsic apoptotic pathway. It represents an ideal target for anti-cancer drug design, since it is mutated in more than half of human tumours. Most of the remaining tumours, although carrying wild-type p53, have defects in the p53-mediated apoptotic pathway. Unlike most other tumour suppressor genes, mutant p53 is overexpressed in tumour cells. Therefore it can function as a tumour antigen (432-434). However, the approach that was investigated here (**chapter 2**) aimed at restoring a tumour-suppressor function in mutant p53 variants. CP-31398 is a prototype small molecule that stabilizes the active conformation of p53 and promotes p53 activity in cancer cell lines with mutant or wild-type p53 (19). CP-31398 was found to induce p53-like activity in all of 11 glioma cell lines harbouring wild-type or mutant p53, but not in p53 null LN-308 cells. However, upon prolonged exposure to CP-31398, all glioma cell lines, irrespective of their p53 status, undergo caspase-independent cell death displaying some characteristics of apoptosis. Posttranscriptional repression of p53 by an intracellularly transcribed siRNA as well as analysis of p53 transgenes in p53-deleted glioma cells allowed to delineate two pathways of CP-31398-induced cell death: an early, p53-dependent pathway that requires new p53 protein synthesis and a late, p53-independent pathway characterized by calcium release and epiphenomenal free radical formation. These observations point out some of the liabilities of CP-31398 as a prototype p53-based therapeutic and define a rationale for the further refinement of small molecules which specifically target the p53 pathway, but lack the p53-independent effects. At the current stage of development, CP-31398 has promising effects on

mutant and wild-type p53 in cancer cell lines, but its strong p53-independent side effects are likely to prevent its use in the clinic.

Surprisingly, posttranscriptional repression of p53 by an intracellularly transcribed siRNA in a p53 mt cell line resulted in the induction of a low, but detectable p53-like reporter gene activity. This observation prompted us to investigate the specificity of Stratagene´s p53 *PathDetect* reporter plasmid **(chapter 3)**, a widely used luciferase-coupled reporter gene for the detection of the transcriptional activity of p53. Both p63 and p73 were found to activate the promoter sequence contained in the p53-luc vector. This shows that data obtained using this system (or any similar one) should be interpreted with caution because they may not actually reflect p53 activity, but rather provide an integrated signal derived from different members of the p53 family. However, this does not seriously challenge the reporter gene data obtained with CP-31398, since a net effect of CP-31398 on p53, p63 and p73 is a physiologically perfectly sensible measure of CP-31398-dependent p53-related activity. In fact, treatment of glioma cells with CP-31398 also increases the cellular level of p73, while p63 is absent from most glioma cell lines (data not shown). Further, the potency of CP-31398 as an inducer of apoptosis may even be enhanced by a cooperative effect on further members of the p53 protein family (176).

Whereas in glioma cells CP-31398 activates an intrinsic, caspase-independent cell death pathway, the extrinsic or death receptor mediated apoptotic pathway may also potentially be exploited for an anti-cancer therapy, since the distribution of death receptors found on tumour cells apparently differs from that found on non-transformed cells. Further, the signalling originating from these receptors may be different in tumour cells. This has been described for CD40 (246), one of several members of the TNFR family that lack a death domain and yet can induce apoptosis (183, 435, 436). Physiologically, CD40 transduces antiapoptotic signalling in B and T cells whereas CD40-mediated apoptosis appears to be restricted to transformed cells (183, 246). Therefore adverse effects like the massive hepatotoxicity of CD95/FasL (179) are unlikely to occur with CD40. Instead, ligation of CD40 can induce antitumour immunity *in vivo* in mice (148, 185, 276, 437). CD40 is expression was detected in all of 12 human glioma cell lines (**chapter 4**), even though in most cell lines the expression seems to be mainly intracellular. In contrast to various non-glial carcinoma cell lines, CD40-expressing glioma cells resist cytotoxic effects of CD40L. Resistance to CD40L-induced cell death has been described as the result of CD40 downregulation during long-term culture (285). CD40

gene transfer into LN-18 glioma cells induces (or restores?) susceptibility to cell death by soluble CD40L. Similar to CD95L- or Apo2L/TRAIL-induced apoptosis, CD40-dependent cell death is potentiated by CHX and involves receptor clustering and caspase 8 and 3 processing. Surprisingly, CD40-transfected LN-18 cells acquire resistance to CD95L, resulting from the down-regulation of CD95 expression via a posttranslational, proteasome inhibitor-sensitive mechanism. In contrast, subtoxic concentrations of CD40L strongly sensitize these cells for TNF-α-induced apoptosis via a mechanism involving intracellular crosstalk between CD40 and TNF-R1 (p55). This suggests complex patterns of modulation of death receptor-mediated glioma cell apoptosis by CD40/CD40L interactions. Further, bispecific CD40xCD95, but not CD20xCD95, antibodies kill glioma cells, disclosing the property of endogenous CD40 to facilitate death signalling. However, the data obtained on CD40 in glioma cells do not strongly support a therapeutical application of CD40L as an inducer of apoptosis. On the other hand, CD40L had no stimulatory or antiapoptotic effects on glioma cells and could therefore be used as an adjuvant in a potential anti-glioma immunotherapy.

Another TNFR-related cell surface receptor implicated in T, B and NK cell activation (311, 438, 439) as well as in apoptosis (49, 333) is CD27. The ligand for CD27, CD70 was identified as a radio-inducible gene in U87MG glioma cells (**chapter 5**). A screening of a panel of human glioma cell lines revealed that 11 of 12 cell lines expressed CD70 mRNA and protein. CD70 protein was also detected by immunocytochemistry in 5 of 12 glioblastomas and 3 of 4 anaplastic astrocytomas *in vivo*. CD27 expression was not detected in any glioma cell line, and there was no evidence for autocrine or backward signalling of the CD70 system in human glioma cells. Unexpectedly, CD70 expressed on glioma cells did not increase the immunogenicity of glioma cells *in vitro*. In contrast, CD70-positive glioma cells induced apoptosis in PBMC in a CD70-dependent manner. Neutralization of CD70 expressed on glioma cells prevented apoptosis and enhanced the release of TNF-α in cocultures of glioma cells and PBMC. The effects of CD70-expressing glioma cells on PBMC were mimicked by agonistic CD27 antibodies. Conversely, the shedding of CD27 by PBMC was identified as a possible escape mechanism from glioma cell-induced CD70-dependent apoptosis. Thus, induction of B cell and T cell apoptosis via interactions of CD70 expressed on glioma cells and CD27 expressed on B and T cells may be a novel way for the immune escape of malignant gliomas.

Our *in vitro* results are in contrast to *in vivo* experiments describing CD27-mediated tumour rejection (329, 440). Further, a study using CD27 knockouts (312) supports a role for CD27 in costimulation. However, chronic stimulation via CD70 as occurs in CD70 transgenic mice results in B cell depletion and lethal T cell immunodeficiency (313, 314). Further, the immune system of glioma patients does not reject CD70-expressing tumours *in vivo*. Instead, the high proportion of CD70-positive gliomas found in this and a related (325) study suggests that there may rather be a selection pressure operating in favour of CD70-expressing glioma cells. These apparently contradictory data suggest that CD27 may be functioning *in vivo* together with other receptors that determine the outcome of CD27 stimulation. Thus CD27 may signal either activation or apoptosis, depending on the context. Given the capability of glioma cells to paralyse anti-tumour immune reactions (294), it is well conceivable that the stimulatory pathways originating from CD27 are inhibited in glioma patients whereas the pathway leading to T cell apoptosis may be enforced.

One newly discovered mechanism by which glioma cells apparently inhibit anti-tumour T cell responses is expression and secretion of HLA-G molecules (**chapter 6**). HLA-G is a nonclassical MHC molecule with highly limited tissue distribution that has been implicated in foetal semi-allograft tolerance during pregnancy (342, 345). To delineate the potential role of HLA-G in glioblastoma immunobiology, expression patterns and functional relevance of this MHC class Ib molecule were investigated in glioma cell lines and brain tissue. HLA-G protein was detected in 4 of 12 cell lines in the absence, and in 8 out of 12 cell lines in the presence of IFN-γ. Immunohistochemical analysis of human brain tumours revealed expression of HLA-G in 4 of 5 tissue samples. Functional studies showed that expression of membrane-bound HLA-G1 and soluble HLA-G5 inhibited alloreactive and antigen-specific immune responses. However, HLA-G dependent T cell apoptosis was not detected (353). Gene transfer of HLA-G1 or HLA-G5 into HLA-G-negative glioma cells rendered these cells highly resistant to direct alloreactive lysis, inhibited the alloproliferative response and prevented efficient priming of cytotoxic T cells. The inhibitory effects of HLA-G were directed against $CD8^+$ and $CD4^+$ T cells, but appeared to be NK cell-independent. Interestingly, few HLA-G-positive cells within a population of HLA-G-negative tumour cells exerted significant immune inhibitory effects. These data suggest that aberrant expression of HLA-G may contribute to immune escape in human glioblastoma.

A long-established determinant of glioblastoma-induced immunosuppression is the cytokine TGF-β (155, 192, 417). However, TGF-β does not only compromise anti-tumour immune responses and induce T cell apoptosis (441), but also stimulates angiogenesis and invasion (193, 330, 415, 442). Therefore, TGF-β has become a major target for the experimental treatment of human malignant gliomas (443). The effects of TGF-β on NKG2D-mediated anti-tumour immunity (131, 406, 444) were investigated (**chapter 8**). NKG2D is an activating immunoreceptor expressed by NK, $CD8^+$ αβ and γδ T cells. Human NKG2DL comprise MHC class I-chain related molecules A (MICA) and MICB and UL16-binding proteins (ULBP) 1, 2, 3, and 4. These ligands are expressed by infected and transformed cells and transmit danger signals to immune cells, leading to the lysis of NKG2DL-expressing cells. An effect of TGF-β on the expression of the activating immunoreceptor NKG2D in $CD8^+$ T and NK cells has been shown by us and others *in vitro* (194, 445). Accordingly, a downregulation of NKG2D is also observed in glioblastoma patients *in vivo*. Moreover, TGF-β inhibits the transcription of the NKG2D ligands MICA, ULBP2 and ULBP4 and reduces their protein level at the cell surface. In contrast, MICB, ULBP1 and ULBP3 are unaffected by TGF-β. Further, TGF-β promotes the release of matrix metalloproteinases (MMP) by glioma cells which in turn mediate the shedding of MICA from the surface of glioma cells. siRNA-mediated "knock-down" of TGF-β synthesis in LN-229 glioma cells suppresses MMP expression and strongly enhances the immunogenicity of glioma cells by enhancing MICA, ULBP2 and ULBP4 expression and by preventing NKG2D down-regulation on immune cells treated with glioma cell SN. Further, the TGF-β knock-down leads to a decreased migratory and invasive tumour phenotype. Altogether, the knock-down of TGF-β results in a glioma cell phenotype which is less motile, more sensitive to immune cell lysis, and non-tumorigenic in nude mice. These data define downregulation of NKG2D expression on immune effector cells and of NKG2DL expression on glioma cells as a further mechanism by which TGF-β may promote immune escape.

This confirms the importance of TGF-β as a principle inhibitor of anti-glioma immune responses. Strategies to counteract the immunosuppressive activities of TGF-β may be crucial to improve the current cancer immunotherapeutic approaches. In this context, a novel TGF-βRI kinase inhibitor, SD-208, was characterized for its effects on the growth and immunogenicity of murine SMA-560 and human LN-308 glioma cells *in vitro* and the growth of, and immune response to, intracranial SMA-560 gliomas in syngeneic VM/Dk mice *in vivo* (**chapter 7**). SD-208 blocks autocrine and paracrine TGF-β signalling in glioma cells as

detected by phosphorylation of Smad2 or TGF-β reporter assays and strongly inhibits constitutive and TGF-β-evoked migration and invasion. PBL or purified T cells, cocultured with TGF-β-releasing LN-308 glioma cells in the presence of SD-208, exhibit enhanced lytic activity against LN-308 targets. The release of IFN-γ and TNF-α by these immune effector cells is enhanced by SD-208 whereas the release of IL-10 is reduced. SD-208 restores the lytic activity of polyclonal NK cells against glioma cells in the presence of recombinant TGF-β or TGF-β-containing glioma cell SN. The oral bioavailability of SD-208 was verified by demonstrating the inhibition of TGF-β-induced Smad phosphorylation in spleen and brain. Systemic SD-208 treatment initiated three days after the implantation of SMA-560 cells into the brains of syngeneic VM/Dk mice prolongs their median survival from 18.6 to 25.1 days. Importantly, SD-208 could be administered together with adjuvant chemotherapy or an immunotherapeutic vaccine. Such a combined treatment might further improve the effect achieved by SD-208 alone. Thus, TGF-βRI kinase inhibitors such as SD-208 are promising novel agents for the treatment of human malignant glioma and other conditions associated with pathological TGF-β activity.

In my Ph.D. research I have thus explored several novel approaches aiming at the selective induction of apoptosis in glioma cells and at an improved understanding of the immune-paralysing capacities of glioma cells. While the connections between these various aspects of glioma biology may not be apparent at first sight, there are good reasons for taking a combined look at apoptosis and tumour immunology: Tumour immunosurveillance is mediated by immune effector cells that selectively induce apoptosis in cancer cells. Activated T and NK attack their targets by expression death ligands (446, 447) and by secretion cytotoxic granules (88, 406) and thus seek to activate both the death receptor and the intracellular apoptotic pathway. An apoptosis-resistant target cell is therefore less susceptible to immune-mediated lysis. Sensitization of tumour cells for apoptotic stimuli could therefore enhance the efficacy of ongoing anti-tumour immune responses. Further, the tumour may strike back and induce apoptosis in tumour infiltrating lymphocytes by various mechanisms, including the expression of CD95/FasL, HLA-G, TGF-β (262, 353, 441, 448, 449) and, under specific circumstances, CD70 (see section 5). Prevention of tumour cell-induced apoptosis of immune effector cells could also support endogenous anti-tumour responses. Finally, therapeutic induction of apoptosis in tumour cells is thought to provide a source of antigens that can be taken up and presented by professional APC, resulting in an anti-tumour immune response (68-71, 450). This, of course, implies that the low rates of spontaneously occurring apoptosis *in vivo* (451)

are simply insufficient to trigger an anti-glioma immune response. Further, the mounting of a productive anti-tumour immune response may be prevented by immune-inhibitory signals sent out by the tumour itself. Therefore, an apoptosis-based reduction of large tumour masses may require the simultaneous relief of tumour-dependent immunosuppression in order to be followed by a productive immune response that can finally clear residual glioma cells dispersed in the brain.

Whether the emerging concepts outlined in this Ph.D. thesis have the potential to improve current glioma treatments will, of course, have to be explored in further models. Thus, the present work finally confirms George Bernard Shaw's notion: "Science... never solves a problem without creating ten more."

Zusammenfassung

Gliomzellen zeichnen sich durch Resistenz gegenüber apoptotischen Stimuli aus. Die Überwindung dieser intrinsischen Apoptose-Resistenz ist daher ein wichtiges Ziel der Gliomforschung. Therapeutische Induktion von Apoptose in Tumorzellen führt *in vivo* zur Bereitstellung von antigenem Tumorzellmaterial. Dieses kann von dendritischen Zellen aufgenommen und präsentiert werden, sodass eine anti-Tumor-Immunantwort ermöglicht wird. Allerdings verfügen Gliomzellen über eine Reihe immuninhibitorisch wirksamer Mechanismen, die eine Tumorabstoßung verhindern. Zudem stellt die Apoptose-Resistenz von Gliomzellen auch für einen immuntherapeutischen Ansatz ein Hindernis dar, da immun-vermittelte anti-Tumor-Effekte ebenfalls auf der (durch NK und T Zellen vermittelten) Induktion von Apoptose in Krebszellen beruhen. Darüber hinaus können Immunzellen bei Kontakt mit Gliomzellen ebenfalls apoptotisch werden. Daher befasst sich diese Arbeit mit den zellbiologischen Prinzipien des programmierten Zelltods (Apoptose) in Gliomzellen sowie mit den wechselseitigen Beziehungen zwischen Immuneffektorzellen und Gliomzellen, ebenfalls unter besonderer Berücksichtigung der Apoptose.

Ein interessantes Agens zur Induktion von Apoptose in Tumorzellen ist das experimentelle Pharmakon CP-31398, das von der Firma Pfizer in den USA mit dem Ziel der Wiederherstellung funktioneller Aktivität in mutanten p53-Proteinen entwickelt wurde. Zur Charakterisierung dieser Substanz wurde unter Zuhilfenahme verschiedene Gentransfer-Techniken ein p53-abhängiger und ein p53-unabhängiger Zelltodweg charakterisiert, die beide durch CP-31398 aktiviert werden. Somit erwies sich CP-31398 als interessante, für den klinischen Gebrauch auf Grund unspezifischer Effekte jedoch nicht hinreichend weit entwickelte Substanz. Die erzielten Ergebnisse könnten aber für die Entwicklung verbesserter p53-modulierender anti-Tumor-Agenzien von Bedeutung sein. Im Rahmen dieser Untersuchungen stellte sich heraus, dass klassische Reporter-Assays für transkriptionelle p53-Aktivität nicht ausschließlich die Aktivität von p53 reflektieren, sondern ein umfassendes Bild der Gesamt-Aktivität von p53, p63, p73 und möglicherweise weiterer, noch nicht bekannter Mitglieder dieser Proteinfamilie liefern. Aufgrund dieses Befundes müssen zahlreiche bisher mit derartigen Reporter-Assays publizierte Daten neu interpretiert werden.

In Ergänzung zu CP-31398, das auf die Aktivierung des intrinsischen apoptotischen Mechanismus abzielt (und in Gliomzellen Caspasen-unabhängigen Zelltod induziert), wurde auch der extrinsische oder rezeptor-vermittelte Apoptosemechanismus untersucht. Die

bekannten Todesrezeptoren gehören zur Familie der Tumor-Nekrose-Faktor (TNF)-Rezeptoren, die auch bei Immunreaktionen eine wichtige Rolle spielen. Da sich das Expressionsmuster dieser Rezeptoren auf Tumorzellen von demjenigen auf nicht-transformierten Zellen unterscheidet, bieten Todesrezeptoren potentielle therapeutische Angriffspunkte. Systemische Aktivierung des CD95/Fas-Rezeptors führt aber in Mäusen zu Leberversagen und auch die gegenwärtig verfügbaren Präparationen von Apo2L/TRAIL sind klinisch nicht einsetzbar oder ineffektiv. CD40L vermag nach dem bisherigen Kenntnisstand nur in transformierten Zellen Apoptose zu induzieren, was auf eine veränderte Signaltransduktion in Tumorzellen hindeutet. Zudem ist CD40L bereits in immuntherapeutischen Studien klinisch erprobt. Daher wurde im Kontext dieser Arbeit erstmals die Expression und funktionelle Bedeutung von CD40 auf Gliomen untersucht. Dabei wurde CD40-Expression auf allen 12 untersuchten Gliomzelllinien sowie *in vivo* nachgewiesen. Dennoch wurden keine zytotoxischen Effekte von CD40L auf Gliomzelllinien beobachtet. Da bei Tumoren eine Herunterregulation der CD40-Expression im Verlauf von Langzeit-Kulturen beschrieben ist, wurde eine CD40-überexprimierende Gliomzelllinie generiert. In dieser induziert CD40L Caspasen-abhängigen Zelltod, der durch Hemmung der Proteinbiosynthese potenziert wird. Gleichzeitig kommt es zu einem verstärkten proteasomalen Abbau von CD95/Fas, wodurch die Zellen ihre Sensitivität gegenüber CD95/Fas-vermittelter Apoptose weitgehend verlieren. TNF-α-abhängige Apoptose wird hingegen durch subtoxische Konzentrationen von CD40L verstärkt, was durch eine neu entdeckte intrazelluläre Wechselwirkung zwischen CD40 und TNF-R1 (p55) erklärt werden kann. Schließlich wurde gezeigt, dass die endogene CD40-Expression von Gliomzellen dazu benützt werden kann, Apoptose mittels eines bispezifischen CD40xCD95 Antikörpers zu induzieren. Somit wurden in diesem Teil der Arbeit komplexe Wechselwirkungen zwischen CD40 und verschiedenen anderen TNF-Rezeptoren nachgewiesen.

Ein weiteres Molekül der TNF-Rezeptor-Familie ist CD27, dessen Ligand CD70 im Rahmen einer Array-Analyse als radio-induzierbares Gen in U87MG-Gliomzellen identifiziert wurde. Dieser Befund war überraschend, weil CD70-Expression bisher lediglich auf T- und B-Zellen nachgewiesen worden war. Während CD70/CD27-Interaktionen dort immunstimulatorisch wirkt (T, B und NK Zell-Aktivierung), zeigten umfangreiche immunologische Versuche, dass die Expression von CD70 auf Gliomen CD27-vermittelte Apoptose in Immuneffektorzellen zu induzieren vermag und somit möglicherweise zur Immuninhibition bei

Gehirntumorpatienten beiträgt. Als potentieller Schutzmechanismus wurde die Abspaltung von löslichem CD27 von Immunzellen beobachtet.

Ein bereits bekannter Mediator der Immuninhibition in der Plazenta und bei Tumoren ist HLA-G, dessen funktionelle Relevanz auf Gliomen erstmals untersucht wurde. Dabei gelang der Nachweis der Expression *in vitro* und *in vivo* sowie die Charakterisierung einer Reihe T Zell-vermittelter immunsuppressiver Effekte: So wird sowohl die durch allogene Gliomzellen induzierte Proliferation als auch die direkte allogene und die antigen-spezifische Lyse nach Stimulation mit bestrahlten Tumorzellen durch lösliches und membranständiges HLA-G inhibiert. Interessanterweise genügt auch in Abwesenheit von löslichem HLA-G ein relativ geringer Anteil HLA-G positiver Tumorzellen, um einen Schutz der benachbarten HLA-G negativen Gliomzellen zu vermitteln.

Neben diesen hier erstmals bei Gliomen beschriebenen Mediatoren der tumor-induzierten Immunsuppression wurden auch noch Untersuchungen zu TGF-β durchgeführt, das bereits 1987 von Adriano Fontana als „glioblastoma derived T cell suppressive factor“ identifiziert wurde. Insbesondere wurden die Effekte von TGF-β auf NKG2D und die zugehörigen Liganden untersucht. NKG2D ist ein aktivatorischer Rezeptor, der auf NK, $CD8^+$ αβ und γδ T Zellen exprimiert wird. TGF-β supprimiert die NKG2D-Expression auf NK und $CD8^+$ T Zellen. Klinisch korreliert dies mit einer verringerten NKG2D-Expression bei Gliompatienten. Die NKG2D Liganden MICA/B (MHC class I-chain related molecule A/B) und ULBP1-4 (UL16-binding proteins 1-4) werden selektiv von infizierten und von transformierten Zellen exprimiert und können die immunvermittelte Lyse dieser Zellen induzieren. Anhand von TGF-$\beta_{1,2}$ siRNA-Zellen, in denen die Expression von TGF-β1 und 2 durch plasmidbasierte RNA-Interferenz inhibiert ist, konnte gezeigt werden, dass TGF-β nicht nur die Expression des NKG2D-Rezeptors, sondern auch die mRNA und Protein-Expression der NKG2D-Liganden MICA, ULBP2 und ULBP4 inhibiert, während sich kein Effekt auf MICB, ULBP1 und ULBP3 zeigte. Zudem fördert TGF-β die Freisetzung der Matrix Metalloproteinasen MMP-2 und MMP-9 (nicht von MT1-MMP), die wiederum die Abspaltung von MICA von der Zelloberfläche vermitteln, sodass es auch noch einen posttranslationalen Effekt von TGF-β auf NKG2D-vermittelte anti-Tumor Immunreaktionen gibt. Zudem führt der „knock-down“ von TGF-β zum Verlust des migratorischen und invasiven Potentials der Tumorzellen, vermutlich ebenfalls aufgrund der Herunterregulation der Matrix Metalloproteinasen. Die geringere Motilität und die erhöhte Immunogenität der

„TGF-β knock-down Zellen“ führt zu einem Phänotyp, der in Nacktmäusen nicht mehr tumorigen ist.

Diese Daten zeigen bisher unbekannte Wechselwirkungen zwischen TGF-β und dem NKG2D Signalweg und belegen somit die Bedeutung von TGF-β als einem zentralen Molekül der Immunsuppression bei Gliomen. Anti-TGF-β-Strategien könnten daher therapeutische Bedeutung erlangen. In diesem Zusammenhang wurde die Wirksamkeit von SD-208, einem neuen TGF-βRI Kinase Inhibitor, auf Wachstum und Immunogenität von murinen SMA-560 und humanen LN-308 Gliomzellen untersucht. SD-208 blockiert die autokrine und die parakrine TGF-β Signaltransduktion in Gliom- und Immunzellen, wie über die Phosphorylierung von Smad2 und die Induktion TGF-β abhängiger Reportergene nachgewiesen wurde. Zudem wird die TGF-β-abhängige Migration und Invasion von Gliomzellen gehemmt. Die allogene Lyse von Gliomzellen durch restimulierte humane Lymphozyten wird durch SD-208 erhöht, zudem sezernieren mit Gliomzellen kokultivierte T Zellen in Gegenwart von SD-208 mehr IFN-γ und TNF-α und weniger IL-10. Zudem kann SD-208 die durch Zugabe von Gliomzellüberstand bewirkte Inhibition polyklonaler NK Zellen aufheben. Die orale Bioverfügbarkeit von SD-208 wurde durch einen phospho-Smad2-ELISA aus Milz und Gehirn TGF-β behandelter Mäuse nachgewiesen. Systemische Behandlung von VM-Dk Mäusen mit SD-208 verlängert das mediane Überleben der Mäuse nach intrakranieller Inokulation mit syngegen SMA-560 Gliomzellen von 18.6 auf 25.1 Tage. Dieser therapeutische Effekt liesse sich durch geeignete Kombinationen mit adjuvanter Chemo- oder Immuntherapie möglicherweise noch verbessern. Somit stellen TGF-βRI Kinase Inhibitors wie SD-208 vielversprechende neue Therapeutika für die Behandlung von malignen Gliomen und anderen TGF-β-abhängigen Erkrankungen dar.

Somit könnten einzelne der im Rahmen dieser Dissertation zusammengefassten Projekte Grundlagen für neue, molekular definierte Therapieansätze bei Gliomen liefern. Bis zu einer klinischen Anwendung der hier vorgestellten Konzepte müssen die immun-inhibitorischen Eigenschaften von Gliomzellen noch weiter erforscht und insbesondere klinisch einsetzbare Agenzien für eine kombinierte Apoptose-Immuntherapie entwickelt werden.

References

1. A. Behin, K. Hoang-Xuan, A. F. Carpentier and J. Y. Delattre. 2003. Primary brain tumours in adults. *Lancet* 361:323-331.
2. P. Kleihues and W.K. Cavenee. 2000. Pathology and Genetics of Tumours of the nervous system. IARC Press, Lyon.
3. J. Hildebrand, O. Dewitte, P. Y. Dietrich and N. De Tribolet. 1997. Management of malignant brain tumours. *Eur Neurol* 38:238-253.
4. M. Weller and D.G.T. Thomas. 2003. Primary tumours of the central and peripheral nervous system. In: Course and Treatment of Neurological Disorders. C.L. Brandt T, Dichgans J, Diener HC, Kennard C, editor. Academic Press, San Diego, CA, USA. 827-863.
5. L. M. DeAngelis. 2001. Brain tumours. *N Engl J Med* 344:114-123.
6. L. A. Stewart. 2002. Chemotherapy in adult high-grade glioma: a systematic review and meta-analysis of individual patient data from 12 randomised trials. *Lancet* 359:1011-1018.
7. D. Schiff and M. E. Shaffrey. 2003. Role of resection for newly diagnosed malignant gliomas. *Expert Rev Anticancer Ther* 3:621-630.
8. R. D. Kortmann, B. Jeremic, M. Weller, L. Plasswilm and M. Bamberg. 2003. Radiochemotherapy of malignant glioma in adults. Clinical experiences. *Strahlenther Onkol* 179:219-232.
9. M. Garcia-Barros, F. Paris, C. Cordon-Cardo, D. Lyden, S. Rafii, A. Haimovitz-Friedman, Z. Fuks and R. Kolesnick. 2003. Tumour response to radiotherapy regulated by endothelial cell apoptosis. *Science* 300:1155-1159.
10. L. M. DeAngelis, P. C. Burger, S. B. Green and J. G. Cairncross. 1998. Malignant glioma: who benefits from adjuvant chemotherapy? *Ann Neurol* 44:691-695.
11. L. M. DeAngelis. 2003. Benefits of adjuvant chemotherapy in high-grade gliomas. *Semin Oncol* 30:15-18.
12. J. N. Rich and D. D. Bigner. 2004. Development of novel targeted therapies in the treatment of malignant glioma. *Nat Rev Drug Discov* 3:430-446.
13. P. S. Mischel and T. F. Cloughesy. 2003. Targeted molecular therapy of GBM. *Brain Pathol* 13:52-61.
14. K. Watanabe, O. Tachibana, K. Sata, Y. Yonekawa, P. Kleihues and H. Ohgaki. 1996. Overexpression of the EGF receptor and p53 mutations are mutually exclusive in the

evolution of primary and secondary glioblastomas. *Brain Pathol* 6:217-223; discussion 223-214.

15. N. Ishii, D. Maier, A. Merlo, M. Tada, Y. Sawamura, A. C. Diserens and E. G. van Meir. 1999. Frequent co-alterations of TP53, p16/CDKN2A, p14ARF, PTEN tumour suppressor genes in human glioma cell lines. *Brain Pathol* 9:469-479.
16. W. Wick, F. B. Furnari, U. Naumann, W. K. Cavenee and M. Weller. 1999. PTEN gene transfer in human malignant glioma: sensitization to irradiation and CD95L-induced apoptosis. *Oncogene* 18:3936-3943.
17. E. G. van Meir, T. Kikuchi, M. Tada, H. Li, A. C. Diserens, B. E. Wojcik, H. J. Huang, T. Friedmann, N. De Tribolet and W. K. Cavenee. 1994. Analysis of the p53 gene and its expression in human glioblastoma cells. *Cancer Res* 54:649-652.
18. P. Wersall, I. Ohlsson, P. Biberfeld, V. P. Collins, S. Von Krusenstjerna, S. Larsson, H. Mellstedt and J. Boethius. 1997. Intratumoral infusion of the monoclonal antibody, mAb 425, against the epidermal-growth-factor receptor in patients with advanced malignant glioma. *Cancer Immunol Immunother* 44:157-164.
19. B. A. Foster, H. A. Coffey, M. J. Morin and F. Rastinejad. 1999. Pharmacological rescue of mutant p53 conformation and function. *Science* 286:2507-2510.
20. V. J. Bykov, N. Issaeva, A. Shilov, M. Hultcrantz, E. Pugacheva, P. Chumakov, J. Bergman, K. G. Wiman and G. Selivanova. 2002. Restoration of the tumour suppressor function to mutant p53 by a low-molecular-weight compound. *Nat Med* 8:282-288.
21. J. F. Kerr, A. H. Wyllie and A. R. Currie. 1972. Apoptosis: a basic biological phenomenon with wide-ranging implications in tissue kinetics. *Br J Cancer* 26:239-257.
22. J. Yuan, S. Shaham, S. Ledoux, H. M. Ellis and H. R. Horvitz. 1993. The C. elegans cell death gene ced-3 encodes a protein similar to mammalian interleukin-1 beta-converting enzyme. *Cell* 75:641-652.
23. J. Yuan and H. R. Horvitz. 2004. A first insight into the molecular mechanisms of apoptosis. *Cell* 116:S53-56, 51 p following S59.
24. N. N. Danial and S. J. Korsmeyer. 2004. Cell death: critical control points. *Cell* 116:205-219.
25. R. E. Ellis, J. Y. Yuan and H. R. Horvitz. 1991. Mechanisms and functions of cell death. *Annu Rev Cell Biol* 7:663-698.
26. Y. Chen and X. Zhao. 1998. Shaping limbs by apoptosis. *J Exp Zool* 282:691-702.

27. C. Y. Kuan, K. A. Roth, R. A. Flavell and P. Rakic. 2000. Mechanisms of programmed cell death in the developing brain. *Trends Neurosci* 23:291-297.
28. J. Yuan and B. A. Yankner. 2000. Apoptosis in the nervous system. *Nature* 407:802-809.
29. A. Strasser and P. Bouillet. 2003. The control of apoptosis in lymphocyte selection. *Immunol Rev* 193:82-92.
30. M. Lenardo, K. M. Chan, F. Hornung, H. McFarland, R. Siegel, J. Wang and L. Zheng. 1999. Mature T lymphocyte apoptosis--immune regulation in a dynamic and unpredictable antigenic environment. *Annu Rev Immunol* 17:221-253.
31. S. W. Lowe and A. W. Lin. 2000. Apoptosis in cancer. *Carcinogenesis* 21:485-495.
32. J. Lotem, M. Peled-Kamar, Y. Groner and L. Sachs. 1996. Cellular oxidative stress and the control of apoptosis by wild-type p53, cytotoxic compounds, and cytokines. *Proc Natl Acad Sci U S A* 93:9166-9171.
33. G. Evan and T. Littlewood. 1998. A matter of life and cell death. *Science* 281:1317-1322.
34. D. C. Huang and A. Strasser. 2000. BH3-only proteins-essential initiators of apoptotic cell death. *Cell* 103:839-842.
35. K. Nakano and K. H. Vousden. 2001. PUMA, a novel proapoptotic gene, is induced by p53. *Mol Cell* 7:683-694.
36. E. Oda, R. Ohki, H. Murasawa, J. Nemoto, T. Shibue, T. Yamashita, T. Tokino, T. Taniguchi and N. Tanaka. 2000. Noxa, a BH3-only member of the Bcl-2 family and candidate mediator of p53-induced apoptosis. *Science* 288:1053-1058.
37. J. Yu, L. Zhang, P. M. Hwang, K. W. Kinzler and B. Vogelstein. 2001. PUMA induces the rapid apoptosis of colorectal cancer cells. *Mol Cell* 7:673-682.
38. T. Miyashita, S. Krajewski, M. Krajewska, H. G. Wang, H. K. Lin, D. A. Liebermann, B. Hoffman and J. C. Reed. 1994. Tumour suppressor p53 is a regulator of bcl-2 and bax gene expression in vitro and in vivo. *Oncogene* 9:1799-1805.
39. K. Polyak, Y. Xia, J. L. Zweier, K. W. Kinzler and B. Vogelstein. 1997. A model for p53-induced apoptosis. *Nature* 389:300-305.
40. J. M. Adams and S. Cory. 1998. The Bcl-2 protein family: arbiters of cell survival. *Science* 281:1322-1326.
41. M. C. Wei, W. X. Zong, E. H. Cheng, T. Lindsten, V. Panoutsakopoulou, A. J. Ross, K. A. Roth, G. R. Macgregor, C. B. Thompson and S. J. Korsmeyer. 2001.

Proapoptotic BAX and BAK: a requisite gateway to mitochondrial dysfunction and death. *Science* 292:727-730.

42. A. Letai, M. C. Bassik, L. D. Walensky, M. D. Sorcinelli, S. Weiler and S. J. Korsmeyer. 2002. Distinct BH3 domains either sensitize or activate mitochondrial apoptosis, serving as prototype cancer therapeutics. *Cancer Cell* 2:183-192.
43. N. A. Thornberry and Y. Lazebnik. 1998. Caspases: enemies within. *Science* 281:1312-1316.
44. Y. Huang, Y. C. Park, R. L. Rich, D. Segal, D. G. Myszka and H. Wu. 2001. Structural basis of caspase inhibition by XIAP: differential roles of the linker versus the BIR domain. *Cell* 104:781-790.
45. T. Shirai, H. Yamaguchi, H. Ito, C. W. Todd and R. B. Wallace. 1985. Cloning and expression in Escherichia coli of the gene for human tumour necrosis factor. *Nature* 313:803-806.
46. T. Takahashi, M. Tanaka, J. Inazawa, T. Abe, T. Suda and S. Nagata. 1994. Human Fas ligand: gene structure, chromosomal location and species specificity. *Int Immunol* 6:1567-1574.
47. S. R. Wiley, K. Schooley, P. J. Smolak, W. S. Din, C. P. Huang, J. K. Nicholl, G. R. Sutherland, T. D. Smith, C. Rauch, C. A. Smith and Et Al. 1995. Identification and characterization of a new member of the TNF family that induces apoptosis. *Immunity* 3:673-682.
48. A. Ashkenazi and V. M. Dixit. 1998. Death receptors: signalling and modulation. *Science* 281:1305-1308.
49. K. V. Prasad, Z. Ao, Y. Yoon, M. X. Wu, M. Rizk, S. Jacquot and S. F. Schlossman. 1997. CD27, a member of the tumour necrosis factor receptor family, induces apoptosis and binds to Siva, a proapoptotic protein. *Proc Natl Acad Sci U S A* 94:6346-6351.
50. G. Pan, J. Ni, Y. F. Wei, G. Yu, R. Gentz and V. M. Dixit. 1997. An antagonist decoy receptor and a death domain-containing receptor for TRAIL. *Science* 277:815-818.
51. R. M. Pitti, S. A. Marsters, D. A. Lawrence, M. Roy, F. C. Kischkel, P. Dowd, A. Huang, C. J. Donahue, S. W. Sherwood, D. T. Baldwin, P. J. Godowski, W. I. Wood, A. L. Gurney, K. J. Hillan, R. L. Cohen, A. D. Goddard, D. Botstein and A. Ashkenazi. 1998. Genomic amplification of a decoy receptor for Fas ligand in lung and colon cancer. *Nature* 396:699-703.

52. W. Roth, S. Isenmann, M. Nakamura, M. Platten, W. Wick, P. Kleihues, M. Bähr, H. Ohgaki, A. Ashkenazi and M. Weller. 2001. Soluble decoy receptor 3 is expressed by malignant gliomas and suppresses CD95 ligand-induced apoptosis and chemotaxis. *Cancer Res* 61:2759-2765.

53. F. C. Kischkel, S. Hellbardt, I. Behrmann, M. Germer, M. Pawlita, P. H. Krammer and M. E. Peter. 1995. Cytotoxicity-dependent APO-1 (Fas/CD95)-associated proteins form a death-inducing signalling complex (DISC) with the receptor. *Embo J* 14:5579-5588.

54. C. Scaffidi, I. Schmitz, P. H. Krammer and M. E. Peter. 1999. The role of c-FLIP in modulation of CD95-induced apoptosis. *J Biol Chem* 274:1541-1548.

55. M. Irmler, M. Thome, M. Hahne, P. Schneider, K. Hofmann, V. Steiner, J. L. Bodmer, M. Schröter, K. Burns, C. Mattmann, D. Rimoldi, L. E. French and J. Tschopp. 1997. Inhibition of death receptor signals by cellular FLIP. *Nature* 388:190-195.

56. C. Scaffidi, S. Fulda, A. Srinivasan, C. Friesen, F. Li, K. J. Tomaselli, K. M. Debatin, P. H. Krammer and M. E. Peter. 1998. Two CD95 (APO-1/Fas) signalling pathways. *Embo J* 17:1675-1687.

57. C. Scaffidi, I. Schmitz, J. Zha, S. J. Korsmeyer, P. H. Krammer and M. E. Peter. 1999. Differential modulation of apoptosis sensitivity in CD95 type I and type II cells. *J Biol Chem* 274:22532-22538.

58. X. Luo, I. Budihardjo, H. Zou, C. Slaughter and X. Wang. 1998. Bid, a Bcl2 interacting protein, mediates cytochrome c release from mitochondria in response to activation of cell surface death receptors. *Cell* 94:481-490.

59. H. Li, H. Zhu, C. J. Xu and J. Yuan. 1998. Cleavage of BID by caspase 8 mediates the mitochondrial damage in the Fas pathway of apoptosis. *Cell* 94:491-501.

60. S. J. Korsmeyer, M. C. Wei, M. Saito, S. Weiler, K. J. Oh and P. H. Schlesinger. 2000. Pro-apoptotic cascade activates BID, which oligomerizes BAK or BAX into pores that result in the release of cytochrome c. *Cell Death Differ* 7:1166-1173.

61. T. Glaser, B. Wagenknecht and M. Weller. 2001. Identification of p21 as a target of cycloheximide-mediated facilitation of CD95-mediated apoptosis in human malignant glioma cells. *Oncogene* 20:4757-4767.

62. J. Rieger, U. Naumann, T. Glaser, A. Ashkenazi and M. Weller. 1998. APO2 ligand: a novel lethal weapon against malignant glioma? *FEBS Lett* 427:124-128.

63. M. Weller, P. Kleihues, J. Dichgans and H. Ohgaki. 1998. CD95 ligand: lethal weapon against malignant glioma? *Brain Pathol* 8:285-293.

64. U. Naumann and M. Weller. 1998. Retroviral BAX gene transfer fails to sensitize malignant glioma cells to CD95L-induced apoptosis and cancer chemotherapy. *Int J Cancer* 77:645-648.

65. B. Wagenknecht, T. Glaser, U. Naumann, S. Kügler, S. Isenmann, M. Bähr, R. Korneluk, P. Liston and M. Weller. 1999. Expression and biological activity of X-linked inhibitor of apoptosis (XIAP) in human malignant glioma. *Cell Death Differ* 6:370-376.

66. T. A. Röhn, B. Wagenknecht, W. Roth, U. Naumann, E. Gulbins, P. H. Krammer, H. Walczak and M. Weller. 2001. CCNU-dependent potentiation of TRAIL/Apo2L-induced apoptosis in human glioma cells is p53-independent but may involve enhanced cytochrome c release. *Oncogene* 20:4128-4137.

67. S. Fulda, W. Wick, M. Weller and K. M. Debatin. 2002. Smac agonists sensitize for Apo2L/TRAIL- or anticancer drug-induced apoptosis and induce regression of malignant glioma in vivo. *Nat Med* 8:808-815.

68. R. S. Goldszmid, J. Idoyaga, A. I. Bravo, R. Steinman, J. Mordoh and R. Wainstok. 2003. Dendritic cells charged with apoptotic tumour cells induce long-lived protective CD4+ and CD8+ T cell immunity against B16 melanoma. *J Immunol* 171:5940-5947.

69. S. R. Scheffer, H. Nave, F. Korangy, K. Schlote, R. Pabst, E. M. Jaffee, M. P. Manns and T. F. Greten. 2003. Apoptotic, but not necrotic, tumour cell vaccines induce a potent immune response in vivo. *Int J Cancer* 103:205-211.

70. V. Russo, S. Tanzarella, P. Dalerba, D. Rigatti, P. Rovere, A. Villa, C. Bordignon and C. Traversari. 2000. Dendritic cells acquire the MAGE-3 human tumour antigen from apoptotic cells and induce a class I-restricted T cell response. *Proc Natl Acad Sci U S A* 97:2185-2190.

71. M. H. M. G. M. den Brok, R. P. M. Sutmuller, R. van der Voort, E. J. Bennink, C. G. Figdor, T. J. M. Ruers and G. J. Adema. 2004. In Situ Tumour Ablation Creates an Antigen Source for the Generation of Antitumour Immunity. *Cancer Res* 64:4024-4029.

72. W. B. Coley. 1893. The treatment of malignant tumours by repeated inoculations of erysipelas: with a report of ten original cases. *Am J Med Sci* 105:487-511.

73. P. Ehrlich. 1909. Über den jetzigen Stand der Karzinomforschung. *Ned Tijdschr Geneeskd* 5:273-290.

74. L. Thomas. 1959. Cellular and humoral aspects of hypersensitive states. *In* Discussion to P.B. Medawar´s paper. H. Lawrence, editor. Hoeber-Harper, New York. 529-534.

75. F. M. Burnet. 1957. Cancer: a biological approach. *Br Med J* 1:779-786.

76. F. M. Burnet. 1967. Immunological aspects of malignant disease. *Lancet* 1:1171-1174.

77. F. M. Burnet. 1970. The concept of immunological surveillance. *Prog Exp Tumour Res* 13:1-2.

78. J. Rygaard and C. O. Povlsen. 1974. The mouse mutant nude does not develop spontaneous tumours. An argument against immunological surveillance. *Acta Pathol Microbiol Scand [B] Microbiol Immunol* 82:99-106.

79. O. Stutman. 1974. Tumour development after 3-methylcholanthrene in immunologically deficient athymic-nude mice. *Science* 183:534-536.

80. S. E. Street, J. A. Trapani, D. Macgregor and M. J. Smyth. 2002. Suppression of lymphoma and epithelial malignancies effected by interferon gamma. *J Exp Med* 196:129-134.

81. M. E. van den Broek, D. Kägi, F. Ossendorp, R. Toes, S. Vamvakas, W. K. Lutz, C. J. Melief, R. M. Zinkernagel and H. Hengartner. 1996. Decreased tumour surveillance in perforin-deficient mice. *J Exp Med* 184:1781-1790.

82. V. Shankaran, H. Ikeda, A. T. Bruce, J. M. White, P. E. Swanson, L. J. Old and R. D. Schreiber. 2001. IFNgamma and lymphocytes prevent primary tumour development and shape tumour immunogenicity. *Nature* 410:1107-1111.

83. Y. Shinkai, G. Rathbun, K. P. Lam, E. M. Oltz, V. Stewart, M. Mendelsohn, J. Charron, M. Datta, F. Young, A. M. Stall and Et Al. 1992. RAG-2-deficient mice lack mature lymphocytes owing to inability to initiate V(D)J rearrangement. *Cell* 68:855-867.

84. R. M. Zinkernagel and P. C. Doherty. 1974. Immunological surveillance against altered self components by sensitised T lymphocytes in lymphocytic choriomeningitis. *Nature* 251:547-548.

85. R. Medzhitov and C. Janeway, Jr. 2000. Innate immune recognition: mechanisms and pathways. *Immunol Rev* 173:89-97.

86. V. Hornung, S. Rothenfusser, S. Britsch, A. Krug, B. Jahrsdörfer, T. Giese, S. Endres and G. Hartmann. 2002. Quantitative expression of toll-like receptor 1-10 mRNA in cellular subsets of human peripheral blood mononuclear cells and sensitivity to CpG oligodeoxynucleotides. *J Immunol* 168:4531-4537.

87. M. J. Robertson and J. Ritz. 1990. Biology and clinical relevance of human natural killer cells. *Blood* 76:2421-2438.

88. J. A. Trapani and M. J. Smyth. 2002. Functional significance of the perforin/granzyme cell death pathway. *Nat Rev Immunol* 2:735-747.

89. R. Medzhitov and C. A. Janeway, Jr. 2002. Decoding the patterns of self and nonself by the innate immune system. *Science* 296:298-300.

90. G. Ferlazzo and C. Münz. 2004. NK cell compartments and their activation by dendritic cells. *J Immunol* 172:1333-1339.

91. A. B. Bakker, J. H. Phillips, C. G. Figdor and L. L. Lanier. 1998. Killer cell inhibitory receptors for MHC class I molecules regulate lysis of melanoma cells mediated by NK cells, gamma delta T cells, and antigen-specific CTL. *J Immunol* 160:5239-5245.

92. P. Matzinger. 2002. The danger model: a renewed sense of self. *Science* 296:301-305.

93. L. L. Lanier. 1998. NK cell receptors. *Annu Rev Immunol* 16:359-393.

94. S. Bauer, V. Groh, J. Wu, A. Steinle, J. H. Phillips, L. L. Lanier and T. Spies. 1999. Activation of NK cells and T cells by NKG2D, a receptor for stress-inducible MICA. *Science* 285:727-729.

95. D. Cosman, J. Mullberg, C. L. Sutherland, W. Chin, R. Armitage, W. Fanslow, M. Kubin and N. J. Chalupny. 2001. ULBPs, novel MHC class I-related molecules, bind to CMV glycoprotein UL16 and stimulate NK cytotoxicity through the NKG2D receptor. *Immunity* 14:123-133.

96. P. J. Peters, J. Borst, V. Oorschot, M. Fukuda, O. Krähenbühl, J. Tschopp, J. W. Slot and H. J. Geuze. 1991. Cytotoxic T lymphocyte granules are secretory lysosomes, containing both perforin and granzymes. *J Exp Med* 173:1099-1109.

97. J. H. Russell and T. J. Ley. 2002. Lymphocyte-mediated cytotoxicity. *Annu Rev Immunol* 20:323-370.

98. P. Parham. 2003. Innate immunity: the unsung heroes. *Nature* 423:20.

99. P. Cresswell. 1994. Assembly, transport, and function of MHC class II molecules. *Annu Rev Immunol* 12:259-293.

100. S. M. Alam, P. J. Travers, J. L. Wung, W. Nasholds, S. Redpath, S. C. Jameson and N. R. Gascoigne. 1996. T-cell-receptor affinity and thymocyte positive selection. *Nature* 381:616-620.

101. J. W. Kappler, N. Roehm and P. Marrack. 1987. T cell tolerance by clonal elimination in the thymus. *Cell* 49:273-280.

102. R. M. Zinkernagel and P. C. Doherty. 1974. Restriction of in vitro T cell-mediated cytotoxicity in lymphocytic choriomeningitis within a syngeneic or semiallogeneic system. *Nature* 248:701-702.

103. J. Nikolich-Zugich, M. K. Slifka and I. Messaoudi. 2004. The many important facets of T-cell repertoire diversity. *Nat Rev Immunol* 4:123-132.

104. K. Falk, O. Rotzschke and H. G. Rammensee. 1990. Cellular peptide composition governed by major histocompatibility complex class I molecules. *Nature* 348:248-251.

105. H. G. Rammensee, K. Falk and O. Rotzschke. 1993. Peptides naturally presented by MHC class I molecules. *Annu Rev Immunol* 11:213-244.

106. O. Rotzschke, K. Falk, K. Deres, H. Schild, M. Norda, J. Metzger, G. Jung and H. G. Rammensee. 1990. Isolation and analysis of naturally processed viral peptides as recognized by cytotoxic T cells. *Nature* 348:252-254.

107. Ayu Rudensky, P. Preston-Hurlburt, S. C. Hong, A. Barlow and C. A. Janeway, Jr. 1991. Sequence analysis of peptides bound to MHC class II molecules. *Nature* 353:622-627.

108. R. M. Steinman, D. S. Lustig and Z. A. Cohn. 1974. Identification of a novel cell type in peripheral lymphoid organs of mice. 3. Functional properties in vivo. *J Exp Med* 139:1431-1445.

109. R. M. Steinman and Z. A. Cohn. 1974. Identification of a novel cell type in peripheral lymphoid organs of mice. II. Functional properties in vitro. *J Exp Med* 139:380-397.

110. J. Banchereau, F. Briere, C. Caux, J. Davoust, S. Lebecque, Y. J. Liu, B. Pulendran and K. Palucka. 2000. Immunobiology of dendritic cells. *Annu Rev Immunol* 18:767-811.

111. J. Banchereau, B. Pulendran, R. Steinman and K. Palucka. 2000. Will the making of plasmacytoid dendritic cells in vitro help unravel their mysteries? *J Exp Med* 192:F39-44.

112. G. Grouard, M. C. Rissoan, L. Filgueira, I. Durand, J. Banchereau and Y. J. Liu. 1997. The enigmatic plasmacytoid T cells develop into dendritic cells with interleukin (IL)-3 and CD40-ligand. *J Exp Med* 185:1101-1111.

113. M. L. Albert, S. F. Pearce, L. M. Francisco, B. Sauter, P. Roy, R. L. Silverstein and N. Bhardwaj. 1998. Immature dendritic cells phagocytose apoptotic cells via alphavbeta5 and CD36, and cross-present antigens to cytotoxic T lymphocytes. *J Exp Med* 188:1359-1368.

114. S. Gallucci, M. Lolkema and P. Matzinger. 1999. Natural adjuvants: endogenous activators of dendritic cells. *Nat Med* 5:1249-1255.

115. G. M. Barton and R. Medzhitov. 2002. Control of adaptive immune responses by Toll-like receptors. *Curr Opin Immunol* 14:380-383.

116. L. Alexopoulou, A. C. Holt, R. Medzhitov and R. A. Flavell. 2001. Recognition of double-stranded RNA and activation of NF-kappaB by Toll-like receptor 3. *Nature* 413:732-738.

117. J. Li, B. Schuler-Thurner, G. Schuler, C. Huber and B. Seliger. 2001. Bipartite regulation of different components of the MHC class I antigen-processing machinery during dendritic cell maturation. *Int. Immunol.* 13:1515-1523.

118. B. M. Carreno and M. Collins. 2002. The B7 family of ligands and its receptors: new pathways for costimulation and inhibition of immune responses. *Annu Rev Immunol* 20:29-53.

119. S. J. Khoury and M. H. Sayegh. 2004. The roles of the new negative T cell costimulatory pathways in regulating autoimmunity. *Immunity* 20:529-538.

120. R. H. Schwartz. 2003. T cell anergy. *Annu Rev Immunol* 21:305-334.

121. P. van der Bruggen, C. Traversari, P. Chomez, C. Lurquin, E. de Plaen, B. van den Eynde, A. Knuth and T. Boon. 1991. A gene encoding an antigen recognized by cytolytic T lymphocytes on a human melanoma. *Science* 254:1643-1647.

122. M. J. Smyth, D. I. Godfrey and J. A. Trapani. 2001. A fresh look at tumour immunosurveillance and immunotherapy. *Nat Immunol* 2:293-299.

123. L. L. Lanier. 2001. A renaissance for the tumour immunosurveillance hypothesis. *Nat Med* 7:1178-1180.

124. J. A. Berzofsky, M. Terabe, S. K. Oh, I.M. Belyakov, J. D. Ahlers, J. E. Janik and J. C. Morris. 2004. Progress on new vaccine strategies for the immunotherapy and prevention of cancer. *J Clin Invest* 113:1515-1525.

125. O. Tureci, U. Sahin, I. Schobert, M. Koslowski, H. Scmitt, H. J. Schild, F. Stenner, G. Seitz, H. G. Rammensee and M. Pfreundschuh. 1996. The SSX-2 gene, which is involved in the t(X;18) translocation of synovial sarcomas, codes for the human tumour antigen HOM-MEL-40. *Cancer Res* 56:4766-4772.

126. H. Singh-Jasuja, N. P. Emmerich and H. G. Rammensee. 2004. The Tübingen approach: identification, selection, and validation of tumour-associated HLA peptides for cancer therapy. *Cancer Immunol Immunother* 53:187-195.

127. R. Ueda, Y. Iizuka, K. Yoshida, T. Kawase, Y. Kawakami and M. Toda. 2004. Identification of a human glioma antigen, SOX6, recognized by patients' sera. *Oncogene* 23:1420-1427.

128. M. J. Scanlan, A. O. Gure, A. A. Jungbluth, L. J. Old and Y. T. Chen. 2002. Cancer/testis antigens: an expanding family of targets for cancer immunotherapy. *Immunol Rev* 188:22-32.

129. C. Lengauer, K. W. Kinzler and B. Vogelstein. 1998. Genetic instabilities in human cancers. *Nature* 396:643-649.

130. L. Müller and G. Pawelec. 2003. Cytokines and antitumour immunity. *Technol Cancer Res Treat* 2:183-194.

131. M. A. Friese, M. Platten, S. Z. Lutz, U. Naumann, S. Aulwurm, F. Bischof, H. J. Bühring, J. Dichgans, H. G. Rammensee, A. Steinle and M. Weller. 2003. MICA/NKG2D-mediated immunogene therapy of experimental gliomas. *Cancer Res* 63:8996-9006.

132. M. Movassagh, A. Spatz, J. Davoust, S. Lebecque, P. Romero, M. Pittet, D. Rimoldi, D. Lienard, O. Gugerli, L. Ferradini, C. Robert, M. F. Avril, L. Zitvogel and E. Angevin. 2004. Selective accumulation of mature DC-Lamp+ dendritic cells in tumour sites is associated with efficient T-cell-mediated antitumour response and control of metastatic dissemination in melanoma. *Cancer Res* 64:2192-2198.

133. A. Heiser, D. Coleman, J. Dannull, D. Yancey, M. A. Maurice, C. D. Lallas, P. Dahm, D. Niedzwiecki, E. Gilboa and J. Vieweg. 2002. Autologous dendritic cells transfected with prostate-specific antigen RNA stimulate CTL responses against metastatic prostate tumours. *J. Clin. Invest.* 109:409-417.

134. D. Ridgway. 2003. The first 1000 dendritic cell vaccinees. *Cancer Invest* 21:873-886.

135. L. Fong and E. G. Engleman. 2000. Dendritic Cells in Cancer Immunotherapy. *Annual Review of Immunology* 18:245-273.

136. E. G. Engleman. 2003. Dendritic cell-based cancer immunotherapy. *Semin Oncol* 30:23-29.

137. D. M. Klinman. 2004. Immunotherapeutic uses of CpG oligodeoxynucleotides. *Nat Rev Immunol* 4:249-258.

138. D. M. Klinman, A. K. Yi, S. L. Beaucage, J. Conover and A. M. Krieg. 1996. CpG motifs present in bacteria DNA rapidly induce lymphocytes to secrete interleukin 6, interleukin 12, and interferon gamma. *Proc Natl Acad Sci U S A* 93:2879-2883.

139. A. F. Carpentier, L. Chen, F. Maltonti and J. Y. Delattre. 1999. Oligodeoxynucleotides containing CpG motifs can induce rejection of a neuroblastoma in mice. *Cancer Res* 59:5429-5432.

140. A. D. Sandler, H. Chihara, G. Kobayashi, X. Zhu, M. A. Miller, D. L. Scott and A. M. Krieg. 2003. CpG oligonucleotides enhance the tumour antigen-specific immune response of a granulocyte macrophage colony-stimulating factor-based vaccine strategy in neuroblastoma. *Cancer Res* 63:394-399.

141. M. Heikenwalder, M. Polymenidou, T. Junt, C. Sigurdson, H. Wagner, S. Akira, R. Zinkernagel and A. Aguzzi. 2004. Lymphoid follicle destruction and immunosuppression after repeated CpG oligodeoxynucleotide administration. *Nat Med* 10:187-192.

142. S. S. Diebold, T. Kaisho, H. Hemmi, S. Akira and C. Reis E Sousa. 2004. Innate antiviral responses by means of TLR7-mediated recognition of single-stranded RNA. *Science* 303:1529-1531.

143. B. Scheel, S. Braedel, J. Probst, J. P. Carralot, H. Wagner, H. Schild, G. Jung, H. G. Rammensee and S. Pascolo. 2004. Immunostimulating capacities of stabilized RNA molecules. *Eur J Immunol* 34:537-547.

144. F. André, N. Chaput, N. E. Schartz, C. Flament, N. Aubert, J. Bernard, F. Lemonnier, G. Raposo, B. Escudier, D. H. Hsu, T. Tursz, S. Amigorena, E. Angevin and L. Zitvogel. 2004. Exosomes as potent cell-free peptide-based vaccine. I. Dendritic cell-derived exosomes transfer functional MHC class I/peptide complexes to dendritic cells. *J Immunol* 172:2126-2136.

145. F. André, N. E. Schartz, N. Chaput, C. Flament, G. Raposo, S. Amigorena, E. Angevin and L. Zitvogel. 2002. Tumour-derived exosomes: a new source of tumour rejection antigens. *Vaccine* 20 Suppl 4:A28-31.

146. V. Mazzaferro, J. Coppa, M. G. Carrabba, L. Rivoltini, M. Schiavo, E. Regalia, L. Mariani, T. Camerini, A. Marchiano, S. Andreola, R. Camerini, M. Corsi, J. J. Lewis, P. K. Srivastava and G. Parmiani. 2003. Vaccination with autologous tumour-derived heat-shock protein gp96 after liver resection for metastatic colorectal cancer. *Clin Cancer Res* 9:3235-3245.

147. M. Campoli, C. C. Chang and S. Ferrone. 2002. HLA class I antigen loss, tumour immune escape and immune selection. *Vaccine* 20 Suppl 4:A40-45.

148. C. J. Melief, S. H. van der Burg, R. E. Toes, F. Ossendorp and R. Offringa. 2002. Effective therapeutic anticancer vaccines based on precision guiding of cytolytic T lymphocytes. *Immunol Rev* 188:177-182.

149. L. Al-Harthi, G. Marchetti, C. M. Steffens, J. Poulin, R. Sekaly and A. Landay. 2000. Detection of T cell receptor circles (TRECs) as biomarkers for de novo T cell

synthesis using a quantitative polymerase chain reaction-enzyme linked immunosorbent assay (PCR-ELISA). *J Immunol Methods* 237:187-197.

150. R. J. De Boer and A. J. Noest. 1998. T cell renewal rates, telomerase, and telomere length shortening. *J Immunol* 160:5832-5837.
151. P. G. Coulie, V. Karanikas, C. Lurquin, D. Colau, T. Connerotte, T. Hanagiri, A. van Pel, S. Lucas, D. Godelaine, C. Lonchay, M. Marchand, N. van Baren and T. Boon. 2002. Cytolytic T-cell responses of cancer patients vaccinated with a MAGE antigen. *Immunol Rev* 188:33-42.
152. P. Romero, J. C. Cerottini and D. E. Speiser. 2004. Monitoring tumour antigen specific T-cell responses in cancer patients and phase I clinical trials of peptide-based vaccination. *Cancer Immunol Immunother* 53:249-255.
153. G. P. Dunn, A. T. Bruce, H. Ikeda, L. J. Old and R. D. Schreiber. 2002. Cancer immunoediting: from immunosurveillance to tumour escape. *Nat Immunol* 3:991-998.
154. G. P. Dunn, L. J. Old and R. D. Schreiber. 2004. The Three Es of Cancer Immunoediting. *Annu Rev Immunol* 22:329-360.
155. M. Weller and A. Fontana. 1995. The failure of current immunotherapy for malignant glioma. Tumour-derived TGF-beta, T-cell apoptosis, and the immune privilege of the brain. *Brain Res Brain Res Rev* 21:128-151.
156. W. F. Hickey. 2001. Basic principles of immunological surveillance of the normal central nervous system. *Glia* 36:118-124.
157. R. M. Ransohoff, P. Kivisakk and G. Kidd. 2003. Three or more routes for leukocyte migration into the central nervous system. *Nat Rev Immunol* 3:569-581.
158. M. Schwartz and I. R. Cohen. 2000. Autoimmunity can benefit self-maintenance. *Immunol Today* 21:265-268.
159. R. Hohlfeld, M. Kerschensteiner, C. Stadelmann, H. Lassmann and H. Wekerle. 2000. The neuroprotective effect of inflammation: implications for the therapy of multiple sclerosis. *J Neuroimmunol* 107:161-166.
160. F. Aloisi, F. Ria, G. Penna and L. Adorini. 1998. Microglia are more efficient than astrocytes in antigen processing and in Th1 but not Th2 cell activation. *J Immunol* 160:4671-4680.
161. H. F. Cserr and P. M. Knopf. 1997. Cervical lymphatics, the blood-brain barrier and immunoreactivity of the brain. *In* Immunology of the nervous system. R.W. Keane and W.F. Hickey, editors. Oxford University Press, New York. 134-154.

162. H. F. Cserr, C. J. Harling-Berg and P. M. Knopf. 1992. Drainage of brain extracellular fluid into blood and deep cervical lymph and its immunological significance. *Brain Pathol* 2:269-276.

163. C. J. Harling-Berg, T. J. Park and P. M. Knopf. 1999. Role of the cervical lymphatics in the Th2-type hierarchy of CNS immune regulation. *J Neuroimmunol* 101:111-127.

164. H. Neumann. 2000. The immunological microenvironment in the CNS: implications on neuronal cell death and survival. *J Neural Transm Suppl* 59:59-68.

165. C. Choi and E. N. Benveniste. 2004. Fas ligand/Fas system in the brain: regulator of immune and apoptotic responses. *Brain Res Brain Res Rev* 44:65-81.

166. T. Suter, G. Biollaz, D. Gatto, L. Bernasconi, T. Herren, W. Reith and A. Fontana. 2003. The brain as an immune privileged site: dendritic cells of the central nervous system inhibit T cell activation. *Eur J Immunol* 33:2998-3006.

167. G. Perrin, V. Schnuriger, A. L. Quiquerez, P. Saas, C. Pannetier, N. De Tribolet, J. M. Tiercy, J. P. Aubry, P. Y. Dietrich and P. R. Walker. 1999. Astrocytoma infiltrating lymphocytes include major T cell clonal expansions confined to the CD8 subset. *Int Immunol* 11:1337-1350.

168. U. Sahin, O. Tureci, H. Schmitt, B. Cochlovius, T. Johannes, R. Schmits, F. Stenner, G. Luo, I. Schobert and M. Pfreundschuh. 1995. Human neoplasms elicit multiple specific immune responses in the autologous host. *Proc Natl Acad Sci U S A* 92:11810-11813.

169. M. C. Kuppner, M. F. Hamou and N. De Tribolet. 1988. Immunohistological and functional analyses of lymphoid infiltrates in human glioblastomas. *Cancer Res* 48:6926-6932.

170. M. Platten, A. Kretz, U. Naumann, S. Aulwurm, K. Egashira, S. Isenmann and M. Weller. 2003. Monocyte chemoattractant protein-1 increases microglial infiltration and aggressiveness of gliomas. *Ann Neurol* 54:388-392.

171. D. P. Lane. 1992. Cancer. p53, guardian of the genome. *Nature* 358:15-16.

172. J. E. Chipuk, U. Maurer, D. R. Green and M. Schuler. 2003. Pharmacologic activation of p53 elicits Bax-dependent apoptosis in the absence of transcription. *Cancer Cell* 4:371-381.

173. J. E. Chipuk, T. Kuwana, L. Bouchier-Hayes, N. M. Droin, D. D. Newmeyer, M. Schuler and D. R. Green. 2004. Direct activation of Bax by p53 mediates mitochondrial membrane permeabilization and apoptosis. *Science* 303:1010-1014.

174. M. Schuler and D. R. Green. 2001. Mechanisms of p53-dependent apoptosis. *Biochem Soc Trans* 29:684-688.

175. A. N. Bullock and A. R. Fersht. 2001. Rescuing the function of mutant p53. *Nat Rev Cancer* 1:68-76.

176. E. R. Flores, K. Y. Tsai, D. Crowley, S. Sengupta, A. Yang, F. Mckeon and T. Jacks. 2002. p63 and p73 are required for p53-dependent apoptosis in response to DNA damage. *Nature* 416:560-564.

177. T. R. Brummelkamp, R. Bernards and R. Agami. 2002. A system for stable expression of short interfering RNAs in mammalian cells. *Science* 296:550-553.

178. S. M. Elbashir, J. Harborth, W. Lendeckel, A. Yalcin, K. Weber and T. Tuschl. 2001. Duplexes of 21-nucleotide RNAs mediate RNA interference in cultured mammalian cells. *Nature* 411:494-498.

179. J. Ogasawara, R. Watanabe-Fukunaga, M. Adachi, A. Matsuzawa, T. Kasugai, Y. Kitamura, N. Itoh, T. Suda and S. Nagata. 1993. Lethal effect of the anti-Fas antibody in mice. *Nature* 364:806-809.

180. U. Naumann, R. Waltereit, J. B. Schulz and M. Weller. 2003. Adenoviral (full-length) Apo2L/TRAIL gene transfer is an ineffective treatment strategy for malignant glioma. *J Neurooncol* 61:7-15.

181. P. Sova, X. W. Ren, S. Ni, K. M. Bernt, J. Mi, N. Kiviat and A. Lieber. 2004. A tumour-targeted and conditionally replicating oncolytic adenovirus vector expressing TRAIL for treatment of liver metastases. *Mol Ther* 9:496-509.

182. G. Jung, L. Grosse-Hovest, P. H. Krammer and H. G. Rammensee. 2001. Target cell-restricted triggering of the CD95 (APO-1/Fas) death receptor with bispecific antibody fragments. *Cancer Res* 61:1846-1848.

183. S. Hess and H. Engelmann. 1996. A novel function of CD40: induction of cell death in transformed cells. *J Exp Med* 183:159-167.

184. N. Fujita, H. Kagamu, H. Yoshizawa, K. Itoh, H. Kuriyama, N. Matsumoto, T. Ishiguro, J. Tanaka, E. Suzuki, H. Hamada and F. Gejyo. 2001. CD40 ligand promotes priming of fully potent antitumour CD4(+) T cells in draining lymph nodes in the presence of apoptotic tumour cells. *J Immunol* 167:5678-5688.

185. R. H. Vonderheide, J. P. Dutcher, J. E. Anderson, S. G. Eckhardt, K. F. Stephans, B. Razvillas, S. Garl, M. D. Butine, V. P. Perry, R. J. Armitage, R. Ghalie, D. A. Caron and J. G. Gribben. 2001. Phase I study of recombinant human CD40 ligand in cancer patients. *J Clin Oncol* 19:3280-3287.

186. R. Q. Hintzen, S. M. Lens, G. Koopman, S. T. Pals, H. Spits and R. A. Van Lier. 1994. CD70 represents the human ligand for CD27. *Int Immunol* 6:477-480.

187. O. Micheau and J. Tschopp. 2003. Induction of TNF receptor I-mediated apoptosis via two sequential signalling complexes. *Cell* 114:181-190.

188. H. Shinohara, H. Yagita, Y. Ikawa and N. Oyaizu. 2000. Fas drives cell cycle progression in glioma cells via extracellular signal-regulated kinase activation. *Cancer Res* 60:1766-1772.

189. H. Wiendl, M. Mitsdoerffer and M. Weller. 2003. Hide-and-seek in the brain: a role for HLA-G mediating immune privilege for glioma cells. *Semin Cancer Biol* 13:343-351.

190. E. D. Carosella, P. Paul, P. Moreau and N. Rouas-Freiss. 2000. HLA-G and HLA-E: fundamental and pathophysiological aspects. *Immunol Today* 21:532-534.

191. M. Wrann, S. Bodmer, R. De Martin, C. Siepl, R. Hofer-Warbinek, K. Frei, E. Hofer and A. Fontana. 1987. T cell suppressor factor from human glioblastoma cells is a 12.5-kd protein closely related to transforming growth factor-beta. *Embo J* 6:1633-1636.

192. R. de Martin, B. Haendler, R. Hofer-Warbinek, H. Gaugitsch, M. Wrann, H. Schlüsener, J. M. Seifert, S. Bodmer, A. Fontana and E. Hofer. 1987. Complementary DNA for human glioblastoma-derived T cell suppressor factor, a novel member of the transforming growth factor-beta gene family. *Embo J* 6:3673-3677.

193. M. Platten, W. Wick and M. Weller. 2001. Malignant glioma biology: role for TGF-β in growth, motility, angiogenesis, and immune escape. *Microsc Res Tech* 52:401-410.

194. R. Castriconi, C. Cantoni, M. Della Chiesa, M. Vitale, E. Marcenaro, R. Conte, R. Biassoni, C. Bottino, L. Moretta and A. Moretta. 2003. Transforming growth factor-β 1 inhibits expression of NKp30 and NKG2D receptors: consequences for the NK-mediated killing of dendritic cells. *Proc Natl Acad Sci U S A* 100:4120-4125.

195. Y. Cho, S. Gorina, P. D. Jeffrey and N. P. Pavletich. 1994. Crystal structure of a p53 tumour suppressor-DNA complex: understanding tumorigenic mutations. *Science* 265:346-355.

196. F. Schmidt, J. Rieger, J. Wischhusen, U. Naumann and M. Weller. 2001. Glioma cell sensitivity to topotecan: the role of p53 and topotecan-induced DNA damage. *Eur J Pharmacol* 412:21-25.

197. M. Weller, J. Rieger, C. Grimmel, E. G. Van Meir, N. De Tribolet, S. Krajewski, J. C. Reed, A. Von Deimling and J. Dichgans. 1998. Predicting chemoresistance in human

malignant glioma cells: the role of molecular genetic analyses. *Int J Cancer* 79:640-644.

198. M. Weller, A. M. Marini and S. M. Paul. 1992. Niacinamide blocks 3-acetylpyridine toxicity of cerebellar granule cells in vitro. *Brain Res* 594:160-164.
199. J. P. Morgenstern and H. Land. 1990. A series of mammalian expression vectors and characterisation of their expression of a reporter gene in stably and transiently transfected cells. *Nucleic Acids Res* 18:1068.
200. U. Naumann, S. Durka and M. Weller. 1998. Dexamethasone-mediated protection from drug cytotoxicity: association with p21WAF1/CIP1 protein accumulation? *Oncogene* 17:1567-1575.
201. Z. Y. Jiang, A. C. Woollard and S. P. Wolff. 1991. Lipid hydroperoxide measurement by oxidation of Fe2+ in the presence of xylenol orange. Comparison with the TBA assay and an iodometric method. *Lipids* 26:853-856.
202. R. Dringen, L. Kussmaul and B. Hamprecht. 1998. Detoxification of exogenous hydrogen peroxide and organic hydroperoxides by cultured astroglial cells assessed by microtiter plate assay. *Brain Res Brain Res Protoc* 2:223-228.
203. U. Naumann, S. Kügler, H. Wolburg, W. Wick, G. Rascher, J. B. Schulz, E. Conseiller, M. Bähr and M. Weller. 2001. Chimeric tumour suppressor 1, a p53-derived chimeric tumour suppressor gene, kills p53 mutant and p53 wild-type glioma cells in synergy with irradiation and CD95 ligand. *Cancer Res* 61:5833-5842.
204. T. Glaser, B. Wagenknecht, P. Groscurth, P. H. Krammer and M. Weller. 1999. Death ligand/receptor-independent caspase activation mediates drug-induced cytotoxic cell death in human malignant glioma cells. *Oncogene* 18:5044-5053.
205. S. Llanos, P. A. Clark, J. Rowe and G. Peters. 2001. Stabilization of p53 by p14ARF without relocation of MDM2 to the nucleolus. *Nat Cell Biol* 3:445-452.
206. W. Wang, R. Takimoto, F. Rastinejad and W. S. El-Deiry. 2003. Stabilization of p53 by CP-31398 inhibits ubiquitination without altering phosphorylation at serine 15 or 20 or MDM2 binding. *Mol Cell Biol* 23:2171-2181.
207. J. Yu, Z. Wang, K. W. Kinzler, B. Vogelstein and L. Zhang. 2003. PUMA mediates the apoptotic response to p53 in colorectal cancer cells. *Proc Natl Acad Sci U S A* 100:1931-1936.
208. W. Wick, C. Grimmel, B. Wagenknecht, J. Dichgans and M. Weller. 1999. Betulinic acid-induced apoptosis in glioma cells: A sequential requirement for new protein

synthesis, formation of reactive oxygen species, and caspase processing. *J Pharmacol Exp Ther* 289:1306-1312.

209. K. Takuma, E. Lee, M. Kidawara, K. Mori, Y. Kimura, A. Baba and T. Matsuda. 1999. Apoptosis in Ca2 + reperfusion injury of cultured astrocytes: roles of reactive oxygen species and NF-kappaB activation. *Eur J Neurosci* 11:4204-4212.
210. S. Kaku, A. Albor and M. Kulesz-Martin. 2001. Dissociation of DNA binding and in vitro transcriptional activities dependent on the C terminus of P53 proteins. *Biochem Biophys Res Commun* 280:204-211.
211. W. Wang, R. Takimoto, D. T. Dicker, F. Rastinejad, J. Lyssikatos and W. S. El-Deiry. 2002. The mutant p53-modifying drug, CP-31398, can induce apoptosis of human cancer cells and can stabilize wild-type p53 protein. *Cancer Biology and Therapy* 1:47-55.
212. Y. Haupt, S. Rowan, E. Shaulian, A. Kazaz, K. Vousden and M. Oren. 1997. p53 mediated apoptosis in HeLa cells: transcription dependent and independent mechanisms. *Leukemia* 11 Suppl 3:337-339.
213. Y. Haupt, S. Rowan, E. Shaulian, K. H. Vousden and M. Oren. 1995. Induction of apoptosis in HeLa cells by trans-activation-deficient p53. *Genes Dev* 9:2170-2183.
214. T. M. Rippin, V. J. Bykov, S. M. Freund, G. Selivanova, K. G. Wiman and A. R. Fersht. 2002. Characterization of the p53-rescue drug CP-31398 in vitro and in living cells. *Oncogene* 21:2119-2129.
215. R. Takimoto, W. Wang, D. T. Dicker, F. Rastinejad, J. Lyssikatos and W. S. El-Deiry. 2002. The mutant p53-conformation modifying drug, CP-31398, can induce apoptosis of human cancer cells and can stabilize wild-type p53 protein. *Cancer Biol Ther* 1:47-55.
216. V. De Laurenzi, A. Costanzo, D. Barcaroli, A. Terrinoni, M. Falco, M. Annicchiarico-Petruzzelli, M. Levrero and G. Melino. 1998. Two new p73 splice variants, gamma and delta, with different transcriptional activity. *J Exp Med* 188:1763-1768.
217. A. Yang, M. Kaghad, Y. Wang, E. Gillett, M. D. Fleming, V. Dötsch, N. C. Andrews, D. Caput and F. McKeon. 1998. p63, a p53 homolog at 3q27-29, encodes multiple products with transactivating, death-inducing, and dominant-negative activities. *Mol Cell* 2:305-316.
218. M. Kaghad, H. Bonnet, A. Yang, L. Creancier, J. C. Biscan, A. Valent, A. Minty, P. Chalon, J. M. Lelias, X. Dumont, P. Ferrara, F. McKeon and D. Caput. 1997.

Monoallelically expressed gene related to p53 at 1p36, a region frequently deleted in neuroblastoma and other human cancers. *Cell* 90:809-819.

219. P. Monti, P. Campomenosi, Y. Ciribilli, R. Iannone, A. Inga, A. Abbondandolo, M. A. Resnick and G. Fronza. 2002. Tumour p53 mutations exhibit promoter selective dominance over wild type p53. *Oncogene* 21:1641-1648.
220. P. Chene. 1998. In vitro analysis of the dominant negative effect of p53 mutants. *J Mol Biol* 281:205-209.
221. J. Milner and E. A. Medcalf. 1991. Cotranslation of activated mutant p53 with wild type drives the wild-type p53 protein into the mutant conformation. *Cell* 65:765-774.
222. K. Bensaad, M. Le Bras, K. Unsal, S. Strano, G. Blandino, O. Tominaga, D. Rouillard and T. Soussi. 2003. Change of conformation of the DNA-binding domain of p53 is the only key element for binding of and interference with p73. *J Biol Chem* 278:10546-10555.
223. C. Gaiddon, M. Lokshin, J. Ahn, T. Zhang and C. Prives. 2001. A subset of tumour-derived mutant forms of p53 down-regulate p63 and p73 through a direct interaction with the p53 core domain. *Mol Cell Biol* 21:1874-1887.
224. J. Wischhusen, U. Naumann, H. Ohgaki, F. Rastinejad and M. Weller. 2003. CP-31398, a novel p53-stabilizing agent, induces p53-dependent and p53-independent glioma cell death. *Oncogene* 22:8233-8245.
225. T. Watanabe, H. Huang, M. Nakamura, J. Wischhusen, M. Weller, P. Kleihues and H. Ohgaki. 2002. Methylation of the p73 gene in gliomas. *Acta Neuropathol (Berl)* 104:357-362.
226. Z. Serber, H. C. Lai, A. Yang, H. D. Ou, M. S. Sigal, A. E. Kelly, B. D. Darimont, P. H. Duijf, H. Van Bokhoven, F. Mckeon and V. Dötsch. 2002. A C-terminal inhibitory domain controls the activity of p63 by an intramolecular mechanism. *Mol Cell Biol* 22:8601-8611.
227. P. Ghioni, F. Bolognese, P. H. Duijf, H. Van Bokhoven, R. Mantovani and L. Guerrini. 2002. Complex transcriptional effects of p63 isoforms: identification of novel activation and repression domains. *Mol Cell Biol* 22:8659-8668.
228. K. Shiraishi, S. Kato, S. Y. Han, W. Liu, K. Otsuka, M. Sakayori, T. Ishida, M. Takeda, R. Kanamaru, N. Ohuchi and C. Ishioka. 2003. Isolation of temperature-sensitive p53 mutations from a comprehensive missense mutation library. *J Biol Chem*.

229. R. Pochampally, C. Li, W. Lu, L. Chen, R. Luftig, J. Lin and J. Chen. 2000. Temperature-sensitive mutants of p53 homologs. *Biochem Biophys Res Commun* 279:1001-1010.

230. A. C. Willis, T. Pipes, J. Zhu and X. Chen. 2003. p73 can suppress the proliferation of cells that express mutant p53. *Oncogene* 22:5481-5495.

231. A. Shimada, S. Kato, K. Enjo, M. Osada, Y. Ikawa, K. Kohno, M. Obinata, R. Kanamaru, S. Ikawa and C. Ishioka. 1999. The transcriptional activities of p53 and its homologue p51/p63: similarities and differences. *Cancer Res* 59:2781-2786.

232. C. J. Di Como, C. Gaiddon and C. Prives. 1999. p73 function is inhibited by tumour-derived p53 mutants in mammalian cells. *Mol Cell Biol* 19:1438-1449.

233. J. Yu, L. Zhang, P. M. Hwang, C. Rago, K. W. Kinzler and B. Vogelstein. 1999. Identification and classification of p53-regulated genes. *Proc Natl Acad Sci U S A* 96:14517-14522.

234. V. De Laurenzi, A. Rossi, A. Terrinoni, D. Barcaroli, M. Levrero, A. Costanzo, R. A. Knight, P. Guerrieri and G. Melino. 2000. p63 and p73 transactivate differentiation gene promoters in human keratinocytes. *Biochem Biophys Res Commun* 273:342-346.

235. C. Perez-Sanchez, V. S. Budhram-Mahadeo and D. S. Latchman. 2002. Distinct promoter elements mediate the co-operative effect of Brn-3a and p53 on the p21 promoter and their antagonism on the Bax promoter. *Nucleic Acids Res* 30:4872-4880.

236. V. Calabro, G. Mansueto, T. Parisi, M. Vivo, R. A. Calogero and G. La Mantia. 2002. The human MDM2 oncoprotein increases the transcriptional activity and the protein level of the p53 homolog p63. *J Biol Chem* 277:2674-2681.

237. D. Bergamaschi, Y. Samuels, N. J. O'neil, G. Trigiante, T. Crook, J. K. Hsieh, D. J. O'connor, S. Zhong, I. Campargue, M. L. Tomlinson, P. E. Kuwabara and X. Lu. 2003. iASPP oncoprotein is a key inhibitor of p53 conserved from worm to human. *Nat Genet* 33:162-167.

238. A. Y. Nikolaev, M. Li, N. Puskas, J. Qin and W. Gu. 2003. Parc: a cytoplasmic anchor for p53. *Cell* 112:29-40.

239. C. Lagresle, C. Bella, P. T. Daniel, P. H. Krammer and T. Defrance. 1995. Regulation of germinal center B cell differentiation. Role of the human APO-1/Fas (CD95) molecule. *J Immunol* 154:5746-5756.

240. T. L. Rothstein, J. K. Wang, D. J. Panka, L. C. Foote, Z. Wang, B. Stanger, H. Cui, S. T. Ju and A. Marshak-Rothstein. 1995. Protection against Fas-dependent Th1-mediated apoptosis by antigen receptor engagement in B cells. *Nature* 374:163-165.

241. K. Büchner, V. Henn, M. Gräfe, O. J. De Boer, A. E. Becker and R. A. Kroczek. 2003. CD40 ligand is selectively expressed on CD4+ T cells and platelets: implications for CD40-CD40L signalling in atherosclerosis. *J Pathol* 201:288-295.

242. V. Henn, J. R. Slupsky, M. Grafe, I. Anagnostopoulos, R. Forster, G. Müller-Berghaus and R. A. Kroczek. 1998. CD40 ligand on activated platelets triggers an inflammatory reaction of endothelial cells. *Nature* 391:591-594.

243. I. Airoldi, S. Lualdi, S. Bruno, L. Raffaghello, M. Occhino, C. Gambini, V. Pistoia and M. V. Corrias. 2003. Expression of costimulatory molecules in human neuroblastoma. Evidence that CD40+ neuroblastoma cells undergo apoptosis following interaction with CD40L. *Br J Cancer* 88:1527-1536.

244. S. Hess, E. Gottfried, H. Smola, U. Grünwald, M. Schuchmann and H. Engelmann. 1998. CD40 induces resistance to TNF-mediated apoptosis in a fibroblast cell line. *Eur J Immunol* 28:3594-3604.

245. A. G. Eliopoulos, C. W. Dawson, G. Mosialos, J. E. Floettmann, M. Rowe, R. J. Armitage, J. Dawson, J. M. Zapata, D. J. Kerr, M. J. Wakelam, J. C. Reed, E. Kieff and L. S. Young. 1996. CD40-induced growth inhibition in epithelial cells is mimicked by Epstein-Barr Virus-encoded LMP1: involvement of TRAF3 as a common mediator. *Oncogene* 13:2243-2254.

246. C. Dallman, P. W. Johnson and G. Packham. 2003. Differential regulation of cell survival by CD40. *Apoptosis* 8:45-53.

247. M. Grell, G. Zimmermann, E. Gottfried, C. M. Chen, U. Grünwald, D. C. Huang, Y. H. Wu Lee, H. Durkop, H. Engelmann, P. Scheurich, H. Wajant and A. Strasser. 1999. Induction of cell death by tumour necrosis factor (TNF) receptor 2, CD40 and CD30: a role for TNF-R1 activation by endogenous membrane-anchored TNF. *Embo J* 18:3034-3043.

248. A. G. Eliopoulos, C. Davies, P. G. Knox, N. J. Gallagher, S. C. Afford, D. H. Adams and L. S. Young. 2000. CD40 induces apoptosis in carcinoma cells through activation of cytotoxic ligands of the tumour necrosis factor superfamily. *Mol Cell Biol* 20:5503-5515.

249. S. C. Afford, J. Ahmed-Choudhury, S. Randhawa, C. Russell, J. Youster, H. A. Crosby, A. Eliopoulos, S. G. Hubscher, L. S. Young and D. H. Adams. 2001. CD40 activation-induced, Fas-dependent apoptosis and NF-kappaB/AP-1 signalling in human intrahepatic biliary epithelial cells. *Faseb J* 15:2345-2354.

250. S. C. Afford, S. Randhawa, A. G. Eliopoulos, S. G. Hubscher, L. S. Young and D. H. Adams. 1999. CD40 activation induces apoptosis in cultured human hepatocytes via induction of cell surface fas ligand expression and amplifies fas-mediated hepatocyte death during allograft rejection. *J Exp Med* 189:441-446.

251. M. Tada, Y. Sawamura, S. Sakuma, K. Suzuki, H. Ohta, T. Aida and H. Abe. 1993. Cellular and cytokine responses of the human central nervous system to intracranial administration of tumour necrosis factor alpha for the treatment of malignant gliomas. *Cancer Immunol Immunother* 36:251-259.

252. W. Roth, S. Isenmann, U. Naumann, S. Kügler, M. Bähr, J. Dichgans, A. Ashkenazi and M. Weller. 1999. Locoregional Apo2L/TRAIL eradicates intracranial human malignant glioma xenografts in athymic mice in the absence of neurotoxicity. *Biochem Biophys Res Commun* 265:479-483.

253. M. Weller, K. Frei, P. Groscurth, P. H. Krammer, Y. Yonekawa and A. Fontana. 1994. Anti-Fas/APO-1 antibody-mediated apoptosis of cultured human glioma cells. Induction and modulation of sensitivity by cytokines. *J Clin Invest* 94:954-964.

254. W. Roth, A. Fontana, M. Trepel, J. C. Reed, J. Dichgans and M. Weller. 1997. Immunochemotherapy of malignant glioma: synergistic activity of CD95 ligand and chemotherapeutics. *Cancer Immunol Immunother* 44:55-63.

255. A. G. Eliopoulos and L. S. Young. 1998. Activation of the cJun N-terminal kinase (JNK) pathway by the Epstein-Barr virus-encoded latent membrane protein 1 (LMP1). *Oncogene* 16:1731-1742.

256. H. Holtmann, R. Winzen, P. Holland, S. Eickemeier, E. Hoffmann, D. Wallach, N. L. Malinin, J. A. Cooper, K. Resch and M. Kracht. 1999. Induction of interleukin-8 synthesis integrates effects on transcription and mRNA degradation from at least three different cytokine- or stress-activated signal transduction pathways. *Mol Cell Biol* 19:6742-6753.

257. G. Jung, U. Freimann, Z. von Marschall, R. A. Reisfeld and W. Wilmanns. 1991. Target cell-induced T cell activation with bi- and trispecific antibody fragments. *Eur J Immunol* 21:2431-2435.

258. J. Dhein, P. T. Daniel, B. C. Trauth, A. Oehm, P. Möller and P. H. Krammer. 1992. Induction of apoptosis by monoclonal antibody anti-APO-1 class switch variants is dependent on cross-linking of APO-1 cell surface antigens. *J Immunol* 149:3166-3173.

259. T. Fernandez, S. Amoroso, S. Sharpe, G. M. Jones, V. Bliskovski, A. Kovalchuk, L. M. Wakefield, S. J. Kim, M. Potter and J. J. Letterio. 2002. Disruption of transforming

growth factor beta signalling by a novel ligand-dependent mechanism. *J Exp Med* 195:1247-1255.

260. M. Tone, Y. Tone, P. J. Fairchild, M. Wykes and H. Waldmann. 2001. Regulation of CD40 function by its isoforms generated through alternative splicing. *Proc Natl Acad Sci U S A* 98:1751-1756.

261. J. Wischhusen, G. Jung, I. Radovanovic, C. Beier, J. P. Steinbach, A. Rimner, H. Huang, J. B. Schulz, H. Ohgaki, A. Aguzzi, H. G. Rammensee and M. Weller. 2002. Identification of CD70-mediated apoptosis of immune effector cells as a novel immune escape pathway of human glioblastoma. *Cancer Res* 62:2592-2599.

262. Weinstock C Weller M, Will C, Wagenknecht B, Dichgans J, Lang F, Gulbins E. 1997. CD95-dependent T cell killing by glioma cells expressing CD95 ligand: more on tumour immune escape, the CD95 counterattack, and the immune privilege of the brain. *Cell Physiol Biochem* 7:282-288.

263. C. Gratas, Y. Tohma, E. G. Van Meir, M. Klein, M. Tenan, N. Ishii, O. Tachibana, P. Kleihues and H. Ohgaki. 1997. Fas ligand expression in glioblastoma cell lines and primary astrocytic brain tumours. *Brain Pathol* 7:863-869.

264. P. Saas, P. R. Walker, M. Hahne, A. L. Quiquerez, V. Schnuriger, G. Perrin, L. French, E. G. van Meir, N. De Tribolet, J. Tschopp and P. Y. Dietrich. 1997. Fas ligand expression by astrocytoma in vivo: maintaining immune privilege in the brain? *J Clin Invest* 99:1173-1178.

265. J. Rieger, H. Ohgaki, P. Kleihues and M. Weller. 1999. Human astrocytic brain tumours express AP02L/TRAIL. *Acta Neuropathol (Berl)* 97:1-4.

266. A. E. Morris, R. L. Remmele, Jr., R. Klinke, B. M. Macduff, W. C. Fanslow and R. J. Armitage. 1999. Incorporation of an isoleucine zipper motif enhances the biological activity of soluble CD40L (CD154). *J Biol Chem* 274:418-423.

267. S. Ghamande, B. L. Hylander, E. Oflazoglu, S. Lele, W. Fanslow and E. A. Repasky. 2001. Recombinant CD40 ligand therapy has significant antitumour effects on CD40-positive ovarian tumour xenografts grown in SCID mice and demonstrates an augmented effect with cisplatin. *Cancer Res* 61:7556-7562.

268. H. Grassmé, J. Bock, J. Kun and E. Gulbins. 2002. Clustering of CD40 ligand is required to form a functional contact with CD40. *J Biol Chem* 277:30289-30299.

269. A. Cremesti, F. Paris, H. Grassmé, N. Holler, J. Tschopp, Z. Fuks, E. Gulbins and R. Kolesnick. 2001. Ceramide enables fas to cap and kill. *J Biol Chem* 276:23954-23961.

270. H. Grassmé, V. Jendrossek, J. Bock, A. Riehle and E. Gulbins. 2002. Ceramide-rich membrane rafts mediate CD40 clustering. *J Immunol* 168:298-307.

271. E. Tani, H. Kitagawa, H. Ikemoto and T. Matsumoto. 2001. Proteasome inhibitors induce Fas-mediated apoptosis by c-Myc accumulation and subsequent induction of FasL message in human glioma cells. *FEBS Lett* 504:53-58.

272. S. Schütze, T. Machleidt, D. Adam, R. Schwandner, K. Wiegmann, M. L. Kruse, M. Heinrich, M. Wickel and M. Kronke. 1999. Inhibition of receptor internalization by monodansylcadaverine selectively blocks p55 tumour necrosis factor receptor death domain signalling. *J Biol Chem* 274:10203-10212.

273. D. F. Legler, O. Micheau, M. A. Doucey, J. Tschopp and C. Bron. 2003. Recruitment of TNF receptor 1 to lipid rafts is essential for TNFalpha-mediated NF-kappaB activation. *Immunity* 18:655-664.

274. B. G. Werneburg, S. J. Zoog, T. T. Dang, M. R. Kehry and J. J. Crute. 2001. Molecular characterization of CD40 signalling intermediates. *J Biol Chem* 276:43334-43342.

275. S. Kreuz, D. Siegmund, P. Scheurich and H. Wajant. 2001. NF-kappaB inducers upregulate cFLIP, a cycloheximide-sensitive inhibitor of death receptor signalling. *Mol Cell Biol* 21:3964-3973.

276. L. Diehl, A. T. Den Boer, S. P. Schoenberger, E. I. Van Der Voort, T. N. Schumacher, C. J. Melief, R. Offringa and R. E. Toes. 1999. CD40 activation in vivo overcomes peptide-induced peripheral cytotoxic T-lymphocyte tolerance and augments anti-tumour vaccine efficacy. *Nat Med* 5:774-779.

277. U. Bugajska, N. T. Georgopoulos, J. Southgate, P. W. Johnson, P. Graber, J. Gordon, P. J. Selby and L. K. Trejdosiewicz. 2002. The effects of malignant transformation on susceptibility of human urothelial cells to CD40-mediated apoptosis. *J Natl Cancer Inst* 94:1381-1395.

278. L. Biancone, V. Cantaluppi, M. Boccellino, L. Del Sorbo, S. Russo, A. Albini, I. Stamenkovic and G. Camussi. 1999. Activation of CD40 favors the growth and vascularization of Kaposi's sarcoma. *J Immunol* 163:6201-6208.

279. R. Batrla, M. Linnebacher, W. Rudy, S. Stumm, D. Wallwiener and B. Gückel. 2002. CD40-expressing carcinoma cells induce down-regulation of CD40 ligand (CD154) and impair T-cell functions. *Cancer Res* 62:2052-2057.

280. L. Tan, K. B. Gordon, J. P. Mueller, L. A. Matis and S. D. Miller. 1998. Presentation of proteolipid protein epitopes and B7-1-dependent activation of encephalitogenic T cells by IFN-gamma-activated SJL/J astrocytes. *J Immunol* 160:4271-4279.

281. F. Aloisi, G. Penna, E. Polazzi, L. Minghetti and L. Adorini. 1999. CD40-CD154 interaction and IFN-gamma are required for IL-12 but not prostaglandin E2 secretion by microglia during antigen presentation to Th1 cells. *J Immunol* 162:1384-1391.

282. Y. Ruan, S. Rabizadeh, D. Camerini and D. E. Bredesen. 1997. Expression of CD40 induces neural apoptosis. *J Neurosci Res* 50:383-390.

283. J. Tan, T. Town, T. Mori, D. Obregon, Y. Wu, A. Delledonne, A. Rojiani, F. Crawford, R. A. Flavell and M. Mullan. 2002. CD40 is expressed and functional on neuronal cells. *Embo J* 21:643-652.

284. F. K. Chan, H. J. Chun, L. Zheng, R. M. Siegel, K. L. Bui and M. J. Lenardo. 2000. A domain in TNF receptors that mediates ligand-independent receptor assembly and signalling. *Science* 288:2351-2354.

285. N. J. Gallagher, A. G. Eliopoulos, A. Agathangelo, J. Oates, J. Crocker and L. S. Young. 2002. CD40 activation in epithelial ovarian carcinoma cells modulates growth, apoptosis, and cytokine secretion. *Mol Pathol* 55:110-120.

286. E. E. Varfolomeev, M. P. Boldin, T. M. Goncharov and D. Wallach. 1996. A potential mechanism of "cross-talk" between the p55 tumour necrosis factor receptor and Fas/APO1: proteins binding to the death domains of the two receptors also bind to each other. *J Exp Med* 183:1271-1275.

287. P. Juo, C. J. Kuo, J. Yuan and J. Blenis. 1998. Essential requirement for caspase-8/FLICE in the initiation of the Fas-induced apoptotic cascade. *Curr Biol* 8:1001-1008.

288. W. C. Yeh, J. L. Pompa, M. E. Mccurrach, H. B. Shu, A. J. Elia, A. Shahinian, M. Ng, A. Wakeham, W. Khoo, K. Mitchell, W. S. El-Deiry, S. W. Lowe, D. V. Goeddel and T. W. Mak. 1998. FADD: essential for embryo development and signalling from some, but not all, inducers of apoptosis. *Science* 279:1954-1958.

289. H. Hsu, H. B. Shu, M. G. Pan and D. V. Goeddel. 1996. TRADD-TRAF2 and TRADD-FADD interactions define two distinct TNF receptor 1 signal transduction pathways. *Cell* 84:299-308.

290. N. Harper, M. Hughes, M. Macfarlane and G. M. Cohen. 2003. Fas-associated death domain protein and caspase-8 are not recruited to the tumour necrosis factor receptor 1

signalling complex during tumour necrosis factor-induced apoptosis. *J Biol Chem* 278:25534-25541.

291. F. H. Igney and P. H. Krammer. 2002. Death and anti-death: tumour resistance to apoptosis. *Nat Rev Cancer* 2:277-288.
292. J. Leitlein, S. Aulwurm, R. Waltereit, U. Naumann, B. Wagenknecht, W. Garten, M. Weller and M. Platten. 2001. Processing of immunosuppressive pro-tgf-beta1,2 by human glioblastoma cells involves cytoplasmic and secreted furin-like proteases. *J Immunol* 166:7238-7243.
293. P. Y. Dietrich, P. R. Walker, P. Saas and N. De Tribolet. 1997. Immunobiology of gliomas: new perspectives for therapy. *Ann N Y Acad Sci* 824:124-140.
294. T. Roszman, L. Elliott and W. Brooks. 1991. Modulation of T-cell function by gliomas. *Immunol Today* 12:370-374.
295. C. Münz, U. Naumann, C. Grimmel, H. G. Rammensee and M. Weller. 1999. TGF-beta-independent induction of immunogenicity by decorin gene transfer in human malignant glioma cells. *Eur J Immunol* 29:1032-1040.
296. J. P. Zou, L. A. Morford, C. Chougnet, A. R. Dix, A. G. Brooks, N. Torres, J. D. Shuman, J. E. Coligan, W. H. Brooks, T. L. Roszman and G. M. Shearer. 1999. Human glioma-induced immunosuppression involves soluble factor(s) that alters monocyte cytokine profile and surface markers. *J Immunol* 162:4882-4892.
297. M. R. Bowman, M. A. Crimmins, J. Yetz-Aldape, R. Kriz, K. Kelleher and S. Herrmann. 1994. The cloning of CD70 and its identification as the ligand for CD27. *J Immunol* 152:1756-1761.
298. R. G. Goodwin, M. R. Alderson, C. A. Smith, R. J. Armitage, T. Vandenbos, R. Jerzy, T. W. Tough, M. A. Schoenborn, T. Davis-Smith and K. Hennen. 1993. Molecular and biological characterization of a ligand for CD27 defines a new family of cytokines with homology to tumour necrosis factor. *Cell* 73:447-456.
299. H. Akiba, H. Oshima, K. Takeda, M. Atsuta, H. Nakano, A. Nakajima, C. Nohara, H. Yagita and K. Okumura. 1999. CD28-independent costimulation of T cells by OX40 ligand and CD70 on activated B cells. *J Immunol* 162:7058-7066.
300. D. Brugnoni, P. Airo, R. Marino, L. D. Notarangelo, R. A. Van Lier and R. Cattaneo. 1997. CD70 expression on T-cell subpopulations: study of normal individuals and patients with chronic immune activation. *Immunol Lett* 55:99-104.

301. S. M. Lens, P. A. Baars, B. Hooibrink, M. H. van Oers and R. A. van Lier. 1997. Antigen-presenting cell-derived signals determine expression levels of CD70 on primed T cells. *Immunology* 90:38-45.

302. S. M. Lens, K. Tesselaar, M. H. van Oers and R. A. van Lier. 1998. Control of lymphocyte function through CD27-CD70 interactions. *Semin Immunol* 10:491-499.

303. A. M. Orengo, C. Cantoni, F. Neglia, R. Biassoni and S. Ferrini. 1997. Reciprocal expression of CD70 and of its receptor, CD27, in human long term-activated T and natural killer (NK) cells: inverse regulation by cytokines and role in induction of cytotoxicity. *Clin Exp Immunol* 107:608-613.

304. H. Nagumo, K. Agematsu, K. Shinozaki, S. Hokibara, S. Ito, M. Takamoto, T. Nikaido, K. Yasui, Y. Uehara, A. Yachie and A. Komiyama. 1998. CD27/CD70 interaction augments IgE secretion by promoting the differentiation of memory B cells into plasma cells. *J Immunol* 161:6496-6502.

305. K. Agematsu, S. Hokibara, H. Nagumo, K. Shinozaki, S. Yamada and A. Komiyama. 1999. Plasma cell generation from B-lymphocytes via CD27/CD70 interaction. *Leuk Lymphoma* 35:219-225.

306. G. Stuhler, A. Zobywalski, F. Grünebach, P. Brossart, V. L. Reichardt, H. Barth, S. Stevanovic, W. Brugger, L. Kanz and S. F. Schlossman. 1999. Immune regulatory loops determine productive interactions within human T lymphocyte-dendritic cell clusters. *Proc Natl Acad Sci U S A* 96:1532-1535.

307. F. C. Yang, K. Agematsu, T. Nakazawa, T. Mori, S. Ito, T. Kobata, C. Morimoto and A. Komiyama. 1996. CD27/CD70 interaction directly induces natural killer cell killing activity. *Immunology* 88:289-293.

308. G. R. Brown, K. Meek, Y. Nishioka and D. L. Thiele. 1995. CD27-CD27 ligand/CD70 interactions enhance alloantigen-induced proliferation and cytolytic activity in CD8+ T lymphocytes. *J Immunol* 154:3686-3695.

309. V. S. Raman, V. Bal, S. Rath and A. George. 2000. Ligation of CD27 on murine B cells responding to T-dependent and T-independent stimuli inhibits the generation of plasma cells. *J Immunol* 165:6809-6815.

310. K. Sugita, T. Tanaka, J. M. Doshen, S. F. Schlossman and C. Morimoto. 1993. Direct demonstration of the CD27 molecule involved in the negative regulatory effect on T cell activation. *Cell Immunol* 152:279-285.

311. T. Kobata, S. Jacquot, S. Kozlowski, K. Agematsu, S. F. Schlossman and C. Morimoto. 1995. CD27-CD70 interactions regulate B-cell activation by T cells. *Proc Natl Acad Sci U S A* 92:11249-11253.

312. J. Hendriks, L. A. Gravestein, K. Tesselaar, R. A. Van Lier, T. N. Schumacher and J. Borst. 2000. CD27 is required for generation and long-term maintenance of T cell immunity. *Nat Immunol* 1:433-440.

313. R. Arens, K. Tesselaar, P. A. Baars, G. M. Van Schijndel, J. Hendriks, S. T. Pals, P. Krimpenfort, J. Borst, M. H. van Oers and R. A. van Lier. 2001. Constitutive CD27/CD70 interaction induces expansion of effector-type T cells and results in IFNgamma-mediated B cell depletion. *Immunity* 15:801-812.

314. K. Tesselaar, R. Arens, G. M. van Schijndel, P. A. Baars, M. A. van der Valk, J. Borst, M. H. van Oers and R. A. van Lier. 2003. Lethal T cell immunodeficiency induced by chronic costimulation via CD27-CD70 interactions. *Nat Immunol* 4:49-54.

315. E. A. Ranheim, M. J. Cantwell and T. J. Kipps. 1995. Expression of CD27 and its ligand, CD70, on chronic lymphocytic leukemia B cells. *Blood* 85:3556-3565.

316. M. H. Van Oers, S. T. Pals, L. M. Evers, C. E. Van Der Schoot, G. Koopman, J. M. Bonfrer, R. Q. Hintzen, A. E. Von Dem Borne and R. A. Van Lier. 1993. Expression and release of CD27 in human B-cell malignancies. *Blood* 82:3430-3436.

317. R. Zambello, L. Trentin, M. Facco, M. Siviero, S. Galvan, F. Piazza, A. Perin, C. Agostini and G. Semenzato. 2000. Analysis of TNF-receptor and ligand superfamily molecules in patients with lymphoproliferative disease of granular lymphocytes. *Blood* 96:647-654.

318. H. Huang, S. Colella, M. Kurrer, Y. Yonekawa, P. Kleihues and H. Ohgaki. 2000. Gene expression profiling of low-grade diffuse astrocytomas by cDNA arrays. *Cancer Res* 60:6868-6874.

319. K. Agematsu, T. Kobata, K. Sugita, G. J. Freeman, M. P. Beckmann, S. F. Schlossman and C. Morimoto. 1994. Role of CD27 in T cell immune response. Analysis by recombinant soluble CD27. *J Immunol* 153:1421-1429.

320. S. M. Lens, P. Drillenburg, B. F. Den Drijver, G. Van Schijndel, S. T. Pals, R. A. Van Lier and M. H. Van Oers. 1999. Aberrant expression and reverse signalling of CD70 on malignant B cells. *Br J Haematol* 106:491-503.

321. V. A. Fadok, D. L. Bratton, D. M. Rose, A. Pearson, R. A. Ezekewitz and P. M. Henson. 2000. A receptor for phosphatidylserine-specific clearance of apoptotic cells. *Nature* 405:85-90.

322. R. Q. Hintzen, R. De Jong, C. E. Hack, M. Chamuleau, E. F. De Vries, I. J. Ten Berge, J. Borst and R. A. Van Lier. 1991. A soluble form of the human T cell differentiation antigen CD27 is released after triggering of the TCR/CD3 complex. *J Immunol* 147:29-35.

323. W. A. Loenen, E. De Vries, L. A. Gravestein, R. Q. Hintzen, R. A. van Lier and J. Borst. 1992. The CD27 membrane receptor, a lymphocyte-specific member of the nerve growth factor receptor family, gives rise to a soluble form by protein processing that does not involve receptor endocytosis. *Eur J Immunol* 22:447-455.

324. R. Q. Hintzen, R. A. van Lier, K. C. Kuijpers, P. A. Baars, W. Schaasberg, C. J. Lucas and C. H. Polman. 1991. Elevated levels of a soluble form of the T cell activation antigen CD27 in cerebrospinal fluid of multiple sclerosis patients. *J Neuroimmunol* 35:211-217.

325. J. Held-Feindt and R. Mentlein. 2002. CD70/CD27 ligand, a member of the TNF family, is expressed in human brain tumours. *Int J Cancer* 98:352-356.

326. J. D. Nieland, Y. F. Graus, Y. E. Dortmans, B. L. Kremers and A. M. Kruisbeek. 1998. CD40 and CD70 co-stimulate a potent in vivo antitumour T cell response. *J Immunother* 21:225-236.

327. B. Couderc, L. Zitvogel, V. Douin-Echinard, L. Djennane, H. Tahara, G. Favre, M. T. Lotze and P. D. Robbins. 1998. Enhancement of antitumour immunity by expression of CD70 (CD27 ligand) or CD154 (CD40 ligand) costimulatory molecules in tumour cells. *Cancer Gene Ther* 5:163-175.

328. M. G. Lorenz, J. A. Kantor, J. Schlom and J. W. Hodge. 1999. Anti-tumour immunity elicited by a recombinant vaccinia virus expressing CD70 (CD27L). *Hum Gene Ther* 10:1095-1103.

329. J. M. Kelly, P. K. Darcy, J. L. Markby, D. I. Godfrey, K. Takeda, H. Yagita and M. J. Smyth. 2002. Induction of tumour-specific T cell memory by NK cell-mediated tumour rejection. *Nat Immunol* 3:83-90.

330. R. M. Siegel, F. K. Chan, H. J. Chun and M. J. Lenardo. 2000. The multifaceted role of Fas signalling in immune cell homeostasis and autoimmunity. *Nat Immunol* 1:469-474.

331. S. Jacquot, T. Kobata, S. Iwata, S. F. Schlossman and C. Morimoto. 1997. CD27/CD70 interaction contributes to the activation and the function of human autoreactive CD27+ regulatory T cells. *Cell Immunol* 179:48-54.

332. Y. Yoon, Z. Ao, Y. Cheng, S. F. Schlossman and K. V. Prasad. 1999. Murine Siva-1 and Siva-2, alternate splice forms of the mouse Siva gene, both bind to CD27 but differentially transduce apoptosis. *Oncogene* 18:7174-7179.

333. B. Py, C. Slomianny, P. Auberger, P. X. Petit and S. Benichou. 2004. Siva-1 and an alternative splice form lacking the death domain, Siva-2, similarly induce apoptosis in T lymphocytes via a caspase-dependent mitochondrial pathway. *J Immunol* 172:4008-4017.

334. L. Xue, F. Chu, Y. Cheng, X. Sun, A. Borthakur, M. Ramarao, P. Pandey, M. Wu, S. F. Schlossman and K. V. Prasad. 2002. Siva-1 binds to and inhibits BCL-X(L)-mediated protection against UV radiation-induced apoptosis. *Proc Natl Acad Sci U S A* 99:6925-6930.

335. A. Nakajima, H. Oshima, C. Nohara, S. Morimoto, S. Yoshino, T. Kobata, H. Yagita and K. Okumura. 2000. Involvement of CD70-CD27 interactions in the induction of experimental autoimmune encephalomyelitis. *J Neuroimmunol* 109:188-196.

336. J. Font, L. Pallares, J. Martorell, E. Martinez, A. Gaya, J. Vives and M. Ingelmo. 1996. Elevated soluble CD27 levels in serum of patients with systemic lupus erythematosus. *Clin Immunol Immunopathol* 81:239-243.

337. R. Q. Hintzen, D. Paty and J. Oger. 1999. Cerebrospinal fluid concentrations of soluble CD27 in HTLV-I associated myelopathy and multiple sclerosis. *J Neurol Neurosurg Psychiatry* 66:791-793.

338. P. P. Tak, R. Q. Hintzen, J. J. Teunissen, T. J. Smeets, M. R. Daha, R. A. van Lier, P. M. Kluin, A. E. Meinders, A. J. Swaak and F. C. Breedveld. 1996. Expression of the activation antigen CD27 in rheumatoid arthritis. *Clin Immunol Immunopathol* 80:129-138.

339. F. M. Marincola, P. Shamamian, R. B. Alexander, J. R. Gnarra, R. L. Turetskaya, S. A. Nedospasov, T. B. Simonis, J. K. Taubenberger, J. Yannelli, and A. Mixon. 1994. Loss of HLA haplotype and B locus down-regulation in melanoma cell lines. *J Immunol* 153:1225-1237.

340. S. Kovats, E. K. Main, C. Librach, M. Stubblebine, S. J. Fisher and R. Demars. 1990. A class I antigen, HLA-G, expressed in human trophoblasts. *Science* 248:220-223.

341. L. Crisa, M. T. Mcmaster, J. K. Ishii, S. J. Fisher and D. R. Salomon. 1997. Identification of a thymic epithelial cell subset sharing expression of the class Ib HLA-G molecule with foetal trophoblasts. *J Exp Med* 186:289-298.

342. Y. Yang, W. Chu, D. E. Geraghty and J. S. Hunt. 1996. Expression of HLA-G in human mononuclear phagocytes and selective induction by IFN-gamma. *J Immunol* 156:4224-4231.

343. H. Wiendl, L. Behrens, S. Maier, M. A. Johnson, E. H. Weiss and R. Hohlfeld. 2000. Muscle fibers in inflammatory myopathies and cultured myoblasts express the nonclassical major histocompatibility antigen HLA-G. *Ann Neurol* 48:679-684.

344. P. Paul, N. Rouas-Freiss, I. Khalil-Daher, P. Moreau, B. Riteau, F. A. Le Gal, M. F. Avril, J. Dausset, J. G. Guillet and E. D. Carosella. 1998. HLA-G expression in melanoma: a way for tumour cells to escape from immunosurveillance. *Proc Natl Acad Sci U S A* 95:4510-4515.

345. S. K. Sanders, P. A. Giblin and P. Kavathas. 1991. Cell-cell adhesion mediated by CD8 and human histocompatibility leukocyte antigen G, a nonclassical major histocompatibility complex class 1 molecule on cytotrophoblasts. *J Exp Med* 174:737-740.

346. C. Münz, S. Stevanovic and H. G. Rammensee. 1999. Peptide presentation and NK inhibition by HLA-G. *J Reprod Immunol* 43:139-155.

347. C. Münz, P. Nickolaus, E. Lammert, S. Pascolo, S. Stevanovic and H. G. Rammensee. 1999. The role of peptide presentation in the physiological function of HLA-G. *Semin Cancer Biol* 9:47-54.

348. M. Diehl, C. Münz, W. Keilholz, S. Stevanovic, N. Holmes, Y. W. Loke and H. G. Rammensee. 1996. Nonclassical HLA-G molecules are classical peptide presenters. *Curr Biol* 6:305-314.

349. O. Mandelboim, L. Pazmany, D. M. Davis, M. Vales-Gomez, H. T. Reyburn, B. Rybalov and J. L. Strominger. 1997. Multiple receptors for HLA-G on human natural killer cells. *Proc Natl Acad Sci U S A* 94:14666-14670.

350. C. Münz, N. Holmes, A. King, Y. W. Loke, M. Colonna, H. Schild and H. G. Rammensee. 1997. Human histocompatibility leukocyte antigen (HLA)-G molecules inhibit NKAT3 expressing natural killer cells. *J Exp Med* 185:385-391.

351. N. Rouas-Freiss, R. E. Marchal, M. Kirszenbaum, J. Dausset and E. D. Carosella. 1997. The alpha1 domain of HLA-G1 and HLA-G2 inhibits cytotoxicity induced by natural killer cells: is HLA-G the public ligand for natural killer cell inhibitory receptors? *Proc Natl Acad Sci U S A* 94:5249-5254.

352. F. A. Le Gal, B. Riteau, C. Sedlik, I. Khalil-Daher, C. Menier, J. Dausset, J. G. Guillet, E. D. Carosella and N. Rouas-Freiss. 1999. HLA-G-mediated inhibition of antigen-specific cytotoxic T lymphocytes. *Int Immunol* 11:1351-1356.

353. S. Fournel, M. Aguerre-Girr, X. Huc, F. Lenfant, A. Alam, A. Toubert, A. Bensussan and P. Le Bouteiller. 2000. Cutting edge: soluble HLA-G1 triggers CD95/CD95 ligand-mediated apoptosis in activated CD8+ cells by interacting with CD8. *J Immunol* 164:6100-6104.

354. M. Weller, S. Winter, C. Schmidt, P. Esser, A. Fontana, J. Dichgans and P. Groscurth. 1997. Topoisomerase-I inhibitors for human malignant glioma: differential modulation of p53, p21, bax and bcl-2 expression and of CD95-mediated apoptosis by camptothecin and beta-lapachone. *Int J Cancer* 73:707-714.

355. G. Engler-Blum, M. Meier, J. Frank and G. A. Müller. 1993. Reduction of background problems in nonradioactive northern and Southern blot analyses enables higher sensitivity than ^{32}P-based hybridizations. *Anal Biochem* 210:235-244.

356. M. Ulbrecht, T. Honka, S. Person, J. P. Johnson and E. H. Weiss. 1992. The HLA-E gene encodes two differentially regulated transcripts and a cell surface protein. *J Immunol* 149:2945-2953.

357. A. de Baey, B. Fellerhoff, S. Maier, S. Martinozzi, U. Weidle and E. H. Weiss. 1997. Complex expression pattern of the TNF region gene LST1 through differential regulation, initiation, and alternative splicing. *Genomics* 45:591-600.

358. M. M. Bradford. 1976. A rapid and sensitive method for the quantitation of microgram quantities of protein utilizing the principle of protein-dye binding. *Anal Biochem* 72:248-254.

359. S. Maier, D. E. Geraghty and E. H. Weiss. 1999. Expression and regulation of HLA-G in human glioma cell lines. *Transplant Proc* 31:1849-1853.

360. N. Rouas-Freiss, R. M. Goncalves, C. Menier, J. Dausset and E. D. Carosella. 1997. Direct evidence to support the role of HLA-G in protecting the fetus from maternal uterine natural killer cytolysis. *Proc Natl Acad Sci U S A* 94:11520-11525.

361. B. Riteau, C. Menier, I. Khalil-Daher, S. Martinozzi, M. Pla, J. Dausset, E. D. Carosella and N. Rouas-Freiss. 2001. HLA-G1 co-expression boosts the HLA class I-mediated NK lysis inhibition. *Int Immunol* 13:193-201.

362. D. R. Bainbridge, S. A. Ellis and I. L. Sargent. 2000. HLA-G suppresses proliferation of CD4(+) T-lymphocytes. *J Reprod Immunol* 48:17-26.

363. K. Kapasi, S. E. Albert, S. Yie, N. Zavazava and C. L. Librach. 2000. HLA-G has a concentration-dependent effect on the generation of an allo-CTL response. *Immunology* 101:191-200.

364. N. Zavazava and M. Kronke. 1996. Soluble HLA class I molecules induce apoptosis in alloreactive cytotoxic T lymphocytes. *Nat Med* 2:1005-1010.

365. N. Lila, N. Rouas-Freiss, J. Dausset, A. Carpentier and E. D. Carosella. 2001. Soluble HLA-G protein secreted by allo-specific CD4+ T cells suppresses the allo-proliferative response: a CD4+ T cell regulatory mechanism. *Proc Natl Acad Sci U S A* 98:12150-12155.

366. P. Paul, F. A. Cabestre, F. A. Le Gal, I. Khalil-Daher, C. Le Danff, M. Schmid, S. Mercier, M. F. Avril, J. Dausset, J. G. Guillet and E. D. Carosella. 1999. Heterogeneity of HLA-G gene transcription and protein expression in malignant melanoma biopsies. *Cancer Res* 59:1954-1960.

367. Y. Fukushima, Y. Oshika, M. Nakamura, T. Tokunaga, H. Hatanaka, Y. Abe, H. Yamazaki, H. Kijima, Y. Ueyama and N. Tamaoki. 1998. Increased expression of human histocompatibility leukocyte antigen-G in colorectal cancer cells. *Int J Mol Med* 2:349-351.

368. C. Pangault, L. Amiot, S. Caulet-Maugendre, F. Brasseur, F. Burtin, V. Guilloux, B. Drenou, R. Fauchet and M. Onno. 1999. HLA-G protein expression is not induced during malignant transformation. *Tissue Antigens* 53:335-346.

369. E. C. Ibrahim, N. Guerra, M. J. Lacombe, E. Angevin, S. Chouaib, E. D. Carosella, A. Caignard and P. Paul. 2001. Tumour-specific up-regulation of the nonclassical class I HLA-G antigen expression in renal carcinoma. *Cancer Res* 61:6838-6845.

370. S. N. Wagner, V. Rebmann, C. P. Willers, H. Grosse-Wilde and M. Goos. 2000. Expression analysis of classic and non-classic HLA molecules before interferon alfa-2b treatment of melanoma. *Lancet* 356:220-221.

371. G. Frumento, S. Franchello, G. L. Palmisano, M. R. Nicotra, P. Giacomini, Y. W. Loke, D. E. Geraghty, M. Maio, C. Manzo, P. G. Natali and G. B. Ferrara. 2000. Melanomas and melanoma cell lines do not express HLA-G, and the expression cannot be induced by IFN-γ treatment. *Tissue Antigens* 56:30-37.

372. B. Davies, S. Hiby, L. Gardner, Y. W. Loke and A. King. 2001. HLA-G expression by tumours. *Am J Reprod Immunol* 45:103-107.

373. L. M. Real, T. Cabrera, A. Collado, P. Jimenez, A. Garcia, F. Ruiz-Cabello and F. Garrido. 1999. Expression of HLA G in human tumours is not a frequent event. *Int J Cancer* 81:512-518.

374. L. M. Real, T. Cabrera, J. Canton, R. Oliva, F. Ruiz-Cabello and F. Garrido. 1999. Looking for HLA-G expression in human tumours. *J Reprod Immunol* 43:263-273.

375. A. Blaschitz, H. Hutter, V. Leitner, S. Pilz, R. Wintersteiger, G. Dohr and P. Sedlmayr. 2000. Reaction patterns of monoclonal antibodies to HLA-G in human tissues and on cell lines: a comparative study. *Hum Immunol* 61:1074-1085.

376. P. Paul, N. Rouas-Freiss, P. Moreau, F. A. Cabestre, C. Menier, I. Khalil-Daher, C. Pangault, M. Onno, R. Fauchet, J. Martinez-Laso, P. Morales, A. A. Villena, P. Giacomini, P. G. Natali, G. Frumento, G. B. Ferrara, M. Mcmaster, S. Fisher, D. Schust, S. Ferrone, J. Dausset, D. Geraghty and E. D. Carosella. 2000. HLA-G, -E, -F preworkshop: tools and protocols for analysis of non-classical class I genes transcription and protein expression. *Hum Immunol* 61:1177-1195.

377. H. Fakhrai, O. Dorigo, D. L. Shawler, H. Lin, D. Mercola, K. L. Black, I. Royston and R. E. Sobol. 1996. Eradication of established intracranial rat gliomas by transforming growth factor beta antisense gene therapy. *Proc Natl Acad Sci U S A* 93:2909-2914.

378. M. Ständer, U. Naumann, L. Dumitrescu, M. Heneka, P. Löschmann, E. Gulbins, J. Dichgans and M. Weller. 1998. Decorin gene transfer-mediated suppression of TGF-beta synthesis abrogates experimental malignant glioma growth in vivo. *Gene Ther* 5:1187-1194.

379. M. Platten, W. Wick, J. Wischhusen and M. Weller. 2001. N-[3,4-dimethoxycinnamoyl]-anthranilic acid (tranilast) suppresses microglial inducible nitric oxide synthase (iNOS) expression and activity induced by interferon-gamma (IFN-gamma). *Br J Pharmacol* 134:1279-1284.

380. A. Fontana, F. Kristensen, R. Dubs, D. Gemsa and E. Weber. 1982. Production of prostaglandin E and an interleukin-1 like factor by cultured astrocytes and C6 glioma cells. *J Immunol* 129:2413-2419.

381. M. Hishii, T. Nitta, H. Ishida, M. Ebato, A. Kurosu, H. Yagita, K. Sato and K. Okumura. 1995. Human glioma-derived interleukin-10 inhibits antitumour immune responses in vitro. *Neurosurgery* 37:1160-1166; discussion 1166-1167.

382. H. Wiendl, M. Mitsdoerffer, V. Hofmeister, J. Wischhusen, A. Bornemann, R. Meyermann, E. H. Weiss, A. Melms and M. Weller. 2002. A functional role of HLA-

G expression in human gliomas: an alternative strategy of immune escape. *J Immunol* 168:4772-4780.

383. W. Wick, C. Grimmel, C. Wild-Bode, M. Platten, M. Arpin and M. Weller. 2001. Ezrin-dependent promotion of glioma cell clonogenicity, motility, and invasion mediated by BCL-2 and transforming growth factor-β2. *J Neurosci* 21:3360-3368.
384. N. M. Valiante, M. Rengaraju and G. Trinchieri. 1992. Role of the production of natural killer cell stimulatory factor (NKSF/IL-12) in the ability of B cell lines to stimulate T and NK cell proliferation. *Cell Immunol* 145:187-198.
385. J. L. Wrana, L. Attisano, J. Carcamo, A. Zentella, J. Doody, M. Laiho, X. F. Wang and J. Massagué. 1992. TGF-β signals through a heteromeric protein kinase receptor complex. *Cell* 71:1003-1014.
386. L. Zawel, J. L. Dai, P. Buckhaults, S. Zhou, K. W. Kinzler, B. Vogelstein and S. E. Kern. 1998. Human Smad3 and Smad4 are sequence-specific transcription activators. *Mol Cell* 1:611-617.
387. M. Tamaki, W. Mcdonald, V. R. Amberger, E. Moore and R. F. Del Maestro. 1997. Implantation of C6 astrocytoma spheroid into collagen type I gels: invasive, proliferative, and enzymatic characterizations. *J Neurosurg* 87:602-609.
388. R. D. Serano, C. N. Pegram and D. D. Bigner. 1980. Tumorigenic cell culture lines from a spontaneous VM/Dk murine astrocytoma (SMA). *Acta Neuropathol (Berl)* 51:53-64.
389. Y. A. Yang, O. Dukhanina, B. Tang, M. Mamura, J. J. Letterio, J. Macgregor, S. C. Patel, S. Khozin, Z. Y. Liu, J. Green, M. R. Anver, G. Merlino and L. M. Wakefield. 2002. Lifetime exposure to a soluble TGF-β antagonist protects mice against metastasis without adverse side effects. *J Clin Invest* 109:1607-1615.
390. L. Gorelik, S. Constant and R. A. Flavell. 2002. Mechanism of transforming growth factor-β-induced inhibition of T helper type 1 differentiation. *J Exp Med* 195:1499-1505.
391. G. Thomas. 2002. Furin at the cutting edge: from protein traffic to embryogenesis and disease. *Nat Rev Mol Cell Biol* 3:753-766.
392. R. S. Muraoka, N. Dumont, C. A. Ritter, T. C. Dugger, D. M. Brantley, J. Chen, E. Easterly, L. R. Roebuck, S. Ryan, P. J. Gotwals, V. Koteliansky and C. L. Arteaga. 2002. Blockade of TGF-β inhibits mammary tumour cell viability, migration, and metastases. *J Clin Invest* 109:1551-1559.

393. A. Fontana, H. Hengartner, N. De Tribolet and E. Weber. 1984. Glioblastoma cells release interleukin 1 and factors inhibiting interleukin 2-mediated effects. *J Immunol* 132:1837-1844.

394. D. M. Ashley, F. M. Kong, D. D. Bigner and L. P. Hale. 1998. Endogenous expression of transforming growth factor-β1 inhibits growth and tumorigenicity and enhances Fas-mediated apoptosis in a murine high-grade glioma model. *Cancer Res* 58:302-309.

395. A. Diefenbach, A. M. Jamieson, S. D. Liu, N. Shastri and D. H. Raulet. 2000. Ligands for the murine NKG2D receptor: expression by tumour cells and activation of NK cells and macrophages. *Nat Immunol* 1:119-126.

396. H. Das, V. Groh, C. Kuijl, M. Sugita, C. T. Morita, T. Spies and J. F. Bukowski. 2001. MICA engagement by human Vγ2Vδ2 T cells enhances their antigen-dependent effector function. *Immunity* 15:83-93.

397. V. Groh, R. Rhinehart, J. Randolph-Habecker, M. S. Topp, S. R. Riddell and T. Spies. 2001. Costimulation of CD8αβ T cells by NKG2D via engagement by MIC induced on virus-infected cells. *Nat Immunol* 2:255-260.

398. S. Bahram, M. Bresnahan, D. E. Geraghty and T. Spies. 1994. A second lineage of mammalian major histocompatibility complex class I genes. *Proc Natl Acad Sci U S A* 91:6259-6263.

399. V. Groh, S. Bahram, S. Bauer, A. Herman, M. Beauchamp and T. Spies. 1996. Cell stress-regulated human major histocompatibility complex class I gene expressed in gastrointestinal epithelium. *Proc Natl Acad Sci U S A* 93:12445-12450.

400. P. Li, D. L. Morris, B. E. Willcox, A. Steinle, T. Spies and R. K. Strong. 2001. Complex structure of the activating immunoreceptor NKG2D and its MHC class I-like ligand MICA. *Nat Immunol* 2:443-451.

401. A. Steinle, P. Li, D. L. Morris, V. Groh, L. L. Lanier, R. K. Strong and T. Spies. 2001. Interactions of human NKG2D with its ligands MICA, MICB, and homologs of the mouse RAE-1 protein family. *Immunogenetics* 53:279-287.

402. N. J. Chalupny, C. L. Sutherland, W. A. Lawrence, A. Rein-Weston and D. Cosman. 2003. ULBP4 is a novel ligand for human NKG2D. *Biochem Biophys Res Commun* 305:129-135.

403. V. Groh, R. Rhinehart, H. Secrist, S. Bauer, K. H. Grabstein and T. Spies. 1999. Broad tumour-associated expression and recognition by tumour-derived gamma delta T cells of MICA and MICB. *Proc Natl Acad Sci U S A* 96:6879-6884.

404. D. Pende, P. Rivera, S. Marcenaro, C. C. Chang, R. Biassoni, R. Conte, M. Kubin, D. Cosman, S. Ferrone, L. Moretta and A. Moretta. 2002. Major histocompatibility complex class I-related chain A and UL16-binding protein expression on tumour cell lines of different histotypes: analysis of tumour susceptibility to NKG2D-dependent natural killer cell cytotoxicity. *Cancer Res* 62:6178-6186.

405. S. A. Welte, C. Sinzger, S. Z. Lutz, H. Singh-Jasuja, K. L. Sampaio, U. Eknigk, H. G. Rammensee and A. Steinle. 2003. Selective intracellular retention of virally induced NKG2D ligands by the human cytomegalovirus UL16 glycoprotein. *Eur J Immunol* 33:194-203.

406. Y. Hayakawa, J. M. Kelly, J. A. Westwood, P. K. Darcy, A. Diefenbach, D. Raulet and M. J. Smyth. 2002. Cutting edge: tumour rejection mediated by NKG2D receptor-ligand interaction is dependent upon perforin. *J Immunol* 169:5377-5381.

407. A. Cerwenka, J. L. Baron and L. L. Lanier. 2001. Ectopic expression of retinoic acid early inducible-1 gene (RAE-1) permits natural killer cell-mediated rejection of a MHC class I-bearing tumour in vivo. *Proc Natl Acad Sci U S A* 98:11521-11526.

408. A. Diefenbach, E. R. Jensen, A. M. Jamieson and D. H. Raulet. 2001. Rae1 and H60 ligands of the NKG2D receptor stimulate tumour immunity. *Nature* 413:165-171.

409. M. Girardi, D. E. Oppenheim, C. R. Steele, J. M. Lewis, E. Glusac, R. Filler, P. Hobby, B. Sutton, R. E. Tigelaar and A. C. Hayday. 2001. Regulation of cutaneous malignancy by gammadelta T cells. *Science* 294:605-609.

410. V. Groh, J. Wu, C. Yee and T. Spies. 2002. Tumour-derived soluble MIC ligands impair expression of NKG2D and T-cell activation. *Nature* 419:734-738.

411. H. R. Salih, H. G. Rammensee and A. Steinle. 2002. Cutting edge: down-regulation of MICA on human tumours by proteolytic shedding. *J Immunol* 169:4098-4102.

412. H. R. Salih, H. Antropius, F. Gieseke, S. Z. Lutz, L. Kanz, H. G. Rammensee and A. Steinle. 2003. Functional expression and release of ligands for the activating immunoreceptor NKG2D in leukemia. *Blood* 102:1389-1396.

413. M. Egeblad and Z. Werb. 2002. New functions for the matrix metalloproteinases in cancer progression. *Nat Rev Cancer* 2:161-174.

414. C. Wild-Bode, M. Weller and W. Wick. 2001. Molecular determinants of glioma cell migration and invasion. *J Neurosurg* 94:978-984.

415. W. Wick, M. Platten and M. Weller. 2001. Glioma cell invasion: regulation of metalloproteinase activity by TGF-beta. *J Neurooncol* 53:177-185.

416. L. Gorelik and R. A. Flavell. 2002. Transforming growth factor-β in T-cell biology. *Nat Rev Immunol* 2:46-53.

417. S. Bodmer, K. Strommer, K. Frei, C. Siepl, N. De Tribolet, I. Heid and A. Fontana. 1989. Immunosuppression and transforming growth factor-β in glioblastoma. Preferential production of transforming growth factor-beta 2. *J Immunol* 143:3222-3229.

418. B. Pasche. 2001. Role of transforming growth factor-β in cancer. *J Cell Physiol* 186:153-168.

419. J. Rieger, W. Wick and M. Weller. 2003. Human malignant glioma cells express semaphorins and their receptors, neuropilins and plexins. *Glia* 42:379-389.

420. M. J. Robertson, K. J. Cochran, C. Cameron, J. M. Le, R. Tantravahi and J. Ritz. 1996. Characterization of a cell line, NKL, derived from an aggressive human natural killer cell leukemia. *Exp Hematol* 24:406-415.

421. T. R. Brummelkamp, R. Bernards and R. Agami. 2002. Stable suppression of tumorigenicity by virus-mediated RNA interference. *Cancer Cell* 2:243-247.

422. C. Weigert, U. Sauer, K. Brodbeck, A. Pfeiffer, H. U. Häring and E. D. Schleicher. 2000. AP-1 proteins mediate hyperglycemia-induced activation of the human TGF-beta1 promoter in mesangial cells. *J Am Soc Nephrol* 11:2007-2016.

423. E.L. Kaplan and P. Meyer. 1958. Non-parametric estimation from incomplete observations. *J Am Stat Assoc* 53:457-481.

424. N. Mantel. 1966. Evaluation of survival data and two new rank order statistics arising in its consideration. *Cancer Chemother Rep* 50:163-170.

425. P. R. Walker, T. Calzascia and P. Y. Dietrich. 2002. All in the head: obstacles for immune rejection of brain tumours. *Immunology* 107:28-38.

426. A. Diefenbach and D. H. Raulet. 2002. The innate immune response to tumours and its role in the induction of T-cell immunity. *Immunol Rev* 188:9-21.

427. J. S. Rao. 2003. Molecular mechanisms of glioma invasiveness: the role of proteases. *Nat Rev Cancer* 3:489-501.

428. L. Gorelik and R. A. Flavell. 2001. Immune-mediated eradication of tumours through the blockade of transforming growth factor-beta signalling in T cells. *Nat Med* 7:1118-1122.

429. S. Bertone, F. Schiavetti, R. Bellomo, C. Vitale, M. Ponte, L. Moretta and M. C. Mingari. 1999. Transforming growth factor-β-induced expression of CD94/NKG2A inhibitory receptors in human T lymphocytes. *Eur J Immunol* 29:23-29.

430. D. Hanahan and R. A. Weinberg. 2000. The hallmarks of cancer. *Cell* 100:57-70.

431. O. Bögler and M. Weller. 2002. Apoptosis in gliomas, and its role in their current and future treatment. *Front Biosci* 7:339-353.

432. N. Erez-Alon, J. Herkel, R. Wolkowicz, P. J. Ruiz, A. Waisman, V. Rotter and I. R. Cohen. 1998. Immunity to p53 induced by an idiotypic network of anti-p53 antibodies: generation of sequence-specific anti-DNA antibodies and protection from tumour metastasis. *Cancer Res* 58:5447-5452.

433. R. F. Fonseca, M. T. Kawamura, J. A. Oliveira, A. Teixeira, G. Alves and G. Carvalho Mda. 2003. Anti-p53 antibodies in Brazilian brain tumour patients. *Genet Mol Res* 2:185-190.

434. J. Hernandez, A. Ko and L. A. Sherman. 2001. CTLA-4 blockade enhances the CTL responses to the p53 self-tumour antigen. *J Immunol* 166:3908-3914.

435. R. Amakawa, A. Hakem, T. M. Kundig, T. Matsuyama, J. J. Simard, E. Timms, A. Wakeham, H. W. Mittruecker, H. Griesser, H. Takimoto, R. Schmits, A. Shahinian, P. Ohashi, J. M. Penninger and T. W. Mak. 1996. Impaired negative selection of T cells in Hodgkin's disease antigen CD30-deficient mice. *Cell* 84:551-562.

436. M. Majdan, C. Lachance, A. Gloster, R. Aloyz, C. Zeindler, S. Bamji, A. Bhakar, D. Belliveau, J. Fawcett, F. D. Miller and P. A. Barker. 1997. Transgenic mice expressing the intracellular domain of the p75 neurotrophin receptor undergo neuronal apoptosis. *J Neurosci* 17:6988-6998.

437. G. J. van Mierlo, A. T. den Boer, J. P. Medema, E. I. van der Voort, M. F. Fransen, R. Offringa, C. J. Melief and R. E. Toes. 2002. CD40 stimulation leads to effective therapy of CD40(-) tumours through induction of strong systemic cytotoxic T lymphocyte immunity. *Proc Natl Acad Sci U S A* 99:5561-5566.

438. L. A. Gravestein, W. Van Ewijk, F. Ossendorp and J. Borst. 1996. CD27 cooperates with the pre-T cell receptor in the regulation of murine T cell development. *J Exp Med* 184:675-685.

439. T. Kobata, K. Agematsu, J. Kameoka, S. F. Schlossman and C. Morimoto. 1994. CD27 is a signal-transducing molecule involved in CD45RA+ naive T cell costimulation. *J Immunol* 153:5422-5432.

440. R. Arens, K. Schepers, M. A. Nolte, M. F. van Oosterwijk, R. A. W. van Lier, T. N. M. Schumacher and M. H. J. van Oers. 2004. Tumour Rejection Induced by CD70-mediated Quantitative and Qualitative Effects on Effector CD8+ T Cell Formation. *J. Exp. Med.* 199:1595-1605.

441. M. Weller, D. B. Constam, U. Malipiero and A. Fontana. 1994. Transforming growth factor-β 2 induces apoptosis of murine T cell clones without down-regulating bcl-2 mRNA expression. *Eur J Immunol* 24:1293-1300.

442. R. Derynck, R. J. Akhurst and A. Balmain. 2001. TGF-β signalling in tumour suppression and cancer progression. *Nat Genet* 29:117-129.

443. J. N. Rich. 2003. The role of transforming growth factor-β in primary brain tumours. *Front Biosci* 8:e245-260.

444. J. A. Westwood, J. M. Kelly, J. E. Tanner, M. H. Kershaw, M. J. Smyth and Y. Hayakawa. 2004. Cutting edge: novel priming of tumour-specific immunity by NKG2D-triggered NK cell-mediated tumour rejection and Th1-independent CD4+ T cell pathway. *J Immunol* 172:757-761.

445. J. C. Lee, K. M. Lee, D. W. Kim and D. S. Heo. 2004. Elevated TGF-β1 secretion and down-modulation of NKG2D underlies impaired NK cytotoxicity in cancer patients. *J Immunol* 172:7335-7340.

446. D. Rosen, J. H. Li, S. Keidar, I. Markon, R. Orda and G. Berke. 2000. Tumour immunity in perforin-deficient mice: a role for CD95 (Fas/APO-1). *J Immunol* 164:3229-3235.

447. V. Screpanti, R. P. A. Wallin, H. G. Ljunggren and A. Grandien. 2001. A central role for death receptor-mediated apoptosis in the rejection of tumours by NK cells. *J Immunol* 167:2068-2073.

448. F. H. Igney and P. H. Krammer. 2002. Immune escape of tumours: apoptosis resistance and tumour counterattack. *J Leukoc Biol* 71:907-920.

449. A. Jekle, R. Obst, F. Lang, H. G. Rammensee and E. Gulbins. 2000. CD95/CD95 ligand-mediated counterattack does not block T cell cytotoxicity. *Biochemical and Biophysical Research Communications* 272:395-399.

450. A. K. Nowak, R.A. Lake, A. L. Marzo, B. Scott, W. R. Heath, E. J. Collins, J. A. Frelinger and B. W. S. Robinson. 2003. Induction of tumour cell apoptosis *in vivo* increases tumour antigen cross-presentation, cross-priming rather than cross-tolerizing host tumour-specific $CD8^+$ T cells. *J Immunol* 170:4905-4913.

451. J. P. Steinbach and M. Weller. 2002. Mechanisms of apoptosis in central nervous system tumours: application to theory. *Curr Neurol Neurosci Rep* 2:246-253.

List of Publications

Friese MA, **Wischhusen J**, Wick W, Weiler M, Eisele G, Steinle A, Weller M. RNA interference targeting TGF-β enhances NKG2D-mediated anti-glioma immune response, inhibits glioma cell migration and invasiveness and abrogates tumorigenicity *in vivo*. Cancer Research. manuscript in press

Uhl M, Aulwurm S, **Wischhusen** J, Weiler M, Ma JY, Almirez R, Mangadu R, Liu YW, Platten M, Herrlinger U, Murphy A, Wong DH, Wick W, Higgins LS, Weller M. SD-208, a novel TGF-β receptor I kinase inhibitor, inhibits growth and invasiveness and enhances immunogenicity of murine and human glioma cells *in vitro* and *in vivo*. Cancer Research. manuscript in press

Naumann U, **Wischhusen J**, Weit S, Rieger J, Wolburg H, Massing U, Weller M. Alkylphosphocholine-induced glioma cell death is BCL-X(L)-sensitive, caspase-independent and characterized by massive cytoplasmic vacuole formation.Cell Death Differ. 2004 Sep 24 [Epub ahead of print]

Wischhusen J, Melino G, Weller M. p53 and its family members - reporter genes may not see the difference. *Manuscript in press* Cell Death & Differentiation

Wischhusen J, Naumann U, Ohgaki H, Rastinejad F, Weller M. p53-dependent and p53-independent induction of glioma cell death by CP-31398, a p53-stabilizing agent. Oncogene. 2003 Nov 13;22(51):8233-45.

Schreiner B, **Wischhusen J**, Mitsdoerffer M, Schneider D, Bornemann A, Melms A, Tolosa E, Weller M, Wiendl H. Expression of the B7-related molecule ICOSL by human glioma cells in vitro and in vivo. Glia. 2003 Dec;44(3):296-301.

Platten M, Eitel K, **Wischhusen J**, Dichgans J, Weller M. Involvement of protein kinase Cdelta and extracellular signal-regulated kinase-2 in the suppression of microglial inducible nitric oxide synthase expression by N-[3,4-dimethoxycinnamoyl]-anthranilic acid (Tranilast). Biochem Pharmacol. 2003 Oct 1;66(7):1263-70.

Wiendl H, Mitsdoerffer M, Hofmeister V, **Wischhusen J**, Weiss EH, Dichgans J, Lochmüller H, Hohlfeld R, Melms A, Weller M. The non-classical MHC molecule HLA-G protects human muscle cells from immune-mediated lysis: implications for myoblast transplantation and gene therapy. Brain. 2003 Jan;126(Pt 1):176-85.

Watanabe T, Huang H, Nakamura M, **Wischhusen J**, Weller M, Kleihues P, Ohgaki H. Methylation of the p73 gene in gliomas. Acta Neuropathol (Berl). 2002 Oct;104(4):357-62

Hipp MS, Urbich C, Mayer P, **Wischhusen J**, Weller M, Kracht M, Spyridopoulos I. Proteasome inhibition leads to NF-kappaB-independent IL-8 transactivation in human endothelial cells through induction of AP-1. Eur J Immunol. 2002 Aug;32(8):2208-17.

Wischhusen J, Jung G, Radovanovic I, Beier C, Steinbach JP, Rimner A, Huang H, Schulz JB, Ohgaki H, Aguzzi A, Rammensee HG, Weller M. Identification of CD70-mediated apoptosis of immune effector cells as a novel immune escape pathway of human glioblastoma. Cancer Res. 2002 May 1;62(9):2592-9.

Wiendl H, Mitsdoerffer M, Hofmeister V, **Wischhusen J**, Bornemann A, Meyermann R, Weiss EH, Melms A, Weller M. A functional role of HLA-G expression in human gliomas: an alternative strategy of immune escape. J Immunol. 2002 May 1;168(9):4772-80.

Platten M, Wick W, **Wischhusen J**, Weller M. N-[3,4-dimethoxycinnamoyl]-anthranilic acid (Tranilast) suppresses microglial inducible nitric oxide synthase (iNOS) expression and induced by interferon-gamma (IFN-gamma). Br J Pharmacol. 2001 Nov;134(6):1279-84.

Rimner A, **Wischhusen J**, Naumann U, Gleichmann M, Steinbach JP, Weller M. Identification by suppression subtractive hybridization of p21 as a radio-inducible gene in human glioma cells. Anticancer Res. 2001 Sep-Oct;21(5):3505-8.

Naumann U, Weit S, **Wischhusen J**, Weller M. Diva/Boo is a negative regulator of cell death in human glioma cells. FEBS Lett. 2001 Sep 7;505(1):23-6.

Spyridopoulos I, **Wischhusen J**, Rabenstein B, Mayer P, Axel DI, Fröhlich KU, Karsch KR. Alcohol enhances oxysterol-induced apoptosis in human endothelial cells by a calcium-dependent mechanism. Arterioscler Thromb Vasc Biol. 2001 Mar;21(3):439-44.

Schmidt F, Rieger J, **Wischhusen J**, Naumann U, Weller M. Glioma cell sensitivity to topotecan: the role of p53 and topotecan-induced DNA damage. Eur J Pharmacol. 2001 Jan 19;412(1):21-5.

Patents: Participation in the patenting of “Tranilast” as an agent for the treatment of inflammatory neurological disorders (5402P229)

Acknowledgements

First of all I wish to express my gratitude to Prof. Dr. Michael Weller who has left me considerable freedom in my research, but has nevertheless guided this work in his inimitable manner – inspiring, determined, demanding and always good-humoured. Many thanks for your continuous support and for your expert group leadership that allows to work in a remarkable team! Many thanks also for allowing me to go on concert tour whenever my pianistic ambitions took over...

I am also indebted to Prof. Dr. Hans-Georg Rammensee who has supported the present work during many stages with helpful suggestions and discussions and who has volunteered to review this thesis. The collaboration with you and your group has been a real pleasure! Special mention must be made to Prof. Dr. Gundram Jung who has introduced me into the immunological techniques required for various projects.

Our future PD Dr. Ulrike Naumann deserves a special credit for organizing our lab and still finding time to help out with scientific advice. Close collaborators in our group were also Dr. Manuel Friese and my fellow Ph.D. student and biochemist Steffen Aulwurm. Further, I have had the pleasure of guiding a number of diploma theses and laboratory rotations - and I have learnt a lot from this experience. (I hope, it worked the other way round, too.) Thus I wish to thank Dr. Bettina Schreiner, Dr. Patrick Roth, Dr. Günter Eisele, Meike Mistdörffer, Isabella Gekel and Lasse Peters for their (mostly) good collaboration. Thanks for a productive and pleasant working atmosphere characterized by a constant interchange of good ideas also go to Dr. Martin Uhl, Dr. Joachim Steinbach, Dr. Johannes Rieger, Dr. Mirjam Hermisson, Dr. Friederike Schmidt, Dr. Marion Bohatschek, Dr. Wolfgang Wick, Dr. Ghazaleh Tabatabai, Dr. Oliver Bähr, Dr. Markus Weiler, Dr. Robert Waltereit, Brigitte Frank, Andrea Klumpp, Simone Weit and all other former and present members of our group I´ve had the pleasure to work with. Sorry for not mentioning all of you by name!

Further partners in the Department of Neurology were Dr. Heinz Wiendl and his group as well as the group of PD Dr. Jörg B. Schulz (around Dr. Ellen Gerhardt) that tolerated me in a shared laboratory for 18 months. I also wish to thank all collaborators that are mentioned in the respective chapters of this thesis and apologize for everybody who would have deserved being mentioned and got forgotten (shame on me!).

I still enjoy the good contact and fruitful discussions with PD Dr. Ioakim Spyridopoulos who has been the tutor of my diploma thesis and who really taught me the essentials of good laboratory work in a creative and relaxed atmosphere. The additional tutorship of Prof. Dr. Kai-Uwe Fröhlich also supported my beginnings both in the former and in my present laboratory. Further, I could benefit from the dedication of Prof. Bernd Hamprecht who has been a committed mentor to “his” group of biochemistry students.

Eric Reits sent me some marvellous illustrations intended to make the introduction of this thesis somewhat more enjoyable to read. Many thanks! Unfortunately I do not have the gift of drawing myself...

Instead I hope to have a little talent for music that helps me to keep my emotional balance. Special thanks goes to Prof. Friedemann Rieger who has been (and still is) an inspiring and highly motivating teacher and friend. I also thank all my chamber music partners for their patience with a pianist who spends most of his time in the laboratory!

I would not have been able to manage my considerable workload during the last years without the unconditional support of some really close friends. My fellow musician and scientist Boris Orlowsky has been an invaluable asset during the complete course of my studies (and during a wonderful trip to South America). Dr. Andreas Rimner has not only introduced me to this laboratory, but also spent numerous evenings and nice vacations with me. And in the laboratory I got to know Christoph Beier who has since then been a perfect friend and hugely contributed to the present work. Our constant exchange of ideas on all scientific topics as well as on “God and the world” cannot be treasured highly enough! Thanks for this and for countless evenings and week-ends we spent with cultural, sportive or recreational activities. You and your future wife Dr. Dagmar Schneider deserve all the credit you can take! My best wishes for your joint future are with you!

Last, but not least, I am most grateful to my parents and my sister for all kinds of valuable and highly valued support!

Academic teachers

at the University of Tübingen:

Prof. Dr. Hans Bisswanger, Prof. Dr. Karl Walter Bock, Prof. Dr. Ursula Breyer-Pfaff, Prof. Dr. Peter Bohley, Prof. Dr. Johannes Dichgans, PD Dr. Ralf Dringen, Prof. Dr. Michael Duszenko, Prof. Dr. Karl Eisele, Prof. Dr. Kai-Uwe Fröhlich, Prof. Dr. Günter Gauglitz, Prof. Dr. Friedrich Götz, Prof. Dr. Peter Grabmayr, Prof. Dr. Friedrich Gönnenwein, Dr. Hans Günzel, Prof. Dr. Hanspaul Hagenmaier, Prof. Dr. Bernd Hamprecht, Prof. Dr. Dr. h.c. Michael Hanack, Prof. Dr. Günther Jung, Prof. Dr. Gundram Jung, Prof. Dr. Ekkehard Lindner, Prof. Dr. Dieter Mecke, Prof. Dr. Helga Ninnemann (†), Prof. Dr. Erich Pfaff, Prof. Dr. Wolfgang Pfeiffer (†), Prof. Dr. Helmut Pommer, Prof. Dr. Hansgeorg Probst, Prof. Dr. Hans-Georg Rammensee, Prof. Dr. Klaus Reutter, PD Dr. Ioakim Spyridopoulos, Prof. Dr. Günther Staudt, PD Dr. Stefan Stevanovič, Prof. Dr. Dr. h.c. Joachim Strähle, Prof. Dr. Dr. h.c.Wolfgang Voelter, Prof. Dr. Dr. h.c. Klaus Wegmann, Prof. Dr. Michael Weller, Prof. Dr. Joachim Werringloer, Prof. Dr. Ulrich Weser

external:

Prof. Dr. Jürgen Brickmann, Darmstadt, Prof. Dr. Petr Čarsky, Prague, Prof. Dr. Martin Heisenberg, Würzburg, Prof. Dr. Pavel Hobza, Prague, Prof. Dr. Laurenz Lütteken, Zürich, Prof. Dr. Wolfgang Proß, Berne, Prof. Friedemann Rieger, Winterthur, Prof. Dr. Martin Scriba, Aachen, Prof. Dr. Heinz-Walter Trauth, Lübeck

Curriculum vitae

PERSÖNLICHE ANGABEN

Geburtsdatum	25.12.1971 in Kandel/Pfalz
Staatsangehörigkeit	Deutsch
Familienstand	ledig
Eltern	Dr. rer. nat. Robert Wischhusen, Physiker
	Ingeborg Wischhusen, Lehrerin
Geschwister	Anne Wischhusen, Krankenschwester

SCHULAUSBILDUNG

1978-1982	Besuch der Rennbuckel-Grundschule in Karlsruhe
1982-1992	Schulzeit am "Helmholtz-Gymnasium" in Karlsruhe
1989-1990	Auslandsaufenthalt an der Internationalen Privatschule "Concord College" bei Shrewsbury, England, erfolgreicher Abschluss der "A-level exams" in Mathematik, Physik und Chemie sowie Erwerb des "Cambridge Certificate of Proficiency in English"
1992	Abitur (Note: 1,0)

ZIVILDIENST

9/1992-10/1993:	Individuelle Schwerstbehindertenbetreuung körperlich behinderter Studenten in Karlsruhe

HOCHSCHULAUSBILDUNG

10/1993 - 7/1999	Studium der Biochemie an der Eberhard-Karls-Universität Tübingen
1996	Vordiplom in Biochemie
1998	Diplomprüfungen in Organischer Chemie, Pharmakologie und Toxikologie und Biochemie
11/1998-7/1999	Diplomarbeit in der Arbeitsgruppe von PD Dr. med. Ioakim Spyridopoulos unter Betreuung von Prof. Dr. rer. nat. Kai-Uwe Fröhlich über Apoptose in primären humanen Aortenendothelzellen
7/1999	Diplom in Biochemie
1/2000	Beginn der Doktorarbeit in der Neurologischen Universitätsklinik Tübingen in der Arbeitsgruppe von Prof. Dr. Michael Weller, unter externer Betreuung von Prof. Dr. rer. nat. Kai-Uwe Fröhlich und Prof. Dr. rer. nat. Hans-Georg Rammensee
2002	Erwerb der Befähigung zum Projektleiter für Biologische Sicherheit inkl. gentechnischer Arbeiten

STIPENDIEN UND PREISE

1992	Preise für ein hervorragendes Abitur von der Stadt Karlsruhe, dem Land Baden-Württemberg, dem Verband der Chemischen Industrie und der Literarischen Gesellschaft
1993	1. Bundespreis für Klavierbegleitung beim Wettbewerb „Jugend musiziert"
10/1993 - 7/1999	Stipendiat der "Studienstiftung des deutschen Volkes"
11/1999	Preis der Vereinigung Tübinger Biochemiker (MoBBEL) für die beste Diplomarbeit
2004	Auszeichnung beim Internationalen Musikwettbewerb Markneukirchen

WEITERE STUDIEN

1997-1999	Studium der Klavierkammermusik am Konservatorium Winterthur, abgeschlossen mit der "Künstlerischen Reifeprüfung/Reifediplom"

Tübingen, 14. Oktober 2004 Jörg Wischhusen